Investigation of Through-Tenon Keys on the Tensile Strength of Mortise and Tenon Joints

Lance David Shields

Thesis submitted to the faculty of the

Virginia Polytechnic Institute and State University

in partial fulfillment of the requirements for the degree of

MASTER OF SCIENCE

In

CIVIL ENGINEERING

Daniel P. Hindman, Co-Chair

Kamal B. Rojiani, Co-Chair

Joseph R. Loferski

June 10, 2011

Blacksburg, Virginia

Keywords: Timber Frame, Joints, Wood Connections, White Oak, Douglas-fir, Through-Tenon, Keys, Wedges, Tensile Strength

Investigation of Through-Tenon Keys on the Tensile Strength of Mortise and Tenon Joints

Lance David Shields

ABSTRACT

A timber frame is a structural building system composed of heavy timber members connected using carpentry-style joinery that may include metal fasteners. A common variant of mortise-and-tenon joints are keyed (or wedged) through-tenon joints. No research on the behavior of wedged joints in timber frames is available. This research provides design knowledge of keyed through-tenon joints from experimental observations and comparisons between mathematical models and experimental measurement. Evaluation of through-tenon keyed mortise and tenon joints was performed by measuring tensile load and stiffness of white oak (Quercus alba) and Douglas-fir (Pseudotsuga menziesii) joints with four- and 11-inch tenons with one and two keys and comparing these results to mathematical models developed from the *National Design Specification of Wood Construction (NDS), General Dowel Equations for Calculating Lateral Connection Values (TR-12),* and engineering mechanics. Variables included joint species (white oak or Douglas-fir), protruding tenon length (four or 11 inches), and number of keys (one or two). Joints were tested to ultimate load, then model input specimens were cut from tested joints and additional key stock to generate inputs for joint load predictions that were compared to experimental joint load results for validation. Forty joints were tested with white oak keys and six of these joints were retested with ipe (Tabebuia) keys.

Joints with four-inch tenons behaved in a brittle manner with tenon failures. Most joints with 11-inch tenons behaved in a ductile manner with key bending and crushing failures. Joint load and stiffness was similar between white oak and Douglas-fir joints. Joints with 11-inch tenons had greater load and stiffness than with four-inch tenons. Joints with two keys had greater load and stiffness than joints with one key, after normalizing joint load and stiffness responses on key width. Joints retested with ipe keys had greater load than joints originally tested with white oak keys.

Tenon relish (row tear-out) failure was predicted for all joints with four-inch tenons. Horizontal key shearing was predicted for all joints with 11-inch tenons. Ratios of predicted ultimate joint load divided by experimental ultimate joints load (calculated/tested) or C/T ratios were used to validate the models chosen for load prediction. C/T ratios showed that ultimate load model predictions over predicted joint load which was due to occurrence of unpredicted tenon failures and simultaneously occurring key failures where models predicted key failures independently. Design safety factors (DSFs) were developed by dividing experimental ultimate joint load by governing allowable (design) load predictions. C/T ratios and DSFs were most similar between white oak and Douglas-fir joints and most different between joints with one and two keys. Alternative design values (ADVs) were developed for comparison to design load predictions. Comparisons between ADVs and DSFs showed that model predictions were most conservative for joints fastened with denser keys than joint members.

Acknowledgements

I want to give special recognition and thanks to Dr. Robert Brungraber for suggesting this research.

I also want to commemorate David Fischetti who was an outstanding engineer in his field, beloved family member, and who also helped with relocation of Cape Hatteras Lighthouse and many other historic landmark structures. David provided me with suggestions before I started this research.

Special thanks to my mother: Karen Shields, father: Charles Shields III, stepfather: Larry Priest, stepmother: Shean Shields, brother: Charles (Wyatt) Shields IV. Thank you for much love, spiritual and financial support, time, and advice. My father, Charles Shields III, short of my Father in Heaven, is most responsible for my interest in structures and building materials since early childhood. "Love you Dad!" Many others have since continued my interests in pursuing construction and engineering including Larry Priest, Wayne Sachleben, Edward Dunn, Donald Long, Jim Henderson, Bob Shortridge, Bobby Shortridge, Dr. McConnell (J Sargeant Reynolds Community College), Dr. Easterling (Virginia Tech), Dr. Hindman (Virginia Tech), and Mike Koelzer just to name a few. Special thanks to Donald Long for excellent friendship and many years of hands-on construction experience including decks, remodeling, log home construction, and many other opportunities; I do not know anyone who constructs things with more precision and skill than Donald Long. Special thanks to Jim Henderson, high school building trades teacher, for four years of hands-on experience in carpentry including manual and computer drafting, full-scale residential framing, timber framing, and for developing my love for timber frame construction and craftsmanship. Special thanks to Wayne Sachleben for confirming my decision in becoming a structural engineer.

All of my friends at Chi Alpha (XA) Christian Ministries provided me strength and encouragement for continuing my studies as an undergraduate and graduate student. I thank and love you all. Special thanks to Pastor Scott Cooper, Amy Cooper, Jonathan Rice, Anthony Saladino, and close friend Douglas Shank for much advice and support. I also give special thanks and recognition to my friends at the Tang Soo Do club at Virginia Tech, especially to Bill, who always told me, "You can do it, you'll do fine," in martial arts and in life. - Tang Soo!

Thanks to Dreaming Creek Timber Frame Homes, Blue Ridge Timber Wrights, Chisel Craft, and others for guidance in the selection of joints for testing and advice on typical details. Special thanks to Dreaming Creek Timber Frames Homes for providing all joints, materials, manufacturing, and encouragement. Bob and Bobby Shortridge of Dreaming Creek Timber Frame Homes not only initially provided joints and materials but also provided addition ipe key stock, without me asking for it, after stopping by to observe some joint tests. - Thank you Bob and Bobby!

Dr. Robert Brungraber, Dr. Joe Miller, Dr. Richard Schmidt, Jordan Truesdell of Truesdell Engineering, and others have provided much support and guidance whenever I had questions regarding issues related to my research. I have never known anybody to respond to an e-mail quicker than Robert or Joe. Thank you all.

I want to thank my dear friends at the Brooks Forest Products Center at Virginia Tech for guidance and support. Thank you Ryan Bamberg, Monil Patel, Paul Timko, Chayanika Mitra, Choa Wang, Ji Young, Scott Lyon, Johanna Madrigal, Bryan Stinnett, Scott McDonald (assisted me with testing an entire semester), Ezechiel Pamprin, Umit Buyuksari, Louis Anthony Francois Junior, Gi Young Jeong, Omar and Scarlet Espinoza, Michael Sperber, Timo Grueneberg ("Lance, get your research done."), Ralph Rupert (much statistical help and advice), Lori Koch, Jim Bisha, John Bouldin, Jose Maria Villasenor Aguilar, Angela Reigel, David Jones, Rick and Linda Caudill, Kenny Albert ("Oh-no, what do you want!"), Dr. Loferski, and Dr. Hindman, and many others. Special thanks to Angela Reigel, Rick and Linda Caudill, Kenny Albert, and David Jones for advice and allowing me to shoot the breeze when I needed a break. Special thanks to Rick Caudill, David Jones, and Scott McDonald for helping me conduct and complete my testing. Rick always made sure that I was okay when I was stressed out, often with ",You don't need to worry, it'll all work out." Special thanks to John Bouldin and Angela Reigel for providing me much spiritual counsel in times of desperate need, you are excellent friends. A very special thanks to my amigo, Jose Maria Villasenor Aguilar, for excellent friendship, counsel, advice, much help with mathematical and computer issues, and good times; I will always remember you stomping up the stairs, to where I worked, and demanded, "Hey Lance, I'm starving, man, let's go to Texas Roadhouse - Right Now!"

This research would not have been possible without the support and guidance of my committee members Dr. Hindman, Dr. Rojiani, and Dr. Loferski. Thank you all for your knowledge and input into this research.

Best regards to Dr. Hindman. It all started when I was an undergraduate student, in civil engineering, where I took a class called "Design of Wood Structures" under the instruction of Dr. Hindman. I always followed him to his car after class with many questions to which he supplied answers. About one year later, when I was graduating and did not know if I was going to pursue a Master's Degree or look for a job, I got an e-mail from Dr. Hindman asking if I wanted to be his graduate student; to this day I am glad that I replied with 'YES' without hesitation. During "Design of Wood Structures," Dr. Hindman saw that I had an interest in timber framing and supplied me with literature on the engineering design of timber frame joints - that I did not know existed. Since then, Dr. Hindman has seen my research through, from start to finish - it was not always easy, but we got there. I remember when Dr. Hindman and I sat down to talk about what I was going to do for a thesis, he said that I could do whatever I wanted , as long as it related to timber and civil engineering - well, there you go, a pretty simple decision. Dr. Hindman told me that he believes that students do best when they choose their research topic - under supervision, of course. Looking back, some of my scariest moments were looking at all the edits that I had to make to previous editions of sections of my thesis to the tune of "It needs a lot of work, but you're doing good, just keep it up - this is a process." Boy, was that right; my writing skills have drastically improved. Just like Donald Long is a perfectionist when it comes to carpentry, Dr. Hindman is a perfectionist at writing, data analyzing, and experimental design. Dr. Hindman, without you, many skills that I have developed, to date, would be seriously lacking or non-existent, yes, professional skills included. Thank you Dr. Hindman, for selecting me for a graduate position, letting me do research in timber frame engineering, and providing me with vast skill sets!

My Sincerest thanks goes to my Lord God and Savior, Jesus Christ. From the beginning, your guiding hand has led me to the wonderful folks, mentioned above, that you so graciously put in my life. You made sure that I was born into a near perfect family, provided me an interest in construction and engineering, and saw that I would be involved in both - none of it I deserved, including and especially your love. I look forward to whatever is next. Thank you Jesus!

Table of Contents

Table of Contents.....vii
List of Figures.....xi
List of Tables.....xiii
Chapter 1: Introduction.....1
1.1 Background.....1
1.2 Timber Framing.....1
1.3 The Mortise and Tenon Joint.....3
1.4 Goal and Objectives.....5
1.5 Significance.....5
Chapter 2: Literature Review.....6
2.1 Introduction.....6
2.2 Conventional Timber Connections.....6
2.2.1 Implementation of the European Yield Model (EYM).....6
2.2.2 Conventional Connection Design Methodology: Dowel-Type Fasteners.....8
2.2.2.1 Yield Limit Equations.....9
2.2.2.2 Fastener Spacing.....13
2.2.2.3 Net-section Tension and Row/Group Tear-out.....14
2.2.2.4 Allowable Strength Design (ASD) for Connections and other Wood Properties.....16
2.2.2.5 Technical Report 12 (TR-12).....18
2.3 Horizontal Shear in Wood Beams.....19
2.4 Connection Strength Comparison Methods.....21
2.5 Timber Frame Research.....23
2.5.1 Pioneered Timber Frame Research.....23
2.5.2 Joint Tension Research.....23
2.5.2.1 Kessel and Augustin.....24
2.5.2.2 Schmidt and MacKay (1997).....25
2.5.2.3 Schmidt and Daniels (1999).....26
2.5.2.4 Miller (2004).....28
2.5.2.5 Sangree and Schafer (2007).....30

2.5.3 Lateral Loading Research....31
2.5.3.1 Carradine (2000)....31
2.5.3.2 Erickson and Schmidt (2002)....32
2.6 Current Design Practices for Timber Frame Structures....33
2.6.1 TFEC 1-2010....33
2.7 Chronological Summary....39
Chapter 3: Through-tenon Key Joint Test Loads and Comparisons.... 42
3.1 Methods and Materials....42
3.1.1 Materials....42
3.1.2 Joint Testing....44
3.1.2.1 Joint Test Set-up....45
3.1.2.2 Joint Testing Procedure....47
3.2 Results and Discussion....49
3.2.1 Joint Testing Results....49
3.2.1.1 Load and Stiffness of Joints with White Oak Keys....49
3.2.1.2 Load and Stiffness of Joints with Ipe Keys....56
3.2.1.3 Joint Failure at Ultimate Load....60
3.2.1.4 Brittle and Ductile Joint Behavior....66
3.2.1.5 Moisture Content/ Specific Gravity (MC/SG) of Joint Components....69
3.2.2 Effects of Joint Factors on Load and Stiffness of Joints with White Oak Keys....72
3.2.2.1 ANOVA Comparison of Joint Load and Stiffness....72
3.2.2.2 Comparison of Species on Joint Load and Stiffness....73
3.2.2.3 Comparison of Tenon Length on Joint Load and Stiffness....74
3.2.2.4 Comparison of the Number of Keys on Joint Load and Stiffness....75
3.2.3 Influence of Key Specific Gravity of Responses of Joint with Key Failures..77
3.3 Summary and Conclusions....80
Chapter 4: Joint Load Prediction: Through-tenon Key Joint Loads and Comparison 82
4.1 Methods and Materials....82
4.1.1 Materials....83
4.1.2 Model Input Testing Procedures....85

4.1.2.1 Moisture Content and Specific Gravity Tests (All Members)..... 86
4.1.2.2 Tension Parallel-to-grain Tests (Tenon Member)..... 86
4.1.2.3 Shear Parallel-to-grain Tests (Tenon Member and Keys)..... 87
4.1.2.4 Bending Tests (Keys)..... 88
4.1.2.5 Bearing Parallel-to-grain Tests (Tenon Member)..... 89
4.1.2.6 Bearing Perpendicular-to-grain Tests (Mortise Member and Keys)..... 90
4.1.3 Models for Load Prediction of Keyed Through Tenon Joints..... 91
4.1.3.1 Tenon Member Models..... 93
4.1.3.2 Mortise Member Model..... 97
4.1.3.3 Key Models..... 98
4.2 Results and Discussion..... 108
4.2.1 Model Input Specimen Test Results..... 108
4.2.1.1 Tension Parallel-to-grain Input Specimen Tests (Tenon)..... 109
4.2.1.2 Shear Parallel-to-grain Input Specimen Tests (Tenon)..... 110
4.2.1.3 Bearing Parallel-to-grain Input Specimen Tests (Tenon)..... 111
4.2.1.4 Perpendicular-to-grain Bearing Input Specimen Tests (Mortise)..... 112
4.2.1.5 Bending Input Specimen Tests (Keys)..... 114
4.2.1.6 Perpendicular-to-grain Bearing Input Specimen Tests (Keys)..... 115
4.2.1.7 Shear Parallel-to-grain Input Specimen Tests (Keys)..... 117
4.2.2 Model Predictions..... 118
4.2.2.1 Ultimate Load Predictions..... 118
4.2.2.2 Allowable Load Predictions..... 124
4.2.3 C/T Ratios of Minimum Ultimate Predicted Joint Load/ Experimental Ultimate Joint Load..... 131
4.2.3.1 ANOVA Comparisons on C/T Ratios between Joint Factors..... 133
4.2.3.2 Comparison of C/T Ratios between Species..... 134
4.2.3.3 Comparison of C/T Ratios between Tenon Length..... 135
4.2.3.4 Comparison of C/T Ratios between Number of Keys..... 135
4.2.3.5 C/T Ratios of Joints with Ipe Keys..... 136
4.2.4 Design Safety Factors (DSFs) of Experimental Ultimate Joint Load/ Minimum Allowable Predicted Load..... 138

4.2.4.1 ANOVA Comparisons on DSFs between Joint Factors..... 139
4.2.4.2 Comparison of DSFs between Species..... 139
4.2.4.3 Comparison of DSFs between Tenon Length..... 140
4.2.4.4 Comparison of DSFs between Number of Keys..... 141
4.2.4.5 DSFs of Joints with Ipe Keys..... 141
4.2.5 Alternative Design Values (ADV) of Experimental Ultimate Joint Load/ Design Recommendations from Kessel and Augustin (1996)..... 143
4.3 Conclusions..... 146
Chapter 5: Summary and Conclusions..... 149
5.1 Summary..... 149
5.2 Conclusions..... 150
5.2.1 Chapter 3 Conclusions..... 150
5.2.2 Chapter 4 Conclusions..... 151
5.3 Limitations..... 155
5.4 Recommendations for Future Work..... 156
References..... 158
Appendix A - Initial Joint Defects..... 163
Appendix B - Joint Test Values, C/T Ratios, DSFs, and ADVs..... 166
Appendix C - Joint Load-Deflection Plots (Curves)..... 169
Appendix D - Moisture Content and Specific Gravity of All Joint Components..... 178
Appendix E - Ultimate and Allowable Joint Strength Predictions..... 179
Appendix F – Model Input Specimen Test Strength Results..... 182

List of Figures

Figure 1-1: Traditional-Style Timber Frame..... 2

Figure 1-2: Pegged Mortise and Tenon Joint.....3

Figure 1-3: Keyed Through-Tenon Joint..... 3

Figure 1-4a: King post Truss..... 4

Figure 1-4b: Dutch Anchor Beam.....4

Figure 2-1: 5% Offset Yield Point..... 7

Figure 2-2: Mode I_m (Conventional)..... 10

Figure 2-3: Mode I_s (Conventional)..... 11

Figure 2-4: Mode III_s (Conventional)..... 11

Figure 2-5: Mode IV (Conventional)..... 12

Figure 2-6: Bolt Spacing Illustration..... 13

Figure 2-7: Net-section Tension..... 15

Figure 2-8: Row Tear-out..... 15

Figure 2-9: Group Tear-out.....16

Figure 2-10: Scarf Joint..... 30

Figure 2-11: Mode I_m (Timber Frame)..... 34

Figure 2-12: Mode I_s (Timber Frame)..... 35

Figure 2-13: Mode III_s (Timber Frame)..... 36

Figure 2-14: Mode V (Timber Frame)..... 36

Figure 2-15: Pegged Joint Detailing..... 39

Figure 3-1: Keyed Through-tenon Joint and Component Dimensions.....43

Figure 3-2: Joint Testing Setup.....46

Figure 3-3: Joint Load-Deformation Curve..... 48

Figure 3-4: Joint load curve without a 5% offset yield load due to brittle behavior..... 51

Figure 3-5: Tenon Split (keyhole center).....62

Figure 3-6: Plane Shearing.....63

Figure 3-7: Full Tenon Relish Failure at each Keyhole.....64

Figure 3-8: Procession of Tenon Relish Failure after a Defect or a Pre-failure Event.....64

Figure 3-9: Key Bending and Crushing (White Oak Keys).....65

Figure 3-10: Key Bending/ slight Crushing (Ipe Keys).....65
Figure 3-11: Key Wedging..... 66
Figure 3-12: Severed Key from Key Wedging.....66
Figure 3-13: Mortise Split from Key Wedging.....66
Figure 3-14a: WO-4-2-1 (Relish on left key)…….....67
Figure 3-14b: DF-11-1-1: Full Relish…….....67
Figure 3-15: WO-4-2-3.....68
Figure 3-16a: WO-11-1-2 (Key Failure).....69
Figure 3-16b: DF-11-2-5 (Key Failure).....69
Figure 3-17: Joint Load vs. Key SG for White Oak Joints with Key Failures..... 78
Figure 3-18: Joint Stiffness vs. Key SG for White Oak Joints with Key Failures..... 78
Figure 3-19: Load vs. Key SG for Douglas-fir Joints with Key Failures..... 79
Figure 4-1: Order of Research Tasks.....83
Figure 4-2: Model Input Specimen Cutting Plan.....84
Figure 4-3: Tension Test..... 87
Figure 4-4: Shear Test..... 88
Figure 4-5: Bending Test..... 88
Figure 4-6: Bearing Parallel-to-grain Test..... 89
Figure 4-7: Bearing Perpendicular-to-grain Test..... 90
Figure 4-8: Possibilities of Group Tear-out for Single and Double Keyed Joints.....95
Figure 4-9: Key Bending and Bearing Mechanics Model..... 98
Figure 4-10: Shear and Moment Diagram of Loaded Key..... 99
Figure 4-11: General Key Bending Load Equation Derivation Model..... 100
Figure 4-12: Transverse Key Shear..... 104

List of Tables

Table 2-1: Pegged Mortise and Tenon Joint Detailing Requirements (Miller 2004)..... 30

Table 2-2: Pegged Joint Detailing Dimensions Based on Physical Tests..... 39

Table 3-1: Joint Test Schedule.....45

Table 3-2: Proportional-Limit Load of Joints with White Oak Keys..... 50

Table 3-3: 5% Offset Yield Load of Joints with White Oak Keys..... 52

Table 3-4: Ultimate Load of Joints with White Oak Keys..... 53

Table 3-5: Stiffness of Joints with White Oak Keys.....55

Table 3-6: Proportional-limit Load of Joints with Ipe Keys..... 57

Table 3-7: 5% Offset Yield Load of Joints with Ipe Keys..... 58

Table 3-8: Ultimate Load of Joints with Ipe Keys..... 59

Table 3-9: Stiffness of Joints with Ipe Keys..... 60

Table 3-10: Joint Failure at Ultimate Load..... 61

Table 3-11: Joint Member and Key MC and SG.....70

Table 3-12: Joint Member and Key MC and SG ANOVA Comparisons.....71

Table 3-13: Single Factor Analysis of Variance Comparison (α =0.05) Considering all Joints with White Oak Keys..... 72

Table 3-14: Comparison of Species on Load and Stiffness..... 73

Table 3-15: Comparison of Tenon Length on Load and Stiffness..... 74

Table 3-16: Comparison of the Number of Keys on Load and Stiffness..... 76

Table 4-1: Model Input Testing Schedule..... 85

Table 4-2: Models with Abbreviations and Full Name and Associated Joint Component...92

Table 4-3: Average Tensile Properties of Tenon Members.....110

Table 4-4: Average Shear Properties of Tenon Members..... 110

Table 4-5: Average Parallel-to-grain Bearing Properties of Tenon Members.....111

Table 4-6: Comparison of Parallel-to-grain Bearing Strength Results to NDS and ASTM D2555 values..... 112

Table 4-7: Average Perpendicular-to-grain Bearing Properties of Mortise Members..... 113

Table 4-8: Comparison of Adjusted 5% Offset Yield and NDS Allowable Adjusted Perpendicular-to-grain Compression Strength of Mortise Member Tests..... 114
Table 4-9: Average 5% Offset Yield and Ultimate Bending Properties of Keys..... 115
Table 4-10: Average Perpendicular-to-grain Bearing Properties of Keys.....116
Table 4-11: Comparison of Adjusted 5% Offset Yield and NDS Allowable Adjusted Perpendicular-to-grain Bearing Strength of Key Tests.....116
Table 4-12: Average Parallel-to-grain Shear Properties of Keys..... 117
Table 4-13: Average Predicted Ultimate Joint Load with White Oak Keys..... 119
Table 4-14: Percent Differences of Ultimate Key Load Predictions compared to Horizontal Key Shearing (Z_{K_v})..... 122
Table 4-15: Predicted Ultimate Joint Load with Ipe Keys..... 123
Table 4-16: Percent Differences of Ultimate Joint Load Predictions for Joints with Ipe Keys and Joints with White Oak Keys..... 124
Table 4-17: Average Predicted Allowable Joint Load with White Oak Keys..... 125
Table 4-18: Percent Differences between Horizontal Key Shearing (Z_{K_v}) and other Key Load Predictions regarding Allowable Predictions..... 128
Table 4-19: Predicted Allowable Joint Load (Joints with IPE Keys)..... 129
Table 4-20: Percent Difference of Allowable Joint Load Predictions of Joints with Ipe Keys and Joints with White Oak Keys..... 130
Table 4-21: Average C/T Ratios and COVs for Joint Groups with White Oak Keys..... 132
Table 4-22: ANOVA p-value Results for C/T Ratios.....134
Table 4-23: Statistical Comparisons of C/T Ratios Between Species (α =0.05)..... 134
Table 4-24: Statistical Comparisons of C/T Ratios Between Tenon Length (α =0.05)..... 135
Table 4-25: Statistical Comparisons of C/T Ratios Between Number of Keys (α =0.05)...136
Table 4-26: C/T Ratios of Joints retested with Ipe Keys.....137
Table 4-27: Average DSFs and COVs for Joint Groups with white oak keys..... 138
Table 4-28: ANOVA p-value Results for DSFs..... 139
Table 4-29: Statistical Comparisons of DSFs Between Species (α =0.05)..... 140
Table 4-30: Statistical Comparisons of DSFs Between Tenon Length (α =0.05)..... 140
Table 4-31: Statistical Comparisons of DSFs Between Number of Keys (α =0.05)..... 141
Table 4-32: C/T Ratios of Joints retested with Ipe Keys.....142

Table 4-33: ADV values of Joints with White Oak and Ipe Keys.....144

Chapter 1: Introduction

1.1 Background

The *Standard for Design of Timber Frame Structures and Commentary* (TFEC 1-10) defines a timber frame as a structural building system composed of heavy timber members connected using carpentry-style joinery that may also include metal fasteners (TFEC 2010). Many timber frame structures are constructed with pegged mortise-and-tenon joints. Obtaining adequate tension capacity is the most difficult aspect of joining timbers. High tension capacity timber connections are difficult to construct because the members are typically fastened at their ends where connection strength is limited by reduced cross-sections and shear area. A common variant of mortise-and-tenon joints are keyed through-tenon joints (Goldstein 1999). Tenon keys are commonly known as wedges. The TFEC 1-10 states, “No research on the behavior of wedged joints in timber frames is available," which also implies keyed through tenon joints.

1.2 Timber Framing

Timber framing has a long history throughout the world. Many structures are centuries old and still stand using timber joint methods. Archeologists have dated timber framing in India to 200 B.C. consisting of teak frames fastened with bamboo pegs during the same time period as the Japanese were joining timbers to build shrines and temples. In Europe, many cathedral roofs were timber framed including all-wooden stave churches in Northern Europe. Of over 700 stave churches constructed, 25 still stand. (Benson and Gruber 1980)

Timber frame construction can be seen in many wooden structures built prior to the twentieth century. In the eastern United States, thousands of timber frame structures including houses, barns, churches, and town halls are still in use after 250 to 350 years of being constructed (Benson 1999). Some of these structures include the Nantucket windmill built in 1746, the Old Ship Meeting House built in 1681, the Jethro Coffin house built in 1686, and the Fairbanks house built in 1637 (Sobon and Schroeder 1984). Today, some older timber frame structures have been retrofitted and newer buildings have been constructed.

Figure 1-1 shows a model of a traditional-style Timber Frame featured in *Timber Frame Construction* that was reconstructed for the Hancock Shaker Village which is now a museum.

This is a 12-foot by 16-foot shed building with eight-inch by eight-inch posts, sills, and plates, and four-inch by six-inch members for the rafters, braces, and joists (Sobon and Schroeder 1984). During the first 300 years of the New World settlement, nearly all buildings were timber framed. This construction was characterized by the use of joinery between large timbers that comprise the structural framework often secured with wooden pegs (Fischetti 2009).

Figure 1-1: Traditional-Style Timber Frame

During the late nineteenth century in North America, stud framing became the prevalent wood frame building technique due to advancements in sawmill technology and the abundance of wire nail production (O'Connell and Smith 1999). Westward expansion demanded faster construction that stud framing offered which was made possible by improved sawmill technology (Sobon and Schroeder 1984). Stud framing increased building construction speed and required less worker skill than timber framing, causing timber frame construction to become nearly obsolete by the 1920's (Benson 1999).

Timber framing experienced a revival in the early 1970's due to the desired craftsmanship it offered, not seen in many homes of the time. In 1996, 216 timber frame companies were identified in the United States and Canada, with nearly half of these companies located in the northeastern United States (O'Connell and Smith 1999). Today there are 233 timber frame companies in the United States and 54 in Canada (Timber Frame Business Council 2010).

1.3 The Mortise and Tenon Joint

Figure 1-2 shows a pegged mortise and tenon joint which is the most common joint used in timber framing (Goldstein 1999). A mortise is typically a rectangular hole cut into the side of a timber that receives a similarly shaped tenon cut in the end of another timber. Sometimes, peg-holes in a mortise and tenon joint are offset so that peg insertion draws the mortise and tenon members together; this method of pretensioning is known as draw-boring (Sobon and Schroeder 1984).

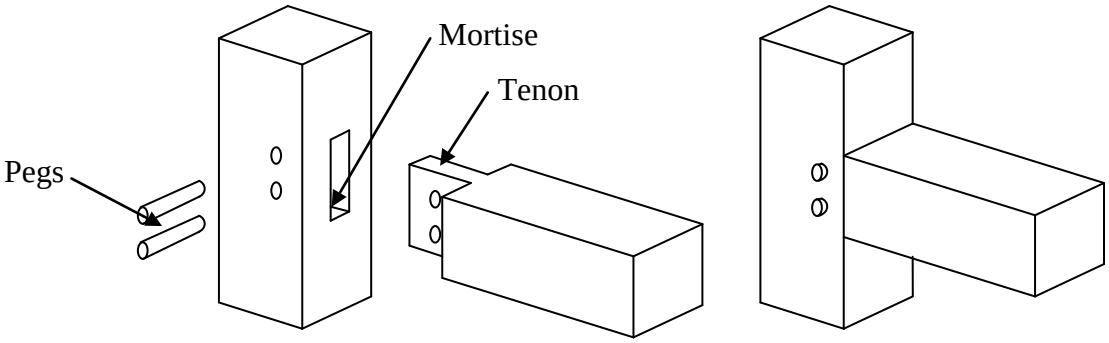

Figure 1-2: Pegged Mortise and Tenon Joint

Figure 1-3 shows a keyed through-tenon joint which has a tenon protruding through the back side of a mortise member which is reinforced with keys on the back side of the mortise member through the tenon. Keys are tapered wooden wedges that are inserted into holes cut through the protruding tenon as a means of fastening. Pegs and keys in mortise and tenon joints serve as wooden fasteners loaded in double-shear when the joint is in tension.

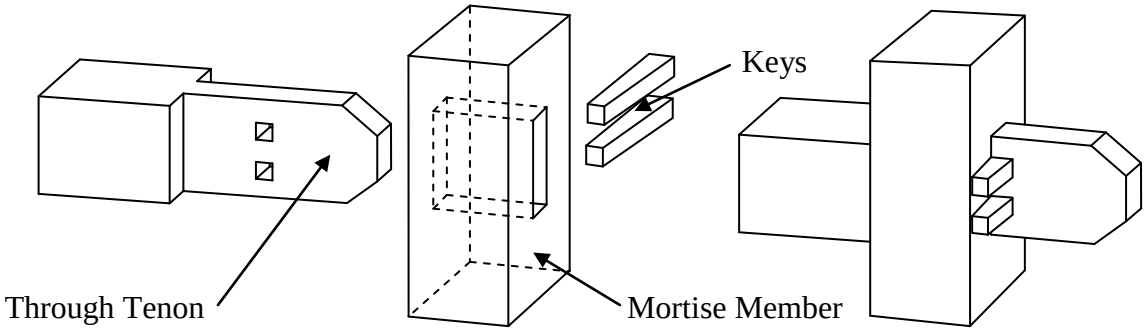

Figure 1-3: Keyed Through-Tenon Joint

Keyed through-tenon joints are often found in king-post trusses, where king-posts are tenoned into rafter-ties as shown in Figure 1-4a. This joint style was notoriously used in Dutch-

style barns where large anchor beams were tenoned into posts at each of their ends to resist large tensile forces (Figure 1-4b). Tensile forces were often exerted on post-to-beam connections when braces underneath anchor beams were compressed from heavy loft loads and lateral loads where compressed braces subjected their adjacent beam-to-post connections to withdrawal forces (Goldstein 1999). Tension in post-to-beam connections can also occur due to rafter thrust.

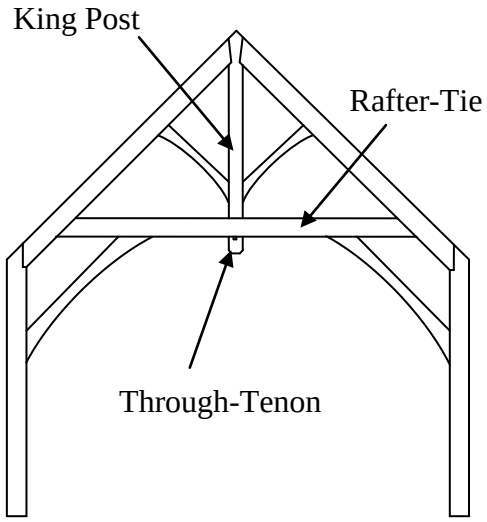

Figure 1-4a: King post Truss

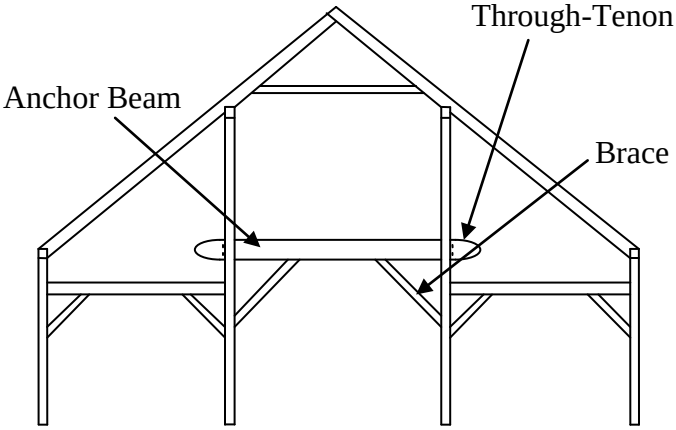

Figure 1-4b: Dutch Anchor Beam

Keyed through-tenon joints cannot be used on building exteriors since the joints would protrude the building envelope. These joints are used on the interior between posts forming central isles in bents as shown in Figure 1-4b. Keys are not constrained against flexural rotation like pegs, however, there is flexibility in sizing keys. Bearing of the tenon key-hole against the key is the smallest area of bearing greatly influencing joint strength. Increasing tenon thickness increases joint tension capacity related to tenon-key interface bearing. Increasing tenon thickness also weakens the mortise member due to widening of the mortise to accommodate a thicker tenon which may require larger mortise members (Goldstein 1999). Keyed through tenon joints under tension loads do not subject mortise walls to perpendicular-to-grain tension like pegged mortise and tenon joints. Loosening of keys due to connection component shrinkage can tremendously reduce initial joint stiffness. After moisture equilibration and periodic tightening, the keys could be secured with a predrilled screw or nail given that interior conditions remain constant after the fact. Reducing key slope may also allow keys to remain in the connection after shrinkage tightening.

1.4 Goal and Objectives

The goal of this research was to examine the load, stiffness, and behavior of keyed through-tenon joints and how joint load could be predicted through comparisons between experimental values and model predictions. Models for comparison were developed using engineering mechanics principles and current design methods. Objectives included:

(1) Develop models for different failure types of keyed-through tenon joints to predict ultimate and allowable joint load.
(2) Measure joint load, stiffness, and behavioral characteristics of full sized, keyed through-tenon joints made in 6x8 White Oak and Douglas-fir timbers.
(3) Make comparisons to determine effects species, tenon length, and number of keys on joint load and stiffness.
(4) Measure material properties of the mortise, tenon, and keys cut from the joints and key stock including tension and shear parallel-to-grain, bearing parallel and perpendicular-to-grain, bending, moisture content, and specific gravity to develop model joint load predictions.
(5) Compare model predictions to the experimental joint test results for model validation and determine the effects of species, tenon length, and number of keys on comparisons.

1.5 Significance

Achievement of the goals of this research provides knowledge of joint load, stiffness, and behavior of keyed through-tenon joints and the effects of species, tenon length, and number of keys on such responses. Design insight of these joints is provided through comparison between model predictions and experimental measurement, and the effects of species, tenon length, and number of keys on such comparisons. This research provides much opportunity for future investigation.

Chapter 2: Literature Review

2.1 Introduction

This literature review describes the development and current design methodology of conventional bolted timber connections and timber frame connections. First, development and design methods of conventional timber connections were summarized. Second, state of the art timber frame design, development, and its relationship to conventional timber design methods was discussed. Lastly, the purpose of keyed through-tenon joint research was summarized.

2.2 Conventional Timber Connections

Currently, steel dowel-type fasteners such as nails, bolts, and screws are prevalent mechanical connectors for timber connections. Other steel connectors include timber rivets, shear plates, and split-rings. Dowel-type fasteners typically transfer load laterally between two or more members by acting in shear perpendicular to the axis. Timber rivets are used in conjunction with steel side-plates in glulam construction acting in single-shear having one shear plane per timber rivet. Shear-plate connectors and split-rings connect wooden members to carry shear loads through being inserted into grooves cut into the members, often concealing them, and are typically aided with the clamping force of bolts to keep the members connected. (AF&PA 2005)

2.2.1 Implementation of the European Yield Model (EYM)

The *2005 National Design Specification of Wood Construction* (AF&PA 2005), abbreviated as the 2005 NDS, uses the European Yield Model (EYM) to predict the strength of timber connections using steel dowels. Additional shear checks including row and group tear-out and fastener spacings account for non-ductile connection behavior (AF&PA 2005). Prior to using the EYM, the design of timber connections in the 1986 edition of the NDS was based on extensive empirical research conducted by Trayer (1932). In 1991, the EYM was adopted for the design of timber connections (Soltis and Wilkinson 1991). EYM design values were adjusted with calibration factors to closely represent that of previous design values (Wilkinson 1993).

Trayer (1932) tested several hundred double-shear connections with various bolt diameters and lengths, softwood and hardwood species, parallel and perpendicular-to-grain

orientations, bolt margins, and bolt spacing. Trayer (1932) presented a proportional-limit-based connection design using bolt-bearing stress influenced primarily by the bolt-length to bolt-diameter ratio (l / D ratio) in the main member. Single-shear connections were verified to have half of the strength of double shear connections (Trayer 1932). Much of the proper bolt-spacing, end, and edge distance spacing, prescribed in the 2005 NDS guidelines are based on the work of Trayer (1932). (AF&PA 2005)

The EYM is a mechanics based model that originated from Johansen (1949) and considers bolted connection bearing capacity when the bearing strength of the wood under the bolt is exceeded and/ or when one or more plastic hinges form in the bolt (Soltis and Wilkinson 1987). A yield point definition for timber connections as 5% offset yield was suggested by Harding and Fowkes (1984), since yield strength is not well defined from connection load-deformation curves (Soltis and Wilkinson 1991). Five percent offset yield connection strength is associated with 5% offset bearing strength which is defined in ASTM D 5764-97a, *Evaluating Dowel-Bearing Strength of Wood and Wood-Based Products* (ASTM 2004a) as the point where a line parallel to the straight portion of the initial load/displacement curve, offset by a distance of 5% of the fastener diameter, intersects the original load displacement curve. Figure 2-1 illustrates the 5% offset yield point.

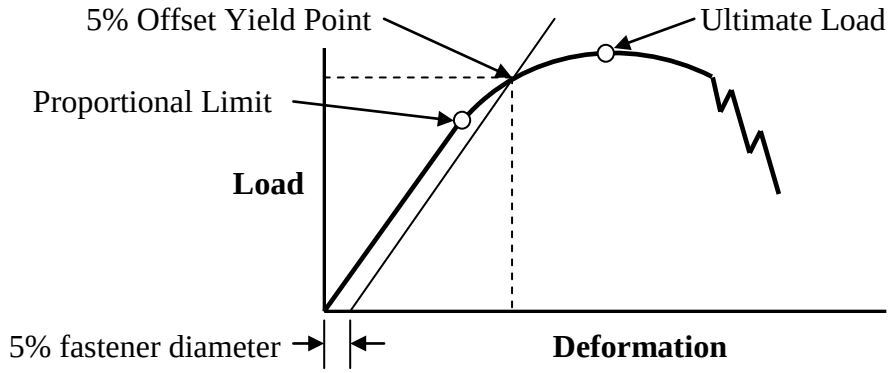

Figure 2-1: 5% Offset Yield Point

Converting to EYM design methodology was desirable because many connections that were not addressed in the 1986 NDS (NFPA 1986) could be predicted using the EYM (Wilkinson 1993). Soltis and Wilkinson (1987) compared the EYM to results of prior experimentation, including the work of Trayer (1932) and others, using the EYM as the basis of comparison. The EYM predicted the general trend of the other experimental results and also

predicted yield curves that were greater than experimental results. However, the experimental results were based on proportional-limit values rather than yield values (Soltis and Wilkinson 1987). Further research by Soltis and Wilkinson (1991) compared EYM predictions to data from over 1,000 bolted connection tests. The predictions were within 10% for parallel-to-grain connection data and within 20% for perpendicular-to-grain connection test data, and were deemed adequate (Soltis and Wilkinson 1991).

Since the 1986 NDS defined allowable strength based on proportional limit data considering a ten-year load duration and the EYM predicted a yield limit state based on a five minute load duration, EYM equations were calibrated to the NDS values upon their adoption (Soltis and Wilkinson 1991) since 1986 NDS connection design values had previously proved satisfactory (Wilkinson 1993). Wilkinson (1993) compared the design values between EYM and the 1986 NDS and developed calibration factors which were distinctly different between parallel and perpendicular-to-grain loading (Wilkinson 1993). The notable differences in the calibration factors between parallel and perpendicular-to-grain values in comparing the EYM design values to the 1986 NDS were verified through Hankinson's formula, which interpolates between parallel and perpendicular-to-grain bearing strength values. Comparing ratios of the adjusted EYM to the 1986 NDS design values determined the change in design values from the original 1986 NDS design values. A ratio of 1.0 signified no change, greater than 1.0 signified an increase, and less than 1.0 a decrease (Wilkinson 1993). The calibration factors from the research of Wilkinson (1991) are the reduction factors (R_d) in the 2005 NDS for connection yield limit values presented in equations 2-2 though 2-5.

2.2.2 Conventional Connection Design Method: Dowel-Type Fasteners

The 2005 NDS defines dowel-type fasteners as bolts, lag screws, wood screws, nails, spikes, and drift pins. Yield limit equations, which incorporate dowel-bearing and bending yield strength, are used to calculate a number of different yield modes. The reference design value for any connection with dowel-type fasteners is the lowest lateral design value from the various yield mode equations. The reference lateral design value must be adjusted for a number of different conditions including load duration, moisture, and adequate spacing. (AF&PA 2005)

Methods for establishing dowel-bearing strength were not available in the United States until the adoption of the EYM. Soltis and Wilkinson (1991) tested 240 specimens concerning relationships between specific gravity of wood species, dowel diameter, and dowel-bearing strength. A weak correlation between bearing strength parallel-to-grain and bolt diameter was observed and thus neglected. The 5% offset yield point was used to determined bolt-bearing strength (Soltis and Wilkinson 1991). The recommended equations for bolt-bearing strength are presented in Equation 2-1a for parallel-to-grain loading and Equation 2-1b for perpendicular-to-grain loading. (AF&PA 2005)

Parallel-to-grain:

$$F_e = 11{,}200G \qquad \textbf{(2-1a)}$$

Perpendicular-to-grain:

$$F_e = 6{,}100G^{1.45} / \sqrt{D} \qquad \textbf{(2-1b)}$$

Where:

F_e = Bolt-Bearing Strength, *psi*

G = Specific Gravity (oven-dry basis)

D = Bolt Diameter, *in*

Dowel-bending yield strength, F_{yb}, is determined from bending tests using the 5% diameter offset value from load-deformation curves. Tension tests have been used for large diameter fasteners to evaluate F_{yb}, where bending tests were impractical. Bolt bending yield strength is approximately equal to the average of yield and ultimate tensile strength, $F_{yb} \approx F_y / 2 + F_u / 2$. For standard A36 and stronger steel bolts, a conservative bending strength value F_{yb} is 45,000 psi (AF&PA 2005).

2.2.2.1 Yield Limit Equations

The yield-limit model for connections with dowel-type fasteners contains yield-limit equations that describe the different possible connection yield modes in regard to the fasteners. These equations include wood bearing strength underneath the fastener and the development of one or more plastic hinges in the fastener. The 5% offset-yield strength of a connection is related

to the 5% offset-bearing strength of the wood and the bending yield strength of the fastener. The reference lateral connection design strength is equal to the minimum value presented by the yield-limit equations multiplied by the number of fasteners. For use of the yield-limit equations, contact must exist between the member faces, load must act perpendicular to the dowel axis, fastener end and edge distances and spacing must be satisfied, and the proper amount of fastener length in the members must be obtained (AF&PA 2005).

Mode I_m represents dowel-bearing yield in the main, or center, member as shown in Figure 2-2. This occurs when the dowel-bearing length is small, with respect to dowel-diameter, avoiding fastener bending. Equation 2-2 shows the reference lateral design value for Mode I_m. The strength of this yield mode is equal to the product of dowel-diameter D, dowel bearing length in the main member l_m, and main member dowel-bearing strength F_{em}, divided by a reduction factor, R_d. R_d is equal to 4.0 when any connection member is oriented parallel-to-grain and 5.0 when perpendicular-to-grain for Mode I_m (AF&PA 2005).

$$Z_{\mathrm{Im}} = \frac{D \times l_m \times F_{em}}{R_d} \qquad \textbf{(2-2)}$$

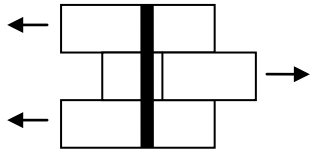

Figure 2-2: Mode I_m

Where:

Z_{Im} = Connection Strength (considering one fastener), *lbs*

D = Dowel Diameter, *in*

l_m = Main Member Dowel-Bearing Length, *in*

F_{em} = Main Member Dowel-Bearing Strength, *psi*

R_d = Reduction Factor ($4\,K_\theta$ for I_m)

K_θ = For Dowel Diameters between one-quarter and one inch: $1 + 0.25(\theta / 90)$

θ = maximum angle of load to the grain, *degrees* (0, parallel-to-grain $\leq \theta \leq 90$, perpendicular-to-grain) for any member in a connection

Mode I_s represents dowel-bearing yield in the side members, as shown in Figure 2-3. This occurs when the dowel-bearing length is small enough, with respect to dowel diameter, avoiding fastener bending. Equation 2-3 shows the reference lateral design value for Mode I_s. The strength of this yield mode is equal to twice the product of dowel-diameter D, side member dowel-bearing length l_s, and side member dowel-bearing strength F_{es}, divided by a reduction factor R_d. R_d is equal to 4.0 when any connection member is oriented parallel-to-grain and 5.0 when perpendicular-to-grain for Mode I_s (AF&PA 2005).

$$Z_{Is} = \frac{2 \times D \times l_s \times F_{es}}{R_d} \qquad \textbf{(2-3)}$$

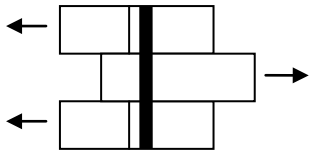

Figure 2-3: Mode I_s

Where:

Z_{Is} = Connection Strength (considering one fastener), *lbs*

l_s = Side Member Dowel-Bearing Length, *in*

F_{es} = Side Member Dowel-Bearing Strength, *psi*

R_d = Reduction Factor ($4 K_\theta$ for I_s)

Mode III_s represents a combination of dowel-bearing and bending with two plastic hinges, or one hinge per shear plane, as shown in Figure 2-4. This occurs when the dowel-bearing length in the main and side members are long enough, with respect to the bolt diameter, to cause bending in the fastener resulting in bearing yield in all members. The side members are not long enough, with respect to dowel-diameter, to cause fastener bending, thus only two plastic hinges develop in the main member with rotation in the side members. Equation 2-4 shows the reference lateral design value for Mode III_s. R_d is equal to 3.2 when any connection member is oriented parallel-to-grain and 4.0 when perpendicular-to-grain for Mode III_s (AF&PA 2005).

$$Z_{IIIs} = \frac{2 \times D \times l_s \times F_{em}}{(2 + R_e) R_d} \left(-1 + \sqrt{\frac{2(1 + R_e)}{R_e} + \frac{2 F_{yb} (2 + R_e) D^2}{3 F_{em} l_s^2}} \right) \qquad \textbf{(2-4)}$$

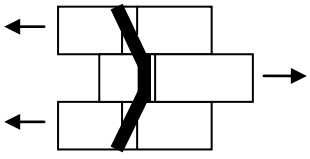

Figure 2-4: Mode III_s

Where:

Z_{IIIs} = Connection Strength (considering one fastener), *lbs*

$R_e = F_{em} / F_{es}$

F_{yb} = Dowel-Bending Yield Strength, *psi*

R_d = Reduction Factor ($3.2\,K_\theta$ for III_s)

Mode IV represents a combination of dowel-bearing and bending with four plastic hinges, or two hinges per shear plane, as shown in Figure 2-5. This occurs when the fastener bearing lengths in the main and side members are long enough, with respect to the bolt diameter, to cause bending in the fastener resulting in bearing deformations in all members. The main and side members are long enough, with respect to fastener diameter, for development of plastic hinges in each member. Equation 2-5 shows the reference lateral design value for Mode IV. R_d is equal to 3.2 when any connection member is oriented parallel-to-grain and 4.0 when perpendicular-to-grain for Mode IV (AF&PA 2005).

$$Z_{IV} = \frac{2D^2}{R_d}\sqrt{\frac{2F_{em}F_{yb}}{3(1+R_e)}} \qquad \textbf{(2-5)}$$

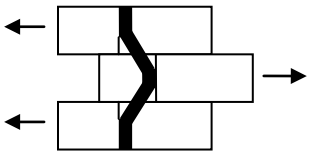

Figure 2-5: Mode IV

Where:

Z_{IV} = Connection Strength (considering one fastener), *lbs*

R_d = Reduction Factor ($3.2\,K_\theta$ for III_s)

The yield-limit equations described above apply to individual dowels in a connection. Connections with more than one fastener, of the same type and of similar size, where each demonstrates the same yield mode, are equal to the strength of the sum of the adjusted values for each fastener. Fasteners in a row are adjusted by a group action factor, C_g, that estimates the load-sharing between bolts in a row, a row being parallel to the direction of the applied load (AF&PA 2005).

2.2.2.2 Fastener Spacing

Figure 2-6 illustrates edge distance, end distance, and spacing between bolts in a row and between bolt rows. The geometry factor, C_{Δ}, is used to adjust the reference lateral design connection strength according to edge distance, end distance, and fastener spacing. C_{Δ} is equal to 1.0 when edge distance, end distance, and spacing are fully utilized and reduced if not. C_{Δ} only applies to dowel-type fasteners of one-quarter inch diameter to one inch diameter (AF&PA 2005).

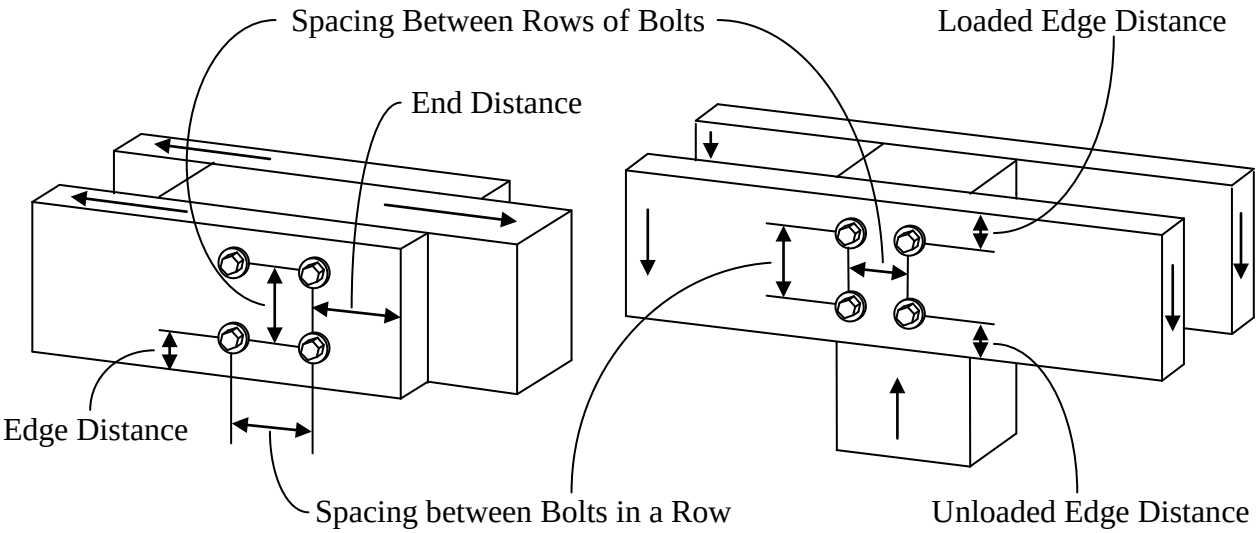

Parallel Connection **Perpendicular Connection**

Figure 2-6 Bolt Spacing Illustration

Edge distance is the distance between the edge of a connection member to the center of the nearest bolt across the grain. Minimum edge distance must be at least one-and-a-half bolt diameters ($1.5D$) for bolt length to diameter (l/D) ratios less than or equal to six and the greater of $1.5D$ or one-half the spacing between rows of bolts for l/D ratios exceeding six for members loaded parallel-to-grain. The l/D ratios correspond to the lesser of bolt length in the main or side member. Loaded and unloaded edge distances are considered in perpendicular connections where some of the members are loaded perpendicular-to-grain. Loaded edge distance is referenced to the edge that the bolt bearing acts toward and requires a spacing of $4D$ or greater. Unloaded edge is referenced to the edge that bolt bearing acts away from and requires a spacing of $1.5D$ or greater. End distance is the distance from the end grain of a member to the center of

the nearest bolt parallel to the loading direction. For a C_Δ value of 1.0, end distance must be at least $4D$ for members loaded perpendicular-to-grain and parallel connections loaded in compression, and at least $7D$ and $5D$ for members loaded in tension parallel-to-grain for softwoods and hardwoods, respectively. Minimum end distances required for a C_Δ of 0.5 are half that for 1.0, any less end distance is prohibited. (AF&PA 2005)

In-row bolt spacing is the center-to-center spacing between bolts that form a line parallel to the loading direction. Minimum in-row bolt spacing parallel-to-grain required for a C_Δ value of 1.0 is $4D$. The absolute minimum spacing requirement is $3D$, for a C_Δ value of 0.75, any less in-row spacing is prohibited. Minimum in-row bolt spacing perpendicular-to-grain is $3D$. Spacing between rows of bolts is the center-to-center spacing between bolts perpendicular to the loading direction. When the load is applied parallel-to-grain, the minimum spacing required is $1.5D$. When the load is applied perpendicular-to-grain, spacing between rows depends on l/D ratios and may not exceed $5D$ (AF&PA 2005).

2.2.2.3 Net-section Tension and Row/ Group Tear-out

Wood failure occurring at closely spaced fasteners may control connection capacity rather than the fastener capacity especially for closely spaced large diameter fasteners such as bolts (AF&PA 2005). Proper edge and end distance spacings help to insure that the strength of a connection is governed by the fastener and surrounding wood rather than shear or tension strength of the associated members which would result in brittle failure modes. Brittle failure modes could include net-section tension, row tear-out, and group tear-out capacity.

Equation 2-6 describes net-section tension as shown in Figure 2-7. The strength regarding net-section tension capacity considers the tensile strength of the member that remains after establishing holes for connection components. Net-section tension capacity is equal to net-section cross-sectional area, which is the total or gross cross-sectional area subtracted by the projected area on the cross-section of holes for fastening, multiplied by the parallel-to-grain tension strength (AF&PA 2005).

$$Z_{NT}' = F_t' A_{net} \quad \textbf{(2-6)}$$

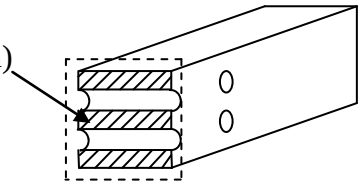

Figure 2-7: Net-section Tension

Where:

Z_{NT}' = Adjusted Tension Capacity of Net-Section Area, *lbs*

F_t' = Adjusted Tension Design Value Parallel-to-grain, *psi*

A_{net} = Net-Section Area, *in^2*

Equation 2-7a describes row tear-out capacity for one row of fasteners while equation 2-7b describes the total connection row tear-out capacity if more than one row of fasteners exist. Figure 2-8 illustrates row tear-out which is regarded as wood material shearing parallel to the grain due to fastener bearing force in members subject to parallel-to-grain tension. Row tear-out strength is equal to half of the adjusted parallel-to-grain shear strength multiplied by member thickness, number of fasteners in a row, two shear lines, and the lesser of minimum in-row fastener spacing or end distance. Half of the adjusted parallel-to-grain strength is used due to the assumption of triangular shear stress distributions on each shear plane. Total row tear-out connection strength is equal to the sum of individual row tear-out strengths (AF&PA 2005).

$$Z_{RTi}' = \frac{F_v' t}{2}\left[n_i s_{critical}\right] \text{ (2 shear lines)} \quad \textbf{(2-7a)}$$

$$Z_{RT}' = \sum_{i=1}^{n_{row}} Z_{RTi}' \quad \textbf{(2-7b)}$$

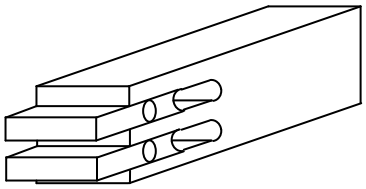

Figure 2-8: Row Tear-out

Where:

Z_{RTi}' = Adjusted Row Tear-Out Capacity of a Row of Fasteners, *lbs*

Z_{RT}' = Total Adjusted Row Tear-Out Capacity of Multiple Rows of Fasteners, *lbs*

F_v' = Adjusted Shear Design Value Parallel-to-grain, *psi*

t = Member Thickness, *in*

n_i = Number of Fasteners in a Row

$s_{critical}$ = Minimum In-Row Spacing (lesser of end spacing or distance between fasteners), *in*

Equation 2-8 describes group tear-out capacity as shown in Figure 2-9. Group tear-out is regarded as wood material surrounding the group of fasteners separating from the rest of the member. Both shear and tension parallel-to-grain strengths of the wood are considered. Group tear-out strength is equal to the shear-plane capacity, $Z_{RT}'/2$, on either side of the fastener group exterior and the net-section tension capacity of the fastener group, $A_{group-net}$, within the exterior bounds of the fastener group. Subscripts in the Z_{RT}' expressions represent the rows of fasteners that form the exterior of the fastener group. For instance, Z_{RT-1}' represents the shear strength along the first row of bolts and Z_{RT-n}' represents the shear strength along the last row of fasteners, where n is equal to the number of fastener rows in a connection (AF&PA 2005).

$$Z_{GT}' = \frac{Z_{RT-1}'}{2} + \frac{Z_{RT-n}'}{2} + F_t' A_{group-net} \qquad \textbf{(2-8)}$$

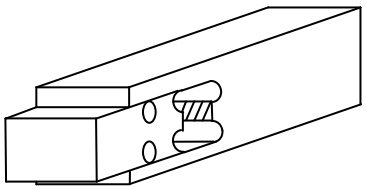

Figure 2-9: Group Tear-out

Where:

Z_{GT}' = Adjusted Group Tear-Out Capacity, *lbs*

Z_{RT-1}' = Adjusted Row Tear-Out Capacity of row 1 of fasteners bounding the fastener group, *lbs*

Z_{RT-n}' = Adjusted Row Tear-Out Capacity of row n of fasteners bounding the fastener group, *lbs*

F_t' = Adjusted Tension Design Value Parallel-to-grain, *psi*

$A_{group-net}$ = Critical Group Net-Section Area between bounding rows, *in^2*

2.2.2.4 Allowable Strength Design (ASD) for Connections and other Wood Properties

Allowable Strength Design (ASD), formally known as Allowable Stress Design, has been used as the main design principle over the past 100 years. The basis of ASD is that a structure's resistance to loads R should be greater than the loads acting on the structure Q, $R > Q$. The margin of safety, known as "safety factor" Ω, is the ratio of nominal strength R_n to nominal service load Q, $\Omega = R_n / Q$. ASD safety factors have been developed based on experience and workmanship. (Salmon et al 2009)

Equations 2-9, 2-10, and 2-11 show the appropriate adjustment factors for obtaining design connection strength considering fasteners, tension parallel-to-grain, and shear parallel-to-grain, respectively. Reference design strength of dowel-type fasteners Z are determined from the minimum value of the yield-limit equations and are further adjusted using adjustment factors C. After all spacing requirements have been satisfied, the fastener strengths are adjusted to obtain the adjusted design strength Z' per fastener. Reference design strengths for tension F_t and shear F_v parallel-to-grain regarding sawn lumber are needed to determine adjusted net-section, row tear-out, and group tear-out connection strengths. Sawn lumber reference design strength is multiplied by adjustment factors to obtain adjusted design values (F_t' and F_v'). The applicable adjustment factors are presented in the equations below. (AF&PA 2005)

$$Z' = Z \times (C_D)(C_M)(C_t)(C_g)(C_\Delta)(C_{eg})(C_{di})(C_{tn}) \quad \textbf{(2-9)}$$

$$F_t' = F_t \times (C_D)(C_M)(C_t)(C_F)(C_i) \quad \textbf{(2-10)}$$

$$F_v' = F_v \times (C_D)(C_M)(C_t)(C_i) \quad \textbf{(2-11)}$$

Where:

Z = Reference Design Strength of a single dowel-type fastener, *lbs*

Z' = Adjusted Design Strength of a single dowel-type fastener, *lbs*

F_t = Reference Tension Parallel-to-grain strength, *psi*

F_t' = Adjusted Tension Parallel-to-grain strength, *psi*

F_v = Reference Shear Parallel-to-grain strength, *psi*

F_v' = Adjusted Shear Parallel-to-grain strength, *psi*

C_D = Load Duration Factor (0.9 for permanent loads, 1.0 for ten-year loads, 1.15 for two-month loads, 1.25 for seven-day loads, and 1.6 for ten minute loads), duration factors greater than 1.6 do not apply to connections

C_M = Wet Service Factor, for connections (1.0 for wood moisture content being less than or equal to 19% at the time of fabrication and in-service, 0.7 for any MC condition at the time of fabrication and greater than 19% in-service); and 1.0 for visually graded timbers regarding F_t' and F_v', at any moisture condition

C_t = Temperature Factor (1.0 for wet and dry wood at a temperature less than 100 degrees Fahrenheit)

C_F = Size Factor (applies to bending strength of beams, stringers, posts, and timbers with a depth exceeding 12 inches and to bending strength and modulus of elasticity of beams and stringers loaded on their wide faces, 1.0 if else); also applies to visually graded dimension lumber

C_i = Incising Factor (applies to incised sawn lumber, 1.0 if else)

C_g = Group Action Factor (applies to a row of more than one fastener that are equal to or less than one inch in diameter, 1.0 for a fastener row with only one fastener)

C_Δ = Geometry Factor (between 1.0 and 0.5, see section 2.2.2.2)

C_{eg} = End Grain Factor (adjustment for fasteners in withdrawal, 1.0 if else)

C_{di} = Diaphragm Factor (1.1 for nails and spikes used in diaphragm construction, 1.0 if else)

C_{tn} = Toe-Nail Factor (used when considering toe-nailed connections, 1.0 if else)

2.2.2.5 Technical Report - 12 (TR-12)

The *General Dowel Equations for Calculating Lateral Connection Values* (AF&PA 1999), also known as TR-12, discusses the calculation of lateral design values using generalized and expanded forms of the 1997 NDS considering single dowel-type fasteners. The TR-12 calculates limit states based on proportional limit load, 5% offset load, and ultimate load. Reduction terms are kept separate from yield mode values to allow for strength calculation at the desired limit state. Reduction terms have not been developed for adjustment of proportional limit or ultimate load to nominal design values, only yield (AF&PA 1999). The TR-12 (AF&PA 1999) document is suitable for use with the 2005 NDS (Finkenbinder 2007).

Input parameters required for the TR-12 general dowel equations include dowel-bearing resistance, dowel moment resistance, dowel bearing length, and gap distance. Gap distance g is the distance between the faces of members comprising a connection and is zero when contact exists. Dowel bearing resistance is the product of dowel diameter and dowel bearing strength. Dowel moment resistance is the product of dowel bending strength and applicable section modulus. Gap distance and dowel moment resistance are not considered in the 1997 or 2005

NDS, the only consideration for moment resistance in the NDS is the fastener bending yield strength, F_{yb}. TR-12 considers both main member dowel moment resistance M_m and side member dowel moment resistance M_s (AF&PA 1999).

Dowel moment and bearing resistance were considered in the yield model used to develop the general dowel equations. Connection strength is assumed to be reached when either the compressive strength of the member beneath the dowel is reached or when the one or more plastic hinges form based on the European Yield Model (EYM). Uniformly distributed dowel loading perpendicular to the dowel axis is assumed and effects of friction, end fixity, and fastener tension forces are ignored. Loading conditions exist on dowels such that they remain in static equilibrium. From static equilibrium, a free body diagram of the fastener can be established and combined with the principles of statics to develop a general dowel equation for that fastener under any loading consideration (AF&PA 1999). A TR-12 derivation is shown in Section 4.1.6.3 but for a fastener similar to Mode III_s as shown in Figure 2-4, fastener rotation was not constrained by the side members.

2.3 Horizontal Shear in Wood Beams

Shear stresses are critical in the design of short, deep beams. Transverse loading in a beam creates vertical shearing forces V and a bending moment couple M. Considering the free body diagram of a finite cube of material in the plane of a beam cross-section, where vertical shear exists from transverse loading, a pair of vertical shear forces V act parallel to the vertical planes of the cube, that are parallel to the beam cross-section, in opposite directions. To maintain static equilibrium, horizontal shear forces ΔH develop on the top and bottom planes of the cube in opposite directions parallel to the beam length which are also influenced by normal forces σdA on the cube, parallel to the beam length, caused by the bending moment couple M. (Beer et al. 2006)

Horizontal shear is created from a bending force differential generated by opposing bending forces from the bending moment couple M and is greatest at the neutral axis where all of the compressive bending forces are on one side while all of the tensile bending forces are on the other generating the largest amount of 'slip' force. The bending force differential in any part

of a beam subject to pure bending is equivalent to zero, because the opposing bending forces are equal, justifying that member sections subject to pure bending do not contain horizontal shear. Any member loaded transversely will contain horizontal shearing stress. Unequal opposing bending forces produce unequal opposing moments which create a moment differential ΔM. Equation 2-12, from Beer et al. (2006), shows the relationship between horizontal shear force and the moment differential.

$$\Delta H = \frac{\Delta M}{I}\int_A ydA \qquad \textbf{(2-12)}$$

Where:

ΔH = Horizontal Shear Force

ΔM = Bending Moment Differential created by unequal opposing bending moments

I = Moment of Inertia of the beam cross-section

$\int_A ydA = Q$ = First Moment of area of a beam cross-section with respect to the neutral axis

Equation 2-13 shows that the bending moment differential is equivalent to the product of the vertical shear force V and a considered finite longitudinal beam length Δx (Beer et al. 2006). Equation 2-14 was developed by combining equation 2-13 and 2-12 and rearranging the expression to show the relationship between shear flow q and vertical shear force (Beer et al. 2006). The shear flow q is known as the horizontal shear force per unit length of beam which is equal to the horizontal shear force ΔH divided by the considered finite longitudinal beam length Δx. Equation 2-15 relates shear flow to the average horizontal shear stress τ_{ave} which is obtained by dividing the shear flow q by the beam width at depth where the horizontal shear is concerned (Beer et al. 2006). Horizontal shear stress τ_{ave} can also be determined by dividing the horizontal shear force ΔH by the area over which it acts, which is the product Δx and beam width t.

$$\Delta M = (dM/dx)\Delta x = (V)\Delta x \qquad \textbf{(2-13)}$$

$$q = \frac{\Delta H}{\Delta x} = \frac{VQ}{I} \qquad \textbf{(2-14)}$$

$$\tau_{ave} = \frac{\Delta H}{\Delta x(t)} = \frac{q}{t} = \frac{VQ}{It} \qquad \textbf{(2-15)}$$

Where:

$(dM/dx) = V$ = Vertical Shear Force (derivative of the bending moment)

Δx = Considered Finite Longitudinal Beam Length

q = Shear Flow (shear force per unit length of beam)

$t =$ Beam Width where horizontal shear is concerned

Shear resistance between fibers in wooden beams is weaker in the longitudinal direction and shearing will occur longitudinally rather than transversely (Beer et al. 2006). Keys in through tenon mortise and tenon joints acting in double shear behave as short deep beams under the transverse loading at the mortise and tenon interface. Horizontal shear splitting of a peg is prevented by full radial confinement in a mortise and tenon joint (Schmidt et al. 1996). Keys are not as confined as pegs and are free to rotate from the mortise sides increasing potential for bending and horizontal shearing.

2.4 Connection Strength Comparison Methods

Understanding connection strength and behavior is critical for design purposes and safety. The safety of a connection depends on its behavior beyond design capacity. To safely design and build connections it is necessary to predict their strength and behavior. Models and equations are used to predict double-shear connection strength and behavior. Comparing model output to experimental connection strength and behavior verifies model accuracy.

Research from Virginia Polytechnic Institute and State University conducted by Smart (2002), Finkenbinder (2007), and Patel (2009) compared experimental test data to models. Each collected experimental test data to compare to mathematical models developed to predict connection behavioral characteristics. Direct comparisons were made between the data and models using calculated divided by tested (C/T) ratios between connection sets of similar variables. Statistical comparisons were made between average C/T ratios of connection sets to determine the effects of the variables using an analysis of variance (ANOVA) with an alpha value (significance level) of 0.05. Safety factors, calculated as capacity divided by allowable strength, were determined for connections. (Patel 2009, Finkenbinder 2007, and Smart 2002)

Smart (2002) conducted 681 laterally loaded single shear connection tests of various residential and commercial products using bolts and nails. His objective was to collect physical test data to quantify safety factors and over-strength of design values in the 1997 NDS (AF&PA 1997) and the *Load and Factor Resistance Design Manual for Engineered Wood Construction* (AF&PA 1996), on the basis of capacity. Smart (2002) observed that the yield theory usually under predicted capacity resistance, with C/T ratios equal-to or less than 1.0, while safety factor and over-strength trends were inversely proportional to C/T ratios. (Smart 2002)

Finkenbinder (2007) conducted 120 double shear single-bolted connection tests using solid-sawn lumber, parallel strand lumber (PSL), and laminated veneer lumber (LVL) with different loaded edge distances and span-to-depth ratios. Finkenbinder (2007) examined perpendicular-to-grain loading of a single loaded bolt with the objectives of quantifying the accuracy of the general dowel equations of the TR-12 (AF&PA 1999) and two fracture mechanics models including Van der Put & Leijten (2000) and Jensen et al. (2003) by comparing them to experimental data. In general, material type and span-to-depth ratios did not have an effect on TR-12 predictions considering C/T ratios and C/T ratios were lower at greater loaded edge distances. Greater loaded edge distances corresponded to higher safety factors using the TR-12 (AF&PA 1999) model. The fracture mechanics models were generally unaffected by span-to-depth ratios and C/T ratios were generally higher for smaller loaded edge distances regarding the Jensen et al. (2003) model. (Finkenbinder 2007)

Patel (2009) conducted 130 perpendicular-to-grain double shear bolted connection tests using LVL from two different manufacturers with one and two bolts per connection fastened in a single row, with different loaded edge distances and bolt diameters. Patel (2009) compared connection resistance to the TR-12, 2005 NDS, Van der Put & Leijten model (2000), Jensen et al. (2003) model, and Eurocode-5 (ENV 2005-1-1, 2004). The Design Safety Factor, calculated as test value divided by 2005 NDS ASD lateral design value, was unaffected by material type and inversely proportional to the number of bolts. The TR-12, Eurocode-5, and fracture models showed that loaded edge distance and connection resistance were directly proportional. The TR-12 model best predicted the single-bolt, $7D$ loaded edge distance configuration and over-predicted the rest. The Van der Put & Leijten (2000) model over-predicted capacity resistance for all test configurations while the Jensen et al. (2003) model only over-predicted capacity

resistance values for configurations with one of the LVL materials. The Eurocode-5 showed a greater design capacity regarding splitting for one of the LVL materials due to its greater width. (Patel 2009)

2.5 Timber Frame Research

Since many early timber frames were built in different forms than ones built today it is unwise to assume that historical practice is always applicable. Designers and builders in historical preservation rebuild and restore historical structures including mills, barns, bridges, and churches while others are designing and building new timber frame structures including homes and public facilities using traditional joinery methods. The NDS does not include the design of traditional joints with wooden fasteners (Schmidt et al. 1996).

2.5.1 Pioneered Timber Frame Research

Brungraber (1985) pioneered timber frame engineering research using two testing programs that were coupled with computer analysis. The first test program included full-sized bents that were subject to gravity and lateral (racking) loads. Linear plane frame analysis was used to analyze the bents and to provide a source of comparison. Axial compression and tension, shear, and moment tests were performed on full-sized joints, coupled with finite element analysis (FEA), to provide spring models for the linear plane frame analysis. Contributions of Brungraber's research included an analysis procedure for the design and construction of timber frame structures and recommendations on analysis method improvements and future research. (Brungraber 1985)

2.5.2 Joint Tension Research

A typical mortise and tenon joint under compression obtains capacity from the bearing of the tenon shoulders against the sides of the mortise member. A mortise and tenon joint subject to shear can obtain great capacity by allowing the entire width of the beam to bear against a housing cut into the receiving member rather than just the bearing surface of the tenon in the mortise. Tension capacity in typical pegged mortise and tenon joints is limited to the double shear strength of round wooden dowels if proper joint detailing is ensured. It is nearly impossible to build a timber frame structure where none of the joints will experience tension

forces. Tension forces develop in post-to-beam joints where rafter thrust exists from opposing rafter pairs, in joints that are adjacent to compression braces resulting from lateral loads, and in the end joints of tension braces (Nehil and Warren 1997 and 1998).

2.5.2.1 Kessel and Augustin

German timber frame research used structural analysis and selection of high quality oak to validate the reconstruction of an eight-story timber frame structure using historical construction techniques. This presented a major engineering task when justifying historic construction techniques with modern building codes. The German standard prohibited the original timber sizes used in the structure based on permissible stresses until higher quality grades of oak timber were selected. Wind loads on the structure were shown to generate significant tensile forces in the posts by analyzing the load carrying behavior of the structure with plane finite element analysis (Kessel et al. 1988).

In the reconstruction efforts of the eight-story timber frame, twelve post-to-sill connections were tested in tension to determine the ability of oak pegs to transfer tensile load between timbers. Peg spacing details were optimized during testing with the goal of reaching all possible failure strengths in a connection simultaneously. Testing showed that the structure could be reconstructed using traditional carpenter-style connections with wooden pegs as intended. (Kessel and Augustin 1995)

Another study by Kessel and Augustin (1996) included testing of pegged mortise and tenon connections to determine allowable tensile strength. Eighty perpendicular and 30 parallel tension connections of oak and spruce were tested. The oak connections were freshly cut and the spruce connections were dry. Each connection was fastened with pegs. Peg diameters included 24mm (15/16"), 32 mm (1-1/4"), and 40mm (1-9/16"). A sample size of five was selected for connections of the same species and detail, making 16 distinct groups among perpendicular connections and six amongst parallel connections. (Kessel and Augustin 1996)

A general positive trend was observed between peg diameter and connection capacity. Typical connection failures for the perpendicular connections included mortise wall splitting, peg failure, and tenon shear failure. Side member shear, or row tear-out failures were observed in parallel connections. Ten additional perpendicular connections of different species were

preloaded to 40% of the anticipated maximum load while green and then loaded to failure after seasoning, no apparent influence of moisture content was observed considering connection load bearing capacity. Design recommendations were based upon connection groups with details that best demonstrated peg, tenon, and mortise failures simultaneously. A design recommendation was developed for connection groups of the same size, species, and details as the minimum of the average value of maximum load divided by 3.0, the average load value at a 1.5mm (<1/16") displacement, and the smallest maximum load divided by 2.25. (Kessel and Augustin 1996)

2.5.2.2 Schmidt and MacKay (1997)

Schmidt and MacKay (1997) used the yield model (EYM) approach to predict the tension strength of pegged mortise and tenon connections. Six connection tests with different peg configurations utilized Douglas-fir dimensional 2x6s, one for the tenon member and two for the mortise member, fastened with two red oak pegs. Separate peg tests included bending, shear, and dowel bearing yield strength with peg diameters of 1.25, 1.0, and 0.75 inches. Pegs were tested in double shear with shear spans a equal to 1/4, 1/2, and 1.0 of peg diameter D. Dowel bearing yield strength included the peg and surrounding base material. Five percent exclusion values were obtained from yield strength test data assuming a normal distribution and with a 75% confidence level. Five percent exclusion represents a value that 95% of the data exceeds. These exclusion values were modified by safety factors to establish design values. (Schmidt and MacKay 1997)

NDS yield model equations were found to apply to pegged mortise and tenon connections, however, with a few additional yield modes. A yield mode similar to Mode IV double shear was observed in the connections. Peg hinge spans were much smaller than steel dowel hinge spans indicating combined bending and shear in the peg cross-section. Tight peg hinge spans prompted a new yield mode, termed Mode V, which was seen in 0.75 inch diameter pegs during testing. (Schmidt and MacKay 1997)

NDS Mode III_s for double shear timber connections using steel dowels considers the formation of two dowel plastic hinges in the main member. Formation of a single plastic hinge in wood pegs in tenons occurred and was termed Mode III_s'. Other failure modes included tenon shear (tenon relish failure) behind the pegs and mortise wall splitting. Mortise splitting

occurred as a result of perpendicular-to-grain tension in the mortise wall accompanied by spreading of the mortise walls due to peg bending. (Schmidt and MacKay 1997)

Specific gravity was the major factor affecting peg bending and shear yield strength with a positive correlation. A negative correlation existed between average peg shear yield strength and diameter, as well shear span. Eastern white pine and recycled Douglas-fir bearing blocks loaded parallel-to-grain with a peg showed peg crushing while bearing blocks of the same species loaded perpendicular-to-grain showed crushing of the bearing blocks. Minimum end distances to prevent tenon relish failure were determined to be at least three peg diameters from the tenon end to the peg center while the minimum edge distance to prevent mortise splitting was determined to be at least four peg diameters from the loaded edge of the mortise to the peg center. Edge distance in this research was conservative due to the fact that only two 2x6s constituted the mortise member. In an actual mortise and tenon joint, the tenon is completely surrounded by mortise member material that will decrease the tendency of mortise splitting at a given edge distance. (Schmidt and MacKay 1997)

2.5.2.3 Schmidt and Daniels (1999)

Schmidt and Daniels (1999) determined design guidelines for pegged mortise and tenon connections concerning strength and detailing. Mortise and tenon joint species included southern yellow pine, recycled Douglas-fir, and red oak. Separate peg tests included bending, shear, and dowel bearing yield strength on 1.0 inch diameter white oak pegs. Pegs were tested in double shear with shear spans a equal to 1/8, 1/4, 1/2, and 1.0 of peg diameter D. A correlation equation was developed to relate joint yield strength to peg shear span. A springs-in-series model was used to predict combined peg and base material bearing strength and behavior. All strength data was analyzed at 5% exclusion values where safety factors could be applied. (Schmidt and Daniels 1999)

Joint test data was divided by recommendations from Kessel and Augustin (1996) to obtain design values representative of ten minute load durations. Safety factors relating Kessel and Augustin's design values to the 5% exclusion values were determined by dividing the 5% exclusion values by Kessel and Augustin's design values. The average safety factor between all joints was 2.0. Combining the safety factor with the NDS (AF&PA 1997) load duration factor of

1.6 to obtain a safety factor relating 5% exclusion values to a ten year design load was equal to 3.2, which corresponds to the calibration factor for the design of conventional connections using the NDS (AF&PA 1997). However, a load duration factor, C_D, for timber frame connections has not been determined. (Schmidt and Daniels 1999)

Joint failures included peg failures, mortise splitting, and tenon splitting. Shear/bending was the dominant peg failure mode. Southern yellow pine joints with 1.25 inch diameter octagonal oak pegs did not reach 5% offset yield, but rather failed due to the development of a single flexural peg hinge within the tenon. A peg bearing failure identified as Mode I_d was discovered from a review of previous research. Joint stiffness was not determined. Specific gravity was the major factor affecting peg bending yield strength with a positive correlation of 0.73. Peg shear yield strength increased with specific gravity. (Schmidt and Daniels 1999)

An equation was developed to associate joint yield loads with peg shear spans for given details and materials. R-squared values between yield stress and peg shear span ratio were 0.70 for average values and 0.88 for 5% exclusion values. Characteristic shear span-to-diameter ratios, for 1.0 inch diameter white oak pegs were 1.14, 0.40, and 0.11 inches in southern yellow pine, recycled Douglas-fir, and red oak, respectively. The high shear span value for southern yellow pine joints is likely from the use of pegs at fiber saturation point. The characteristic shear span-to-diameter ratios were inserted into the 5% exclusion correlation equation to predict the 5% exclusion values of the 5% offset yield joint strength for the three joint species. (Schmidt and Daniels 1999)

Combined bearing strength of base material and pegs was tested under the assumption that each could be tested separately and then mathematically combined in a springs-in-series (spring theory) model. A few combined bearing tests were conducted for verification of the model. The spring theory model yield strength results were an average of 0.4% less than actual test results and the initial stiffness predicted by the spring theory model was always lower than the actual with an average difference of 21.6%. The weaker bearing material dominated the combined bearing strength and the bearing strength of the combined materials could be defined be the weaker material. (Schmidt and Daniels 1999)

A methodology for determining end distance, edge distance, and spacing for pegged mortise and tenon connections known as the equivalent steel bolt theory was presented by Schmidt and MacKay (1997) and investigated by Schmidt and Daniels (1999). This theory involves using conventional distance and spacing requirements for steel bolts that are equivalent in strength to pegs in double shear. The smallest joint capacity from timber frame yield equations was used to determine an equally strong steel bolt in the connection per peg. Proper end distance, edge distance, and spacing were then calculated based on NDS spacing requirements using the largest steel bolt diameter calculated for the particular capacity. End and edge distances regarding the equivalent steel bolt theory were conservative in comparison to recommended values except for spacing. Recommended edge distance, end distance, and spacing respectively for joint detailing was $2D$, $2D$, and $3D$ for southern yellow pine, $2.5D$, $2D$, and $2.5D$ for recycled Douglas-fir, and $2D$, $2D$, and $2.5D$ for red oak joints to ensure peg failure. For example, a pegged southern yellow pine mortise and tenon connection using one inch diameter pegs would require a two-inch edge distance, a two-inch tenon end distance, and a three-inch peg spacing. (Schmidt and Daniels 1999)

2.5.2.4 Miller (2004)

Miller (2004) conducted research to quantify peg shear strength of mortise and tenon joints using full-sized joint tests and finite element modeling. Mortise and tenon joint species were yellow poplar. The primary goal of the research was to establish a design method for tension loaded pegged mortise and tenon joints based on a correlation between allowable shear stress in pegs and specific gravities of wood from physical tests and finite element analysis. The secondary goal was to establish minimum detailing for yellow poplar mortise and tenon joints. (Miller 2004)

Testing included pegged mortise and tenon joints loaded in tension and shear, and dowel bearing tests. Moisture content of the yellow poplar ranged from 20-63% with no attempt of equilibration. Joints tested in tension were successively optimized to determine minimum detailing requirements. Joint failures included mortise splitting, tenon splitting and relish failure, peg bending with one flexural hinge, and peg shear at two interfaces. Combinations of peg bending and shearing occurred in most of the joints with greater recognition of peg bending attributing to the low bearing strength of yellow poplar compared to oak pegs. Joint shear tests

showed that bearing of the tenon inside a mortise is considerably stronger and stiffer than a joint in shear only reliant on pegs for load transfer. (Miller 2004)

A nonlinear finite element model (FEM) was developed to predict the 5% offset yield strength of mortise and tenon joints loaded in tension and shear. The FEM was calibrated to accurately predict test results of known data in order to provide yield load data for joints using materials that were not tested. This aided in developing a numerical correlation between joint yield strength and specific gravity with the goal of decreasing the need for vast amounts of physical testing. (Miller 2004)

Joint test data was fitted with a statistical curve to determine an equation that predicted joint shear yield stress with respect to specific gravity using data from previous research at the University of Wyoming, yellow poplar joint tests, and FEM results. Equation 2-16a resulted from the curve considering the interface yield strength of the four shear planes in a double pegged mortise and tenon joint. The fitted equation presented an R-squared value of 0.803 and was based on red and white oak pegs and various timber base materials and therefore was applicable to peg specific gravities of 0.6 to 0.8 and timber base materials of 0.35 to 0.75. A safety factor of 2.20 for shear yield stress was determined by dividing correlated yield loads by allowable Mode III_s loads. Combining the safety factor to a load duration factor of 1.6 provided equation 2-16b which is the allowable tension shear stress for a ten-year load duration. (Miller 2004)

$$F_{vy} = 4{,}810 G_{PEG}^{0.926} G_{BASE}^{0.778} \quad \textbf{(2-16a)}$$

$$F_{v} = 1{,}365 G_{PEG}^{0.926} G_{BASE}^{0.778} \quad \textbf{(2-16b)}$$

Where:

F_{vy} = Shear Yield Stress, *psi*

F_{v} = Allowable Peg Shear Stress (ten year loading), *psi*

G_{PEG} = Peg Specific Gravity

G_{BASE} = Base Material Specific Gravity

Table 2-1 shows the minimum detailing requirements from Schmidt and Scholl (2000) combined with yellow poplar data from 1.0 inch diameter peg tests based on the short-term

loading of unseasoned joints. A $0.5D$ increase of detailing requirements from Schmidt and Scholl (2000) showed to be appropriate for load duration, seasoning, and drawboring effects. Yellow poplar dowel bearing tests were 3.5 times stiffer and 2.2 times stronger when loaded parallel-to-grain than perpendicular-to-grain. (Miller 2004)

Table 2-1: Pegged Mortise and Tenon Joint Detailing Requirements (Miller 2004)

Detail Requirements	End Distance, D	Edge Distance, D	Spacing, D
Douglas-Fir	2.0	2.5	2.5
Eastern White Pine	4.0	4.0	3.0
Red & White Oak	2.0	2.0	2.5
Southern Yellow Pine	2.0	2.0	3.0
Yellow Poplar	2.5	2.5	3.0

2.5.2.5 Sangree and Schafer (2007)

Sangree and Schafer (2007) conducted research on scarf joints found in covered bridges, particularly Pine Grove Bridge in Pennsylvania. A scarf joint is known as a traditional splice that was constructed by fastening two timbers at their ends to transfer tensile loads. Figure 2-10 shows a typical scarf joint. Scarf joints were previously determined to be the primary cause of decreased structural stiffness of covered wood bridges. Research by Sangree and Schafer (2007) included experimental tests performed on replicated scarf joints coupled with finite element modeling with the intent of providing information to engineers regarding their strength. The key was determined to have the greatest influence on scarf joint behavior because it was loaded perpendicular-to-grain. Research showed that without the aid of a clamping force, the key would roll in its confinement causing the joint to spread transversely introducing axial and bending forces in the joint components. Using bolts to clamp the joint components to eliminate the transverse spreading created a shear parallel-to-grain failure limit state which led to greater ultimate strength. (Sangree and Schafer 2007)

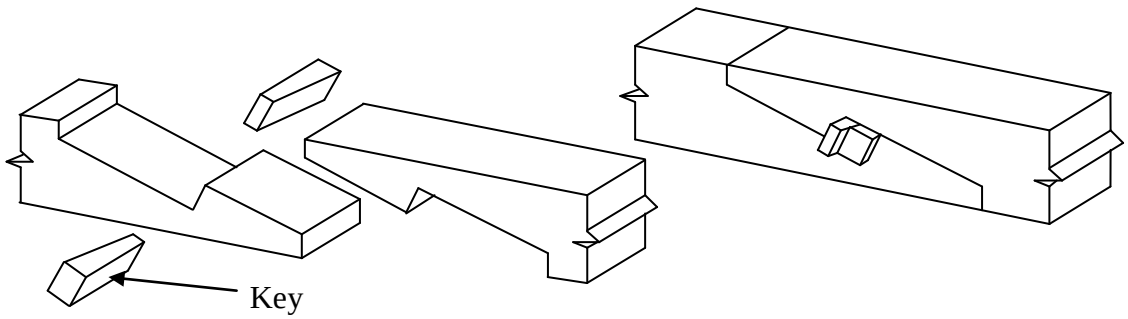

Figure 2-10: Scarf Joint

2.5.3 Lateral Loading Research

Timber frames can be designed a few ways to carry lateral loads including stand-alone timber frames, coupled timber frames and diaphragms, and lean-on timber frames. Stand-alone timber frames are designed such that all of the lateral load is carried by the timber frame. Coupled timber frames and diaphragms are designed such that the timber frame and diaphragm in combination bear the lateral load. Lean-on timber frames rely completely on the diaphragm to carry all of the lateral load (TFEC 1-10). Research by Carradine (2000) and Erikson and Schmidt (2002) concluded that the addition of Structural Insulated Panels (SIPs) as diaphragm elements to timber frames greatly increased their strength and stiffness for carrying lateral loads. Erikson and Schmidt (2002) concluded that bare timber frames are usually strong enough to carry expected design lateral loads, however, are not usually stiff enough and that the global stiffness of bare timber frames is greatly dependant on the stiffness of the individual joints.

2.5.3.1 Carradine (2000)

Carradine (2000) studied timber frame roof systems that used SIPs as diaphragm elements in an effort to develop design and test procedures that considered the strength and stiffness contribution of SIPs under lateral loading. The guidelines for the testing program came from the ASAE standard for wooden post frame buildings with metal wall diaphragms (ASAE EP 484.2, 1999). Strength and stiffness data provided by testing was used to develop a design procedure for timber frame structures with SIPs as lateral load resistant diaphragm elements. At the time of this research, timber frame design neglected the structural contributions of SIPs. Bare timber frames alone were usually well within safety limits considering gravity loads, however, tensile loads often overstressed tenons under lateral loads when diaphragm action was not included as a structural contributor. (Carradine 2000)

Five roof diaphragms of southern pine timbers and 6.5 inch thick SIPs were tested monotonically and cyclically. Three diaphragms were eight feet deep and 24 feet wide and two were 20 feet deep and 24 feet wide. The tests were setup such that each roof assembly was composed of three rafters connected with roof purlins spaced four feet on center. The two outer rafters were secured to the testing surface while the center rafter was pushed or pulled at its end. Timber frame - SIP assemblies demonstrated effective behavior as diaphragms which could be

used to reduce forces in timber frame members subject to wind or seismic loads. Material properties of the screws used to attach the SIPs to the timber frame limited ultimate shear capacity of the test assemblies. Decreasing screw spacing and adding perimeter edge boards to the SIPs increased the cyclical stiffness and strain energy of the roof assemblies. Chord failures did not occur in any of the assemblies which used spline joints secured with four 1.0 inch diameter oak pegs. (Carradine 2000)

2.5.3.2 Erikson and Schmidt (2003)

Erikson and Schmidt (2003) examined sheathed and unsheathed timber frame behavior when subjected to lateral loading. Unsheathed timber frames included one story with one bay (1S1B) with Eastern white pine, Douglas-fir, Port Orford cedar, ponderosa pine, and white oak. As well as two story with two bay timber frames (2S2B) with Eastern white pine, Douglas-fir, Port Orford cedar, and white oak. Sheathed timber frames included a 1S1B Douglas-fir frame, a 1S1B white oak frame, a 2S2B Douglas-fir frame, and a 2S2B Eastern white pine frame. Structural Insulated Panels (SIPs) were used for sheathing. Lateral tests were performed on SIP panel-to-timber connection specimens to determine factors that influence SIP attachment. Modeling of unsheathed timber frames was conducted in a nonlinear computer program to determine joint detailing effects on global frame stiffness. (Erikson and Schmidt 2003)

Lateral tests of the unsheathed white oak timber frames demonstrated more than twice the stiffness of the other frame species for the given number of stories and bays due to having two pegs, instead of one, in each brace joint and a relatively higher joint stiffness. Removal of one of the pegs from the two-pegged brace joints in the unsheathed 2S2B white oak frame still resulted in more stiffness than the other unsheathed 2S2B frames. Post-to-beam connection separations were observed at the top of the unsheathed white oak frames at the leeward post. The unsheathed 2S2B Eastern white pine frame continued to sustain increasing load after some joints failed. However, failure was imminent because the lower beams pulled out of the posts. Removal of brace joint pegs from the unsheathed Eastern white pine 1S1B frame resulted in slightly less frame stiffness due to the compressive brace resisting the full lateral load. Installing a load cell in one of the braces of the Port Orford cedar 1S1B frame showed that the brace sustained a compressive load 75 percent greater than the tensile load, demonstrating that most of a lateral load was carried in compressive braces. All of the unsheathed frames continued to

sustain increasing load beyond design loads and serviceability limits, while the stiffness of each frame was lower than the minimum stiffness required. (Erikson and Schmidt 2003)

Unsheathed timber frames relying on knee braces for lateral load resistance are likely to have adequate strength but not sufficient stiffness. Modeling showed that unsheathed timber frame global stiffness under lateral loads is greatly dependent upon brace joint stiffness more than beam-to-post joint stiffness. Member actions (forces) in the more redundant unsheathed 2S2B timber frames were much more affected by joint stiffness than the 1S1B frames. The addition of SIPs greatly increased lateral timber frame strength and stiffness to levels accepted for serviceability. (Erikson and Schmidt 2003)

2.6 Current Design Practices for Timber Frame Structures

Some timber frame structures built centuries ago are still standing today. Fully relying on traditional timber frame methods to build newer contemporary style timber frame structures with differing site conditions and greater complexity is not appropriate. Timber frame structures are designed like other structures such that once the shape of the structure is determined the loads that act upon it are determined, individual members are sized, structural analysis on global structural behavior is executed, then any revisions to members or connections are performed until results are satisfactory (Nehil and Warren 1997). Design of mortise and tenon joints in tension includes the use of the yield equations in the NDS and the TFEC 1 (Miller 2009a).

2.6.1 TFEC 1-2010

Timber frame engineering has been practiced by a small group of specialized structural engineers and has always been challenging accordingly. The NDS uses design procedures that are useful for sizing timbers and provides design provisions for timber connections using steel fasteners but does not mention timber frame joinery. The Timber Frame Engineering Council (TFEC) is an organization of structural engineers that specialize in timber frame engineering who developed the *Standard for Design of Timber Frame Structures and Commentary* (TFEC 1-07). Much of TFEC document is based on research performed at the University of Wyoming and includes methodologies for evaluating structural capacity of joints with hardwood pegs, and provides guidance for proportioning mortises, tenons, and timber notches. (DeStefano 2008)

The most recent TFEC 1 document, TFEC 1-2010, serves as a supplement to NDS provisions. If contradictory requirements arise between and TFEC 1 and the NDS, the NDS provisions apply. The TFEC 1 contains design provisions including seasoning effects and notching of structural members, mortise and tenon connections loaded in shear and tension, and describes lateral load carrying systems. TFEC 1 connection design provisions include yield limit equations, dowel bearing strength, peg diameter and bending yield strength, seasoning and creep effects, spacing requirements, adjustment factors, tenon size and quality, and mortise placement for pegged mortise and tenon joints loaded in tension. (TFEC 2010)

Yield modes for double shear presented in the TFEC 1 for pegged mortise and tenon connections are similar to the yield modes presented in the NDS (AF&PA 2005) for steel-doweled timber connections with the exception of Mode IV and the addition of Mode V. Mode IV has not been observed in pegged mortise and tenon tension tests and was not included in the TFEC 1. Mode V represents double shear peg failure which has been observed in previous research including Miller (2004), Schmidt and Daniels (1999), and Bulleit et al. (1999), and Schmidt and MacKay (1997) to name a few. The nominal peg strength value Z is calculated using equations 2-13 to 2-16. Nominal design strength Z for a single peg is equal to the minimum value presented by these equations. Connection capacity is equal to the minimum design strength of one peg multiplied by the number of pegs in the connection. (TFEC 2010)

Mode I_m represents bearing crushing in the main member and peg material as shown in Figure 2-11. This occurs when peg bending resistance is sufficient enough to overcome bending while peg and tenon material crushing take place. Equation 2-17 shows the nominal lateral connection strength concerning Mode I_m. The strength of this yield mode is equal to the product of peg diameter D, tenon breadth l_m, and tenon dowel bearing strength parallel-to-grain F_{em}, divided by a reduction factor R_d. R_d is equal to 4.0 when any connection member is oriented parallel-to-grain and 5.0 when perpendicular-to-grain for Mode I_m. (TFEC 2010)

$$Z_{\mathrm{Im}} = \frac{D \times l_m \times F_{em}}{R_d} \qquad \textbf{(2-17)}$$

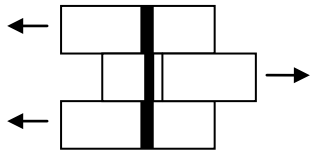

Figure 2-11: Mode I_m

Where:

Z_{Im} = Nominal Design Value (considering one peg), *lbs*

D = Peg Diameter, *in*

l_m = Tenon Breadth, *in*

F_{em} = Tenon Dowel Bearing Strength Parallel-to-grain, *psi*

R_d = Reduction Factor ($4\,K_\theta$ for I_m)

K_θ = Reduction Factor Adjustment according to grain orientation: $1+(\theta/360)$

θ = Maximum Angle of Load to the grain, *degrees* (0, parallel-to-grain $\leq \theta \leq 90$, perpendicular-to-grain) for any member in a connection

Mode I_s represents bearing crushing in the side member and peg material as shown in Figure 2-12. This occurs when peg bending resistance is sufficient enough to overcome bending while peg and mortise wall material crushing take place. Equation 2-18 shows the nominal lateral connection strength concerning Mode I_s. The strength of this yield mode is equal to twice the product of peg diameter D, minimum mortise side wall thickness on one side of tenon l_s, and mortise side wall dowel bearing strength perpendicular-to-grain F_{es}, divided by a reduction factor R_d. R_d is equal to 4.0 when any connection member is oriented parallel-to-grain and 5.0 when perpendicular-to-grain for Mode I_s. (TFEC 2010)

$$Z_{Is} = \frac{2 \times D \times l_s \times F_{es}}{R_d} \qquad \textbf{(2-18)}$$

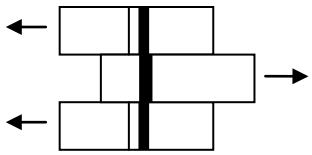

Figure 2-12: Mode I_s

Where:

Z_{Is} = Nominal Design Value (considering one peg), *lbs*

l_s = Minimum Mortise Side Wall Thickness on one side of Tenon, *in*

F_{es} = Mortise Side Wall Dowel Bearing Strength Perpendicular-to-grain, *psi*

R_d = Reduction Factor ($4\,K_\theta$ for I_s)

Mode III_s represents combined flexure of the peg and crushing of the timber material as shown in Figure 2-13. This occurs when peg bending resistance is sufficient enough to overcome flexural failure in the mortise walls but not throughout its length creating a single flexural peg hinge in the tenon and rotation in the mortise walls. Equation 2-19 shows the nominal lateral design value for Mode III_s. R_d is equal to 3.2 when any connection member is oriented parallel-to-grain and 4.0 when perpendicular-to-grain for Mode III_s. (TFEC 2010)

$$Z_{IIIs} = \frac{2 \times D \times l_s \times F_{em}}{(2+R_e)R_d}\left(-1+\sqrt{\frac{2(1+R_e)}{R_e}+\frac{2F_{yb}(2+R_e)D^2}{3F_{em}l_s^2}}\right) \quad \textbf{(2-19)}$$

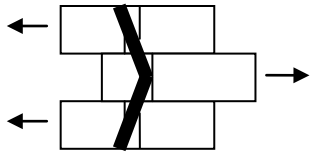

Figure 2-13: Mode III_s

Where:

Z_{IIIs} = Nominal Design Value (considering one peg), *lbs*

$R_e = F_{em} / F_{es}$

F_{yb} = Peg Bending Yield Strength, *psi*

R_d = Reduction Factor ($3.2\,K_\theta$ for III_s)

Mode V represents peg double shear failure as shown in Figure 2-14. This occurs when the dowel bearing resistance in the timber material is sufficient enough to cause peg shear failure at the mortise and tenon interfaces. Equation 2-20 shows the nominal lateral design value for Mode V. R_d is equal to 3.5 when any connection member is oriented parallel-to-grain and 4.375 when perpendicular-to-grain for Mode V. (TFEC 2010)

$$Z_V = \frac{\pi D^2 F_{yv}}{2R_d} \quad \textbf{(2-20)}$$

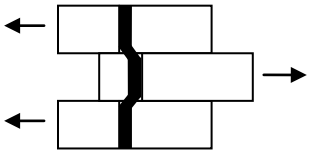

Figure 2-14: Mode V

Where:

Z_V = Nominal Design Value (considering one peg), *lbs*

F_{yv} = Effective Peg Yield Strength, *psi*

R_d = Reduction Factor ($3.5\,K_\theta$ for III_V)

Dowel bearing strength parallel and perpendicular-to-grain consider the combination of peg and timber material crushing. The crushing of a steel dowel against wood is highly negligible. The dowel bearing strengths of pegged connections are presented in equations 2-21a and b. Dowel bearing at an angle to the grain is determined as in the 2005 NDS by use of Hankinson's formula. (TFEC 2010)

Parallel-to-grain:

$$F_{em} = 4{,}770 G_p^{1.32} \qquad \textbf{(2-21a)}$$

Perpendicular-to-grain:

$$F_{es} = 4{,}900 G_p G_t^{0.50} \qquad \textbf{(2-21b)}$$

Where:

F_{em} = Main Member Dowel Bearing Strength, *psi*

F_{es} = Side Member Dowel Bearing Strength, *psi*

G_p = Specific Gravity of Peg Material

G_t = Specific Gravity of Tenon Member

The yield-limit equations described above apply to individual pegs in a connection. The nominal connection design capacity Z, presented by the minimum of the value of equations 2-13 to 2-16, must be multiplied by adjustment factors to obtain the allowable connection design value Z'. The adjustment factors include load duration factor C_D, wet service factor C_M, temperature factor C_t, group action factor C_g, and geometry factor C_Δ. Equation 2-22 shows the application of adjustment factors to nominal design values to obtain the allowable design value. (TFEC 2010)

$$Z' = Z \times \left\lfloor C_D C_M C_t C_g C_\Delta \right\rfloor \qquad \textbf{(2-22)}$$

Where:

Z' = Allowable Connection Design Value, lbs

Z = Nominal Connection Design Capacity, lbs

C_D = Load Duration Factor

C_M = Wet Service Factor

C_t = Temperature Factor

C_g = Group Action Factor

C_Δ = Geometry Factor

Determination of the applicability of various adjustment factors for pegged connections has not been fully satisfied. For instance, research by Schmidt and Scholl (2000) has shown no discernable effect on mortise and tenon joint capacity regarding load duration. Until resolution of its applicability, use of the NDS load duration factor is permitted. Adjustment factors for pegged connections are similar to the ones in the NDS for steel dowel connections with a few exceptions including the wet service factor and geometry factor. The difference in the wet service factor, from the NDS, is that a direct factor is not applied to connections fabricated at a moisture content greater than 19% and less than or equal to 19 % in service. It is thought that the splitting of timbers caused by transverse shrinkage may be eliminated by peg flexibility. (TFEC 2010)

Table 2-2 shows end distances, edge distances, and spacings justified by physical tests that develop full strength of pegged mortise and tenon joints without splitting of the timber. These distances and spacings are defined in figure 2-15 and are the same detailing requirements as in Table 2-1 except for red and white oak end distance which increased one peg diameter. Edge distance is the distance between the edge of a member to the center of the nearest fastener across the grain as well as the loaded edge distance while end distance is the distance from the end of a member to the center of the nearest fastener parallel to the grain. Spacing is the distance between peg centers. End and edge distances for pegged connections to prevent splitting are less than that prescribed in the NDS because the lateral load capacity of a wooden peg is significantly less than a steel dowel of the same diameter. One method for establishing proper end and edge distances in pegged joints is to use NDS spacing requirements for a steel dowel of diameter with the same capacity of a considered wooden peg. Spacing between pegs should conform to the ones prescribed in the NDS with no adjustment for diameter. (TFEC 2010)

Table 2-2 Pegged Joint Detailing Dimensions Based on Physical Tests

Timber Species	End Distance	Edge Distance	Spacing
Douglas Fir	2*D**	2.5*D*	2.5*D*
Eastern White Pine	4*D*	4*D*	3*D*
Red & White Oak	3*D*	2*D*	2.5*D*
Southern Yellow Pine	2*D*	2*D*	3*D*
Yellow Poplar	2.5*D*	2.5*D*	3*D*

**D* = Peg Diameter

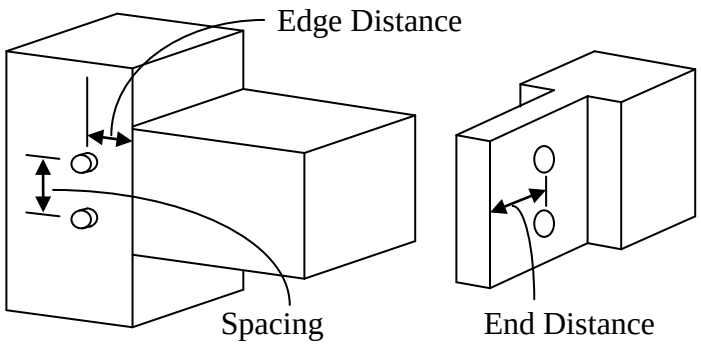

Figure 2-15: Pegged Joint Detailing

2.7 Chronological Summary

Shortly after the timber frame revival a need for structural knowledge of timber frames arose. Brungraber (1985) pioneered timber frame engineering research regarding pegged mortise and tenon joints including full sized joints and bent tests coupled with computer structural analysis (Brungraber 1985). In Germany, an eight story timber frame was reconstructed. Structural analysis validated the use of traditional construction techniques after high quality grades of oak were selected (Kessel et al. 1988). Connection testing further validated the construction of the eight story frame and provided design recommendations (Kessel and Augustin 1995 and 1996). Research by Drewek (1997), O'Bryant (1996), and Weaver (1993) included computer modeling of pegged mortise and tenon joints and frames.

Bearing behavior of pegged mortise and tenon joints was studied by Church and Tew (1997) by observing the bearing behavior of wooden dowels against wooden members. Schmidt and MacKay (1997) investigated strength prediction of pegged mortise and tenon joints using the EYM. Mode *IV* from the NDS was found not to apply to pegged mortise and tenon connections and a new mode known as Mode *V* was discovered which included tight hinge spaces compared to those observed in Mode *IV* with metal fasteners. Schmidt and MacKay

also observed that Mode III_s for pegged mortise and tenon joints included a single peg hinge in the tenon rather than two observed in steel fastener connections (Schmidt and MacKay 1997). Research by Bulleit et al. (1999) investigated the strength and behavior of four types of pegged mortise and tenon connections using primarily white oak and Douglas-fir and discovered the structural benefits of certain details and how certain details should be modeled.

Schmidt and Daniels (1999) developed design guidelines concerning strength and detailing of pegged mortise and tenon joints. Mode V was further investigated and the 'equivalent steel bolt theory' presented by Schmidt and MacKay (1997) was investigated. Schmidt and Daniels (1999) also developed a spring model to predict bearing strengths of different combinations of wood and found that the bearing characteristics of the weaker wood material dominated the bearing characteristics of the combination (Schmidt and Daniels 1999). Sandberg et al. (2000) studied the strength of simplified pegged mortise and tenon joints and developed models to predict the strength and stiffness. Each simplified joint was composed of three wooden blocks and a peg in double shear tested under compression. Sandberg et al. (2000) discovered that the simplified joints were capable of evaluating the strength and stiffness of typical joints in timber framing.

Carradine (2000) studied timber framed roof systems sheathed with SIPs panels as diaphragm elements and discovered that these roof systems behave as effective diaphragm structural elements. Erikson and Schmidt (2003) studied lateral behavior of sheathed and unsheathed timber frame wall systems and concluded that unsheathed knee-braced timber frame wall systems may have adequate strength to carry lateral loads but may not be stiff enough for deflection limitations. Erikson and Schmidt (2003) discovered that timber framed wall systems sheathed with SIPs panels greatly increase the lateral timber frame strength and stiffness to levels accepted for serviceability.

Miller (2004) tested poplar pegged mortise and tenon joints and used finite element modeling to predict the strength of the joints and previous joints tested with the goal of establishing a design method for tension loaded pegged mortise and tenon joints. This design methodology was based on a correlation between allowable shear stress in pegs and the specific gravity of the peg and surrounding base materials. The work by Schmidt and Daniels (1999),

Miller (2004), and Schmidt and Scholl (2000) have greatly contributed to the joint detailing requirements seen in the TFEC standard.

Shanks and Walker (2005) conducted a study on the pull-out (tension), bending, and shear behavior of pegged mortise and tenon joints of green oak. It was found that tension failure of pegged mortise and tenon connections are ductile, peak load resistance of connections in pull-out tests is related to the dry density (SG) of the peg material, and that tenon fit in the mortise greatly influences load carrying capacity of mortise and tenon connections in tension, bending, and shear (Shanks and Walker 2005). Hill et al. (2007) investigated structural performance of five arch-braced green oak sub-frames in the reconstruction efforts of the restoration of Pilton Barn. Sangree and Schafer (2007) investigated tensile properties of keyed scarf joints in covered bridges. Research showed that the key had the greatest influence on joint behavior due to being loaded perpendicular-to-grain. Clamping force from bolts was shown to eliminate transverse bolt spreading under tensile loads increasing joint capacity (Sangree and Schafer 2007).

Currently, some historic timber framed structures are in need of strengthening, repair, or structural evaluation. Traditional joinery methods are still being used to construct residential and commercial buildings (Goldstein 1999). Connections are one of the weakest links in wood construction and when tested in tension are more representative of behavior in service than those tested in compression (ASTM D 5652-95, 2004b). Creating tension joints is among the most difficult aspect in timber construction because it is nearly impossible to cut traditional joinery that is as strong as the timbers that are connected. Cutting tension joinery limits the tensile capacity of the timber to the net-section tension capacity left over from cutting the joinery, this capacity is further reduced by using shear components such as fasteners to connect the members. (Goldstein 1999).

Keyed through tenon joints are able to generate withdrawal resistance due to a long tenon exposed on the back of a mortise member without further weakening the mortise member with peg holes (Goldstein 1999). The only known research pertaining to keys includes studies on bending members including scarf joints and keyed beams. No research on keyed through mortise and tenon joints may be partly due to the fact that there have been classical ways to design such joints using a mechanics approach (Miller 2009b). Performing tensile strength tests on keyed through-tenon joints will validate classical methods that can be used for analysis.

Chapter 3: Through-tenon Key Joint Test Loads and Comparisons

This chapter discusses the test results of through-tenon keyed joints constructed of white oak and Douglas-fir with different tenon lengths and number of keys. The proportional-limit load, 5% offset yield load, ultimate load, and stiffnesses of joint groups were compared to examine the effects of species, tenon length, and number of keys. Much literature uses 'joint strength' to define joint resistance (in pounds), for purposes of this research 'joint load' is used to define joint resistance. This chapter was written as the methods, results and discussion, and conclusions of a paper to be submitted to the *Journal of Materials in Civil Engineering.*

3.1 Methods and Materials

This section describes the methods and materials for joint testing. Joints and other materials were shipped from Dreaming Creek Timber Frame Homes located in Floyd, Virginia and headquartered in Powhatan, Virginia and were constructed of white oak (*Quercus alba*) and Douglas-fir (*Pseudotsuga menziesii*) and fastened with white oak and ipe (*Tabebuia spp.*) keys. The joints were subject to tension by withdrawing the tenon from the mortise with the keys acting in double-shear as the only means of load resistance. Forty-six joints were tested in all, 40 with white oak keys and six retested with ipe keys.

3.1.1 Materials

Figure 3-1 shows the dimensions of the individual joint elements and a typical assembled joint. Each joint consisted of a mortise member and a tenon member fastened with one or two keys. Nominal 6x8s (5.5 inches by 7.5 inches actual) were used for mortise and tenon members of the same species for each joint, either white oak (*Quercus alba*) or Douglas-fir (*Pseudotsuga menziesii*). Mortise members were 24 inches long with a 7.63 inch long by 2.13 inch wide through mortise centered in the wide face (8x dimension). Tenon members with four-inch long tenons protruding beyond the mortise backside were 39.5 inches long, and tenon members with 11-inch long tenons protruding beyond the mortise backside were 46.5 inches long. Tenons were 7.5 inches wide, 2.0 inches thick, and centered in the tenon member cross-section. White oak keys were used for joint fastening, then ipe keys were retested in six selected joints after testing with white oak keys. Tenons were shortened by less than an inch when retested with ipe keys due to retooling of the keyholes. All white oak keys were eight inches long, with a slope

(rise/run) of 1:8, and widths of 1.5 inches for double-keyed joints and 2.0 inches for single-keyed joints. Ipe keys were the same size as the white oak keys, but were one-sixteenth to one-eighth of an inch shallower in depth. The keyholes were centered in the tenon faces for single-keyed joints and symmetric about the tenon face for the double-keyed joints.

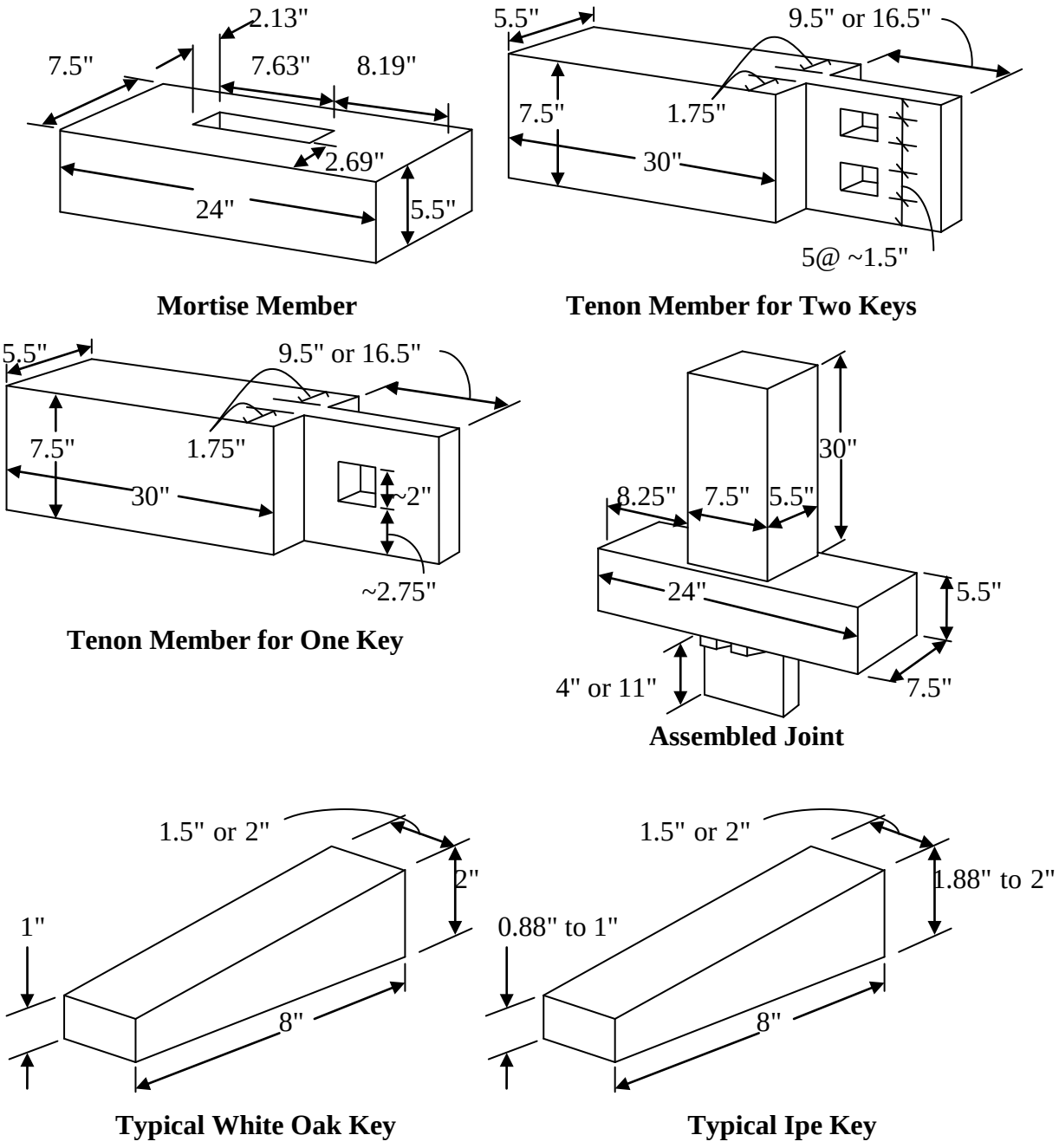

Mortise Member

Tenon Member for Two Keys

Tenon Member for One Key

Assembled Joint

Typical White Oak Key

Typical Ipe Key

Figure 3-1: Keyed Through-tenon Joint and Component Dimensions

The joints were cut on a computer numerical control (CNC) machine then hand-tooled before assembly. All joints were end-grain sealed, identified, and wrapped in plastic prior to arrival then stored until testing. All testing was conducted at the Brooks Forest Products Center at the Virginia Polytechnic Institute and State University.

3.1.2 Joint Testing

Joint testing procedures were adopted from ASTM D 5652-95, *Bolted Connections in Wood and Wood-Based Products* (ASTM 2004b). Keys were used to fastened the joints (connections) with the tenon members loaded in tension parallel-to-grain. Bolt-hole tolerances for bolted connections, prescribed in ASTM D 5652-95 (ASTM 2004b), resulted in approximately a 0.0625 inch clearance between key-keyhole and mortise-tenon interface surfaces to maintain shrinkage tolerance.

Table 3-1 shows the test variables and sample size for joint tests. Three joint factors, each with two levels, produced eight variable combinations. Factors included joint species, tenon length (protruding beyond mortise backside), and the number of keys in a joint. Five repetitions of the eight joint variable combinations were tested for a total of forty tests, creating 20 white oak and 20 Douglas-fir joints. A sample size of five joints per test variable combination was chosen based upon previous research by Kessel and Augustin (1996) who used the same sample size for testing pegged mortise and tenon joints. Additionally, ipe key stock was provided for retesting of six joints which were chosen based on undamaged mortise and tenon members from initial testing with white oak keys (see Table 3-1).

Table 3-1: Joint Test Schedule

Joint Species (Mortise and Tenon)	Tenon Length (inches)	Keys per Joint	Number of Specimens
White Oak	4	1	5
		2	5
	11	1	5
		2	5
Douglas-fir	4	1	5
		2	5
	11	1	5
		2	5
White Oak (retested with Ipe Keys)	11	1	3
		2	1
Douglas-fir (retested with Ipe Keys)	11	1	1
		2	1
Total			**46**

Joint Identification

Joints were identified by species, tenon length, number of keys, and then by consecutive numbering per group. Mortise and tenon members were identified as "WO" for white oak and "DF" for Douglas-fir. Tenon length was identified as "4" for four-inch tenons and "11" for eleven-inch tenons. The number of keys in a joint was identified as "1" for single-key joints and "2" for double-keyed joints. For instance, WO-11-2-3 was the third joint specimen in a group of five white oak mortise and tenon joints with 11 inch tenons fastened with two keys.

3.1.2.1 Joint Test Set-up

Figure 3-2 is a photograph showing a joint test specimen and the testing fixture with applied loading indicated by the vertical arrows. The mortise member was supported by blocks allowing adequate space for the tenon. Steel tubes (hold-downs) were placed on top of the mortise member ends to transfer force to the connecting components. The hold-downs were pre-drilled for bolts extending to the testing base. Proper alignment of the cross-head fixture to the tenon member was ensured before the hold-downs were clamped. Once the cross-head was

attached to the tenon member, the hold-downs were lightly tightened against the mortise member. This method ensured proper alignment of the joint and load direction.

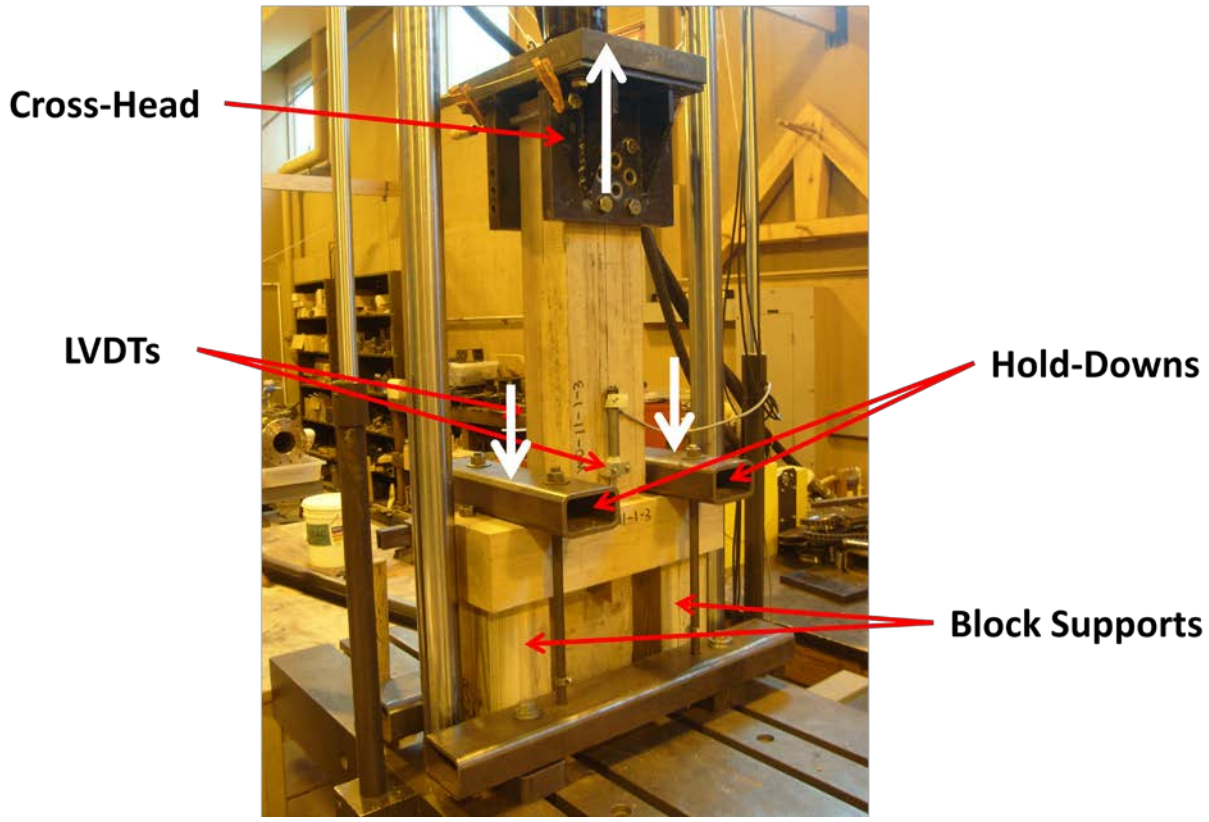

Figure 3-2: Joint Testing Setup

Joints were tested on an MTS Servo-Hydraulic Test Machine with a load cell with a range of 50 kips and an error less than 1% of the load. Two linear variable differential transducers (LVDTs), with a range of two inches and sensitivity of 0.001 inches, were attached at opposite sides of the joint to measure the tenon member slip relative to the mortise member. Joint slip was taken as the average of the LVDT readings. Load-deformation data measured by the load cell and LVDTs was processed through MTS FlexTest 40 data acquisition software to generate load-deformation curves. Initial joint stiffness, proportional-limit load, 5% offset yield load, and ultimate load were recorded from the curves.

3.1.2.2 Joint Testing Procedure

Joint testing was randomized to avoid bias. Once a joint was selected for testing, it was unwrapped, placed in the machine, and then bolt holes were drilled for the cross-head attachment. Moisture content (MC) of white oak joint members was approximately 60%, while Douglas-fir was typically less than 20%. Once the joint assembly was aligned and secured, the keys were tightened with the light tap of a 16 ounce hammer. Testing concluded when the load dropped at least 20% of the ultimate load with no sign of recovery or when wedging action of the keys occurred at the shear planes. Expected time to reach the maximum load was approximately ten minutes, ranging from five to 20 minutes based on ASTM D 5652-95 (ASTM 2004b). Maximum load for the joints with 11-inch tenons was obtained between five and 20 minutes, except for two Douglas-fir joints with 11-inch tenons with one key that displayed brittle failures. Joints with four-inch tenons obtained maximum load in less than five minutes due to brittle failures, except for one white oak joint with a four-inch tenon with one key and two white oak joints with two keys. All joints retested with ipe keys failed within the five to 20 minute time range. Joints within and out of the time range were treated identically for analysis. The displacement rate was initially 0.02 inches per minute and then increased to 0.03 inches per minute after the third joint, in an attempt to achieve the time range, which was used to accommodate the majority of the joints.

Proportional-limit load, 5% offset yield load, ultimate load, and stiffness were found as shown in figure 3-3. Proportional-limit load was found by scaling all curves and selecting the initial longest and straightest portion of each curve by eye. A set of parallel lines were drawn on either side of the selected curve portion and the first deviation from the lines was taken as the proportional-limit. This visual analysis was performed separately by two researchers. Five percent offset yield load was found by offsetting a line, parallel to the initial linear portion of the load-deformation curve, 5% of the key width, and then finding the point of intersection with the load-deformation curve. If the 5% offset line intersected the load curve after ultimate load or not at all, the joint was not considered to have a 5% offset yield load. Ultimate load was the maximum load prior to a post-failure event, such as key wedging. Stiffness was the slope of initial linear portion of the load-deformation curve.

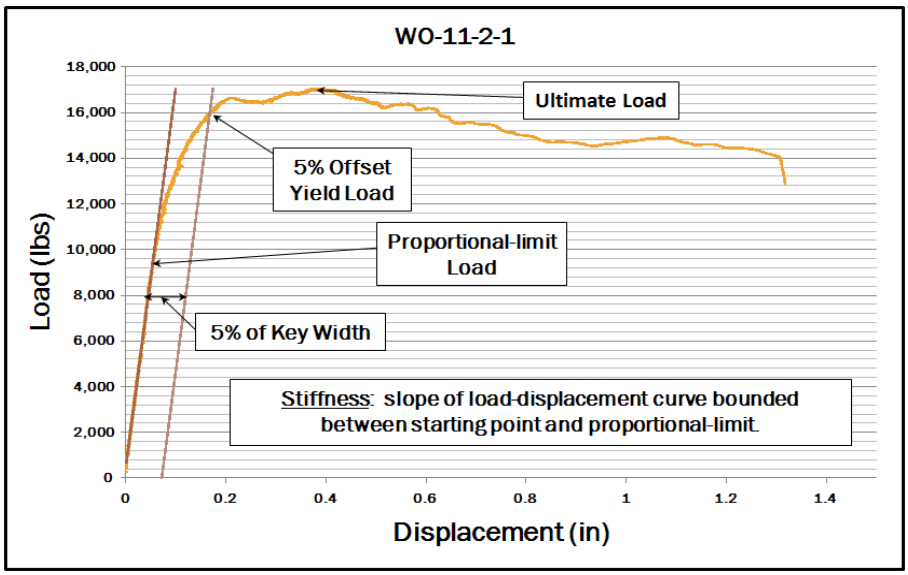

Figure 3-3: Joint Load-Deformation Curve

Joints retested with ipe keys were disassembled, after being tested with white oak keys, before being tested with ipe keys. The bearing surfaces of the tenon keyholes were re-cut and re-sloped while the mortise members were turned over on the tenon to provide fresh bearing surfaces for the ipe keys. The joints were then reassembled with the ipe keys and tested again using the same procedures described above. Ipe keys were rough cut to the dimensions of the finished white oak keys and then surface sanded for flat surfaces. Sanding the ipe keys after being rough cut to the dimensions of the white oak keys decreased the depth by one-sixteenth to one-eighth of an inch from the depth of the finished white oak keys.

After joint testing, one moisture content and specific gravity (MC/SG) sample per tenon, key, and mortise was cut, weighed, and placed in a drying oven. ASTM D4442, *Direct Moisture Content Measurement of Wood and Wood-Base Materials* (ASTM 2004c) method A, oven-drying, was used to determine the moisture content (MC) of the joint members and keys. ASTM D 2395, *Specific Gravity of Wood and Wood-Based Materials* (ASTM 2004d) oven-dry basis displacement method, was used to determine specific gravity (SG) of joint members and keys.

3.2 Results and Discussion

This section presents joint testing results including load and stiffness and the effects of joint factors (joint species, tenon length, and number of keys) on joint load and stiffness. Joint group coefficient of variation (COV) was determined by dividing standard deviations by associated averages and were presented as percentages. The three joint factors included species (white oak or Douglas-fir), protruding tenon length (4" or 11"), and number of keys (one or two). Joint testing results are presented in section 3.2.1. The effects of joint factors on load and stiffness are presented in section 3.2.2. Effects of key specific gravity on joint load and stiffness are presented in section 3.2.3 for joints with key failures.

3.2.1 Joint Testing Results

Joint test results present data from testing including load and stiffness, failure modes and behaviors, and moisture content (MC) and specific gravity (SG) of the joint components. Joint load and stiffness results with white oak keys are presented in section 3.2.1.1 and results of joints with ipe keys are presented in section 3.2.1.2. Joint failure modes are presented in section 3.2.1.3 and joint behaviors are presented in section 3.2.1.4. Joint component MC and SG is presented in section 3.2.1.5. 'Joint load' is used to define joint resistance in terms of force (lbs).

3.2.1.1 Load and Stiffness of Joints with White Oak Keys

Proportional-Limit Load

Table 3-2 shows the average proportional-limit load for joints with white oak keys along with coefficient of variation (COV) values and percent differences of average load regarding species, tenon length, and number of keys. The average proportional-limit load ranged from 2,300 lbs to 6,200 lbs. The COV values ranged from 8.1% to 30.0%. Douglas-fir joints consistently produced greater COVs than white oak joints between joints groups with similar details. COVs from greatest to least, concerning proportional-limit load, were 11-inch tenons with two keys, four-inch tenons with one key, 11-inch tenons with one key, and four-inch tenons with two keys for white oak and Douglas-fir joints.

Table 3-2: Proportional-Limit Load of Joints with White Oak Keys

Species	Tenon Length	Number of Keys	Average Proportional Limit Load, lbs (COV,%)	% Differences		
				Species [1]	Tenon Length [2]	Number of Keys [3]
WO	4	1	2,300 (21.1)	-----	-----	-----
		2	5,820 (8.1)	-----	-----	153
	11	1	2,960 (11.6)	-----	29	-----
		2	6,200 (26.2)	-----	6.5	109
DF	4	1	2,670 (25.3)	16	-----	-----
		2	4,740 (16.9)	-19	-----	78
	11	1	3,440 (20.6)	16	29	-----
		2	6,020 (30.0)	-2.9	27	75

[1] (Douglas-fir - White Oak)/White Oak x 100% (between same tenon length and number of keys)
[2] (11" Tenon - 4" Tenon)/4" Tenon x 100% (between same species and number of keys)
[3] (2 Keys - 1 Key)/1 Key x 100% (between same species and tenon length)

The least difference in proportional-limit load existed between white oak and Douglas-fir joints with similar tenon length and number of keys where the species with the greatest proportional-limit load could be not distinguished. Douglas-fir joints with one key had 16% greater proportional-limit load than white oak joints with one key considering both four- and 11-inch tenons. Douglas-fir joints had average proportional-limit load 19% less than white oak joints with four-inch tenons with two keys and 2.9% less than the white oak joints with 11-inch tenons with two keys.

Average proportional-limit load was consistently greater for joints with 11-inch tenons than with four-inch tenons which was 29% greater for white oak joints with one key, 6.5% greater for white oak joints with two keys, 29% greater for Douglas-fir joints with one key, and 27% greater for Douglas-fir joints with two keys. The small difference of average proportional-limit load between white oak joints with four- and 11-inch tenons with two keys (6.5%) indicated that the four-inch white oak tenons with two keys may be close to the balanced tenon length and key size that would cause simultaneous tenon and key failure for the species used.

The number of keys produced the greatest difference in proportional-limit load of joint groups which was consistently greater for joints with two keys. White oak joints with four-inch tenons with two keys had approximately 2.5 times the average proportional-limit load than with

one key. White oak joints with 11-inch tenons with two keys had over twice the average proportional-limit load than one key. Douglas-fir joints with two keys were approximately 75% greater in average proportional-limit load than with one key, per tenon length.

5% Offset Yield Load

Twenty one joints did not produce a 5% offset yield load value due to brittle behavior. Figure 3-4 shows the load-deformation curve of a Douglas-fir with a four-inch tenon with two keys where the 5% offset line did not contact the load-deformation curve. ASTM D 5652-95 (ASTM 2004b) recommends using the maximum (ultimate) load for the 5% offset yield load if the 5% offset line does not intersect with the load-deformation curve. Joints where the 5% offset yield load values did not intersect the load curve, as shown in Figure 3-4, or intersected the load curve after ultimate load was obtained were not considered to have a 5% offset yield load. The 5% offset yield load of these joints were listed as 'N/A' (Not Applicable) for the purposes of this research.

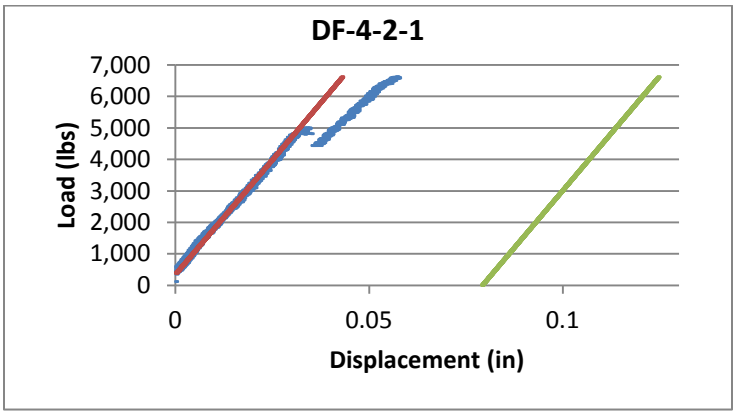

Figure 3-4: Joint load curve without a 5% offset yield load due to brittle behavior

There were only three groups of joints where each joint, in the group, produced a 5% offset yield load value - white oak joints with 11-inch tenons with one and two keys, and Douglas-fir joints with 11-inch tenons with two keys. These joint groups obtained 5% offset yield load due to keys failures. One white oak joint with a four-inch tenon with two keys produced failure in one key accompanied by tenon failure where the 5% offset yield line intersected the load deflection curve directly after ultimate load. Only two of five white oak joints with four-inch tenons with two keys and two of five Douglas-fir joints with 11-inch tenons with one key produced 5% offset yield loads with accompanying key failures.

Table 3-3 shows the 5% offset yield load values of joints with white oak keys. Average 5% offset yield loads ranged from 6,480 lbs to 13,900 lbs. The average 5% offset yield load was similar between white oak and Douglas-fir joints with 11-inch tenons with two keys, and between white oak and Douglas-fir joints with 11-inch tenons with one key. White oak joints with 11-inch tenons with two keys had approximately twice the 5% offset yield load of the white oak joints with 11-inch tenons with one key, which was also true for Douglas-fir joints with 11-inch tenons. No 5% offset yield load values were obtained for Douglas-fir joints with four-inch tenons. COV values ranged from 8.5% to 12.3% for joint groups, where every joint produced 5% offset yield load.

Table 3-3: 5% Offset Yield Load of Joints with White Oak Keys

Species	Tenon Length	Number of Keys	Average 5% Offset Yield Load, lbs (COV,%)	% Differences		
				Species [1]	Tenon Length [2]	Number of Keys [3]
WO	4	1	N/A	-----	-----	-----
		2 [4]	12,500 (4.9)	-----	-----	N/A
	11	1	6,480 (8.5)	-----	N/A	-----
		2	13,300 (12.0)	-----	6.4	105
DF	4	1	N/A	N/A	-----	-----
		2	N/A	N/A	-----	N/A
	11	1 [4]	6,780 (1.6)	4.5	N/A	-----
		2	13,900 (12.3)	4.8	N/A	105

[1] (Douglas-fir - White Oak)/White Oak x 100% (between same tenon length and number of keys)
[2] (11" Tenon - 4" Tenon)/4" Tenon x 100% (between same species and number of keys)
[3] (2 Keys - 1 Key)/1 Key x 100% (between same species and tenon length)
[4] Only two of Five Joints Produced 5% Offset Yield Load

Ultimate Load

Table 3-4 shows the average ultimate load for joints with white oak keys including COV values and percent differences with respect to species, tenon length, and number of keys. The average ultimate load ranged from 3,340 lbs to 15,600 lbs. Two white oak joints with 11-inch tenons with two keys (WO-11-2-2 and WO-11-2-3) experienced key wedging which was considered a post-failure event. A deformation of 0.35 inches was established, to eliminate the selection key wedging for ultimate load of these joints, based on similar deflection at ultimate

load within the same joint group since distinguishing between ultimate load and key wedging was difficult between the two joints. The COV values ranged from 6.4% to 29.7%. Joints with four-inch tenons produced greater COV values (13.6 to 29.7%) than joints with 11-inch tenons (6.4 to 10.1%) for each joint species indicating that joints with key failures produce more consistent ultimate load values than joints with tenon failures.

Table 3-4: Ultimate Load of Joints with White Oak Keys

Species	Tenon Length	Number of Keys	Average Ultimate Joint Load, lbs (COV,%)	% Differences		
				Species [1]	Tenon Length [2]	Number of Keys [3]
WO	4	1	4,700 (22.4)	-----	-----	-----
		2	12,100 (13.6)	-----	-----	158
	11	1	7,810 (10.1)	-----	66	-----
		2	15,400 (6.4)	-----	27	97
DF	4	1	3,340 (27.4)	-29	-----	-----
		2	7,370 (29.7)	-39	-----	121
	11	1	7,160 (8.9)	-8.3	115	-----
		2	15,600 (8.0)	1.8	112	118

[1] (Douglas-fir - White Oak)/White Oak x 100% (between same tenon length and number of keys)
[2] (11" Tenon - 4" Tenon)/4" Tenon x 100% (between same species and number of keys)
[3] (2 Keys - 1 Key)/1 Key x 100% (between same species and tenon length)

Comparisons of average ultimate joint load between joint species, with similar tenon length and number of keys, showed white oak joints with greater ultimate load than Douglas-fir joints, other than joints with 11-inch tenons with two keys where Douglas-fir joints had 1.8% greater average ultimate load than white oak joints. Douglas-fir joints with four-inch tenons with one key had 29% less average ultimate load than white oak joints. Douglas-fir joints with four-inch tenons with two keys had 39% less average ultimate load than white oak joints. Douglas-fir joints with 11-inch tenons with one key had 8.3% less average ultimate load than white oak joints. The greatest differences between white oak and Douglas-fir joints occurred in joints with four-inch tenons indicating that the ultimate load of joints with tenon failures are more dependent on joint member species than joints with key failures.

Joints with 11-inch tenons produced greater average ultimate load than joints with four-inch tenons. White oak joints with 11-inch tenons were 66 and 27% greater in average ultimate

load than white oak joints with four-inch tenons, for joints with one and two keys respectively. Douglas-fir joints with 11-inch tenons produced more than twice the average ultimate load than Douglas-fir joints with four-inch tenons, for joints with one and two keys. The smaller difference of average ultimate load between white oak joints with four- and 11-inch tenons with two keys indicated that four-inch white oak tenons with two keys were close to the balanced tenon length and key size that would cause simultaneous tenon and key failure for the species used.

The greatest differences in average ultimate load were between joints with one and two keys per species and tenon length. The least difference in average ultimate joint load, regarding the number of keys, was between the white oak joints with 11-inch tenons where the joints with two keys produced an average ultimate load nearly twice that of joints with one key. The greatest difference in average ultimate joint load, regarding the number of keys, was among the white oak joints with four-inch tenons where the joints with two keys produced an average ultimate load 158% greater than with one key. Douglas-fir joints with two keys produced over twice the average ultimate load than Douglas-fir joints with one key, for both four- and 11-inch tenons. Greater average ultimate load for joints with four-inch tenons with two keys than with one key was likely due to the double number of tenon shear planes. Greater average ultimate load for joints with 11-inch tenons with two keys than with one was likely due to greater total key width which provided more key bending, bearing, and shear resistance.

Stiffness

Table 3-5 shows the average stiffness for joints with white oak keys along with COV values and percent differences regarding species, tenon length, and number of keys. Average stiffness values ranged from 76,100 lbs/in to 191,000 lbs/in, and COVs ranged from 7.5% to 28.5%. COVs were similar between species. Joint groups with four-inch tenons with one key produced the largest COVs for both white oak and Douglas-fir. The COVs for white oak and Douglas-fir joints with four-inch tenons with one key were more than twice that of any other joint groups indicating that joints with tenon failures produced the largest stiffness variation.

Table 3-5: Stiffness of Joints with White Oak Keys

Species	Tenon Length	Number of Keys	Average Ultimate Joint Load, lbs/in (COV,%)	% Differences		
				Species [1]	Tenon Length [2]	Number of Keys [3]
WO	4	1	76,100 (27.0)	-----	-----	-----
		2	163,000 (13.1)	-----	-----	115
	11	1	99,200 (11.6)	-----	30	-----
		2	191,000 (7.5)	-----	17	92
DF	4	1	77,900 (28.5)	2.4	-----	-----
		2	127,000 (10.9)	-22	-----	63
	11	1	81,000 (11.4)	-18	3.9	-----
		2	165,000 (13.5)	-14	30	103

[1] (Douglas-fir - White Oak)/White Oak x 100% (between same tenon length and number of keys)
[2] (11" Tenon - 4" Tenon)/4" Tenon x 100% (between same species and number of keys)
[3] (2 Keys - 1 Key)/1 Key x 100% (between same species and tenon length)

White oak joints had greater average stiffness values than Douglas-fir joints, however, Douglas-fir joints with four-inch tenons with one key were 2.4% greater in average stiffness than the white oak joints. The average stiffness of Douglas-fir joints were 22 and 18% less than white oak joints for four-inch tenons with two keys and 11-inch tenons with one key, respectively. Average stiffness of Douglas-fir joints with 11-inch tenons with two keys were 14% less than white oak joints with the same details. Lower average stiffness of Douglas-fir joints may be due to lower perpendicular-to-grain bearing strength observed for Douglas-fir mortise members. Joints with four-inch tenons with one key typically produced tenon relish failure before stresses were great enough to produce perpendicular-to-grain crushing of the mortise members at the keys, which may explain the similarity between the average stiffness of white oak and Douglas-fir joints with four-inch tenons with one key.

Joints with 11-inch tenons had greater average stiffness values than joints with 4-inch tenons. White oak joints with 11-inch tenons with one key were 30% greater in average stiffness than with four-inch tenons with one key, while white oak joints with 11-inch with two keys were 17% greater than with four-inch tenons with two keys. Douglas-fir joints with 11-inch tenons with one key were 3.9% greater in average stiffness than with four-inch tenons with one key,

while Douglas-fir joints with 11-inch with two keys were 30% greater than with four-inch tenons with two keys.

Joints with two keys were consistently greater in average stiffness than joints with one key which produced greater differences than between species or tenon length. White oak joints with four-inch tenons with two keys were 115% greater in average stiffness than with one key, while white oak joints with 11-inch tenons with two keys were 92% greater than with one key. Douglas-fir joints with four-inch tenons with two keys were 63% greater in average stiffness than with one key, while Douglas-fir joints with 11-inch tenons with two keys were 103% greater than with one key.

3.2.1.2 Load and Stiffness of Joints with Ipe Keys

This section discusses the test results of joints retested with ipe keys and comparisons to the same joints originally tested with white oak keys. A total of six joints were retested with ipe keys including three white oak joints with 11-inch tenons with one key (WO-11-1-2,3, and 4), one white oak joint with an 11-inch tenon with two keys (WO-11-2-2), one Douglas-fir joint with an 11-inch tenon with one with one key (DF-11-1-4), and one Douglas-fir joint with an 11-inch tenon with two keys (DF-11-2-2). Joints with 11-inch tenons were selected due to the prevalence of key failures with minimal damage to the tenons. Joints with ipe keys had greater load and generally greater stiffness responses than the same joints tested with white oak keys due to the greater specific gravity (SG) of the ipe keys compared to the white oak keys, resulting in higher key bending and bearing strength. DF-11-2-2 was retested with ipe keys on the same bearing surface of the mortise member that was originally tested with white oak keys, leaving pre-crushed bearing surfaces for the ipe keys, which had a decreasing effect on stiffness. WO-11-1-4 and DF-11-1-4 experienced tenon failures. Full-width splintering occurred on the tension side of the ipe key in WO-11-1-4, that indicated the start of a key bending failure.

Proportional-limit Load

Table 3-6 shows the proportional-limit load of joints retested with ipe keys and the percent differences between the identical joints previously tested with white oak keys. Proportional-limit load for joints retested with ipe keys ranged from 5,100 lbs to 9,300 lbs. Joints retested with ipe keys consistently produced greater proportional-limit load than when

originally tested with white oak keys. The average proportional-limit load of white oak joints with 11-inch tenons retested with one ipe key was twice as great as when originally tested with white oak keys. Proportional-limit load of WO-11-2-2 was 63% greater retested with ipe keys than when originally tested with white oak keys. Proportional-limit load of DF-11-1-4 was 89% greater retested with an ipe key than when originally tested with a white oak key. Proportional-limit load of DF-11-2-2 was 84% greater retested with ipe keys than when originally tested with white oak keys. A difference in the proportional-limit load between joint species did not appear to exist. The number of keys caused a difference in load, where joints with two ipe keys had greater proportional-limit load than joints with one ipe key. The difference in proportional-limit load between joints retested with ipe keys and white oak keys was greatest for joints with one key, however, less different for DF-11-1-4 which had a tenon relish failure. The percent difference in proportional-limit load being greater for joints with one key indicated a direct relationship between joint load and key SG, since white oak keys in joints with two keys had a greater SG than with one key (see Section 3.2.1.5). Correlations between joint load and key SG, for joints with key failures, were performed in Section 3.2.3 where positive correlations of proportional-limit load and key SG produced r-squared values of 0.809 and 0.475 for the keys in white oak and Douglas-fir joints, respectively.

Table 3-6: Proportional-limit Load of Joints with Ipe Keys

Joint Group	Average Proportional-limit Load (COV, %) of Joints retested with Ipe Keys, lbs	% Difference Compared to white oak keyed joints [1]
WO-11-1	6,000 (12.0) - [5,200 6,600 6,200] [2]	100
WO-11-2-2	9,300 (N/A - one joint)	63
DF-11-1-4	5,100 (N/A - one joint)	89
DF-11-2-2	9,200 (N/A - one joint)	84

[1] (Ipe Keyed Joint - White Oak Keyed Joint)/White Oak Keyed Joint x 100%

[2] Individual Values of WO-11-1-2,3, and 4 respectively

5% Offset Yield Load

Table 3-7 shows the 5% offset yield load of joints retested with ipe keys and the percent differences between joints previously tested with white oak keys. Five percent offset yield load for joints retested with ipe keys ranged from 12,400 lbs to 19,700 lbs. Joints retested with ipe keys consistently produced greater 5% offset yield load than when originally tested with white

oak keys. The average 5% offset yield load of white oak joints with 11-inch tenons retested with one ipe key was 130% greater than when originally tested with white oak keys. Five percent offset yield load values of WO-11-2-2 and DF-11-2-2 retested with ipe keys were 51 and 41% greater, respectively, than when tested with white oak keys. DF-11-1-4 retested with one ipe key had 85% greater 5% offset yield load than when tested with one white oak key. A difference in the 5% offset yield load between joint species did not appear to exist. The number of keys caused a difference in load, where joints with two ipe keys had greater 5% offset yield load than joints with one ipe key. The difference in 5% offset yield load between joints retested with ipe keys and white oak keys was greatest for joints with one key, however, less different for the DF-11-1-4 which had a tenon relish failure, however still produced a 5% offset yield load. The percent difference in 5% offset yield load being greater for joints with one key indicated a direct relationship between joint load and key SG, since white oak keys in joints with two keys had a greater SG than with one key (see Section 3.2.1.5). Correlations between joint load and key SG, for joints with key failures, were performed in Section 3.2.3 where positive correlations of 5% offset yield load and key SG produced r-squared values of 0.951 and 0.976 for the keys in white oak and Douglas-fir joints, respectively.

Table 3-7: 5% Offset Yield Load of Joints with Ipe Keys

Joint Group	Average 5% Offset Yield Load (COV, %) of Joints retested with Ipe Keys, lbs	% Difference Compared to white oak keyed joints [1]
WO-11-1	14,900 (2.7) - [14,900 14,600 15,400] [2]	130
WO-11-2-2	19,600 (N/A - one joint)	51
DF-11-1-4	12,400 (N/A - one joint)	85
DF-11-2-2	19,700 (N/A - one joint)	41

[1] (Ipe Keyed Joint - White Oak Keyed Joint)/White Oak Keyed Joint x 100%

[2] Individual Values of WO-11-1-2,3, and 4 respectively

Ultimate Load

Table 3-8 shows the ultimate load of joints retested with ipe keys and the percent differences between joints previously tested with white oak keys. Ultimate load for joints retested with ipe keys ranged from 12,500 lbs to 21,100 lbs. Joints retested with ipe keys consistently produced greater ultimate load than when originally tested with white oak keys. The average ultimate load of white oak joints with 11-inch tenons retested with one ipe key was 92%

greater than when originally tested with white oak keys. Ultimate load of WO-11-2-2 and DF-11-2-2 retested with ipe keys were 41 and 29% greater, respectively, than when tested with white oak keys. DF-11-1-4 retested with one ipe key was 73% greater than when tested with one white oak key. The lower percentage differences of the joints with two keys may be explained by the lower density of white oak keys in joints with one key compared to that of the white oak keys in joints with two keys. Also, DF-11-1-4, with one ipe key, had a less percent difference than the white oak joints with 11-inch tenons with one key because it failed at the tenon. A difference in the ultimate load between joint species did not appear to exist among joints retested with ipe keys whereas the number of keys showed much difference.

Table 3-8: Ultimate Load of Joints with Ipe Keys

Joint Group	Average Ultimate Load (COV, %) of Joints retested with Ipe Keys, lbs	% Difference Compared to white oak keyed joints [1]
WO-11-1	15,300 (2.1) - [15,200 15,000 15,600] [2]	92
WO-11-2-2	20,800 (N/A - one joint)	41
DF-11-1-4	12,500 (N/A - one joint)	73
DF-11-2-2	21,100 (N/A - one joint)	29

[1] (Ipe Keyed Joint - White Oak Keyed Joint)/White Oak Keyed Joint x 100%

[2] Individual Values of WO-11-1-2,3, and 4 respectively

Stiffness

Table 3-9 shows the stiffness of joints retested with ipe keys and the percent differences between joints previously tested with white oak keys. Stiffness for joints retested with ipe keys ranged from 84,600 to 189,000 lbs/in. The average stiffness of white oak joints with 11-inch tenons retested with one ipe key was 43% greater than when originally tested with white oak keys. Stiffness of WO-11-2-2 retested with ipe keys was 5.6% less than when tested with white oak keys. Ipe keys were one-eighth of an inch less in depth than the white oak keys originally used for WO-11-2-2 which may explain the similar, but yet slightly less, stiffness of WO-11-2-2 with ipe keys. The stiffness of DF-11-1-4 with one ipe key was 101% greater than when tested with one white oak key. The stiffness of DF-11-2-2 retested with ipe keys was 54% less than tested with white oak keys. This was due to the ipe keys bearing on the pre-crushed surface of the mortise member from initially testing with white oak keys where the mortise member was not turned over afterward to provide a fresh bearing surface for the ipe keys. The pre-crushed

surfaces were deformed greatest at the mortise and least at the edges of the mortise member, limiting initial joint stiffness to the bending stiffness of the replacement (ipe) keys. Replacement keys should be cut to match crushed surfaces of the mortise member to eliminate loss of joint stiffness, however, special care is needed to make certain that tenon load would be greater than replacement keys, to avoid constructing a brittle joint.

Table 3-9: Stiffness of Joints with Ipe Keys

Joint Group	Average Stiffness (COV, %) of Joints retested with Ipe Keys, lbs/in	% Difference Compared to white oak keyed joints [1]
WO-11-1	150,000(5.7) - [155,000 140,000 155,000] [2]	43
WO-11-2-2	189,000 (N/A - one joint)	-5.6
DF-11-1-4	188,000 (N/A - one joint)	101
DF-11-2-2	84,600 (N/A - one joint) [3]	-54

[1] (Ipe Keyed Joint - White Oak Keyed Joint)/White Oak Keyed Joint x 100%

[2] Individual Values of WO-11-1-2,3, and 4 respectively

[3] Retested Ipe Keys on same bearing surface of mortise member that white oak keys were tested

3.2.1.3 Joint Failure at Ultimate Load

Table 3-10 shows joint failures at ultimate load for each joint tested. Failure was defined as a decrease in joint load by 20% with little to no sign of load recovery or the greatest load prior to key wedging or mortise splitting. Events such as key wedging and mortise splitting were considered post-failure events. Tenon splitting and single plane shearing were considered failures if these events occurred at the ultimate load of a joint. Otherwise, these events were termed as pre-failure events as shown in the footnotes of Table 3-10. In joints that experienced pre-failure events such as tenon splitting or single plane shearing, the joint load recovered promptly after a sharp decrease and then increased beyond the former maxima.

All joints with four-inch tenons displayed brittle failure of the tenon upon reaching ultimate load including row tear-out (relish failure), tenon splits over the keys, single shear plane failures, and various combinations of these failures. Most of the joints with four-inch tenons did not have a 5% offset yield load before failure due to the brittle nature of these joints. All of the white oak joints with 11" tenons displayed ductile behavior except for one retested with an ipe key (WO-11-1-4-IPE). Three of the Douglas-fir joints with 11-inch tenons with one key

displayed ductile behavior, however one of these experienced a tenon split prior to key bending and crushing, while the other two experienced tenon relish failure. Joints with 11" tenons, with exception of three Douglas-fir joints with one key (two with white oak keys and one with an ipe key), produced key bending and crushing failures. WO-11-1-4-IPE had a tenon failure, but showed the initiation of key bending. Key wedging was a post-failure seen in most of the white oak joints with 11" tenons.

Table 3-10: Joint Failure at Ultimate Load

Joint Group	Joint 1	Joint 2	Joint 3	Joint 4	Joint 5
WO-4-1	Tenon Split	Tenon Split Spread	Relish [1]	Tenon Split Spread	Tenon Split Spread
WO-4-2	Tenon Split at One Key	Tenon Split at One Key	Relish at One Key [1] [2]	Relish at One Key	Relish at One Key
WO-11-1	Key Bending and Crushing [2]	Key Bending and Crushing [2]	Key Bending and Crushing [2]	Key Bending and Crushing [2]	Key Bending and Crushing
WO-11-2	Key Bending and Crushing [2]	Key Bending and Crushing [2]	Key Bending and Crushing [2]	Key Bending and Crushing [2]	Key Bending and Crushing
DF-4-1	Plane Shearing	Plane Shearing	Plane Shearing [1]	Tenon Split	Tenon Split
DF-4-2	Relish at Both Keys [1]	Relish at Both Keys	Relish (three sheared planes)	Relish at Both Keys [1]	Relish at Both Keys
DF-11-1	Checks and Splits Opened - relish	Key Bending and Crushing [1]	Tenon Split near Shear Plane - Relish	Key Bending and Crushing	Key Bending and Crushing
DF-11-2	Key Bending and Crushing [2]	Key Bending and Crushing	Key Bending and Crushing [2]	Key Bending and Crushing	Key Bending and Crushing
WO-11-1-Ipe	----------	Key Bending and slight Crushing	Key Bending and slight Crushing	Tenon Split Spread - Shear Plane Sheared	----------
WO-11-2-Ipe	----------	Key Bending and slight Crushing [3]	----------	----------	----------
DF-11-1-Ipe	----------	----------	----------	Relish	----------
DF-11-2-Ipe	----------	Key Bending and slight Crushing	----------	----------	----------

[1] Pre-failure event resulting in a decrease in load prior to ultimate load

[2] Joints that experienced key wedging (WO-4-2-3 had this in one key), after ultimate load

[3] Joints that experienced a mortise split, after ultimate load

Five different failure types were observed at ultimate load and are defined below.

- **Tenon Split (Brittle)**

A tenon split occurred as a result of perpendicular-to-grain tension in the wood fibers of the tenon at the location of a key as shown in Figure 3-5. This was a brittle failure that was usually audible. Tenon splits produced failure in some of the white oak and Douglas-fir joints with four-inch tenons and in one Douglas-fir joint with an 11-inch tenon (DF-11-1-3) which occurred prior to full relish failure. A 'tenon split at one key' was where a tenon split occurred at one key in a joint with two keys. Tenon splitting occurred as a pre-failure event in one white oak and in one Douglas-fir joint with a four-inch tenon with one key (WO-4-1-3 and DF-4-1-3). Tenon splitting at one key occurred as a pre-failure event in a white oak joint with a four-inch tenon with two keys (WO-4-2-3).

Figure 3-5: Tenon Split (keyhole center)

- **Tenon Split Spread (Brittle - often gradual)**

A tenon split spread occurred when a joint with an initial split defect, usually from drying, in the tenon spread farther apart due to perpendicular-to-grain tension stresses in the tenon. This failure type occurred in three white oak joints with four-inch tenons with one key, and one white joint with an 11-inch tenon with one ipe key (WO-11-1-4-IPE). This failure type usually occurred prior to shear plane or relish failure. Tenon split spreading often occurred gradually which may have been due to the high joint moisture content of approximately 60% for white oak joint members. An abrupt and audible tenon split spread occurred in a Douglas-fir joint with an 11-inch tenon with one key (DF-11-1-2) as a brittle pre-failure event. This joint had a check and a shake around its pith in the end of the tenon situated over the key prior to

testing. At the time of the split, the load dropped by 26.4%, but increased promptly showing immediate load recovery and was termed as a pre-failure event and not a failure.

- **Plane shearing (Brittle)**

Plane shearing was where shearing of a single tenon plane, securing a key, occurred as shown in Figure 3-6 at the right shear plane of keyhole 'A'. This failure was usually brittle and abrupt. Plane shearing at ultimate load occurred in three Douglas-fir joints with four-inch tenons with one key, and at one key of one Douglas-fir joint with a four-inch tenon with two keys (DF-4-2-3), which also had a tenon relish failure at the other key. Plane shearing was a pre-failure event in two Douglas-fir joints with four-inch tenons with two keys (DF-4-2-1 and DF-4-2-4). Ultimate load of the Douglas-fir joint with plane shear pre-failure events at each key (DF-4-2-4) was less than half of the other Douglas-fir joints with simultaneous relish failures at each key without any pre-failure events. The ultimate load of the Douglas-fir joint with plane shear pre-failure events at one key (DF-4-2-1) was 70% of the other Douglas-fir joints with relish failures at each key without any pre-failure events.

Figure 3-6: Plane Shearing 'A', Relish Failure 'B'

- **Relish Failure (Brittle)**

Relish failure occurred when two shear planes, securing a key, sheared simultaneously as shown in Figure 3-7 and at keyhole 'B' in Figure 3-6. Failure was brittle and usually occurred after pre-failure events such as a tenon split or a single shear plane failure. Three white oak joints with four-inch tenons with two keys experienced relish failure in one key. Two of the Douglas-fir joints with four-inch tenons with two keys experienced relish failure in both keys simultaneously (DF-4-2-2 and DF-4-2-5).

Figure 3-7: Full Tenon Relish Failure at each Keyhole

Relish failures may have been weakened by pre-failure events as indicated by the load-deformation plots for the Douglas-fir joints with four-inch tenons with two keys shown in Appendix C. The two joints that experienced relish failures with no pre-failure events had approximately 50% more ultimate load than the joints with three shear plane failures, and slightly more than twice the load of the joint with that had a single plane shearing pre-failure at each key.

Figure 3-8 illustrates how a pre-failure event such as a tenon split or single plane shearing failure contributed to a relish failure. A tenon split or single shear plane failure weakens the intact shear planes as the two tenon halves become two eccentrically loaded tension members, producing perpendicular-to-grain tension in the remaining intact shear planes nearest the key edges prior to full tenon relish failure, due to slight flexural rotation in the tenon-halves. Relish failure due to single shear plane failure can be conceptualized by moving the tenon split to the location of one of the shear planes in the tenon.

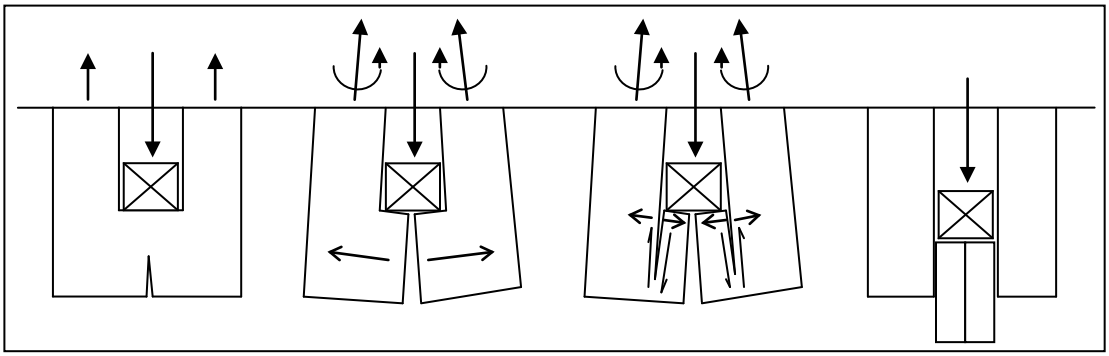

Figure 3-8: Procession of Tenon Relish Failure after a Defect or a Pre-failure Event

- **Key Bending and Crushing/ Slight Crushing (Ductile)**

Key bending and crushing, shown in Figure 3-9, occurred in most joints with 11-inch tenons and in one key of a white oak joint with a four-inch tenon with two keys (WO-4-2-3). Tenons in joints with key bending and crushing had greater shear resistance than the key bending/crushing resistance. Identifying key bending or crushing during testing was difficult since the portion of the key that experienced bending/crushing was hidden within the tenon. White oak keys experienced slight crushing before bending, and then bending and crushing simultaneously. Key crushing reduced the key cross-section, reducing the section modulus and damaging the cell structure, resulting in reduced bending resistance. Ipe keys were denser than white oak keys and experienced bending, with less crushing. Figure 3-10 shows the ipe keys with key bending and slight crushing. Distinguishing horizontal key shearing from crushing was difficult and no conclusions where made as to if or when key shearing occurred.

Figure 3-9: Key Bending and Crushing (White Oak Keys)

Figure 3-10: Key Bending/ slight Crushing (Ipe Keys)

Many of the joints with 11-inch tenons had key wedging post-failures as shown in Figure 3-11. Key wedging took place after the key(s) experienced bending failures in an inverted 'V' shape and were often observed at deformations of 0.5" or greater. One key wedging post-failure completely severed a white oak key as shown in Figure 3-12. Key wedging also subjected mortise members to perpendicular-to-grain tension which caused complete splitting of the mortise member of the white oak joint with an 11-inch tenon with two ipe keys (WO-11-2-2-IPE), shown in Figure 3-13. Key wedging was not as common in Douglas-fir joints as in white

oak joints, since the Douglas-fir mortise members had lower bearing strength than white oak mortise members. Softer bearing surfaces allow keys to bend more than harder bearing surfaces.

Figure 3-11: Key Wedging

Figure 3-12: Severed Key from Wedging

Figure 3-13: Mortise Split from Key Wedging

3.2.1.4 Brittle and Ductile Joint Failures

A brittle joint was defined by brittle behavior at ultimate load, such as tenon failure. Tenon failures included tenon splitting, tenon split spreading, single plane shearing, and relish failure. All joints with four-inch tenons were brittle as well as one white oak and one Douglas-fir joint with 11-inch tenons with one ipe key (WO-11-1-4-IPE and DF-11-1-4-IPE), and two Douglas-fir joints with 11-inch tenons with one white oak key (DF-11-1-1 and DF-11-1-3). One Douglas-fir joint with an 11-inch tenon with one white oak key experienced a tenon split prior to a key bending and crushing failure due to an initial tenon defect (DF-11-1-2).

Figure 3-14 shows load-deformation plots of typical brittle joints with photos of corresponding failures beneath. The white oak joint with a four-inch tenon with two keys (WO-

4-2-1) showed a tenon split at ultimate load, followed by relish failure of the same key. The intersection of the 5% offset line and the load-deformation curve occurred after ultimate load (Figure 3-14a). Figure 3-14b shows relish failure that occurred in a Douglas-fir joint with an 11-inch tenon with one key (DF-11-1-1). This brittle failure may have been due to a tenon split observed prior to testing.

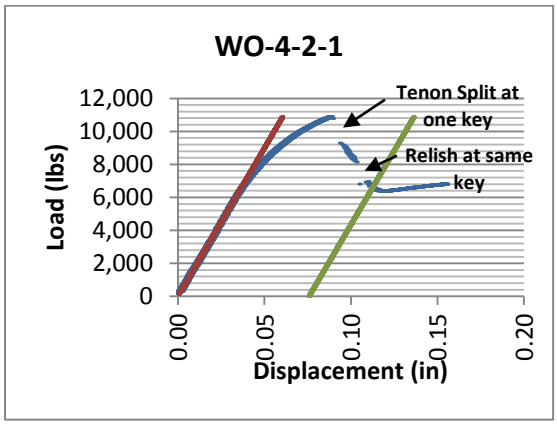

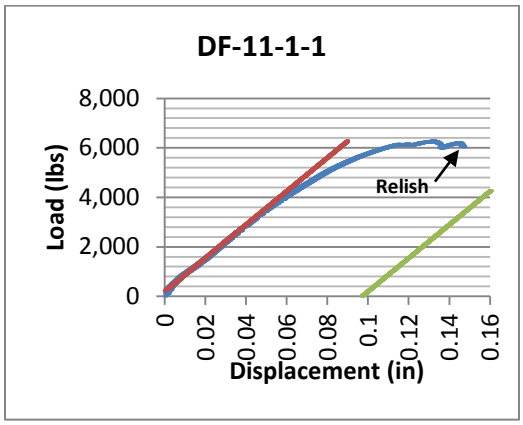

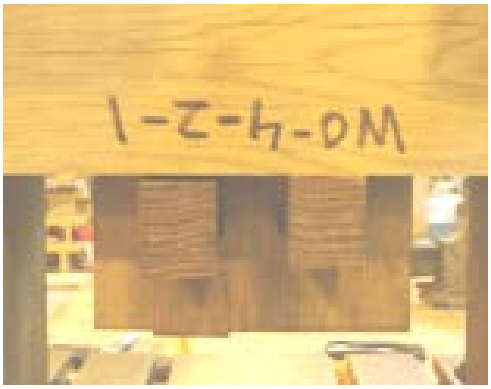

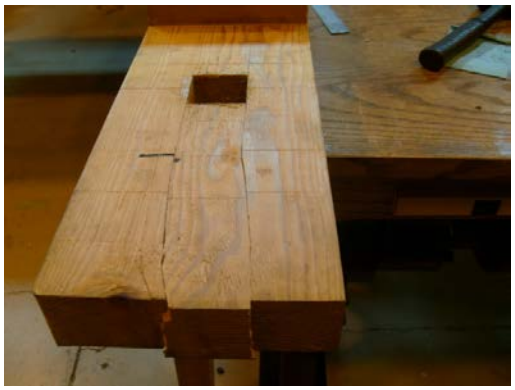

Figure 3-14a: WO-4-2-1 (Relish on left key) **Figure 3-14b: DF-11-1-1: Full Relish**

The only four-inch tenon joint that produced ductile behavior, but was still brittle in accordance with the definition above, was a white oak joint with two keys (WO-4-2-3), shown and photographed in Figure 3-15. This joint was termed brittle because a relish failure occurred at one of the keys, establishing ultimate load, prior to the intersection of the 5% offset line and the load-deformation curve. The other key experienced failure and the loading was stopped at approximately one-inch of deformation when the tenon split at the failed key.

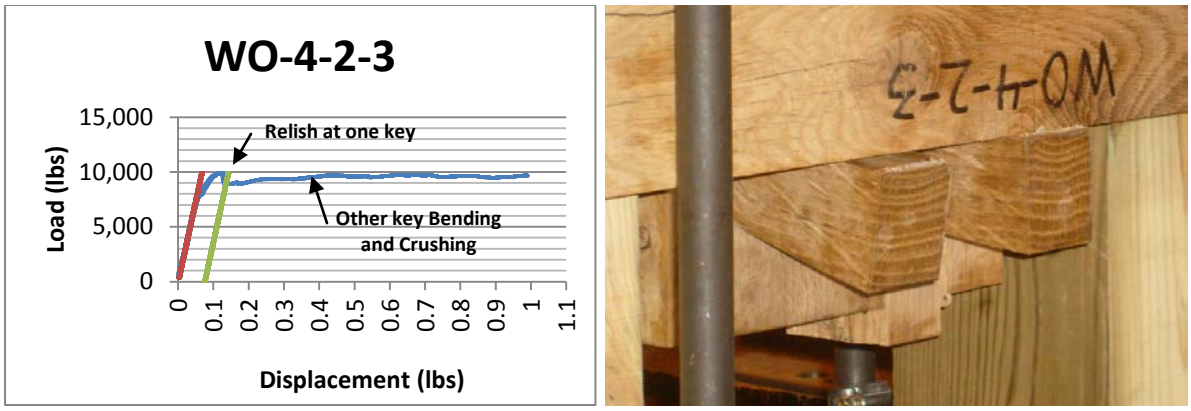

Figure 3-15: WO-4-2-3 (Photo: Bent and Crushed Key on left, Tenon Relish on right)

Figure 3-16 shows the load-deformation curves of typical ductile joints with photographs of the corresponding failures beneath. Two criteria had to be met when defining a ductile joint: (1) a ductile behavior must occur at ultimate load such, as a key failure, and (2) the joint in consideration must have had a 5% offset line intersection with the load curve prior to ultimate load. Most joints with 11-inch tenons were ductile by producing key failures. A good example of ductile behavior was a white oak joint with an 11-inch tenon with one key (WO-11-1-2) that showed a key bending/crushing failure that occurred after the intersection of the 5% offset line and load-deformation curve. Key wedging occurred in this joint as shown in Figure 3-16a. Figure 3-16b shows key bending and crushing failure that occurred in a Douglas-fir joint with an 11-inch tenon with two keys (DF-11-2-5). This joint did not produce key wedging.

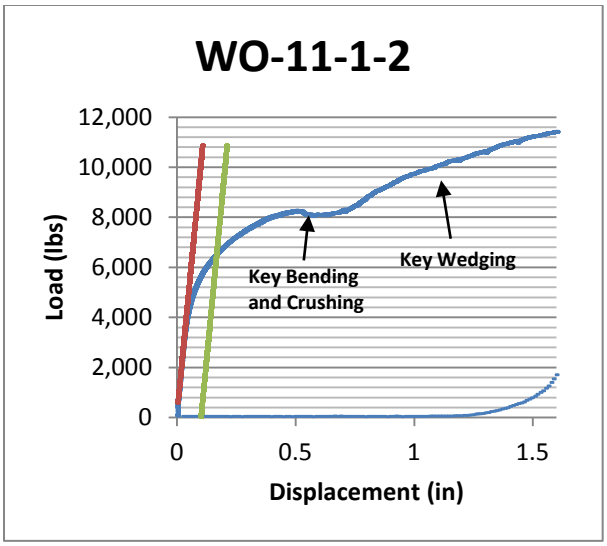

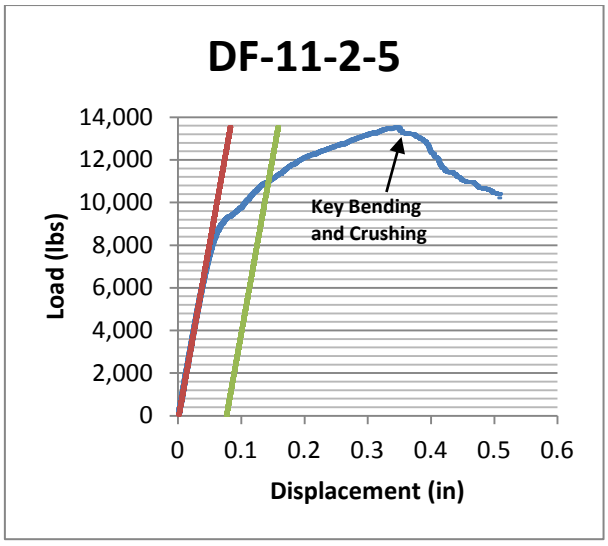

Figure 3-16a: WO-11-1-2 (Key)

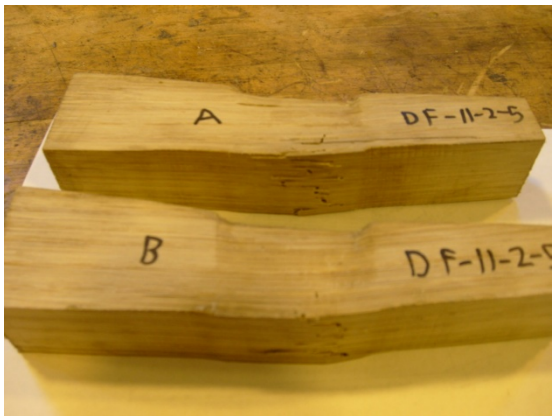

Figure 3-16b: DF-11-2-5 (Keys)

3.2.1.5 Moisture Content/ Specific Gravity (MC/SG) of Joint Components

Table 3-11 shows the averages and COVs for moisture content (MC) and specific gravity (SG) of all joint members and keys. White oak mortise and tenon members had higher MC and SG values than Douglas-fir mortise and tenon members. Average MC values for white oak and Douglas-fir tenon members were 63.4% (7.6% COV) and 17.3% (18.3% COV), respectively. Average SG values for white oak and Douglas-fir tenon members were 0.78 (5.9% COV) and 0.47 (8.0% COV), respectively. Average MC values for white oak and Douglas-fir mortise members were 58.6% (11.8% COV) and 14.9% (12.2% COV), respectively. Average SG values for white oak and Douglas-fir mortise members were 0.77 (9.0% COV) and 0.48 (9.8% COV), respectively. The more brittle behavior seen in the Douglas-fir joints than in the white oak joints, particularly with 11-inch tenons with one key, may have been due to lower moisture

content compared to that of the white oak joint members, which were above fiber saturation point, while Douglas-fir joint members were below fiber saturation point.

Table 3-11: Joint Member and Key MC and SG

Joint Member	Species	MC: AVG (COV)	SG: AVG (COV)
Tenon	White Oak	63.4% (7.6%)	0.78 (5.9%)
	Douglas-fir	17.3% (18.3%)	0.47 (8.0%)
Mortise	White Oak	58.6% (11.8%)	0.77 (9.0%)
	Douglas-fir	14.9% (12.2%)	0.48 (9.8%)
Key(s)	White Oak Keys (1)	16.7% (17.1%)	0.68 (4.6%)
	White Oak Keys (2)	16.7% (15.5%)	0.76 (7.5%)
	Ipe Keys	11.8% (10.9%)	1.03 (1.2%)

The average MC between white oak keys in joints with one and two keys were similar. However, the average SG of white oak keys in joints with two keys was greater than white oak keys in joints with one key. The COV values of MC and SG for white oak keys between joints with one and two white oak keys were similar. Average MC values for one and two white oak keys were 16.7% (17.1% COV) and 16.7% (15.5% COV), respectively. Average SG values for one and two white oak keys were 0.68 (4.6% COV) and 0.76 (7.5% COV), respectively. Ipe keys had less MC and greater SG values than white oak keys. Average MC and SG of ipe keys were 11.8% (10.9% COV) and 1.03 (1.2%), respectively. The higher SG of ipe keys explains the greater joint loads compared to joints with white oak keys regarding key failures.

Table 3-12 shows the single factor ANOVA results between the MC and SG of joint components with an alpha value (α) of 0.05, where the null hypothesis was that no difference existed between MC or SG values of joint components. The MC and SG of white oak mortise and tenon members were significantly different than those of Douglas-fir (p-values less than 0.05). The SG for white oak keys in joints with two white oak keys was significantly different than white oak keys in joints with one (p-value less than 0.05). The SG value of ipe keys was significantly different than white oak keys (p-value less than 0.05). The MC of white oak keys in white oak joints was significantly different than white oak keys in Douglas-fir joints (p-value less than 0.05) which may have due to the effect of MC of joint members since joints were wrapped in plastic prior to testing where the moisture of the joints may have been transferred to

the keys. Comparisons involving SG for joint members were taken from joint members directly after testing as well as MC/SG samples of the material tests cut from the members due to availability. Moisture content samples of the joint components were only measured from MC/SG samples taken from the joints directly after testing because the material tests were conducted after the joint tests which would have influenced MC results. The SG of keys being greatest for ipe and least for white oak keys in joints with one key, indicated a trend between key SG and joint loads with keys failures, which is investigated in Section 3.2.3 based upon normalized key width. The MC and SG differences between white oak and Douglas-fir joint members are important when considering the effects of bearing strength on joint load.

Table 3-12: Joint Member and Key MC and SG ANOVA Comparisons

ANOVA Comparisons (alpha value of 0.05)			
p-values	Rank		
0.000	SG, white oak tenon members	>	SG, Douglas-fir tenon members
0.000	SG, white oak mortise members	>	SG, Douglas-fir mortise members
0.000	SG, white oak keys in 2-key joints	>	SG, white oak keys in 1-key joints
0.000	SG, Ipe keys	>	SG, white oak keys (1 and 2 keys)
0.000	MC, white oak tenon members	>	MC, Douglas-fir tenon members
0.000	MC, white oak mortise members	>	MC, Douglas-fir mortise members
0.000	MC, white oak keys in WO joints	>	MC, white oak keys in DF joints

The *Standard for Design of Timber Frame Structures and Commentary* (TFEC 1-10) states that oven-dry SG of wedges (keys) shall not be less than the oven-dry SG of the species or species group of timber comprising the connection, as assigned in the NDS, and that the oven-dry SG of wedge (key) material must be at least 0.57 (TFEC 2010). Given the SG values in Table 3-11, white oak and ipe keys would suffice for fastening Douglas-fir joints, however, only ipe keys would suffice for fastening the white oak joints because the joint members were denser than the white oak keys. According to the NDS, the oven-dry SG of white oak is 0.73. Making joints from the joint members and key stock, above, may be permissible due to the guidelines in the TFEC 1-10 which regard oven-dry SG according to that presented in the NDS (TFEC 1-10).

3.2.2 Effects of Joint Factors on Load and Stiffness of Joints with White Oak Keys

This section compares the load and stiffness of the joints based on factors of species, tenon length, and number of keys. Joint responses for all 40 joints with white oak keys were first compared using a single factor analysis of variance (ANOVA) to determine which factors produced differences among load and stiffness responses (section 3.3.2.1). For example, comparisons between species compared all white oak joints against all Douglas-fir joints to determine if the responses were significantly different. Joints were then compared using a series of single factor ANOVAs to determine if the factors produced differences among joint load and stiffness of the joints based on single joint groups where two factors, other than the comparison factor, remained constant. All p-values less than the alpha value (0.05) indicated a significant difference. No ANOVA comparisons were performed on joints with ipe keys due to limited sample size. Comparisons between the number of keys were normalized to key width to account for different key widths rather than number of shear planes since key failures were more prevalent than any individual tenon failure type. The null hypothesis for all ANOVA comparisons was that no significance existed between species, tenon length, or number of keys. ANOVA comparisons did not account for different MC and SG between white oak and Douglas-fir joint members.

3.2.2.1 ANOVA Comparison of Joint Load and Stiffness

Table 3-13 shows the p-values of the single factor ANOVA considering the factors of species, tenon length, and number of keys tested with white oak keys. All p-values less than 0.05 indicating a significant difference, are bold-faced. No significant difference existed for the species comparisons for proportional-limit, 5% offset yield, or ultimate load, or stiffness.

Table 3-13: Single Factor Analysis of Variance Comparison (α =0.05) Considering all Joints with White Oak Keys

Joint Response	Species	Tenon Length	Number of Keys
Proportional-Limit Load	0.857	0.173	**0.000**
5% Offset Yield Load	0.377	0.524	**0.000**
Ultimate Load	0.297	**0.001**	**0.001**
Stiffness	0.177	0.118	**0.000**

A significant difference existed between tenon length for ultimate load with a p-value of 0.001. Proportional-limit load, 5% offset yield load, and stiffness responses did not produce significant differences between tenon length. Significant differences between number of keys were displayed for all joint load and stiffness responses. The responses for the ANOVA comparison used normalized key width joint responses when comparing between the number of keys.

3.2.2.2 Comparison of Species on Joint Load and Stiffness

Table 3-14 shows the single factor ANOVA comparisons between different joint species (white oak and Douglas-fir) among individual joint groups on proportional limit, 5% offset yield, and ultimate load, and stiffness. Comparisons marked 'N/A' (not applicable) are for joints in certain groups that did not produce 5% offset yield load where comparisons could not be performed. P-values less than 0.05 are bold-faced and the rank (showing the greater comparison) shaded when a significant difference existed.

Table 3-14: Comparison of Species on Load and Stiffness

Effect of Species on:	ANOVA Comparison			p-value	Rank		
Proportional Limit Load	WO-11-1	to	DF-11-1	0.210	WO-11-1	=	DF-11-1
	WO-11-2	to	DF-11-2	0.873	WO-11-2	=	DF-11-2
	WO-4-1	to	DF-4-1	0.351	WO-4-1	=	DF-4-1
	WO-4-2	**to**	**DF-4-2**	**0.031**	**WO-4-2**	**>**	**DF-4-2**
5% Offset Load	WO-11-1	to	DF-11-1	N/A	WO-11-1	N/A	DF-11-1
	WO-11-2	to	DF-11-2	0.557	WO-11-2	=	DF-11-2
	WO-4-1	to	DF-4-1	N/A	WO-4-1	N/A	DF-4-1
	WO-4-2	to	DF-4-2	N/A	WO-4-2	N/A	DF-4-2
Ultimate Load	WO-11-1	to	DF-11-1	0.224	WO-11-1	=	DF-11-1
	WO-11-2	to	DF-11-2	0.706	WO-11-2	=	DF-11-2
	WO-4-1	to	DF-4-1	0.060	WO-4-1	=	DF-4-1
	WO-4-2	**to**	**DF-4-2**	**0.005**	**WO-4-2**	**>**	**DF-4-2**
Stiffness	**WO-11-1**	**to**	**DF-11-1**	**0.024**	**WO-11-1**	**>**	**DF-11-1**
	WO-11-2	to	DF-11-2	0.056	WO-11-2	=	DF-11-2
	WO-4-1	to	DF-4-1	0.895	WO-4-1	=	DF-4-1
	WO-4-2	**to**	**DF-4-2**	**0.013**	**WO-4-2**	**>**	**DF-4-2**

No significant difference was detected between species by the single factor ANOVA, in Table 3-13, when comparing between all white oak and Douglas-fir joints for each response. However, the comparison between white oak and Douglas-fir joints with four-inch tenons with two keys showed a significant difference in the proportional-limit and ultimate load and stiffness,

where white oak joint responses were greater than Douglas-fir joint responses. White oak joints with four -inch tenons with two keys failed in tenon splitting and relish failure at one key where Douglas-fir joints with four-inch tenons with two keys primarily failed in combinations of single shear plane failure and relish failure at both keys, which also indicated that white oak tenons had greater shear resistance than Douglas-fir tenons. No significant difference was found between 5% offset yield load for species. A significant difference was found between stiffness of white oak and Douglas-fir joints with 11-inch tenons with one key. The species comparison between white oak and Douglas-fir joints with 11-inch tenons with two keys almost produced a significant difference (p-value 0.056). White oak joints with 11-inch tenons with one key and four-inch tenons with two keys had greater stiffness than Douglas-fir joints with the same details. The white oak mortise and tenon members had greater SG than the Douglas-fir joints which produced a greater bearing strength in the white oak mortise members increasing joint stiffness.

3.2.2.3 Comparison of Tenon Length on Joint Load and Stiffness

Table 3-15 shows the single factor ANOVA comparisons between four- and 11-inch tenons on proportional limit, 5% offset yield, and ultimate load, and stiffness. Comparisons marked 'N/A' (not applicable) are for joints that did not produce 5% offset yield load. P-values less than 0.05 are bold-faced and the rank shaded when a significant difference existed.

Table 3-15: Comparison of Tenon Length on Load and Stiffness

Effect of Tenon Length on:	ANOVA Comparison			p-value	Rank		
Proportional Limit Load	**WO-11-1**	**to**	**WO-4-1**	**0.038**	**WO-11-1**	**>**	**WO-4-1**
	WO-11-2	to	WO-4-2	0.629	WO-11-2	=	WO-4-2
	DF-11-1	to	DF-4-1	0.116	DF-11-1	=	DF-4-1
	DF-11-2	to	DF-4-2	0.186	DF-11-2	=	DF-4-2
5% Offset Load	WO-11-1	to	WO-4-1	N/A	WO-11-1	N/A	WO-4-1
	WO-11-2	to	WO-4-2	N/A	WO-11-2	N/A	WO-4-2
	DF-11-1	to	DF-4-1	N/A	DF-11-1	N/A	DF-4-1
	DF-11-2	to	DF-4-2	N/A	DF-11-2	N/A	DF-4-2
Ultimate Load	**WO-11-1**	**to**	**WO-4-1**	**0.001**	**WO-11-1**	**>**	**WO-4-1**
	WO-11-2	**to**	**WO-4-2**	**0.005**	**WO-11-2**	**>**	**WO-4-2**
	DF-11-1	**to**	**DF-4-1**	**0.000**	**DF-11-1**	**>**	**DF-4-1**
	DF-11-2	**to**	**DF-4-2**	**0.000**	**DF-11-2**	**>**	**DF-4-2**
Stiffness	WO-11-1	to	WO-4-1	0.059	WO-11-1	=	WO-4-1
	WO-11-2	**to**	**WO-4-2**	**0.044**	**WO-11-2**	**>**	**WO-4-2**
	DF-11-1	to	DF-4-1	0.785	DF-11-1	=	DF-4-1
	DF-11-2	**to**	**DF-4-2**	**0.013**	**DF-11-2**	**>**	**DF-4-2**

White oak joints with 11- and four-inch tenons with one key were significantly different regarding proportional-limit load where white oak joints with 11-inch tenons were greater. No other comparisons were significantly different for proportional-limit load. Comparisons could not be made between tenon length for 5% offset yield load, as only two joints with four-inch tenons produced 5% offset yield load values. Significant differences were found between all tenon length comparisons for ultimate load. Joints with 11-inch tenons produced greater ultimate load than joints with four-inch tenons between each combination of species and number of keys. Joints with four-inch tenons produced tenon failure, which did not permit full load usage of the keys, whereas joints with 11-inch tenons often produced key failure, fully using key load. For stiffness comparisons, significant differences were detected among white oak and Douglas-fir joints with two keys between four- and 11-inch tenons. White oak and Douglas-fir joints with 11-inch tenons with two keys had greater stiffness than with four-inch tenons with two keys. The tenon length comparison for stiffness between white oak joints with four- and 11-inch tenons with one key was almost significantly different regarding stiffness (p-value 0.059).

3.2.2.4 Comparison of the Number of Keys on Joint Load and Stiffness

Table 3-16 shows the single factor ANOVA comparisons between the number of keys for proportional limit, 5% offset yield, and ultimate load, and stiffness. Comparisons marked 'N/A' (not applicable) are for joints in groups that did not produce 5% offset yield load. Significant differences, where p-values were less than 0.05, are bold-faced and the rank shaded. Load and stiffness joint responses with one and two keys were normalized according to key width to account for different key sizes. Keys in joints with one key had a width of two inches and keys in joints with two keys had a width of one-and-a-half inches. Joint responses were not normalized to number of tenon shear planes since key failures were more prevalent than any individual tenon failure type

Table 3-16: Comparison of the Number of Keys on Load and Stiffness

Effect of Number of Keys on:	ANOVA Comparison			p-value	Rank		
Proportional Limit Load	**WO-11-1**	**to**	**WO-11-2**	**0.0496**	**WO-11-1**	**<**	**WO-11-2**
	WO-4-1	**to**	**WO-4-2**	**0.000**	**WO-4-1**	**<**	**WO-4-2**
	DF-11-1	to	DF-11-2	0.386	DF-11-1	=	DF-11-2
	DF-4-1	to	DF-4-2	0.236	DF-4-1	=	DF-4-2
5% Offset Load	**WO-11-1**	**to**	**WO-11-2**	**0.002**	**WO-11-1**	**<**	**WO-11-2**
	WO-4-1	to	WO-4-2	N/A	WO-4-1	N/A	WO-4-2
	DF-11-1	to	DF-11-2	N/A	DF-11-1	N/A	DF-11-2
	DF-4-1	to	DF-4-2	N/A	DF-4-1	N/A	DF-4-2
Ultimate Load	**WO-11-1**	**to**	**WO-11-2**	**0.001**	**WO-11-1**	**<**	**WO-11-2**
	WO-4-1	**to**	**WO-4-2**	**0.001**	**WO-4-1**	**<**	**WO-4-2**
	DF-11-1	**to**	**DF-11-2**	**0.000**	**DF-11-1**	**<**	**DF-11-2**
	DF-4-1	to	DF-4-2	0.075	DF-4-1	=	DF-4-2
Stiffness	**WO-11-1**	**to**	**WO-11-2**	**0.003**	**WO-11-1**	**<**	**WO-11-2**
	WO-4-1	**to**	**WO-4-2**	**0.019**	**WO-4-1**	**<**	**WO-4-2**
	DF-11-1	**to**	**DF-11-2**	**0.006**	**DF-11-1**	**<**	**DF-11-2**
	DF-4-1	to	DF-4-2	0.550	DF-4-1	=	DF-4-2

For proportional-limit load comparisons, significant differences were detected among white oak joints with four- and 11-inch tenons between one and two keys. White oak joints with two keys had greater proportional-limit load than with one key for each tenon length. The only comparison that could be made for 5% offset yield load was between white oak joints with 11-inch tenons with one key and two keys, since all joints in these groups produced key failures. White oak joints with 11-inch tenons with two keys had greater 5% offset yield load than with one key. Every comparison between joints with one and two keys, except among Douglas-fir joints with four-inch tenons, produced significant differences for both ultimate load and stiffness. The increased load and stiffness performances were due to greater total key width (for bending and bearing strength) of joints with two keys. However, increased load and stiffness responses, after normalization, were likely due to greater specific gravity of white oak keys in joints with two keys compared to white oak keys in joints with one key (greater key bending and bearing strength).

3.2.3 Influence of Key Specific Gravity on Responses of Joints with Key Failures

Correlations between key specific gravity (SG) and joint load and stiffness were made due to the significantly different values among SG of white oak keys between joints with one and two white oak keys and ipe keys, as shown in Table 3-12. White oak keys in joints with two keys had significantly greater SG than white oak keys in joints with one key due to keys of joints with one key being cut from separate stock than the keys in joints with two keys. Ipe keys had significantly greater SG than white oak keys. Since all white oak keys had similar depth to ipe keys, which were usually a 1/16" to an 1/8" less due to finish tooling, correlations could be made between key SG and normalized joint responses per inch of key width. Correlations were performed separately for white oak and Douglas-fir joints to examine effects of key SG on each joint species, and were made on joints showing key failures since the load and stiffness of these joints was dependant on keys.

Figure 3-17 shows the relationship of proportional-limit, 5% offset yield, and ultimate load versus key SG of white oak joints with key failures. This data contains all ten joints with 11-inch tenons with white oak keys, three joints with 11-inch tenons with one ipe key, and one joint with an 11-inch tenon with two ipe keys. Even though one of the three white oak joints with an 11-inch tenon with one ipe key (WO-11-1-4-IPE) experienced a tenon failure, this joint was still used because the key showed full-width tension-side splintering. R-squared values were 0.809 for proportional-limit, 0.951 for 5% offset yield load, and 0.947 for ultimate load indicating a good fit. Positive correlations showed that each joint load response increased as key SG increased for a given key width, for white oak joints. Five percent offset yield load was shown to be the most influenced by key SG, closely followed by ultimate, and then proportional-limit load.

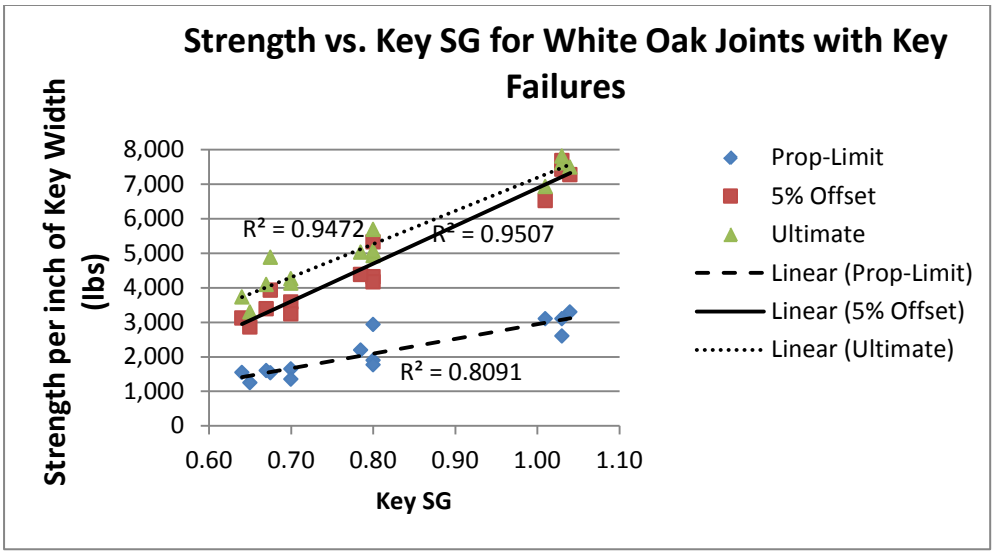

Figure 3-17: Joint Load vs. Key SG for White Oak Joints with Key Failures

Figure 3-18 shows the correlation between joint stiffness and key SG for the white oak joints with key failures. Positive correlations showed that joint stiffness increased as key SG increased for a given key width, for white oak joints. This correlation presented an r-squared value of 0.586, which was not as strong as correlations between joint load and key SG. Joint load was more dependent on key SG than joint stiffness.

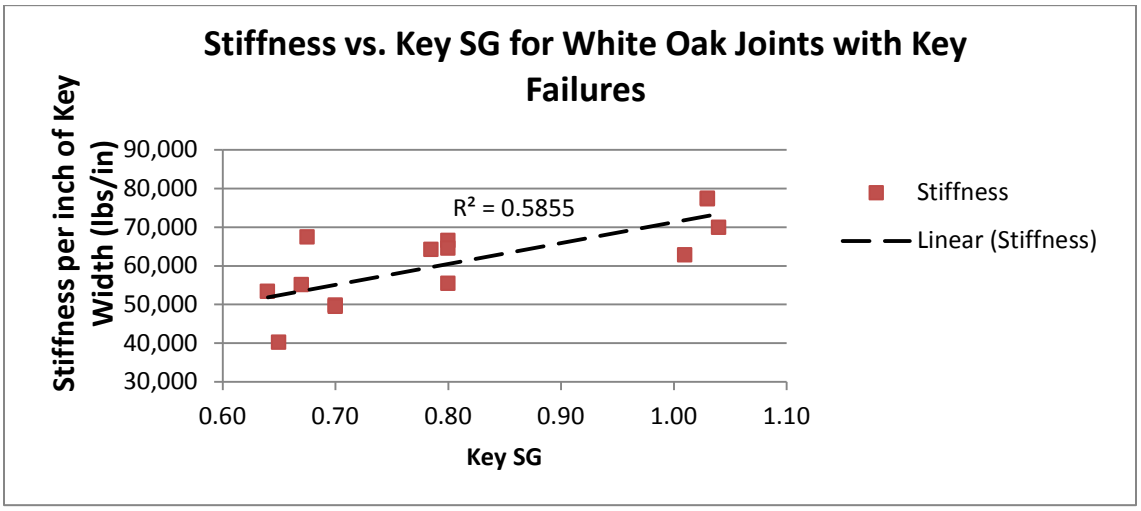

Figure 3-18: Joint Stiffness vs. Key SG for White Oak Joints with Key Failures

Figure 3-19 shows the relationship of proportional-limit, 5% offset yield, and ultimate load versus key SG of Douglas-fir joints that had key failures. This data contains seven joints with 11-inch tenons with white oak keys (two with one key and five with two keys) and one joint

with an 11-inch tenon with two ipe keys. R-squared values for 5% offset yield load (0.976) and ultimate load (0.928) showed a good fit to key SG. The correlation was not as strong for proportional-limit load with an r-squared value of 0.475. A correlation between joint stiffness and key SG was not performed on Douglas-fir joints because the only Douglas-fir joint that produced an ipe key failure (DF-11-2-2-IPE) was retested on the same mortise member bearing face that was tested with white oak keys. This altered joint stiffness because it was reliant on the bending stiffness of the keys since the keys did not fully contact the pre-crushed surfaces initially.

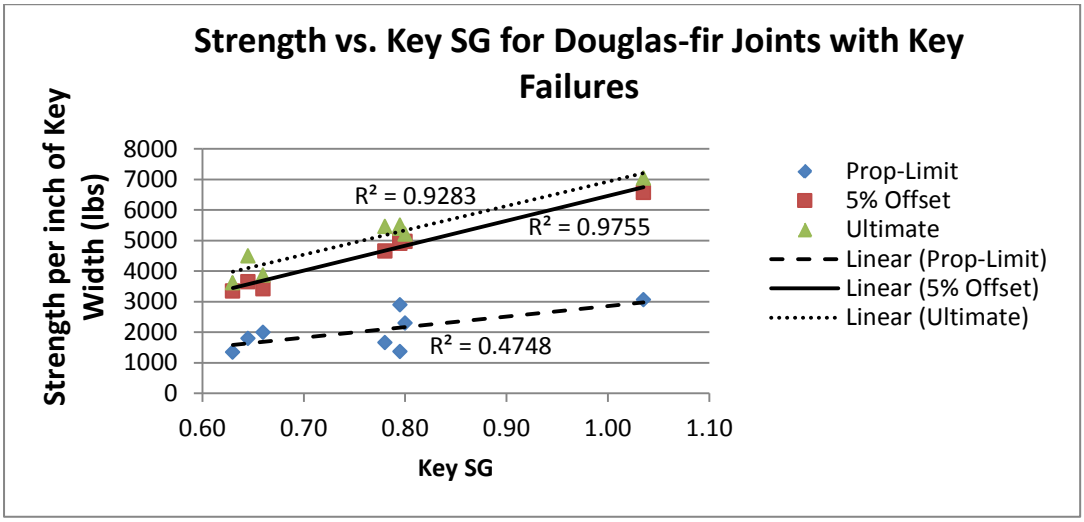

Figure 3-19: Load vs. Key SG for Douglas-fir Joints with Key Failures

Correlations were strongest between joint 5% offset yield load and key SG, closely followed by ultimate, and then proportional-limit load for both white oak and Douglas-fir joints. The lower r-squared values for proportional-limit could be due to the method of selection described in Section 3.1.2.2. The lower r-squared values for white oak joint stiffness, than load, indicated that joint load is more dependent on key SG than joint stiffness. Meaning that, for white oak joints with key failures, as key SG increased, joint stiffness also increased, but not as much as load increased. This section showed that as key SG increased, joint load and stiffness also increased. This indicates the possibility of using correlation values of key SG and different joint species (or SG) to predict joint capacities, for given key sizes, of joints with appropriately sized tenons. However, it should be noted that denser keys experienced bending and less crushing while less dense keys experienced bending and more crushing, especially white oak keys in white oak joints.

3.3 Summary and Conclusions

This paper examined joint load, stiffness, and behavior of full sized, keyed through-tenon joints made in 6x8 white oak and Douglas-fir timbers and compared joint group responses based on species and connection details. Joint behavior and ductility, and comparisons among moisture content (MC) and specific gravity (SG) of joint members and keys are also discussed as well as comparisons between key width-normalized joint responses versus key SG. In general, white oak joints with greater specific gravity had load and stiffness responses equal to or greater than Douglas-fir joints. However, differences in moisture content of the samples complicated these comparisons. Four-inch tenons displayed brittle failures involving the tenon, and 11-inch tenons displayed ductile failures involving the keys. In general, joints with 11-inch tenons had load and stiffness responses greater than or equal to joints with four-inch tenons since joints with 11-inch tenons often utilized the entire key resistance where joints with four-inch tenons did not due to tenon failure. In general, joints with two keys had load and stiffness responses greater than or equal to joints with one key. Joints with four-inch tenons with two keys had twice the shear planes causing greater load and stiffness responses than joints with four-inch tenons with one key. Joints with 11-inch tenons with two keys had greater load and stiffness responses than joints with 11-inch tenons with one key, due to greater total key width in joints with two keys. Key properties between keys in joints with one and two keys were confounded to where white oak keys in joints with two keys had greater specific gravity (greater strength properties) than white oak keys in joints with one key. Many significant differences were found among load and stiffness responses between joint groups with one and two white oak keys after normalizing responses to key width. Differences in the specific gravity of the keys for use in one- and two-key joints were significantly different, affecting these comparisons. Joints with ipe keys had greater load and generally greater stiffness than the same joints originally tested with white oak keys due to the greater specific gravity (greater strength properties) of the ipe keys. For joints producing key failures, white oak keys experienced key bending and crushing while ipe keys experienced key bending and less crushing due to greater specific gravity. When a keyed through-tenon joint produced key failure, joint stiffness was reduced upon installation of replacement keys due to the original key failure that pre-deformed the mortise bearing surface causing reliance of joint stiffness on replacement key bending stiffness, even if the replacement keys are denser than the original. Replacement keys should be cut to match crushed surfaces of

the mortise member to eliminate loss of joint stiffness. Special care is needed to make certain that tenon load would be greater than replacement keys, to avoid constructing a brittle joint. For joints with ductile failure, good correlations existed between key-width normalized joint load and key specific gravity, while a weaker correlation existed between joint stiffness and key specific gravity for white oak joints. This indicated that key specific gravity could be used to predict joint load for given key sizes and appropriately sized tenons. However, it should be noted that denser keys experienced bending and less crushing while less dense keys experienced bending and more crushing, especially in denser (white oak) joints.

Chapter 4: Joint Load Prediction: Through-tenon Key Joint Test Loads and Comparisons

This chapter discusses model input specimen test results, predicted ultimate and allowable joint load, and comparison of experimental joint load to model predictions. Allowable predictions were reduced from 5% offset yield load. Experimental ultimate joint load was compared to predicted ultimate joint load to verify the models in the form of C/T (calculated/ tested) ratios. Allowable joint load predictions were compared to experimental ultimate joint load to determine design safety factors (DSF). Experimental ultimate joint load values were also adjusted by recommendations from Kessel and Augustin (1996) to obtain alternative design values (ADV) which were compared to allowable predicted joint load. 'Joint load' is used to define joint resistance at a given limit state. This chapter is written as the methods, results and discussion, and conclusions of a paper to be submitted to the *Journal of Materials in Civil Engineering.*

4.1 Methods and Materials

This research examined load predictability of keyed through-tenon joints by comparing experimental joint test data to model predictions. Material property samples (hereon known as model input specimens or input specimens) cut from tested joints were used as input parameters for the models. All testing was conducted at the Brooks Forest Products Center at the Virginia Polytechnic Institute and State University.

Figure 4-1 shows the general order of research. First, mathematical models were developed to predict ultimate and allowable joint load. These models incorporated engineering mechanics principles, sections of the *National Design Specification for Wood Construction* (NDS) (AF&PA 2005), and a derivation from the *General Dowel Equations for Calculating Lateral Connection Values, Technical Report 12* (TR-12) (AF&PA 1999). Next, joint tests were conducted to ultimate load to obtain load/displacement data, discussed in the previous chapter. Specimens were cut from tested joints and additional key stock for model inputs. These input specimens included tension parallel-to-grain strength F_t, shear parallel-to-grain strength F_v, bearing parallel and perpendicular-to-grain strength F_e, bending strength F_b, moisture content MC, and specific gravity SG. Finally, the experimental data from the joint tests was compared to the model predictions for model validation.

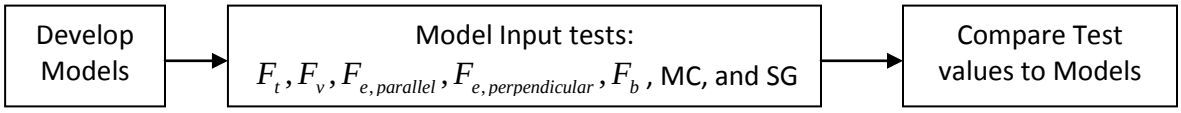

Figure 4-1: Order of Research Tasks

4.1.1 Materials

Mortise and tenon joint members were fabricated from white oak (*Quercus alba*) and Douglas-fir (*Pseudotsuga menziesii*) and fastened with white oak keys. Ipe (*Tabebuia spp*) keys were used to refasten six joints after being tested with white oak keys. Additional key property test species included red oak (*Quercus rubra*), black walnut (*Juglans nigra*), and cherry (*Prunus serotina*). These additional species were not used in joints and only provide material strength test results that could be used for joint load prediction if used as keys.

Figure 4-2 shows input specimen locations of the rough cut (rectangular prisms) and final form as the shapes of the final specimens drawn on the rectangular prisms of joint specimens previously tested. MC and SG specimens representative of mortise and tenon member and keys were discussed in the previous chapter and are only illustrated in Figure 4-2. Tension parallel-to-grain (F_t), shear parallel-to-grain (F_v) and parallel-to-grain bearing ($F_{e,parallel}$) specimens were cut from tenon members. Perpendicular-to-grain bearing ($F_{e,perpendicular}$) specimens were cut from mortise members. Shear parallel-to-grain (F_v), bending (F_b), and perpendicular-to-grain bearing ($F_{e,perpendicular}$) specimens were cut from additional key stock. It should be noted that the SG of the white key stock most closely represented that of white oak keys in joints with one key, indicating similar strength properties. Moisture content (MC) and specific gravity (SG) samples were cut from each input specimen. Input specimens were cut from tenon shoulders and away from mortises to obtain clear specimens and preserve failure locations for observation. Input specimens were initially rough cut from the joint members using a band saw, then end-grain sealed and wrapped in plastic after joint testing. The specimens were later cut to their final dimensions before testing.

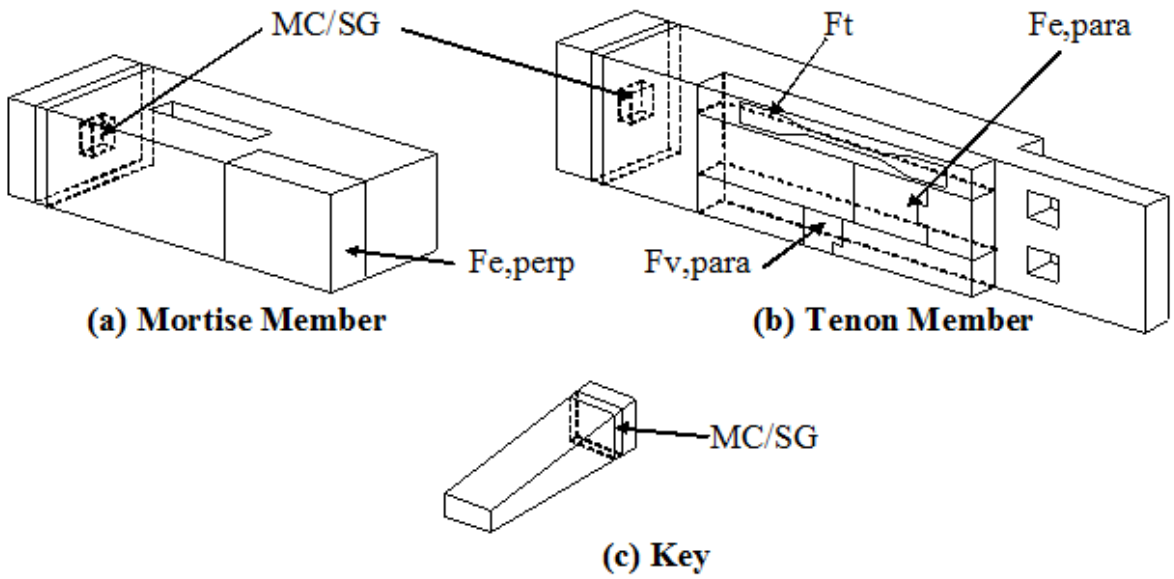

Figure 4-2: Model Input Specimen Cutting Plan

Table 4-1 shows the input specimens conducted and the sample sizes. Forty samples of F_t, F_v, and $F_{e,parallel}$ were cut from the tenon members and forty $F_{e,perpendicular}$ samples were cut from the mortise members, providing a set of matched samples with the joints tested. Key input specimens were of white oak and ipe other species tested included red oak, black walnut, and cherry. Only white oak and ipe keys were used in joint testing. Additional key species testing allowed investigation of mechanical strength properties for keys species other than white oak and ipe. Key input specimens were cut from separate key stock due to size limitations of the keys which created unmatched specimens. Twenty-eight specimens of each key property were tested per species except for ipe. Ipe input specimens were limited in sample size and included only six F_v tests, four F_b tests, and four $F_{e,perpendicular}$ tests. Moisture content and specific gravity specimens were cut from each input specimen. A total of 510 input specimens were tested not including MC/SG samples.

Table 4-1: Model Input Specimen Testing Schedule

Joint Member	Input Specimen [1]	White oak	Douglas-fir	Black walnut	Red oak	Cherry	Ipe	Total
Tenon	Tension parallel-to-grain, F_t	20	20	N/A	N/A	N/A	N/A	40
	Shear parallel-to-grain, F_v	20	20	N/A	N/A	N/A	N/A	40
	Bearing parallel-to-grain, $F_{e,parallel}$	20	20	N/A	N/A	N/A	N/A	40
Mortise	Bearing perpendicular-to-grain, $F_{e,perpendicular}$	20	20	N/A	N/A	N/A	N/A	40
Key(s)	Shear parallel-to-grain, F_v	28	N/A	28	28	28	6	118
	Bending, F_b	28	N/A	28	28	28	4	116
	Bearing perpendicular-to-grain, $F_{e,perpendicular}$	28	N/A	28	28	28	4	116
Total		164	80	84	84	84	14	**510**

[1] Corresponding MC/SG samples were cut from each specimen

4.1.2 Model Input Specimen Testing Procedures

The following sections discuss the model input specimen testing procedures. Each title contains the type of member that specimens represented (tenon, mortise, and/or key). Tension parallel-to-grain specimens and the white oak, red oak, black walnut, and cherry parallel-to-grain shear specimens were tested on an MTS GL10 Electrical Mechanical Test Machine having a load cell with a 10,000 lb range, a displacement sensitivity of 0.001 inches, and an error less than 1% of the load. Data was recorded using MTS Test Works 4 data acquisition software. All other input specimens were tested on an MTS 50 kip Servo-Hydraulic Test Machine where the loads and displacements were measured by the machine's load cell and built-in LVDT with a range of 50,000 lbs, sensitivity of 0.001 inches, and error less than 1% of the load, respectively. The bending tests used a load cell with a 5,500 lb range with an error less than 1% of the load, and a separate LVDT attached to a yoke as described in section 4.1.2.4. Data was recorded using Test Flex 40 data acquisition software.

4.1.2.1 Moisture Content and Specific Gravity Tests (All Members)

ASTM D 4442-92 (ASTM 2004c), *Standard Test Methods for Direct Moisture Content Measurement of Wood-Based Materials, Method A - Primary Oven-Drying Method*, was used to determine moisture content (MC) of the MC/SG test specimens. ASTM D 2395-02 (ASTM 2004d), *Standard Test Methods for Specific Gravity of Wood and Wood-Based Materials, Method B (Mode II), Volume by Water Immersion*, was used to determine specific gravity (SG). MC/SG samples were taken from all mortise, tenon, key, and model input specimens tested.

4.1.2.2 Tension Parallel-to-grain Tests (Tenon Member)

ASTM D 143-94 (ASTM 2004e), Standard *Test Methods for Small Clear Specimens of Timber*, was used for testing tension parallel-to-grain specimens. One specimen was cut per tenon member along with extras, due to testing difficulty, in accordance with Figure 4-2. Specimens were cut in accordance with the standard at 18 inches long with a cross-section of one-inch by one -inch. Four-inches, from each end, remained at the original one-inch by one-inch cross-section and the cross-section of the middle 10 inches was reduced to one-inch by one-half-inches with the largest dimension perpendicular to the growth rings, which produced one-quarter-inch shoulders for the grips of the testing device. The middle two-and-a-half inches of the specimen was reduced to three-eighths of an inch by three-sixteenths of an inch with the direction of the growth rings perpendicular to the greater cross-sectional dimension. The middle two-and-a-half inches, with the smallest cross-section, gradually met the one-inch by one-half inch cross-section using 17.5 inch radii, on each face. The smallest cross-section of some specimens deviated from that specified in the standard with cross-sections as small as one-eighth of an inch by one-quarter of an inch. Difficulty of testing tension specimens was due to limited clear and straight grain specimens with long and small cross-sections and due to cutting small dimensions. Tension specimens were rejected when failure did not occur within the smallest cross-section. Each specimen cut from the tenon member, for WO-4-2-1-T-tn produced failure outside of the smallest cross-section, therefore the tensile strength was taken as the average of the best two of three specimens.

Each specimen was inserted into tension grips as shown in Figure 4-3. Only the maximum load for the tension tests was obtained and no extensometer was used to measure

deformation over the gage length. The load rate was 0.05 inches per minute and testing was terminated upon failure. Six of the Douglas-fir specimens were mistakenly tested at 0.10 inches per minute, however an analysis of variance (ANOVA test) with an alpha (α) value of 0.05 showed no statistically significant difference between the strengths of the two groups (p-value of 0.326). Strength was calculated by dividing the ultimate load by the smallest cross-sectional dimension.

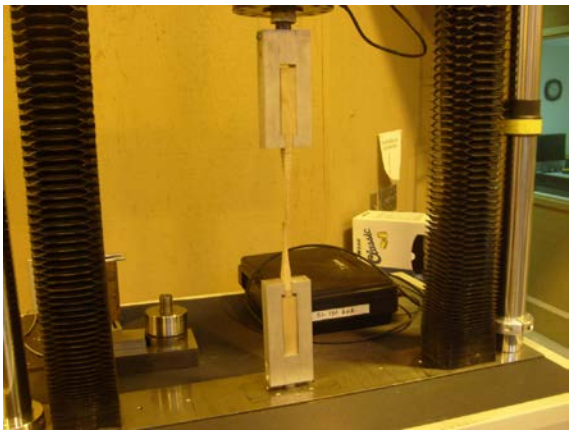

Figure 4-3: Tension Test

4.1.2.3 Shear Parallel-to-grain Tests (Tenon Member and Keys)

The ASTM D 143-94 (ASTM 2004e) procedure was followed for testing shear parallel-to-grain specimens. One specimen per tenon member was cut and 28 specimens per key species were cut from separate stock representing the keys except for ipe, where six specimens were tested. Tenon member shear specimens were cut 2.5 inches along the grain at various thicknesses and widths. Special care was taken in cutting the shear specimens to match the grain orientation of the actual shear planes in the joint tenons. Key stock specimens were cut 2.5 inches along the grain, 2.0 inches thick, and 1.5 inches wide. Each specimen was inserted into a shearing device with a one-eighth inch offset between the inner edge of the supporting surface and the plane of the adjacent edge of the loading surface as shown in Figure 4-4. The load rate was 0.024 inches per minute for tenon member shear specimens and key specimens with white oak, ipe, and six of the red oak specimens. The load rate was 0.020 inches per minute for key specimens of red oak, black walnut, and cherry. The tests were terminated once the specimens sheared. The maximum load was used to calculate the shear strength by dividing by the area of the shear plane.

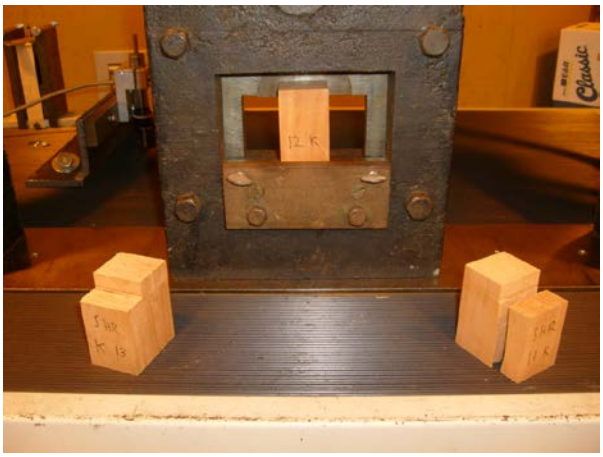

Figure 4-4: Shear Test

4.1.2.4 Bending Tests (Keys)

The ASTM D 143-94 (ASTM 2004e) procedure was followed for the bending input specimens using the secondary method specimen size of a 1.0 inch by 1.0 inch cross-section and a 16-inch length along the grain. The cross section of ipe specimens was 0.9 inches by 0.9 inches due to available stock size. The sample size was 28 per key species as specified in Table 4-1. An LVDT, with a sensitivity of 0.001 inches, was mounted on a yoke suspended from screws over the support points to measure the center-span displacement with respect to the ends of the specimen as shown in Figure 4-5. The load rate was 0.05 inches per minute. The test was terminated when the load decreased by one half the maximum value with no sign of recovery. This was usually accompanied by audible cracking. Proportional-limit and ultimate bending strength were obtained from the load-deformation curve of each specimen.

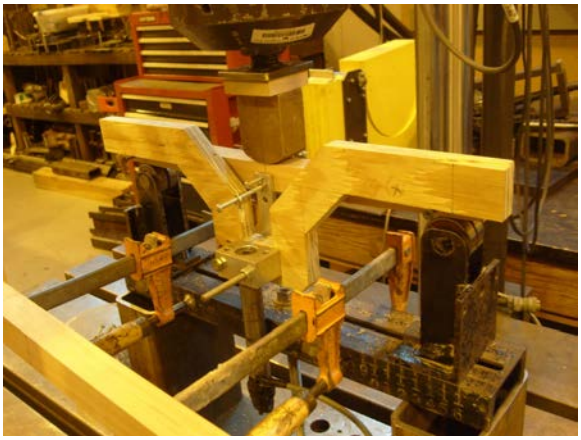

Figure 4-5: Bending Test

4.1.2.5 Bearing Parallel-to-grain Tests (Tenon Member)

ASTM D 5764-97 (ASTM 2004a), *Standard Test Method for Evaluating Dowel-Bearing Strength of Wood and Wood-Based Products*, was used for parallel-to-grain specimen testing. One test per tenon member was cut in accordance with Figure 4-2, totaling 40 specimens. Rough cut specimens were unwrapped and cut five inches along the grain, one-and-a-half inches thick, and four inches wide. A square saddle notch 0.75 inches deep and 1.0 inch wide was cut into one end of each specimen and centered in the width as shown in Figure 4-6. A square notch, instead of a half-round hole, was cut due to key geometry. A steel bearing block, 1.0 inch wide by 2.0 inches long was placed in the saddle notch. The steel block size was chosen to eliminate concerns of exceeding the machine capacity. Specimens were placed in the test machine fitted with a spherical loading block to ensure uniform bearing pressure that compressed the specimens at the saddle notch seat parallel to the grain. The load rate was 0.050 inches per minute. Each test was terminated upon reaching 0.9 inches or once the load decreased by 20% with no sign of recovery. The ultimate bearing load was measured as the maximum load within 0.5 inches of displacement (one-half of the bearing block width). The 5% offset yield load was measured by offsetting a line parallel to the proportional-limit line by 5% of the steel block width (0.05 inches). If the 5% offset yield load occurred after the ultimate load, the 5% offset yield load and ultimate load were taken as the same value in accordance with ASTM D 5764-97 (ASTM 2004a). Strength was calculated by dividing load by bearing area.

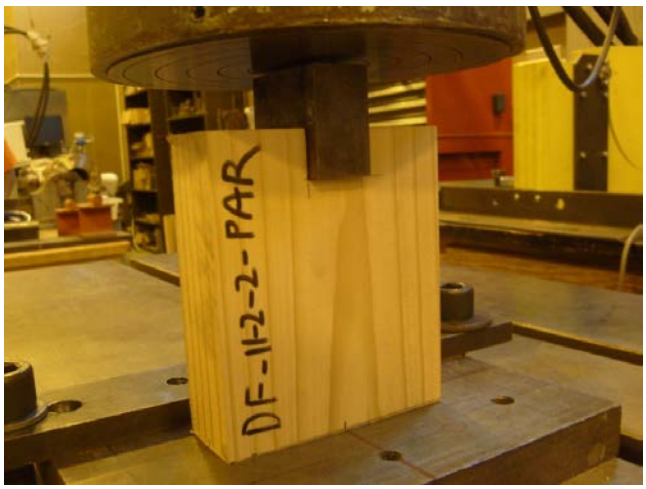

Figure 4-6: Bearing Parallel-to-grain Test

4.1.2.6 Bearing Perpendicular-to-grain Tests (Mortise Member and Keys)

The ASTM D 5764-97 (ASTM 2004a) procedure was followed for perpendicular-to-grain bearing tests. One specimen per mortise member was cut in accordance with Figure 4-2, totaling 20 white oak and 20 Douglas-fir specimens. Mortise bearing specimens were cut at full width of the 5.5 inch-thick mortise members at varying thicknesses and were eight to nine inches along the grain. A steel bearing block 1.0 inch wide, for consistency with the 1.0 inch parallel-to-grain bearing width, by 3.0 inches long, due to varying specimen thicknesses, was used for testing as shown in Figure 4-7. Twenty-eight specimens representative of the keys were cut from separate stock per specie, except for ipe where only four specimens were tested. Key bearing specimens were cut 5.0 inches along the grain, 4.0 inches wide, and 1.5 inches thick for white oak, red oak, black walnut, and cherry. Ipe key bearing input specimens were cut approximately 3.0 inches wide, 1.0 inches thick, and 8.0 inches along the grain. Specimens were placed in the test machine fitted with a spherical loading block to ensure uniform bearing pressure that compressed the specimens perpendicular to the grain. The load rate was 0.075 inches per minute. Each test was terminated upon reaching 0.9 inches or once the load dropped by 20% with no sign of recovery. The ultimate load was measured as the maximum load within 0.5 inches of displacement (one-half of the bearing block width). If the 5% offset yield load occurred after the ultimate load, the 5% offset yield load and ultimate load were taken as the same value in accordance with ASTM D 5764-97 (ASTM 2004a). Strength was calculated by dividing load by bearing area.

Figure 4-7: Bearing Perpendicular-to-grain Test

4.1.3 Models for Joint Load Prediction of Keyed Through-Tenon Joints

The following models were developed to predict the ultimate and allowable joint load and behavior of keyed through-tenon joints. Ultimate joint load predictions were developed for direct comparison to experimental values. Allowable (ASD) joint load predictions were developed to predict design values which were the minimum of allowable predictions for a joint. Models are based on engineering mechanics principles, including sections of the NDS (AF&PA 2005) and TR-12 (AF&PA 1999). Ultimate material strengths from input specimens were used for ultimate joint load predictions, while allowable design (ASD) strengths, and 5% offset yield strength of input specimens with appropriate reduction factors were used for allowable joint load predictions. Key strength input specimens were averaged from key stock specimen tests, while mortise and tenon input specimens strengths where taken from matched specimens.

The minimum model prediction of each joint was chosen as the governing joint load, which was termed 'design load' for allowable predictions. All members were analyzed separately including the tenon member, mortise member, and key(s). All models considered only short duration loading and neither friction between the mortise and tenon members nor the pretensioning forces from key insertion were accounted for. Joint loading is described as follows:

- As the tenon member was tensioned, the tenon keyholes bore against the keys resulting in parallel-to-grain bearing stress against the tenon keyholes and perpendicular-to-grain bearing stress against the keys.
- Bearing stresses against tenon keyholes produced parallel-to-grain tensile stress in the tenon net-section and shear parallel-to-grain stress in the tenon, resulting in the possibility of row tear-out (relish failure) and variations of group tear out (block shear).
- Tenon keyhole bearing stress was transferred through the keys to the mortise member, subjecting the keys to bending, perpendicular-to-grain bearing, and parallel-to-grain shear stress from transverse loading.
- Transverse key loading imposed perpendicular-to-grain bearing stress against the mortise member which was restrained by the test fixture. Restraining the mortise member did not alter load results since keys were installed on the backside of the mortise member. Mortise wall splitting, due to perpendicular-to-grain tension, caused by pegs would have

been prohibited, altering load results for pegged joints if restrained as these joints were with tie-downs close to the tenon member as shown in figure 3-2 in the previous chapter.

Table 4-2 shows models used for joint load prediction with the abbreviation, full name, and associated joint component. Tenon Net-section Tension at keyholes (Z_{NT}), Tenon Parallel-to-grain Keyhole Bearing (Z_{Im}), Tenon Row Tear-out/ Tenon Relish (Z_{RT}), and Tenon Group Tear-out/ Block Shear (Z_{GT} a,b,c,d) were associated with tenon failures. Mortise Bearing (Z_{Is}) was associated with the mortise member. Key Bending ($Z_{III_m,M,T}$ and $Z_{III_m,K}$), Key Bearing ($Z_{\mathrm{Im}-K}$ and Z_{Is-K}), and Key Horizontal Shear (Z_{K_v}) were associated with key failures. It should be noted that models for joint load predictions were developed prior to experimentation. Failure modes from some of the joint tests occurred that the models did not account for. Such failure modes were tenon splitting, tenon split spreading, relish failure of only one key in a joint with two keys, and failure of a single tenon shear plane, which are described in the previous chapter.

Table 4-2: Models with Abbreviations and Full Name and Associated Joint Component

Model	Full Name of Model	Joint Member
Z_{NT}	Tenon Net-section Tension (at keyholes)	Tenon Member
Z_{Im}	Tenon Parallel-to-grain Keyhole Bearing	
Z_{RT}	Tenon Row Tear-out/ Tenon Relish	
Z_{GT} [1]	Tenon Group Tear-out/ Block Shear	
Z_{Is}	Mortise Bearing	Mortise
$Z_{III_m,M,T}$	Key Bending (considering Mortise and Tenon Member Bearing strength only)	Key(s)
$Z_{III_m,K}$	Key Bending (considering Bearing strength of all Joint Components)	
$Z_{\mathrm{Im}-K}$	Key Bearing (against Tenon Keyhole)	
Z_{Is-K}	Key Bearing (against Mortise Member)	
Z_{K_v}	Key Horizontal Shear	

[1] See section 4.1.6.1 for Z_{GT} (a,b,c,d)

4.1.3.1 Tenon Member Models (Figure 4-2b)

Tenon Net-Section Tension (at Keyholes)

Tension loading was entirely transferred through the tenon net-section at the keyholes. Joint load was calculated by multiplying the net-section area $\left[T_t\left(T_w - nK_h\right)\right]$ by tension parallel-to-grain strength, F_t. Ultimate load predictions used ultimate parallel-to-grain tension strength from specimen tests. Allowable load predictions used adjusted ASD parallel-to-grain tension strength from the NDS (AF&PA 2005).

$$Z_{NT} = F_t\left[T_t\left(T_w - nK_h\right)\right] \quad \textbf{(4-1)}$$

Where:

Z_{NT} = Tenon Net-section Tension Joint Load, *lbs*

F_t = Parallel-to-Grain Tension Strength, *psi*

T_t = Tenon Thickness, *in*

T_w = Tenon Width, *in*

n = Number of Keys

K_h = Keyhole Width, *in*

Tenon Parallel-to-grain Keyhole Bearing

Joint loading caused parallel-to-grain bearing against the tenon keyholes. Bearing area is the product of key width, K_w, tenon thickness, T_t, and number of keys, n. Ultimate load predictions used the ultimate strength of parallel-to-grain bearing specimen tests. Allowable load predictions used the 5% offset yield strength of the parallel-to-grain bearing input specimen tests, divided by a reduction factor of 4.0, which represents main member bearing for yield Mode I_m (AF&PA 2005).

$$Z_{\mathrm{Im}} = \frac{F_{e-t,para}\left(nT_tK_w\right)}{R_{d,\mathrm{Im}}} \quad \textbf{(4-2)}$$

Where:

Z_{Im} = Tenon Parallel-to-Grain Keyhole Bearing Joint Load, *lbs*

$F_{e-t,para}$ = Tenon Parallel-to-grain Bearing Strength (ultimate strength for ultimate load prediction and 5% offset strength for allowable load prediction), *psi*

n = Number of Keys

T_t = Tenon Thickness, *in*

K_w = Key Width, *in*

$R_{d,\mathrm{Im}}$ = Reduction Factor (1.0 for ultimate load, 4.0 for allowable load)

Tenon Row Tear-out/ Tenon Relish

Key bearing against tenon keyholes caused parallel-to-grain shear stress in the tenon. This failure type was associated with a sheared block of the tenon, behind each key, protruding from the tenon end. The total shear area was multiplied by the material shear strength, and divided by two to account for triangular shear stress distributions (AF&PA 2005). The area of one shear plane was determined by the product of tenon thickness, T_t, and the quantity of greatest key depth at the tenon face, $D_{\max,tenon}$, subtracted from the protruding tenon length, T_l. Ultimate load predictions used ultimate material parallel-to-grain shear strength from input specimen tests and the allowable load predictions used ASD parallel-to-grain shear strength, F_v, from the NDS (AF&PA 2005).

$$Z_{RT} = nF_v\left[T_t\left(T_l - D_{\max,tenon}\right)\right] \qquad \textbf{(4-3)}$$

Where:

Z_{RT} = Tenon Row Tear-out Joint Load, *lbs*

n = Number of Keys

F_v = Parallel-to-Grain Shear Strength, *psi*

T_t = Tenon Thickness, *in*

T_l = Protruding Tenon Length, *in*

$D_{\max.tenon}$ = Greatest Key Depth at Tenon Face, *in*

Tenon Group Tear-out/ Block Shear

Bearing against tenon keyholes caused several possible variations of group tear-out. Group tear-out is a combination of tension and shear parallel-to-grain. As shown in Figure 4-8, one group tear-out mode was calculated for single keyed joints (Figure 4-8a), and three modes were calculated for double keyed joints (Figures 4-8b,c, and d). Group tear-out load for joints with two keys was equal to the minimum load of the three cases. The rectangular boxes with an 'x' represent the keys. The rectangles with two 'P/2' loads represent the mortise member while the single 'P' load acts on the tenon member. Shear planes are in the vertical direction while tension planes are horizontal. Ultimate tension and shear parallel-to-grain strengths from input specimen tests were used for ultimate load predictions and adjusted ASD values for tension and shear strength were taken from the NDS (AF&PA 2005) for allowable load predictions.

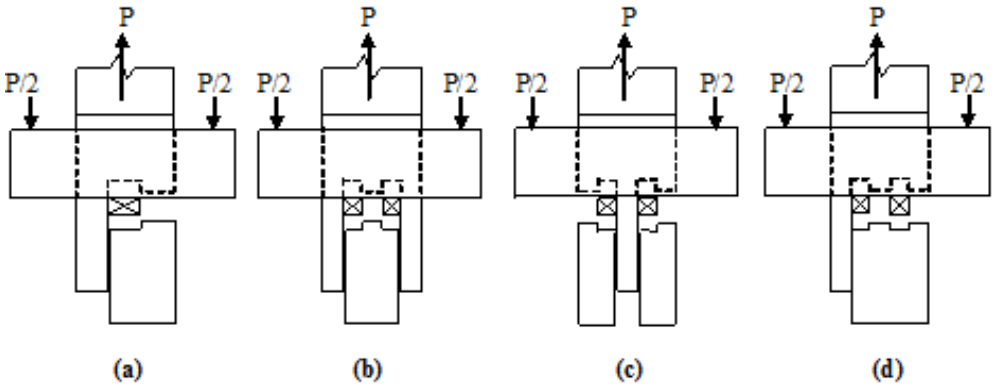

Figure 4-8: Possibilities of Group Tear-out for Single and Double Keyed Joints

Equations 4-4(a-d) predicted the group tear-out loads of joints with one and two keys. Equation 4-4a predicted the group tear-out load of Figure 4-8(a), representing a shear plane on one edge of the key and a net-section tension plane on the other edge. Equation 4-4b predicted the group tear-out load shown in Figure 4-8(b), representing a global tenon tear-out between the outer edges of the keys (two shear planes) with a net-section tension plane forming between the keyholes. Equation 4-4c predicted the group tear-out load of Figure 4-8(c), where two outer blocks separated from the tenon center. This failure type occurred from the development of a shear plane at the inner edge of each key and a net-section tension plane between the outer edge of each key and the tenon edges. Equation 4-4d predicted the group tear-out load of Figure 4-8(d) similar to the single keyed group tear-out. This failure type represented the development of

a shear plane on the outer edge of one of the keys and net-section tension planes between the keyholes and the outer edge of the other keyhole to the tenon edge.

$$Z_{GT} = \frac{nF_v\left[T_t\left(T_l - D_{\max,tenon}\right)\right]}{2} + \frac{F_t T_t\left(T_w - K_h\right)}{2}, n = 1 \quad \textbf{(4-4a)}$$

$$Z_{GT} = \frac{nF_v\left[T_t\left(T_l - D_{\max,tenon}\right)\right]}{2} + F_t T_t D_k, n = 2 \quad \textbf{(4-4b)}$$

$$Z_{GT} = \frac{nF_v\left[T_t\left(T_l - D_{\max,tenon}\right)\right]}{2} + F_t T_t\left[T_w - \left(D_k + nK_h\right)\right], n = 2 \quad \textbf{(4-4c)}$$

$$Z_{GT} = \frac{nF_v\left[T_t\left(T_l - D_{\max,tenon}\right)\right]}{4} + F_t T_t\left[D_k + \left(\frac{T_w - \left(D_k + nK_h\right)}{2}\right)\right], n = 2 \quad \textbf{(4-4d)}$$

Where:

Z_{GT} = Tenon Group Tear-out Joint Load, *lbs*

n = Number of Keys

F_v = Parallel-to-Grain Shear Strength, *psi*

T_t = Tenon Thickness, *in*

T_l = Protruding Tenon Length, *in*

$D_{\max,tenon}$ = Greatest Key Depth at Tenon Face, *in*

F_t = Parallel-to-Grain Tension Strength, *psi*

T_w = Tenon Width, *in*

K_h = Keyhole Width, *in*

D_k = Distance Between Keyholes, *in*

4.1.3.2 Mortise Member Model (Figure 4-2a)

Mortise Bearing

Load prediction of the mortise member included perpendicular-to-grain bearing due to the load acting through the keys with the assumption of uniform bearing. Joint load was calculated by multiplying the bearing area and mortise-member bearing strength, $F_{e-m,perp}$. The bearing area was the product of key width, K_w, length of key in contact with the mortise member $(M_w - T_t - 2Gap)$, and the number of keys, n. This model also assumed that the key was in contact with the entire width of the mortise. Ultimate load predictions used the ultimate bearing strength of the mortise-member perpendicular-to-grain input specimen tests. Allowable load predictions used the 5% offset bearing yield strength of the mortise-member perpendicular-to-grain input specimen tests divided by reduction factor of 5.0, representative of yield Mode I_s (AF&PA 2005). The 5% offset distance was 5% of the width of the steel bearing block (0.05 inches).

$$Z_{Is} = \frac{F_{e-m,perp}(nK_w)(M_w - T_t - 2Gap)}{R_{d,Is}} \quad \textbf{(4-5)}$$

Where:

Z_{Is} = Mortise Bearing Joint Load, *lbs*

$F_{e-m,perp}$ = Mortise Perpendicular-to-grain Bearing Strength (ultimate strength for ultimate model and 5% offset strength for allowable model), *psi*

n = Number of Keys

K_w = Key Width, *in*

M_w = Mortise Member Width, *in*

T_t = Tenon Thickness, *in*

Gap = Gap between Mortise and Tenon surfaces, *in*

$R_{d,Is}$ = Reduction Factor, (1.0 for ultimate load, 5.0 for allowable load)

4.1.3.3 Key Models (Figure 4-2c)

Key Bending

The key bending mode was predicted using TR-12 (AF&PA 1999) considering key (as well as mortise and tenon) bearing strength, key bending strength, and any gaps between the mortise and tenon from dimensional tolerances. Figure 4-9 shows the external and internal key forces considering only bending due the loading that generated the shear and moment diagrams presented in Figure 4-10. The load 'P' is the bearing of the tenon keyhole against one key, while the '$P/2$' loads are the assumed bearing reactions against the mortise member, per key. Key bending stress increased as a result of increased bearing force as load increased. Joint load relied on key bending resistance to transverse bearing forces from tension loading. Bearing was assumed to be uniformly distributed emanating outward from the mortise and tenon interfaces, where shear forces were greatest, and then terminating at a location along the key length at the mortise sides once a bending stress in the key at the center tenon thickness matched its associated bending resistance. Key slope was assumed to have a negligible effect on bending.

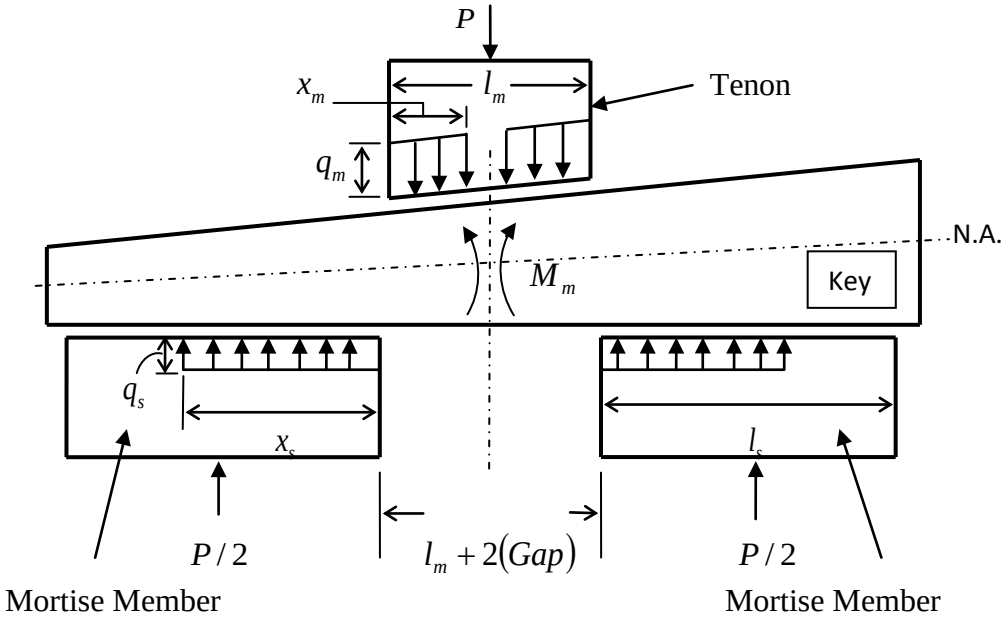

Figure 4-9: Key Bending and Bearing Mechanics Model

Where:

P = Transverse Shear per Key, lbs

l_m = Main Member Width (Tenon Thickness, T_t), *in*

x_m = Main Member Bearing Length, *in*

q_m = Main Member or Key Bearing Resistance, *lbs/in*

l_s = Contact Interface between Key and Mortise Member, *in*

x_s = Side Member Bearing Length, *in*

q_s = Side Member or Key Bearing Resistance, *lbs/in*

M_m = Key Moment Resistance, *lb-in*

Gap = Distance between Mortise and Tenon, *in*

Figure 4-10 shows the shear and moment diagrams for transversely loaded keys. Gaps existed between the mortise and tenon resulting from dimensional tolerances and were assumed to be equal at each interface. Bearing of the tenon key-hole against the keys caused an opposite bearing reaction of the mortise member generating shear and bending stress in each key. Tenon bearing resistance is represented by q_m, while mortise member bearing resistance is represented by q_s. Maximum shear occurred at the gaps between the mortise and tenon interfaces and maximum moment occurred in each key at the center tenon thickness.

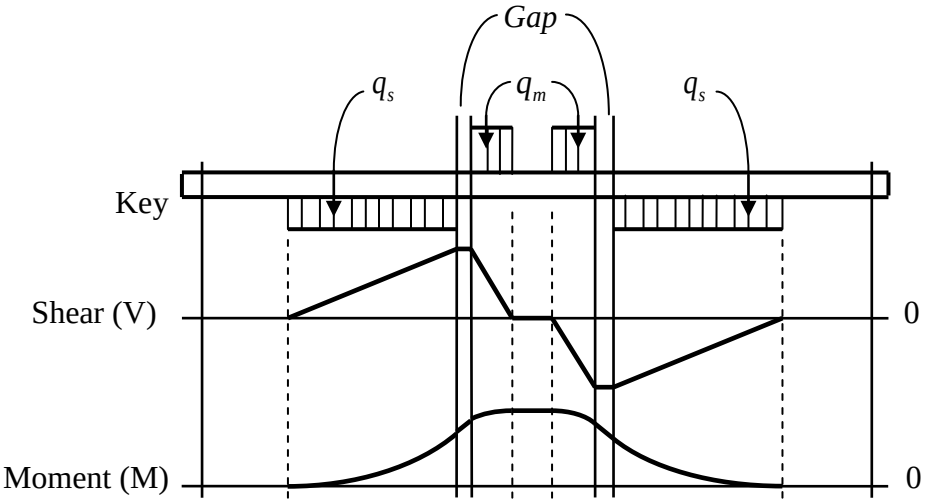

Figure 4-10: Shear and Moment Diagram of Loaded Key

TR-12 (AF&PA 1999) discussed the derivation of single dowel connection load, using generalized and expanded forms of the NDS (AF&PA 1997). Figure 4-11 shows the free body diagram to derive a yield, or load, limit equation representative of the failure type for a sloped, rectangular, wooden fastener (or key) in an unrestrained double shear connection. Unrestrained

means that the key ends are unrestrained against upward rotation upon flexure. Joint load related to key bending resistance was derived using Equations 4-6 through 4-9. Half of the key is shown due to load symmetry.

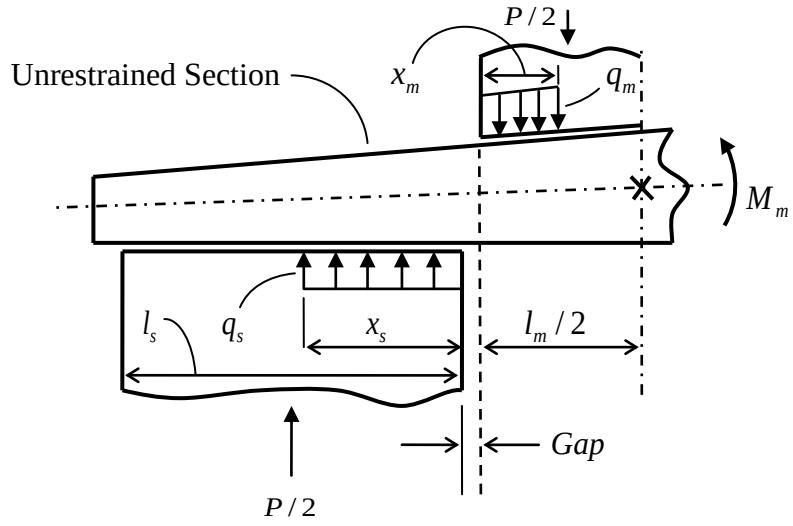

Figure 4-11: General Key Bending Load Equation Derivation Model

Equations in 4-6(a-c) relate bearing length, x, and resistance, q, to load, P. Variables with the subscript 's' represent the side or mortise member, while variables with the subscript 'm' represent the main or tenon member. The load 'P' is equivalent to twice the product of bearing resistance and bearing length because two shear planes exist per key. Moments acting about the neutral-axis of the key at the tenon center, where key bending moment was highest, was assumed for Equation 4-7. Inserting Equations 4-6 into Equation 4-7, substituting bearing length for the transverse load produced Equation 4-8. Equation 4-8 can be simplified to Equation 4-9, producing the general key bending load equation. Note that M_m in Equation 4-9 is equal and opposite to the moment produced by bearing forces of the mortise and tenon member against the key(s).

$$(x)(q) = P/2 \quad \textbf{(4-6a)} \qquad x_s = P/(2q_s) \quad \textbf{(4-6b)} \qquad x_m = P/(2q_m) \quad \textbf{(4-6c)}$$

$$\sum M_X = 0: \; q_m(x_m)\left(\frac{l_m}{2} - \frac{x_m}{2}\right) - q_s(x_s)\left(\frac{x_s}{2} + Gap + \frac{l_m}{2}\right) + M_m = 0 \qquad \textbf{(4-7)}$$

$$\sum M_X = 0: \; q_m\left(\frac{P}{2q_m}\right)\left(\frac{l_m}{2} - \frac{P}{4q_m}\right) - q_s\left(\frac{P}{2q_s}\right)\left(\frac{P}{4q_s} + Gap + \frac{l_m}{2}\right) + M_m = 0 \quad \textbf{(4-8)}$$

$$\frac{P^2}{8}\left(\frac{1}{q_m}+\frac{1}{q_s}\right)+\frac{(P)(Gap)}{2}-M_m=0 \qquad \textbf{(4-9)}$$

The tensile load acting on the joint creating the transverse key load, P, was equal to the total bearing force on either the top or bottom side of the key, $2q_m x_m$ or $2q_s x_s$, multiplied by the number of keys. Key moment resistance, M_m, is equal to the product of key bending strength and the key section modulus at the tenon center. Equation 4-9 requires manual iterations to obtain P. Equation 4-10 was derived from equation 4-9 using Mathematica Version 7 software to eliminate the need for iterations.

$$Z_{III_m}=(n)\frac{2\left[-Gap(q_m q_s)+\sqrt{q_m q_s\left(Gap^2 q_m q_s+2M_m(q_m+q_s)\right)}\right]}{R_{d,III_m}(q_m+q_s)} \qquad \textbf{(4-10)}$$

Where:

Z_{III_m} = Key Bending Joint Load, *lbs*

n = Number of Keys

Gap = Distance Between Mortise and Tenon, *in*

q_m = Main Member or Key Bearing Resistance, *lbs/in*

q_s = Side Member or Key Bearing Resistance, *lbs/in*

M_m = Key Bending Strength; ultimate strength for ultimate load predictions, and addition of half of ultimate strength and half proportional-limit strength for allowable load predictions, *lb-in*

R_{d,III_m} = Reduction Factor (1.0 for ultimate model and 4.0 for allowable model)

Ultimate and allowable joint load predictions for key bending were calculated twice considering the bearing strength of the mortise and tenon members without regard to that of the key and also considering the lesser of the mortise and tenon, or key bearing strength for the respective bearing interface. Joint load for either prediction was the lesser of the output values between bearing strength considerations. Ultimate load predictions used the average ultimate bending and bearing strength from key material bending input specimen testing and ultimate bearing strength from individual mortise and tenon bearing input specimen testing. TR-12

prediction for 5% offset bending strength of bolts, lag screws, and drift pins was the addition of tensile yield strength (proportional-limit strength) and ultimate tensile strength, divided by two (AF&PA 1999). So, the addition of average proportional-limit bending strength and average ultimate bending strength, divided by two, from key bending input specimen tests was used to predict the 5% offset bending strength of the key material used for allowable load predictions. Allowable load predictions used the 5% offset bearing strength from input specimens with an offset of 5% of one inch, or 0.05 inches. The allowable joint load prediction was reduced by 4.0 from Yield Mode III_m in the NDS (AF&PA 2005).

Key Bearing

Equation 4-11a predicts joint load based on the bearing of the tenon against the key surface as the product of key bearing strength and bearing area of contact between the tenon keyhole and the key. The tenon keyhole bearing area was equal to the product of the number of keys, n, key width, K_w, and tenon thickness, T_t. Equation 4-11b predicts joint load based on the bearing area of the mortise member against the key surface as the product of key bearing strength and bearing area of contact between the mortise member and the key. Bearing area of the contact between the mortise member and the key surface is equal to the product of the number of keys, n, key width, K_w, and bearing length which is the mortise member width subtracted by the quantity of tenon thickness and gaps, $M_w - T_t - 2Gap$. Tenon keyhole bearing was assumed to control due to the smaller bearing area compared to the mortise face/key bearing area. Ultimate load predictions used the average ultimate strength of perpendicular-to-grain key bearing specimen tests. Allowable load predictions used the average 5% offset yield strength of perpendicular-to-grain key bearing specimen tests, divided by a reduction factor of 5.0 for perpendicular-to-grain bearing, which was representative of yield modes I_m and I_s in the NDS (AF&PA 2005), for Equations 4-11a and 4-11b.

$$Z_{\mathrm{Im}-K} = \frac{nK_wT_tF_{e-K,perp}}{R_{d,\mathrm{Im}-K}} \qquad \textbf{(4-11a)}$$

$$Z_{Is-K} = \frac{nK_w\left[M_w - T_t - 2Gap\right]\left(F_{e-K,perp}\right)}{R_{d,Is-K}} \qquad \textbf{(4-11b)}$$

Where:

$Z_{\mathrm{Im}-K}$ = Joint load of Key-Tenon Member Perpendicular-to-grain Bearing Strength, *lbs*

Z_{Is-K} = Joint load of Key-Mortise Member Perpendicular-to-grain Bearing Strength, *lbs*

n = Number of Keys

K_w = Key Width, *in*

M_w = Mortise Member Width, *in*

T_t = Tenon Thickness, *in*

Gap = Distance between Mortise and Tenon, *in*

$F_{e-K,perp}$ = Key Perpendicular-to-grain Bearing Strength, *psi*

$R_{d,\mathrm{Im}-K}$ = Reduction Factor (1.0 for ultimate load, 5.0 for allowable load)

$R_{d,Is-K}$ = Reduction Factor (1.0 for ultimate load, 5.0 for allowable load)

Key Horizontal Shear

Each key was subjected to transverse shear as the tenon keyhole and mortise member face bore from tensile loading of the joint. Transverse shear loading on each key is assumed to be halved among the two shear planes at the mortise and tenon interfaces. This model uses one single transverse key shear plane and assumed that the entire key length resists horizontal or parallel-to-grain shear forces from the combined shear at each shear plane. Equation 4-12 shows the key horizontal shear resistance to one transverse shear plane as the product of key width, key shear strength divided by two to account for the assumption of triangular shear stress distribution, and key length divided by two to account for the two transverse shear planes.

$$K_T = K_w(F_v/2)(K_L/2) = \frac{K_w F_v K_L}{4} \quad \textbf{(4-12)}$$

Where:

K_T = Horizontal Shear Resistance (half of one Key), *lbs*

K_w = Key Width, *in*

F_v = Key Shear Strength, *psi*

K_L = Key Length, *in*

The total horizontal shear force produced by transverse shear was assumed to be distributed along the key length, until the maximum key horizontal shear resistance K_T was reached, dictating the maximum joint strength. The maximum transverse load for a key is *P*. Neglecting key slope, Figure 4-12 shows the key loading, the resulting shear diagram, and an enlargement of the shear diagram at one shear plane. The transverse shear, used to determine horizontal key shear, was converted from a trapezoid to an equivalent rectangle for simplicity of horizontal shear calculation.

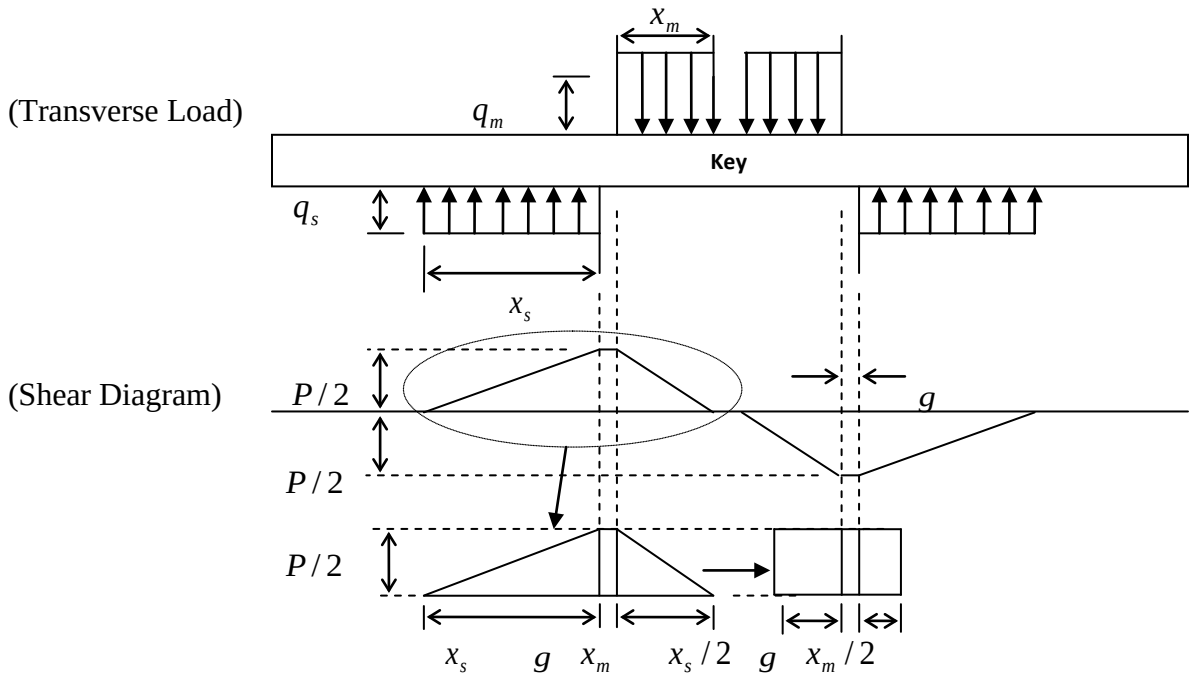

Figure 4-12: Transverse Key Shear

Where:

P = Maximum Joint Load carried be one Key, *lbs*

$P/2$ = Maximum Joint Load carried per Key shear plane, *lbs*

x_m = Main (Tenon) Member Bearing Length, *in*

q_m = Minimum of Main Member or Key Bearing Resistance, *lbs/in*

x_s = Side (Mortise) Member Bearing Length, *in*

q_s = Minimum of Side (Mortise) Member or Key Bearing Resistance, *lbs/in*

$g = Gap =$ Distance between Mortise and Tenon, *in*

Equations 4-13 (a-f) show the derivation of shear flow, *q*, according to Figure 4-12. Equation 4-13b is inserted into equation 4-13a to obtain the shear flow related to the maximum transverse key shear, P, shown in Equation 4-13c. Joint strength was analyzed with respect to the smallest key transverse shear plane with a key depth of K_d. Equations 4-13d and 4-13e are the first moment of area, *Q*, and moment of inertia, *I*, respectively, of the smallest key cross-section at a shear plane with respect to key width, K_w, and the corresponding key depth, K_d. Inserting Equations 4-13d and 4-13e into Equation 4-13c yields the shear flow, q, with respect to maximum transverse key shear, P, and the smallest key cross-section at a shear plane, Equation 4-13f.

$$q = \frac{VQ}{I} \quad \textbf{(4-13a)} \qquad V = P/2 \quad \textbf{(4-13b)} \qquad q = \frac{PQ}{2I} \quad \textbf{(4-13c)}$$

$$Q = \frac{K_w K_d^2}{8} \quad \textbf{(4-13d)} \qquad I = \frac{K_w K_d^3}{12} \quad \textbf{(4-13e)} \qquad q = \frac{3P}{4K_d} \quad \textbf{(4-13f)}$$

Where:

q = Shear Flow, *lbs/in*

$V = P/2$ = Maximum Joint load carried per Key shear plane, *lbs*

Q = First Moment of Area of smallest key cross-section at a shear plane, *in^3*

I = Moment of Inertia of smallest key cross-section at a shear plane, *in^4*

K_d = Key Depth of smallest key cross-section at a shear plane, *in*

K_w = Key Width, *in*

Keys were assumed to fail after the available horizontal shear strength in the entire key length, K_L, was reached, as shown by Equations 4-14a and 4-14b. Bearing length of the main member, x_m, and side member, x_s, are functions of transverse key shear as shown in Equations 4-6 (a-c). Equations 4-6 and 4-13f are inserted into Equation 4-14a to obtain the maximum transverse key shear dictated by the total horizontal key shear load, Equation 4-14b.

$$q\left[\frac{x_m + x_s}{2} + g\right] = K_T \qquad \textbf{(4-14a)}$$

$$\frac{3P}{4K_d}\left[\frac{P}{4q_m} + \frac{P}{4q_s} + g\right] = \frac{K_w K_L F_v}{4} \qquad \textbf{(4-14b)}$$

Equation 4-14b, shown above, contains P and P^2 which requires iterations of P to obtain the maximum transverse key force and ultimately the joint load, Z_{K_v}. To avoid iterations, Equation 4-14b was set to zero and the quadratic formula applied to determine P directly. Equations 4-15 (a-d), below, show the derivation of Equation 4-14b using the quadratic formula to solve for the maximum joint load regarding horizontal key shearing. First, Equation 4-14b was set to zero, as shown in Equation 4-15a. Then the quadratic formula, Equation 4-15b, was applied to equation 4-15a to obtain P, as shown in Equation 4-15c. Equation 4-15c was then multiplied by the number of keys, n, to obtain maximum joint load for horizontal key shear, Z_{K_v} in Equation 4-15d.

$$P^2\left[\frac{3}{4K_d q_m} + \frac{3}{4K_d q_s}\right] + P\left[\frac{3g}{K_d}\right] - K_w K_L F_v = 0 \qquad \textbf{(4-15a)}$$

$$P = \frac{-B + \sqrt{B^2 - 4AC}}{2A} \qquad \textbf{(4-15b)}$$

$$P = \frac{-\left[\frac{12g}{K_d}\right] + \sqrt{\left[\frac{12g}{K_d}\right]^2 + 4\left[\frac{3}{K_d q_m} + \frac{3}{K_d q_s}\right]\left(K_w K_L F_v\right)}}{2\left[\frac{3}{K_d q_m} + \frac{3}{K_d q_s}\right]} \qquad \textbf{(4-15c)}$$

$$Z_{K_v} = (n)\frac{-\left[\frac{12g}{K_d}\right] + \sqrt{\left[\frac{12g}{K_d}\right]^2 + 4\left[\frac{3}{K_d q_m} + \frac{3}{K_d q_s}\right]\left(K_w K_L F_v\right)}}{2\left[\frac{3}{K_d q_m} + \frac{3}{K_d q_s}\right]} \qquad \textbf{(4-15d)}$$

Where:

Z_{K_v} = Maximum Joint Load for horizontal key shear, *lbs*

P = Maximum Joint Load carried be one Key (Z_{K_v}, if joint has only one key), *lbs*

n = Number of Keys

q_m = Minimum of Main (Tenon) Member or Key Bearing Resistance, *lbs/in*

q_s = Minimum of Side (Mortise) Member or Key Bearing Resistance, *lbs/in*

$g = Gap$ = Distance between Mortise and Tenon, *in*

K_d = Key Depth of smallest key cross-section at a shear plane, *in*

K_w = Key Width, *in*

F_v = Key Shear Strength, *psi*

K_L = Key Length, *in*

Ultimate load predictions used average ultimate key shear strength and average ultimate bearing strength values from key, mortise, and tenon bearing input specimens. Allowable load predictions used NDS (AF&PA 2005), ASD, adjusted allowable parallel-to-grain shear key strength. Allowable load predictions regarding bearing strength used 5% offset strength values divided by reduction factors. Reduction factors included 5.0 for perpendicular-to-grain bearing input specimens (mortises and keys), and 4.0 for parallel-to-grain bearing input specimens (tenons).

4.2 Results and Discussion

This section discusses ultimate and allowable joint load predictions and comparisons to experimental joint data. Model input specimen strength results are discussed in Section 4.2.1, and then used to determine load predictions in Section 4.2.2. Comparisons of predicted to experimental ultimate joint load, Section 4.2.3, used C/T (calculated value/ tested value) ratios. Design safety factors (DSFs), Section 4.2.4, were determined by comparing minimum allowable (design) joint load predictions to experimental ultimate joint load. Experimental ultimate joint load values were divided by recommended factors from Kessel and Augustin (1996), for alternative design values (ADVs), which were compared to the design joint load predictions in Section 4.2.5.

4.2.1 Model Input Specimen Test Results

Model input specimens were tested in accordance with Section 4.1.5. The subsections below are organized by joint member and each test associated with the member. Sections 4.2.1.1 through 4.2.1.3 give the results of the input specimens of the tenon members, 4.2.1.4 gives the results of the mortise member input specimens, and 4.2.1.5 through 4.2.1.7 give the results of the key input specimens. MC/SG results of the input specimens are mentioned within the individual subsections.

Tables in this section contain clear wood strength values (+/- two standard deviations), that were obtained from ASTM D2555 (ASTM 2004f), *Establishing Clear Wood Strength Values* for comparison to input specimen strength values. Two standard deviations above and below the average represent 95% of the data for strength values. The ASTM D2555 values for white oak joint members were based on the unseasoned condition, where ASTM D2555 values for Douglas-fir are based on the seasoned condition, based on the MC values from the previous chapter. The test results for individual specimens are in Appendix F. Douglas-fir specimens were assumed to be Douglas-fir South based on the oven-dry specific gravity of approximately 0.47 to 0.48. Allowable NDS predictions used Douglas-fir South values for Douglas-fir specimens. White oak specimens were assumed to be true white oak and red oak specimens were assumed to be Northern red oak for comparison purposes. All timbers considered for allowable predictions were assumed best represented by grade No. 1, post-and-timber values

presented in the NDS. Moisture content of mortise and tenon members decreased from the time of joint testing to the time of input specimen testing since input specimens were tested after joint testing, indicating that end grain sealing and wrapping rough cut specimens in plastic does not completely protect against moisture loss. This loss in moisture content did not affect the models since all white oak specimens remained above fiber saturation point and Douglas-fir joints remained below fiber saturation point.

4.2.1.1 Tension Parallel-to-grain Input Specimen Tests (Tenon)

Table 4-3 shows the average and coefficient of variation (COV) of the average tensile strength, MC, and SG of the white oak and Douglas-fir tension specimens cut from tenon members. Table 4-3 also shows strength values of small clear wood specimens from ASTM D2555, for verification of input specimen strength values. The average tensile strength of white oak was 13.1% greater than Douglas-fir. The average tensile strength of the tension specimens was 15,500 psi for white oak (35.8% COV), and 13,700 psi for Douglas-fir (27.6% COV). The average strength of the white oak tension specimens was greater than the two-standard deviation range of the ASTM D2555 values. However, the SG values were within one standard deviation of the average value presented in ASTM D2555 when converted to the unseasoned SG. The average strength of the Douglas-fir specimens was within the two-standard deviation range of the ASTM D2555 values. The average MC of the white oak was 47.1% (10.5% COV) and 14.3% for the Douglas-fir (15.9% COV). Average MC of the white oak and Douglas-fir tenon members was 63.4% and 17.3% for joint testing, respectively, indicating that the specimens lost moisture from the time of joint testing to the time of tension specimen testing, especially white oak. The average SG was 0.79 for white oak and 0.48 for Douglas-fir. The COVs were highest for tensile strength and lowest for SG. The high COV values are indicative of a limited representation of the total tenon net-section tensile strength by a single cross-section of roughly 3/16" by 3/8". Similar variability for model results can be expected for models incorporating this strength input such as tenon net-section and group tear-out joint load predictions.

Table 4-3: Average Tensile Properties of Tenon Members

	Tension Strength, psi (COV, %)	MC, % (COV, %)	SG (COV, %)	ASTM D2555 (psi) +/-2 stdev
White Oak	15,500 (35.8)	47.1% (10.5%)	0.79 (7.5%)	5,640 to 10,960
Douglas-fir	13,700 (27.6)	14.3% (15.9%)	0.48 (7.5%)	8,700 to 15,050
% Difference [1]	13.1%			

[1] % Difference = (White Oak - Douglas-fir)/Douglas-fir x 100%

4.2.1.2 Shear Parallel-to-grain Input Specimen Tests (Tenon)

Table 4-4 shows the average shear parallel-to-grain strength, MC, and SG of the white oak and Douglas-fir parallel-to-grain tenon specimens with accompanying COVs and ASTM D2555 values for the two species. The average parallel-to-grain shear strength of white oak and Douglas-fir specimens was 1,590 psi (8.9 % COV) and 1,300 psi (11.5% COV), respectively. The average shear strength of white oak was 22% greater than Douglas-fir. The average MC of the white oak and Douglas-fir shear specimens was 45.5% (13.6% COV) and 13.7% (15.0% COV), respectively. The average MC of white oak tenon shear specimens, 45.5%, decreased from tenon members at the time of joint testing, 63.4%. The average MC of Douglas-fir tenon shear specimens, 13.7%, decreased from tenon members at the time of joint testing, 17.3%. The average SG of white oak and Douglas-fir specimens was 0.79 (6.9% COV) and 0.46 (8.5% COV), respectively. The average SG of white oak tenon shear specimens was the same as the tenon tensile specimens. The average SG of Douglas-fir tenon shear specimens, 0.46, was similar to the tenon tensile specimens, 0.48. The COV values for each species were highest for MC and lowest for SG. The average shear strength of each species was within the two-standard deviation range of the ASTM D2555 values.

Table 4-4: Average Shear Properties of Tenon Members

	Shear Strength, psi (COV, %)	MC, % (COV, %)	SG (COV, %)	ASTM D2555 (psi) +/-2 stdev
White Oak	1,590 (8.9%)	45.5% (13.6%)	0.79 (6.9%)	900 to 1,600
Douglas-fir	1,300 (11.5%)	13.7% (15.0%)	0.46 (8.5%)	1,030 to 2,000
% Difference [1]	22.3%			

[1] % Difference = (White Oak - Douglas-fir)/Douglas-fir x 100%

4.2.1.3 Bearing Parallel-to-grain Input Specimen Tests (Tenon)

Table 4-5 shows the average parallel-to-grain bearing strength of the white oak and Douglas-fir specimens cut from the tenon members and the average MC and SG values with associated COVs. The ultimate strength was chosen as the maximum stress within 0.5 inches of displacement to keep consistent with perpendicular-to-grain bearing tests described in the next section. The average 5% offset yield and ultimate strength and COVs of the Douglas-fir specimens are the same since the 5% offset yield line intersection with the load curve occurred after the ultimate strength for all Douglas-fir specimens. This behavior also occurred with four white oak specimens. On average, white oak specimens were lower in strength and more ductile than Douglas-fir specimens which may have due to the higher MC values of the white oak specimens, even though the oak specimens had greater SG. The NDS shows greater parallel-to-grain bearing strength for Douglas-fir South than white oak, which may also agrees with Douglas-fir bearing specimens having greater strength. The average white oak 5% offset yield and ultimate strengths were 18.8% and 14.7% less than the Douglas-fir specimens, respectively. The average MC of white oak tenon bearing specimens, 45.1%, decreased from tenon members at the time of joint testing, 63.4%. The average MC of Douglas-fir tenon bearing specimens, 14.2%, decreased from tenon members at the time of joint testing, 17.3%. The average SG of white oak tenon bearing specimens, 0.78, was similar to the tenon tensile and shear specimens, 0.79. The average SG of Douglas-fir tenon shear specimens, 0.47, was similar to the tenon tensile and shear specimens, 0.48 and 0.46, respectively. White oak and Douglas-fir specimens produced the greatest COVs for 5% offset yield and ultimate strength closely followed by MC, while the SG values presented the smallest COVs.

Table 4-5: Average Parallel-to-grain Bearing Properties of Tenon Members

	5% Offset Yield Strength, psi (COV, %)	Ultimate Strength, psi (COV, %)	MC, % (COV, %)	SG (COV, %)
White Oak [1]	5,090 (11.5%)	5,350 (10.6%)	45.1% (10.4%)	0.78 (5.1%)
Douglas-fir [2]	6,270 (18.3%)	6,270 (18.3%)	14.2% (12.9%)	0.47 (5.9%)
% Difference [3]	-18.8%	-14.7%		

[1] Four samples had 5% offset yield strengths equal to the ultimate strengths

[2] All samples had 5% offset yield strengths equal to the ultimate strengths

[3] % Difference = (White Oak - Douglas-fir)/Douglas-fir x 100%

Table 4-6 shows the average tested 5% offset yield strength divided by the NDS reduction term for parallel-to-grain bearing (bearing yield mode), 4.0, compared to the adjusted NDS parallel-to-grain compression strength (Fc'), since flat bearing surfaces of the keys represented NDS Fc' values. Average tested ultimate strength values were compared to ASTM D2555 values. The NDS Fc' values were modified by a ten minute load duration, 1.6, and wet service factor, 0.91 for white oak and 1.0 for Douglas-fir. Ultimate bearing strength values were compared to the two-standard deviation range of average values presented in ASTM D2555 for parallel-to-grain compressive strength.

Table 4-6: Comparison of Parallel-to-grain Bearing Strength Results to NDS and ASTM D2555 values

	5% Offset Yield Strength			Ultimate Strength	
	Tested Value/4.0 (psi)	NDS Fc'-Adjusted (psi)	% Difference[1]	Tested Value (psi)	ASTM D2555 +/- 2 standard deviations (psi)
White Oak	1,270	1,200	5.8%	5,350	2,280 to 4,840
Douglas-fir	1,570	1,480	6.1%	6,270	4,270 to 8,180

[1] % Difference = [(Tested/4.0)-(Fc')]/Fc' x 100%

On average, the tested 5% offset yield strength of parallel-to-grain bearing specimens divided by the reduction term was approximately 6% greater than the NDS Fc' values, for each species. Therefore, parallel-to-grain bearing strength of tenon keyhole surfaces could be designed using NDS Fc' values. The average ultimate strength of the of the white oak specimens was greater than the two-standard deviation range of the average ASTM D2555 values. However, the SG values were within one standard deviation of the average value presented in ASTM D2555 when converted to the unseasoned SG. The average ultimate strength of the Douglas-fir specimens was within the two-standard deviation of the ASTM D2555 values.

4.2.1.4 Perpendicular-to-grain Bearing Input Specimen Tests (Mortise)

Table 4-7 shows the average perpendicular-to-grain bearing strength of the white oak and Douglas-fir specimens cut from the mortise members along with the MC and SG values. ASTM D5764 (ASTM 2004a), *Evaluating Dowel-Bearing Strength of Wood and Wood-Based Products*,

recommended test termination after an embedment of one-half the fastener diameter or when maximum load was achieved. One-half of the steel bearing block width was taken as half of the fastener diameter (0.5 inches) for testing purposes and to normalize the two different key widths. Typically, bearing strength increased throughout the duration of the tests due to wood compaction, so the ultimate load was chosen as the maximum load within 0.5 inches of displacement. The average 5% offset yield bearing strength was approximately half of the ultimate bearing strength for each species. The white oak 5% offset yield and ultimate strengths were 57.8% and 94.2% greater than the Douglas-fir specimens, respectively, which the was opposite for the parallel-to-grain tenon bearing specimens where the Douglas-fir specimens had greater bearing strength. The NDS also shows greater perpendicular-to-grain bearing strength for white oak than Douglas-fir, for post and timbers. The average MC of white oak mortise bearing specimens, 41.5%, decreased from mortise members at the time of joint testing, 58.6%. The average MC of Douglas-fir mortise bearing specimens, 12.2%, decreased from mortise members at the time of joint testing, 14.9%. White oak and Douglas-fir specimens produced the greatest COVs for 5% offset yield and ultimate strength followed by MC, while the SG values presented the smallest COVs.

Table 4-7: Average Perpendicular-to-grain Bearing Properties of Mortise Members

	5% Offset Yield Strength, psi (COV, %)	Ultimate Strength, psi (COV, %)	MC, % (COV, %)	SG (COV, %)
White Oak	2,430 (25.2%)	5,010 (17.1%)	41.5 (12.4%)	0.74 (4.8%)
Douglas-fir	1,540 (15.7%)	2,580 (19.7%)	12.2 (11.9%)	0.48 (10.2%)
% Difference [1]	57.8%	94.2%		

[1] % Difference = (White Oak - Douglas-fir)/Douglas-fir x 100%

Table 4-8 shows the average tested 5% offset yield strength of mortise members divided by the NDS reduction term for perpendicular-to-grain bearing (bearing yield mode), 5.0, compared to adjusted allowable NDS compression perpendicular-to-grain, since flat bearing surfaces of the keys represented NDS compression perpendicular-to-grain values. The NDS values were modified by a wet service factor (0.67 for white oak and 1.0 for Douglas-fir) to represent actual MC conditions of the members. Ultimate bearing strength values were not compared to values presented in ASTM D2555 for perpendicular-to-grain compressive strength since ASTM D2555 values used a displacement limit of 0.04 inches, which is also used in the

NDS for establishment of perpendicular-to-grain compressive strength. Tested 5% offset yield strength, divided by the reduction term, was approximately 9% less than NDS compression perpendicular-to-grain values for white oak and 40% less for Douglas-fir. This indicated that NDS compression perpendicular-to-grain strength could be used to design the compressive strength of the mortise members instead of using the tested 5% offset yield strength divided by a reduction factor of 5.0 for allowable strength predictions.

Table 4-8: Comparison of Adjusted 5% Offset Yield and NDS Allowable Adjusted Perpendicular-to-grain Compression Strength of Mortise Member Tests

	5% Offset Value/5.0, psi	NDS Fc'perp - Adjusted, psi	% Difference[1]
White Oak	486	536	-9.3%
Douglas-fir	308	520	-40.1%

[1] % Difference = [(Tested/5.0)-(Fc',perp)]/Fc',perp x 100%

4.2.1.5 Bending Input Specimen Tests (Keys)

Table 4-9 shows average values of 5% offset yield and ultimate bending strength, MC, SG, and two-standard deviation range values from ASTM D2555 for bending specimens. Two-standard deviation range values for modulus of rupture from ASTM D2555 were compared to the ultimate bending strength of the key specimens for only white and red oak since values for the other species were not available. The ASTM D2555 values selected for comparison were true white oak and Northern red oak in the seasoned condition considering the MC of the bending specimens. Both white and red oak bending specimens were within the ASTM D2555 value ranges. Five percent offset yield bending strength was considered the average of proportional-limit and ultimate bending strength based on TR-12 (AF&PA 1999) 5% offset bending yield strength values. The average SG of white oak bending specimens, 0.66, was less than the average SG of the keys used to fasten joints which was 0.68 for joints with one key and 0.76 for joints with two keys, since bending specimens were not from the keys. White oak specimens had considerably low average 5% offset yield and ultimate strength compared to the other species considering that SG of the white oak specimens (0.66) was close to that of the red oak specimens (0.67) which had the second greatest bending strength, second to ipe specimens. Ipe specimens produced the greatest bending strength values and also had the greatest SG values of any other species.

Table 4-9: Average 5% Offset Yield and Ultimate Bending Properties of Keys

Species	5% Offset, psi (COV, %)	Ultimate, psi (COV, %)	MC,% (COV, %)	SG (COV, %)	ASTM D2555 (psi) +/- 2 standard deviations
White Oak	8,010 (12.3)	11,000 (12.3)	11.3% (4.2)	0.66 (4.6)	10,300 to 20,000
Red Oak	12,300 (12.0)	16,700 (10.8)	10.5% (21.9)	0.67 (5.9)	9,700 to 18,800
Black Walnut	11,200 (17.3)	15,500 (15.7)	9.8% (4.4)	0.61 (5.0)	
Cherry	11,400 (15.8)	15,000 (17.2)	8.8% (7.0)	0.60 (8.1)	
Ipe[1]	18,500 (15.1)	23,000 (13.4)	8.5% (2.5)	1.04 (3.4)	

[1] Only four ipe bending specimens were tested.

4.2.1.6 Perpendicular-to-grain Bearing Input Specimen Tests (Keys)

Table 4-10 shows average values of 5% offset yield and ultimate perpendicular-to-grain bearing strength, MC, SG of the perpendicular-to-grain bearing specimens with accompanying COV values. The greater 5% offset yield and ultimate bearing strength of the red oak specimens compared to the white oak specimens was likely due to the greater SG of the red oak specimens. The unadjusted NDS compression perpendicular-to-grain strength values of red oak (820 psi) was rated slightly higher than white oak values (800 psi) for dimension lumber, where keys would be cut from (AF&PA 2005). These NDS values give further indication of red oak specimens having greater bearing strength than white oak. However, white oak specimens had the lowest bearing strength compared to the other species and black walnut and cherry had lower average SG values than white oak.

Table 4-10: Average Perpendicular-to-grain Bearing Properties of Keys

	5% Offset Yield, psi (COV, %)	Ultimate, psi (COV, %)	MC, % (COV, %)	SG (COV, %)
White Oak	3,420 (8.7)	5,330 (7.4)	8.4 (10.2)	0.71 (9.2)
Red Oak	4,690 (10.8)	8,540 (9.3)	7.3 (13.1)	0.81 (6.1)
Black Walnut	3,810 (13.9)	6,190 (14.4)	7.2 (13.8)	0.62 (6.3)
Cherry	4,430 (29.1)	7,450 (19.6)	5.4 (5.6)	0.60 (6.4)
Ipe[1]	10,300 (6.2)	10,400 (5.5)	5.8 (5.1)	1.01 (3.0)

[1] Only four ipe bearing specimens were tested.

Table 4-11 shows the average tested 5% offset yield bearing strength of the key stock divided by the NDS reduction term for perpendicular-to-grain bearing (5.0) compared to the adjusted NDS compression perpendicular-to-grain, since flat bearing surfaces of the keys represented NDS compression perpendicular-to-grain values. Only white and red oak were compared since NDS values were not available for the other species. The NDS compression perpendicular-to-grain values were not adjusted for moisture since the MC of the specimens was less than 19%. Ultimate bearing strength values were not compared to values presented in ASTM D2555 for perpendicular-to-grain compressive strength since ASTM D2555 values used a displacement limit of 0.04 inches. The tested 5% offset yield strength, divided by the reduction term was approximately 14.5% less than the NDS compression perpendicular-to-grain values for white oak and 14.4% greater for red oak. This indicated that NDS compression perpendicular-to-grain strength could be used to design the compressive strength of the keys instead of using the tested 5% offset yield strength divided by a reduction factor of 5.0, for allowable strength predictions.

Table 4-11: Comparison of Adjusted 5% Offset Yield and NDS Allowable Adjusted Perpendicular-to-grain Bearing Strength of Key Tests

	5% Offset Value/5.0, psi	NDS Fc'perp - Adjusted, psi	% Difference[1]
White Oak	684	800	-14.5%
Red Oak	938	820	14.4%

[1] % Difference = [(Tested/5.0)-(Fc')]/Fc' x 100%

4.2.1.7 Shear Parallel-to-grain Input Specimen Tests (Keys)

Table 4-12 shows average values of parallel-to-grain shear strength, MC, SG, accompanying COVs, and two-standard deviation range values from ASTM D2555. Two-standard deviation range values for parallel-to-grain shear strength from ASTM D2555 were only compared to the key specimen values for white and red oak since values for the other species were not available. The ASTM D2555 values selected for comparison were true white oak and Northern red oak in the seasoned condition considering the MC of the shear specimens. Parallel-to-grain shear strength of white and red oak specimens were within the two standard deviation range of the ASTM D 2555 values. Unlike the key bending and bearing specimens, white oak shear specimens were shown to have the greatest strength second to only ipe. Unadjusted NDS values for shear parallel-to-grain of white and red oak (220 psi) are the same, for dimension lumber, where keys would be cut from. It is likely that the greater strength of the white oak shear specimens, compared to the red oak shear specimens, was due to greater SG.

Table 4-12: Average Parallel-to-grain Shear Properties of Keys

	Ultimate Shear Strength, psi (COV, %)	MC, % (COV, %)	SG (COV, %)	ASTM D2555 (psi) +/- 2 standard deviations
White Oak	1,910 (9.5)	11.3 (3.1)	0.69 (6.5)	1,440 to 2,560
Red Oak	1,760 (10.5)	12.4 (5.1)	0.66 (7.7)	1,276 to 2,270
Black Walnut	1,640 (12.1)	10.7 (3.7)	0.60 (6.5)	
Cherry	1,510 (16.4)	9.6 (9.1)	0.60 (7.0)	
Ipe[1]	2,667 (10.1)	8.0 (8.9)	1.00 (1.3)	

[1] Only six ipe shear specimens were tested.

4.2.2 Model Predictions

This section contains the ultimate and allowable joint load predictions from the models in Section 4.1.3 using the inputs from Section 4.2.1 along with geometric measurements of the joints taken prior to testing. The load prediction for any joint was the minimum value predicted by the individual models and was termed 'governing ultimate load' for ultimate load predictions and 'design load' for allowable load predictions. Governing ultimate and allowable predictions were consistent in the models for joints with white oak keys including tenon relish (Z_{RT}) in joints with four-inch tenons and key horizontal shearing (Z_{K_v}) in joints with 11-inch tenons. The models are shown with abbreviations including:

- Tenon Net-section Tension (at keyholes) (Z_{NT})
- Tenon Parallel-to-grain Keyhole Bearing (Z_{Im})
- Tenon Row Tear-out/ Tenon Relish (Z_{RT})
- Tenon Group Tear-out/ Block Shear (Z_{GT} a,b,c,d - see section 4.1.6.1)
- Mortise Bearing (Z_{Is})
- Key Bending ($Z_{III_m,M,T}$ and $Z_{III_m,K}$)
- Key Bearing ($Z_{\mathrm{Im}-K}$ and Z_{Is-K})
- Key Horizontal Shear (Z_{K_v})

4.2.2.1 Ultimate Load Predictions

Table 4-13 shows the average ultimate load predictions and COVs for each joint group and model for joints with white oak keys. Ultimate load predictions for the mortise and tenon members used matched specimens cut from the members. Ultimate load predictions for keys used the average strength of the additional key stock due to the limited size of the keys. Governing load predictions are bold-faced and shaded for easy identification. White oak joints are listed as "WO" and Douglas-fir joints are listed as "DF." The first number after species is the protruding tenon length, in inches, and the second number represents the number of keys per joint in a group.

Table 4-13: Average Predicted Ultimate Joint Load with White Oak Keys

Model	WO-4-1	WO-4-2	WO-11-1	WO-11-2	DF-4-1	DF-4-2	DF-11-1	DF-11-2
	lbs (COV)	lbs (COV)	lbs (COV)	lbs (COV)	lbs (COV)	lbs (COV)	lbs (COV)	lbs (COV)
Z_{NT}	174,100 (31.9%)	81,600 (18.4%)	173,700 (33.0%)	167,700 (24.1%)	165,400 (25.6%)	119,900 (30.5%)	145,500 (33.6%)	99,600 (15.4%)
Z_{Im}	21,300 (12.7%)	31,500 (7.9%)	23,900 (8.5%)	31,100 (11.8%)	23,000 (2.4%)	41,800 (21.1%)	28,500 (12.5%)	32,200 (13.1%)
Z_{RT}	**7,400 (10.5%)**	**15,400 (12.1%)**	30,500 (6.4%)	59,200 (13.1%)	**6,300 (6.7%)**	**12,200 (9.3%)**	23,100 (18.6%)	51,600 (9.4%)
Z_{GT} (a)	90,700 (30.8%)	N/A	102,100 (28.3%)	N/A	85,900 (24.7%)	N/A	84,300 (29.9%)	N/A
Z_{GT} (b)	N/A	33,500 (15.1%)	N/A	82,300 (17.7%)	N/A	44,400 (26.1%)	N/A	56,800 (9.7%)
Z_{GT} (c)	N/A	63,600 (16.6%)	N/A	144,600 (20.3%)	N/A	87,700 (27.9%)	N/A	94,400 (11.3%)
Z_{GT} (d)	N/A	57,600 (17.4%)	N/A	125,000 (21.8%)	N/A	82,100 (29.3%)	N/A	78,200 (13.0%)
Z_{Is}	49,400 (5.5%)	84,800 (17.6%)	55,000 (19.6%)	86,000 (21.8%)	29,600 (29.8%)	36,200 (7.9%)	30,800 (12.2%)	38,700 (11.5%)
$Z_{III_m,M,T}$	17,500 (3.5%)	26,400 (2.4%)	18,500 (8.8%)	26,600 (4.8%)	14,800 (9.4%)	21,500 (2.6%)	15,300 (5.6%)	21,100 (3.1%)
$Z_{III_m,K}$	17,400 (2.8%)	26,100 (3.0%)	17,800 (6.9%)	26,100 (2.0%)	14,600 (9.0%)	20,800 (2.5%)	14,600 (3.7%)	20,900 (2.5%)
$Z_{\mathrm{Im}-K}$	21,700 (1.9%)	32,400 (0.2%)	21,800 (1.2%)	32,300 (1.8%)	21,500 (0.4%)	31,900 (1.2%)	21,600 (0.3%)	32,100 (0.4%)
Z_{Is-K}	58,400 (0.9%)	86,400 (0.7%)	58,600 (1.5%)	86,300 (1.5%)	57,000 (0.5%)	85,300 (0.8%)	57,200 (0.3%)	85,100 (0.8%)
Z_{K_v}	16,000 (3.2%)	24,000 (2.6%)	**16,400 (6.5%)**	**24,000 (2.4%)**	13,400 (8.8%)	19,200 (2.6%)	**13,700 (3.5%)**	**19,300 (2.9%)**

Predicted ultimate joint load for all white oak and Douglas-fir joints with four-inch tenons was governed by tenon relish failure (Z_{RT}). Average governing ultimate joint load was 7,400 lbs (10.5% COV) and 15,400 lbs (12.1% COV) for white oak joints with four-inch tenons with one and two keys, respectively, and 6,300 lbs (6.7% COV) and 12,200 lbs (9.3% COV) for Douglas-fir joints with four-inch tenons with one and two keys, respectively. Average governing ultimate load of white oak and Douglas-fir joints with four-inch tenons with two keys was approximately twice that of the same joints with one key since tenons with two keys had twice the number of tenon shear planes than tenons with one key, where tenon relish failure assumed simultaneous failures of each shear plane. White oak joints were predicted to have greater

ultimate load than the Douglas-fir joints, considering tenon relish failure, due to the higher parallel-to-grain shear strength of white oak than Douglas-fir as shown in Section 4.2.1.2.

Predicted ultimate joint load for all white oak and Douglas-fir joints with 11-inch tenons was governed by horizontal key shearing (Z_{K_v}). Average governing ultimate joint load was 16,400 lbs (6.5% COV) and 24,000 lbs (2.4% COV) for white oak joints with 11-inch tenons with one and two keys, respectively, and 13,700 lbs (3.5% COV) and 19,300 lbs (2.9% COV) for Douglas-fir joints with 11-inch tenons with one and two keys, respectively. Average governing ultimate load of white oak and Douglas-fir joints with 11-inch tenons with two keys was approximately one-and-a-half that of the same joints with one key since keys in joints with two keys were 1.5 inches wide, totaling a width of 3.0 inches, and keys in joints with one key were 2.0 inches wide. White oak joints were predicted to have greater ultimate load than the Douglas-fir joints, considering horizontal key shear, due to the higher perpendicular-to-grain bearing strength of white oak mortise members than Douglas-fir mortise members as shown in Section 4.2.1.4.

Ultimate joint load prediction COV values are dependent upon COV values from material input tests which explains the high COV values of the tenon net-section tension results (Z_{NT}) which were calculated using the tension specimens with high COV values. Tension specimens of white oak joints with 11-inch tenons with two keys had greater net-section tension strength than the same joints with four-inch tenons, while both groups had the same tenon net-section area. Measured geometries of the joints had a small influence on the COV values due to dimensional tolerances.

According to ultimate load predictions, white oak and Douglas-fir joints with four-inch tenons were governed by tenon relish failure with no key failures, of the size tested. Second governing ultimate load prediction for joints with four-inch tenons was horizontal key shearing (Z_{K_v}) followed by key bending ($Z_{III_m,M,T}$ and $Z_{III_m,K}$). Predictions for joints with 11-inch tenons were governed by horizontal key shearing which produced key bending and crushing failures, experimentally. Key bending was the second governing prediction for white oak and Douglas-fir joints with 11-inch tenons.

High values for tenon net-section tension at keyholes (Z_{NT}), tenon group tear-out (Z_{GT}), and bearing predictions were due to high bearing strength (considering maximum bearing strength within one-half inches of deformation) and high tension strengths from tension tests. Tension strength was a factor in tenon net-section tension at keyholes (Z_{NT}) and tenon group tear-out (Z_{GT}) which produced the highest predicted ultimate loads, except for the group of white oak joints with four-inch tenons with two white oak keys, where key bearing strength against the mortise member was the greatest prediction. Load optimization (balancing) of these joints can be achieved by increasing the number of keys (greater number of shear planes) and total bearing area on the keys (increased key width), while reducing tenon net-section area. Increasing total key bearing area (width), for a given tenon thickness and key depth, would increase key bearing, bending, and shear strength since the combined key width would increase. Increased number of tenon shear planes (greater shear area) may also allow a reduction in tenon length, if individual key width is also reduced to avoid increasing key resistance relative to relish resistance, constructing a brittle joint.

Table 4-14 shows the percent differences of ultimate joint load predictions, regarding key failure, compared to horizontal key shear load predictions (Z_{K_v}). The minimum percent difference values are bold-faced for easy identification. Key bending predictions, $Z_{III_m,K}$ and $Z_{III_m,M,T}$, were 7.2 to 8.8% and 9.1 to 12.3% greater than horizontal key shear (Z_{K_v}) predictions, respectively, for all joint groups with white oak keys. Ultimate load predictions were most sensitive to horizontal key shearing (Z_{K_v}), closely followed by key bending considering all joint component bearing strengths ($Z_{III_m,K}$) and then by key bending considering only mortise and tenon bearing strength ($Z_{III_m,M,T}$), for the key size tested. Key bearing load predictions regarding the tenon member bearing interface ($Z_{\mathrm{Im}-K}$) were 32.3 to 66.3% greater than horizontal key shear load predictions. Key bearing load predictions regarding the mortise member bearing interface (Z_{Is-K}) were 257 to 344% greater than horizontal key shear load predictions. The differences between Z_{Is-K} and Z_{K_v} were greater than those between $Z_{\mathrm{Im}-K}$ and Z_{K_v} since the bearing surface Z_{Is-K} was approximately three times that of the $Z_{\mathrm{Im}-K}$ area. The higher

predicted joint load of the key bearing models are indicative of the selection of ultimate strength as the maximum strength within a one-half inch bearing deformation and suggest that ultimate bearing strength could be defined at less than 0.5 inches of deformation. Key failure occurred before any joint component experienced 0.5 inches of bearing deformation, during joint testing. Key bearing failure could exist in joints with deep keys, where key bending or shear would occur after a bearing deformation of 0.5 inches.

Table 4-14: Percent Differences of Ultimate Key Load Predictions compared to Horizontal Key Shearing (Z_{K_v})

[1] % Difference	WO-4-1	WO-4-2	WO-11-1	WO-11-2	DF-4-1	DF-4-2	DF-11-1	DF-11-2
$Z_{III_m,M,T}$	9.3%	10.0%	12.3%	11.0%	9.8%	12.0%	11.9%	9.1%
$Z_{III_m,K}$	**8.4%**	**8.6%**	**8.5%**	**8.8%**	**8.6%**	**8.4%**	**7.2%**	**8.3%**
$Z_{\mathrm{Im}-K}$	35.6%	34.9%	32.3%	34.8%	59.8%	65.8%	58.2%	66.3%
Z_{Is-K}	265%	260%	257%	260%	324%	344%	319%	340%

[1] % Difference = (Key Load Prediction - Z_{K_v})/ Z_{K_v} *100%

Table 4-15 shows the ultimate load predictions for joints retested with ipe keys. The average values of the three white oak joints with 11-inch tenons with one ipe and COV values are presented, whereas the other values are displayed for individual joints. The average governing joint load for joints with 11-inch tenons with one ipe key was 19,200 lbs (2.8% COV). Governing joint load was 26,400 lbs for WO-11-2-2, 17,200 lbs for DF-11-1-4, and 22,700 lbs for DF-11-2-2. Horizontal key shear (Z_{K_v}) was the governing ultimate load prediction, except for WO-11-2-2, which estimated tenon keyhole bearing (Z_{Im}) to be the governing prediction. However, horizontal key shearing (26,700 lbs) was close to the governing predicted load for WO-11-2-2.

Table 4-15: Predicted Ultimate Joint Load with Ipe Keys

Model	WO-11-1 [1]	WO-11-2-2	DF-11-1-4	DF-11-2-2
	lbs (COV, %)	lbs	lbs	lbs
Z_{NT}	136,300 (27.9)	152,300	215,000	89,600
Z_{Im}	23,700 (2.9)	**26,400**	30,100	31,500
Z_{RT}	26,100 (8.2)	48,000	27,500	45,200
Z_{GT} (a)	81,200 (22.1)	N/A	121,200	N/A
Z_{GT} (b)	N/A	72,500	N/A	50,700
Z_{GT} (c)	N/A	127,900	N/A	84,100
Z_{GT} (d)	N/A	112,400	N/A	70,200
Z_{Is}	57,300 (13.5)	83,900	35,300	36,000
$Z_{III_m,M,T}$	25,100 (2.8)	34,400	22,600	30,400
$Z_{III_m,K}$	25,100 (2.8)	34,400	22,600	30,400
$Z_{\mathrm{Im}-K}$	40,700 (1.1)	63,500	41,200	63,900
Z_{Is-K}	109,000 (0.5)	169,600	109,100	169,000
Z_{K_v}	**19,200 (2.8)**	26,700	**17,200**	**22,700**

[1] Average value of three joints tested with Ipe Keys (WO-11-1-2,3,4)

Table 4-16 shows the percent differences of ultimate load predictions between joints with white oak keys and joints with ipe keys. Negative percent differences indicated that joints with white oak keys had greater ultimate load prediction values than joints with ipe keys, while positive percent differences indicated the opposite. Differences in ultimate joint load predictions between joints with white oak keys and joints with ipe keys were least for models that predicted the load of the mortise and tenon members (i.e. Z_{NT}, Z_{Im}, Z_{RT}, Z_{GT}, and Z_{Is}) with differences ranging from -11.5 to 1.9%, and were greatest for models that predicted the load of the keys (i.e. $Z_{III_m,M,T}$, $Z_{III_m,K}$, $Z_{\mathrm{Im}-K}$, Z_{Is-K}, and Z_{K_v}) with differences ranging from 12.6 to 99.7%. The relatively low differences in ultimate joint load predictions, considering the mortise and tenon members, was due to retesting the same mortise and tenon members with different keys, which was expected. The consistent negative percent differences for tenon relish failure were due to the decreasing tenon length since the tenon keyholes were retooled for the ipe keys. The larger differences in ultimate joint load predictions, regarding keys, were due to the greater bending, bearing, and shear strength of ipe compared to white oak. The greatest increase of 84.6% to

99.7% was for key bearing since ipe keys had almost twice the ultimate bearing strength of white oak keys. Average ultimate bending strength of ipe was over twice that of white oak, but resulted in only a 28.9% to 47.0% increase for key bending joint load predictions, since the bending predictions also considered the bearing strength of the mortise and tenon members. The least difference of ultimate joint load predictions between joints with white oak and ipe keys, based on key resistance, was parallel-to-grain key shear from 12.6% to 19.6%, where key shear predictions also considered the bearing strength of mortise and tenon members.

Table 4-16: Percent Differences of Ultimate Joint Load Predictions for Joints with Ipe Keys and Joints with White Oak Keys

% Difference[1]	WO-11-1 [2]	WO-11-2-2	DF-11-1-4	DF-11-2-2
Z_{NT}	-0.3%	1.5%	-0.3%	0.0%
Z_{Im}	-5.0%	0.4%	-3.1%	1.9%
Z_{RT}	-11.5%	-6.7%	-1.5%	-2.7%
Z_{GT} (a)	-2.3%	N/A	-0.5%	N/A
Z_{GT} (b)	N/A	-1.4%	N/A	-1.2%
Z_{GT} (c)	N/A	-0.1%	N/A	-0.7%
Z_{GT} (d)	N/A	0.6%	N/A	-0.4%
Z_{Is}	-5.8%	-0.7%	-2.8%	1.9%
$Z_{III_m,M,T}$	28.9%	33.1%	38.9%	47.0%
$Z_{III_m,K}$	35.2%	33.1%	47.4%	47.0%
$Z_{\mathrm{Im}-K}$	86.3%	96.7%	90.0%	99.7%
Z_{Is-K}	84.6%	94.7%	90.5%	99.7%
Z_{K_v}	12.8%	12.6%	19.6%	19.6%

[1] % Difference = (Ipe - White Oak)/ White Oak x 100%

[2] Average value of three joints tested with Ipe Keys (WO-11-1-2,3,4)

4.2.2.2 Allowable Load Predictions

Table 4-17 shows the average allowable load predictions and COVs for each joint group and model for joints with white oak keys. Allowable load predictions use NDS ASD values for tension and shear parallel-to-grain strengths, while reduction terms applied to the 5% offset input test values were used for parallel- and perpendicular-to-grain bearing and bending strength. Allowable parallel-to-grain shear strength for ipe was estimated by dividing the ultimate shear

strength of ipe by the ratio of the ultimate strength of the white oak divided by the allowable strength of the white oak, since ipe properties were not given in the NDS. Governing load (design) predictions are bold-faced and shaded for easy identification. White oak joints are listed as "WO" and Douglas-fir joints are listed as "DF." The first number after species is the protruding tenon length, in inches, and the second number represents the number of keys per joint in a group.

Table 4-17: Average Predicted Allowable Joint Load with White Oak Keys

Model	WO-4-1	WO-4-2	WO-11-1	WO-11-2	DF-4-1	DF-4-2	DF-11-1	DF-11-2
	lbs (COV)	lbs (COV)	lbs (COV)	lbs (COV)	lbs (COV)	lbs (COV)	lbs (COV)	lbs (COV)
Z_{NT}	12,000 (2.1%)	9,410 (1.6%)	12,100 (1.0%)	9,410 (1.5%)	13,300 (1.0%)	10,500 (2.2%)	13,400 (0.6%)	10,500 (1.4%)
Z_{Im}	5,140 (12.7%)	7,420 (6.7%)	5,800 (7.0%)	7,250 (14.0%)	5,760 (2.4%)	10,500 (21.2%)	7,130 (12.5%)	8,040 (13.1%)
Z_{RT}	**1,550 (2.8%)**	**3,110 (2.3%)**	6,160 (1.0%)	12,300 (1.4%)	**1,240 (3.4%)**	**2,500 (1.7%)**	5,030 (0.2%)	9,990 (1.0%)
Z_{GT} (a)	6,770 (2.1%)	N/A	9,110 (1.0%)	N/A	7,250 (1.1%)	N/A	9,230 (0.4%)	N/A
Z_{GT} (b)	N/A	4,530 (0.8%)	N/A	9,130 (1.4%)	N/A	4,590 (1.6%)	N/A	8,250 (1.2%)
Z_{GT} (c)	N/A	8,000 (1.2%)	N/A	12,600 (1.5%)	N/A	8,380 (2. 3%)	N/A	12,200 (1.2%)
Z_{GT} (d)	N/A	6,970 (1.2%)	N/A	9,270 (1.5)	N/A	7,530 (2.0)	N/A	9,360 (1.1)
Z_{Is}	4,580 (7.3%)	8,060 (28.7%)	5,480 (29. 3%)	8,610 (27.7%)	3,320 (17.8%)	4,370 (12.6%)	3,730 (15.8%)	4,820 (6.5%)
$Z_{III_m,M,T}$	2,920 (3.1%)	4,470 (5.6%)	3,150 (13.2%)	4,570 (8.2%)	2,570 (7.4%)	3,750 (4.2%)	2,700 (7.7%)	3,780 (2.1%)
$Z_{III_m,K}$	2,750 (3.0%)	4,170 (4.0%)	2,870 (10.1%)	4,280 (5.7%)	2,410 (6.4%)	3,480 (4.6%)	2,460 (5.6%)	3,580 (2.2%)
$Z_{\mathrm{Im}-K}$	2,790 (1.9%)	4,160 (0.2%)	2,790 (1.2%)	4,140 (1.8%)	2,760 (0.4%)	4,090 (1.2%)	2,770 (0.3%)	4,125 (0.4%)
Z_{Is-K}	7,500 (0.9%)	11,100 (0.7%)	7,520 (1.5%)	11,100 (1.5%)	7,320 (0.5%)	11,000 (0.8%)	7,340 (0.3%)	10,900 (0.8%)
Z_{K_v}	2,270 (2.5%)	3,450 (4.2%)	**2,360 (9.8%)**	**3,540 (5.8%)**	2,000 (6.0%)	2,900 (4.3%)	**2,070 (4.8%)**	**2,990 (2.1%)**

Design load predictions for white oak and Douglas-fir joints were governed by tenon relish failure (Z_{RT}) for joints with four-inch tenons and horizontal key shearing (Z_{K_v}) for joints with 11-inch tenons. The same models governed the ultimate load predictions. Average design

load was 1,550 lbs (2.8% COV) and 3,110 lbs (2.3% COV) for white oak joints with four-inch tenons with one and two keys, respectively, and 1240 lbs (3.4% COV) and 2,500 lbs (1.7% COV) for Douglas-fir joints with four-inch tenons with one and two keys, respectively. Average design load of white oak and Douglas-fir joints with four-inch tenons with two keys was approximately twice that of the same joints with one key since tenons with two keys had twice the number of tenon shear planes, where tenon relish failure assumed simultaneous failure of each shear plane. White oak joints were predicted to have greater design load than Douglas-fir joints, due to greater parallel-to-grain shear strength of white oak than Douglas-fir as provided by the NDS (AF&PA 2005), for joints with four-inch tenons.

Average design load was 2,360 lbs (9.8% COV) and 3,540 lbs (5.8% COV) for white oak joints with 11-inch tenons with one and two keys, respectively, and 2,070 lbs (4.8% COV) and 2,990 lbs (2.1% COV) for Douglas-fir joints with 11-inch tenons with one and two keys, respectively. Average design load of white oak and Douglas-fir joints with 11-inch tenons with two keys was approximately one-and-a-half that of the same joints with one key since keys in joints with two keys were 1.5 inches wide, totaling a width of 3.0 inches, and keys in joints with one key were 2.0 inches wide. White oak joints were predicted to have greater design load than Douglas-fir joints due to the greater experimental perpendicular-to-grain bearing strength of white oak than Douglas-fir, using the same reduction factors, for joints with 11-inch tenons.

The COV values presented in Table 4-17 were generally greatest for model predictions that relied on bearing strength of the mortise and tenon members, especially for models only considering mortise and tenon bearing strength such as tenon keyhole bearing (2.4 to 21.2%) and mortise surface bearing (6.5 to 29.3%) since bearing inputs came from experimental values and not the NDS. The COV values were low for load predictions that considered perpendicular-to-grain bearing strength of the keys (0.2 to 1.9%) since one average value of key stock was used for all predictions. The COV values of the key bending load predictions (2.1 to 13.2%) and key shear load predictions (2.1 to 9.8%) were greater than the key bearing load predictions since the key bending and shear models also incorporated experimental mortise and tenon bearing strength. Predictions using only strength values from the NDS produced low COV values for predicted allowable load such as tenon net-section tension load (0.6 to 2.2%), row tear-out load (0.2 to 3.4%), and group tear-out load (0.4 to 2.3%). The NDS material strengths were

consistent at given moisture contents, where differences among COV values were due to slight differences in joint geometry and moisture content considerations.

Allowable load predictions of joints with four-inch tenons were governed by tenon relish failure. The second governing allowable load prediction for joints with four-inch tenons was horizontal key shearing (Z_{K_v}) followed by key bearing ($Z_{\mathrm{Im}-K}$), for white oak joints with four-inch tenons with two keys and key bending ($Z_{III_m,K}$) for all other joints with four-inch tenons. Allowable load predictions of joints with 11-inch tenons were governed by horizontal key shearing. Key bearing ($Z_{\mathrm{Im}-K}$) was the second governing allowable load prediction for white oak joints with 11-inch tenons, while key bending ($Z_{III_m,K}$) was the second governing allowable load prediction for Douglas-fir joints with 11-inch tenons. The greatest allowable load predictions were the tenon net-section tension load (Z_{NT}) for white oak and Douglas-fir joints with one key. The greatest allowable joint load prediction for white oak and Douglas-fir joints with four-inch tenons with two keys was key bearing against the mortise member (Z_{Is-K}) and tenon block shear (Z_{GT}-c) for white oak and Douglas-fir joints with 11-inch tenons with two keys. Load optimization of these joints can be achieved by increasing the number of keys (greater number of shear planes) and total bearing area of the keys (increased key width), while reducing tenon net-section area. Increasing total key bearing area (width), for a given tenon thickness and key depth, would increase key bearing, bending, and shear resistance since the combined key width would increase. Increased number of tenon shear planes (greater shear area) may also allow a reduction in tenon length, if individual key width is also reduced to avoid increasing key resistance relative to relish resistance, constructing a brittle joint.

Table 4-18 shows percent differences of allowable key load predictions compared to horizontal key shear load predictions. Minimum values are bold-faced for easy identification. Horizontal key shearing (Z_{K_v}) was the governing allowable key load prediction for all joints with 11-inch tenons, of key sizes tested. Key bearing at the tenon bearing interface ($Z_{\mathrm{Im}-K}$) was the second most governing key load prediction, at 17.2% to 20.4% greater than key shear (Z_{K_v}), for white oak joints, however, white oak joints with four-inch tenons with one key were

governed secondly by key bending ($Z_{III_m,K}$) which was 21.1% greater than horizontal key shear predictions on average. Key bearing failure occurring as the second governing load in white oak joints was due to the applied reduction factor (5.0). Key bending relies on mortise and tenon bearing strength and key bearing relies only on bearing strength of the keys, so softer mortise and tenon member surfaces increase the likelihood for key bending. Douglas-fir joints showed key bending ($Z_{III_m,K}$) as the second governing allowable load prediction to horizontal key shearing by 18.7% to 20.2% followed by key bending regarding only the bearing strength of the mortise and tenon members ($Z_{III_m,M,T}$). Key bearing load predictions regarding the tenon member bearing interface ($Z_{\mathrm{Im}-K}$) were 17.2% to 40.9% greater than horizontal key shear load predictions. Key bearing load predictions regarding mortise member bearing interface (Z_{Is-K}) were 213% to 277% greater than horizontal key shear load predictions. Differences between Z_{Is-K} and Z_{K_v} were greater than those between $Z_{\mathrm{Im}-K}$ and Z_{K_v} since the bearing surface Z_{Is-K} was approximately three times that of the $Z_{\mathrm{Im}-K}$ area. The greater allowable load predictions for key bearing suggest that the sizes of the keys tested were not deep enough to allow key bearing failures due to the other key failure predictions, even after the reduction factor (5.0) was applied.

Table 4-18: Percent Differences between Horizontal Key Shearing (Z_{K_v}) and other Key Load Predictions regarding Allowable Predictions

[1] % Difference	WO-4-1	WO-4-2	WO-11-1	WO-11-2	DF-4-1	DF-4-2	DF-11-1	DF-11-2
$Z_{III_m,M,T}$	28.8%	29.2%	33.4%	29.3%	28.2%	29.1%	30.3%	26.5%
$Z_{III_m,K}$	**21.1%**	20.8%	21.5%	21.0%	**20.2%**	**20.0%**	**18.7%**	**19.8%**
$Z_{\mathrm{Im}-K}$	23.0%	**20.4%**	**18.4%**	**17.2%**	37.7%	40.9%	34.1%	37.9%
Z_{Is-K}	231%	221%	219%	213%	266%	277%	255%	265%

[1] % Difference = (Key Load Prediction - Z_{K_v})/ Z_{K_v} *100%

Table 4-19 shows the allowable load predictions for joints retested with ipe keys. The average of the three white oak joints with 11-inch tenons with one ipe are averaged with the COV values presented in parenthesis, whereas the other values are displayed for individual joints. The joint design load values are bold-faced for easy identification. The average design load for joints with ipe keys was 3,090 lbs (10.3% COV) for joints with 11-inch tenons with one

key. The design load was 4,110 lbs for WO-11-2-2, 2,620 lbs for DF-11-1-4, and 3,780 lbs for DF-11-2-2. Horizontal key shear (Z_{K_v}) was the design load prediction followed by key bending (Z_{III_m}). Both key bending models ($Z_{III_m,M,T}$ and $Z_{III_m,K}$) produced the same allowable load predictions since the ipe keys had greater perpendicular-to-grain bearing strength than white oak and Douglas-fir bearing strength, parallel- or perpendicular-to-grain.

Table 4-19: Predicted Allowable Joint Load (Joints with IPE Keys)

Model	WO-11-1 [1]	WO-11-2-2	DF-11-1-4	DF-11-2-2
	lbs (COV, %)	lbs	lbs	lbs
Z_{NT}	12,000 (0.9)	9,500	13,300	10,500
Z_{Im}	5,720 (3.5)	5,930	7,520	7,870
Z_{RT}	5,440 (0.3)	11,400	4,940	9,620
Z_{GT} (a)	8,740 (0.6)	N/A	9,130	N/A
Z_{GT} (b)	N/A	8,720	N/A	8,110
Z_{GT} (c)	N/A	12,200	N/A	12,000
Z_{GT} (d)	N/A	9,110	N/A	9,320
Z_{Is}	5,850 (27.7)	7,010	3,620	4,580
$Z_{III_m,M,T}$	4,550 (10.3)	5,950	3,950	5,770
$Z_{III_m,K}$	4,550 (10.3)	5,950	3,950	5,770
$Z_{\mathrm{Im}-K}$	7,990 (1.1)	12,500	8,100	12,600
Z_{Is-K}	21,400 (0.5)	33,300	21,400	33,200
Z_{K_v}	**3,090 (10.3)**	**4,110**	**2,620**	**3,780**

[1] Average value of three joints tested with Ipe Keys (WO-11-1-2,3,4)

Table 4-20 shows the percent differences of allowable load predictions between joints with white oak keys and joints with ipe keys. Negative percent differences indicated that joints with white keys had greater allowable load prediction values than joints with ipe keys, while positive percent differences indicated the opposite. Differences in allowable joint load predictions between joints with white oak keys and joints with ipe keys were least for models that predicted the load of the mortise and tenon members (i.e. Z_{NT}, Z_{Im}, Z_{RT}, Z_{GT}, and Z_{Is}) with differences ranging from -11.6 to 1.9%, and were greatest for models that predicted the load of the keys (i.e. $Z_{III_m,M,T}$, $Z_{III_m,K}$, $Z_{\mathrm{Im}-K}$, Z_{Is-K}, and Z_{K_v}) with differences ranging from 21.4 to

206%. The relatively low differences in allowable joint load predictions, considering the mortise and tenon members, was due to retesting the same mortise and tenon members with different keys, which was expected. The consistent negative percent differences for tenon relish failure were due to the decreasing tenon length since the tenon keyholes were retooled for the ipe keys. The larger differences in allowable joint load predictions, regarding keys, were due to the greater bending, bearing, and shear strength of ipe compared to white oak. The greatest difference between white oak and ipe keyed joint load prediction was key bearing, from 183% to 206%, since ipe key specimens had almost three times the 5% offset yield bearing strength of white oak. Average 5% offset yield bending strength of ipe was over twice that of white oak, however, differences in key bending predictions, from 35.7% to 62.8%, were far less than for bearing since bending predictions also considered the bearing strength of the mortise and tenon members. Key shear load predictions between joints with white oak and ipe keys showed the least difference of joint load predictions regarding key load, from 21.4% to 28.3%, which also considered the bearing strength of mortise and tenon members.

Table 4-20: Percent Difference of Allowable Joint Load Predictions of Joints with Ipe Keys and Joints with White Oak Keys

% Difference[1]	WO-11-1[2]	WO-11-2-2	DF-11-1-4	DF-11-2-2
Z_{NT}	-0.3%	1.5%	-0.3%	0.0%
Z_{Im}	-4.9%	0.4%	-3.1%	1.9%
Z_{RT}	-11.6%	-6.7%	-1.5%	-2.7%
Z_{GT} (a)	-4.1%	N/A	-0.6%	N/A
Z_{GT} (b)	N/A	-4.0%	N/A	-1.6%
Z_{GT} (c)	N/A	-2.5%	N/A	-1.1%
Z_{GT} (d)	N/A	-1.2%	N/A	-0.7%
Z_{Is}	-5.8%	-0.7%	-2.8%	1.9%
$Z_{III_m,M,T}$	35.7%	40.3%	46.2%	54.9%
$Z_{III_m,K}$	51.0%	43.7%	61.3%	62.8%
$Z_{\mathrm{Im}-K}$	185%	201%	191%	206%
Z_{Is-K}	183%	198%	192%	206%
Z_{K_v}	24.7%	21.4%	26.5%	28.3%

[1] % Difference = (Ipe - White Oak)/ White Oak x 100%

[2] Average value of three joints tested with Ipe Keys (WO-11-1-2,3,4)

4.2.3 C/T Ratios of Minimum Ultimate Predicted Joint Load/ Experimental Ultimate Load

Ultimate joint load predictions were developed for direct comparison to experimental ultimate joint load to validate the models. The predicted load was divided by the experimental load to obtain C/T (Calculated/Tested) ratios, similar to the methods used in Patel (2009), Finkenbinder (2007), and Smart (2002). The C/T ratios were compared for the effects of factors including species (white oak vs. Douglas-fir), tenon length (11" vs. 4"), and number of keys (1 vs. 2). Comparisons between joint groups with the same factors were made using an analysis of variance (ANOVA) with an alpha value (α) of 0.05. The null hypothesis was that no significant differences existed between C/T ratios. Joints with ipe keys were not compared statistically due to a limited sample size of three or one. The C/T ratios were calculated independently of experimental joint failure and were ranked as follows:

- C/T ratio < 0.9: Conservative Prediction
- C/T ratio between 0.9 and 1.1: Reasonably Accurate Prediction
- C/T ratio > 1.1: Non-conservative Prediction

Table 4-21 shows the average and COV of the C/T ratios of the joints with white oak keys. C/T ratios are tabulated for each joint in Appendix B. The models non-conservatively predicted the ultimate joint load for each joint with average C/T ratios ranging from 1.29 to 2.12. The second white oak joint specimen in the four-inch tenons with two keys group was the only joint with a reasonably accurate prediction with a C/T ratio of 1.08. COV values ranged from 7.1% to 33.5%, with the highest COVs in the Douglas-fir joints with four-inch tenons. The white oak joints with four inch tenons produced the next greatest COV values. Joints with 11-inch tenons produced the lowest COV values. Non-conservatively predicting (high) C/T ratios were likely due to tenon splitting, single shear plane failure, and relish failure of one of two keys failures in joints with four-inch tenons. High C/T ratios for joints with 11-inch tenons were likely due to simultaneous key bending and crushing behavior, since models predicted key failures independently.

Table 4-21: Average C/T Ratios and COVs for Joint Groups with White Oak Keys

Joint Species	Tenon Length	Keys per Joint	Average C/T Ratio (COV)
White Oak	4	1	1.61 (14.1%)
		2	1.29 (19.0%)
	11	1	2.12 (9.2%)
		2	1.56 (7.1%)
Douglas-fir	4	1	2.05 (33.4%)
		2	1.75 (24.2%)
	11	1	1.91 (9.4%)
		2	1.24 (11.5%)

Explanation of C/T ratios for White Oak Joints

Tenon relish failure with simultaneous shear plane failure, was predicted for white oak joints with four-inch tenons with one key. However, tenon splitting and split spreading both occurred. Tenon splits were thought to weaken shear planes since the key bears eccentrically on each tenon half inducing perpendicular-to-grain tension as shown in Figure 3-8 of the previous chapter. Weakened shear planes from tenon splits were the likely cause of the high average C/T ratios (1.61) since predictions included full tenon relish failure. Tenon relish failure was also predicted for white oak joints with four-inch tenons with two keys. However, tenon splitting and relish failure of one of two keys occurred. When relish failure occurred at one key, the other two shear planes securing the other key were responsible for the load, decreasing joint load. Tenon splitting and relish failure of one of two keys likely caused the high average C/T ratios (1.29) for joints with four-inch tenons with two keys. Non-conservative predictions (high C/T ratios) due to simultaneous key bending and crushing indicated that yield models, such as those used to predict key failure, were not suitable for predicting ultimate joint load and since yield models were originally developed for joints with steel fasteners where fastener crushing does not occur.

Horizontal key shear was predicted for white oak joints with 11-inch tenons with one and two keys. However, key bending and crushing occurred. Models that predicted key failures, such as bending, crushing (bearing), and horizontal shearing, do not consider failures occurring simultaneously. Key crushing reduces and damages the key section which reduces key bending

resistance and, ultimately, joint load. Unanticipated simultaneous key failures likely produced high C/T ratios for white oak joints with 11-inch tenons with one key (2.12) and two keys (1.56).

Explanation of high C/T ratios for Douglas-fir Joints

Tenon relish failure was predicted for Douglas-fir joints with four-inch tenons with one and two keys. Tenon splitting and single shear plane failures were observed in Douglas-fir joints with four-inch tenons with one key while combinations of tenon relish failure and single shear plane failure were observed in the same joints with two keys. Tenon splitting and single shear plane failure likely contributed to the high C/T ratios for Douglas-fir joints with four-inch tenons with one key. Combinations of partial tenon relish failure and single shear plane failure likely contributed to the high C/T ratios for Douglas-fir joints with four-inch tenons with two keys. However, two Douglas-fir joints with four-inch tenons with two keys produced simultaneous tenon relish failure at both keys which produced the lowest C/T ratios in the group, 1.55 and 1.20, which indicated that further reduction may be necessary for joints governed by tenon relish failure since these joints failed as predicted and still produced high C/T ratios.

Horizontal key shear was predicted for Doulas-fir joints with 11-inch tenons with one and two keys. Douglas-fir joints with 11-inch tenons with one key produced tenon relish failure in one joint, tenon splitting in another, and key bending and crushing in all other joints. Key bending and crushing occurred in each of the Douglas-fir joints with 11-inch tenons with two keys. Simultaneous key bending and crushing likely produced high C/T ratios for the Douglas-fir joints with 11-inch tenons that produced key failures.

4.2.3.1 ANOVA Comparisons on C/T Ratios between Joint Factors

Table 4-22 shows results of a single factor ANOVA (alpha value of 0.05) between all joints with the same factors to examine how factors of species, tenon length, and number of keys influenced C/T ratios. For instance, for species comparisons, all white oak joints were compared against all Douglas-fir joints to determine if a difference existed between C/T ratios for species. The only significant difference in C/T ratios was between the number of keys (p-value of 0.000) which was due to the difference in SG of the keys between joints with one and two keys.

Table 2-22: ANOVA p-value Results for C/T Ratios

C/T Ratio	Species	Tenon Length	Number of Keys
ANOVA	0.551	0.863	0.000

4.2.3.2 Comparison of C/T ratios between Species

Table 4-23 shows the results of the single factor ANOVA ($\alpha = 0.05$) regarding the influence of joint species on the C/T ratios of joint groups with similar details. The C/T ratios of white oak and Douglas-fir joints with 11-inch tenons with two keys were significantly different with the white oak joints having greater a C/T ratio. The difference in C/T ratios between white oak and Douglas-fir joints with 11-inch tenons with two keys was due to the similar tested ultimate loads (15,400 lbs and 15,600 lbs, respectively) yet different governing predicted ultimate loads (24,000 lbs and 19,300 lbs, respectively). Douglas-fir joints had lower experimental bearing strength of the mortise members, which was not shown to influence the experimental joint load. Softer bearing surfaces of the Douglas-fir mortise members better sustained key-section geometry, as the keys failed, than the harder surfaces of the white oak mortise members which had more tendency to 'pinch' the keys, altering key-section geometry. This supports the TFEC 1-10 recommendation to use keys with SG greater than or equal to the that of joint members. White oak and Douglas-fir joints with four-inch tenons with two keys were almost significantly different (p-value of 0.068). These C/T ratios were not significantly different due to the relatively high COV values (18.9% and 24.1%). High COV values of C/T ratios for joints with four-inch tenons were indicative of high load variability produced in joints with tenon failures.

Table 4-23: Statistical Comparisons of C/T Ratios Between Species (α =0.05)

ANOVA Comparison			p-value	Rank		
WO-11-1	to	DF-11-1	0.150	WO-11-1	=	DF-11-1
WO-11-2	**to**	**DF-11-2**	**0.004**	**WO-11-2**	**>**	**DF-11-2**
WO-4-1	to	DF-4-1	0.215	WO-4-1	=	DF-4-1
WO-4-2	to	DF-4-2	0.068	WO-4-2	=	DF-4-2

4.2.3.3 Comparison of C/T ratios between Tenon Length

Table 4-24 shows the single factor ANOVA for the influence of joint tenon length on the C/T ratios of joint groups with similar details. C/T ratios of white oak joints with 11-inch tenons with one key (2.12) were significantly greater than white oak joints with four-inch tenons with one key (1.61). C/T ratios of white oak joints with 11-inch tenons with two keys (1.56), were almost significantly greater than white oak joints with four-inch tenons with two keys (1.29), (p-value: 0.051). C/T ratios of Douglas-fir joints with four-inch tenons with two keys (1.75) were significantly greater than Douglas-fir joints with 11-inch tenons with two keys (1.91). Predictions for white oak joints with simultaneous key failures (where single key failure was predicted) produced greater error than tenon splitting, split spreading, and relish failure of one of two keys, where simultaneous relish failure of each key was assumed. The opposite was true for Douglas-fir joints with two keys where the models non-conservatively predicted tenon failures more than key failures, regarding tenon length for joints with two keys. This was likely due to the relatively smaller C/T ratios of the Douglas-fir joints with 11-inch tenons with two keys where the softer bearing surfaces of the Douglas-fir mortise members allowed more key bending better sustaining key-section geometry.

Table 4-24: Statistical Comparisons of C/T Ratios Between Tenon Length (α =0.05)

ANOVA Comparison			p-value	Rank		
WO-11-1	**to**	**WO-4-1**	**0.005**	**WO-11-1**	**>**	**WO-4-1**
WO-11-2	to	WO-4-2	0.051	WO-11-2	=	WO-4-2
DF-11-1	to	DF-4-1	0.718	DF-11-1	=	DF-4-1
DF-11-2	**to**	**DF-4-2**	**0.035**	**DF-11-2**	**<**	**DF-4-2**

4.2.3.4 Comparison of C/T ratios between Number of Keys

Table 4-25 shows the single factor ANOVA for the influence of the number of keys on the C/T ratios of joint groups with similar details. C/T ratios of white oak joints with 11-inch tenons with one key (2.12) were significantly greater than white oak joints with 11-inch tenons with two keys (1.56). C/T ratios of white oak joints with four-inch tenons with one key (1.61) were almost significantly greater than white oak joints with four-inch tenons with two keys (1.29), (p-value: 0.062). C/T ratios of Douglas-fir joints with 11-inch tenons with one key (1.91)

were significantly greater than Douglas-fir joints with 11-inch tenons with two keys (1.24). The difference in joint group C/T ratios between the number of keys suggests that models more conservatively predicted for joints with two keys than with one key. Greater C/T ratios for white oak and Douglas-fir joints with 11-inch tenons with one key than with two keys was due to the greater SG of the keys in joints with two keys. White oak keys in joints with one key had similar average SG, 0.68, to the white oak key stock used for model inputs, 0.69. Since C/T ratios were greater for joints with one key than with two, indications show further need of reduction in key failure predictions for ultimate load. Greater C/T ratios of joints with 11-inch tenons with one key than with two also indicate that cross-sectional geometry of denser keys is better sustained during failure, producing key bending with less crushing, than less dense keys. Greater C/T ratios of white oak and Douglas-fir joints with four-inch tenons with one key than with two keys, although not significant, suggested that tenon splitting and split spreading failures produced greater C/T ratios than single shear plane failure and partial relish failure (relish failure at one of two keys).

Table 4-25: Statistical Comparisons of C/T Ratios Between Number of Keys (α =0.05)

ANOVA Comparison			p-value	Rank		
WO-11-1	**to**	**WO-11-2**	**0.001**	**WO-11-1**	**>**	**WO-11-2**
WO-4-1	to	WO-4-2	0.062	WO-4-1	=	WO-4-2
DF-11-1	**to**	**DF-11-2**	**0.000**	**DF-11-1**	**>**	**DF-11-2**
DF-4-1	to	DF-4-2	0.434	DF-4-1	=	DF-4-2

4.2.3.5 C/T Ratios of Joints with Ipe keys

Table 4-26 shows the C/T ratios of joints retested with ipe keys. Horizontal key shearing (Z_{K_v}) was predicted for each joint retested with ipe keys, except for WO-11-2-2, where tenon keyhole bearing (Z_{lm}) was predicted to govern ultimate load, however, key shear was close to governing which was predicted within 300 lbs of keyhole bearing. Each joint experienced key bending and crushing, except for WO-11-1-4 which experienced tenon split spreading and shearing of a single shear plane followed by relish failure and DF-11-1-4 which experienced tenon relish failure. The C/T ratios ranged from 1.08 to 1.37. The relatively high C/T ratio of 1.37 for DF-11-1-4, was likely due to an experimental tenon relish failure, not fully using the

resistance of the key, where key failure was predicted. Ipe key crushing was minimal compared to white oak keys, since ipe keys had greater SG (greater bearing strength). The ipe keys showed more of one type of failure, key bending, than the white oak keys with simultaneous key bending and crushing. C/T ratios for ipe keyed joints, being generally lower than white oak keyed joints, suggested that key failure predictions were more accurate for predicting joint load with single key failure rather than simultaneous key failures. Joints with denser keys than the mortise and tenon members, such as white oak joints with ipe keys, produced more of one type of key failure (key bending with less crushing) rather than many simultaneous key failures which supports TFEC 1-10 about using keys with SG greater than or equal to the that of joint members.

Table 4-26: C/T Ratios of Joints retested with Ipe Keys

Joint(s)	C/T Ratio(s)	AVG (COV)
WO-11-1	1.27, 1.24, 1.26[1]	1.26 (1.2%)
WO-11-2-2	1.27	
DF-11-1-4	1.37	
DF-11-2-2	1.08	

[1] Individual Values of WO-11-1-2,3, and 4 respectively

4.2.4 Design Safety Factors (DSF) of Experimental Ultimate Joint Load/ Minimum Allowable Predicted (Design) Load

Minimum allowable (design) joint load predictions were compared to experimental ultimate load using design safety factors (DSF). DSFs were determined by dividing experimental ultimate joint load by design joint load predictions. Comparisons between joint groups with the same factors were made using an analysis of variance (ANOVA) with an alpha value (α) of 0.05. The null hypothesis was that no significant differences existed between DSF comparisons. Compared factors included species (white oak vs. Douglas-fir), tenon length (11" vs. 4"), and number of keys (1 vs. 2). Joints with ipe keys were not compared statistically due to a limited sample size of three or one. DSFs were calculated independently of experimental joint failure.

Table 4-27 shows the average DSF and COV of all joints with white oak keys. DSFs are tabulated for each joint in Appendix B. Average DSFs ranged from 2.72 to 5.23 with COV values ranging from 6.6% to 29.9%. White oak and Douglas-fir joints with 11-inch tenons with two keys produced the greatest average DSFs, 4.35 and 5.23, respectively, and the lowest COV values, 6.6% and 8.3%, respectively. Douglas-fir joints with four-inch tenons with one and two keys produced the lowest DSFs, 2.72 and 2.95, respectively, and greatest COV values, 29.9% each. White oak joints with four-inch tenons with one key produced the lowest average DSF, 3.02, and greatest COV value, 21.0%, within the white oak joint groups. Higher COVs for white oak and Douglas-fir joints with four-inch tenons suggested that experimental tenon failures produced greater load variability than key failures.

Table 4-27: Average DSFs and COVs for Joint Groups with white oak keys

Joint Species	Tenon Length	Keys per Joint	Average DSF (COV)
White Oak	4	1	3.02 (21.0%)
		2	3.90 (14.2%)
	11	1	3.34 (12.7%)
		2	4.35 (6.6%)
Douglas-fir	4	1	2.72 (29.9%)
		2	2.95 (29.9%)
	11	1	3.49 (9.2%)
		2	5.23 (8.3%)

4.2.4.1 ANOVA Comparisons on DSFs between Joint Factors

Table 4-28 shows the results of a single factor ANOVA (alpha value of 0.05) between all joints to examine the factors of species, tenon length, and number of keys. For instance, all white oak joints were compared against all Douglas-fir joints to determine if a difference existed between DSFs for species. The null hypothesis was that no DSFs were significantly different. Significant differences existed in DSFs between tenon length and number of keys. Significant differences in DSFs between different number of keys was likely due to the different SG values (key strength properties) of white oak keys between joints with one and two keys, for joints with 11-inch tenons (see Table 3-11 of the previous chapter).

Table 4-28: ANOVA p-value Results for DSFs

C/T Ratio	Species	Tenon Length	Number of Keys
ANOVA	0.872	0.001	0.001

4.2.4.2 Comparison of DSFs between Species

Table 4-29 shows the results of the single factor ANOVA regarding the influence of joint species on the DSFs between joint groups with similar details. Species showed a significant difference between the DSFs of white oak and Douglas-fir joints with 11-inch tenons with two keys where Douglas-fir joints had greater DSFs. The difference in DSFs between white oak and Douglas-fir joints with 11-inch tenons with two keys was due to the similar ultimate loads (15,400 lbs and 15,600 lbs, respectively) and different design loads (3,540 lbs and 2,990 lbs), respectively. Design loads were lower for the Douglas-fir joints due to the lower experimental bearing strength of the mortise members used as model input. NDS compression perpendicular-to-grain values could be used for mortise member bearing strength since NDS compression perpendicular-to-grain values were greater than the tested 5% offset yield strength of Douglas-fir divided by a reduction factor of 5.0 (see Table 4-7). Greater DSFs of Douglas-fir than white oak joints with 11-inch tenons with two keys indicated that cross-sectional key geometry is better sustained during failure, in Douglas-fir joints which had less mortise member bearing strength than white oak, producing key bending with less crushing. White oak and Douglas-fir joints with four-inch tenons with two keys almost had a significant difference between DSFs (p-value: 0.075), 3.90 and 2.95, respectively. The reason for no significant difference of DSFs between

these two joint groups was likely due to relatively high COV values of the Douglas-fir joints with four-inch tenons with two keys, 29.9%. High COV values considering DSFs in joints with four-inch tenons, were indicative of the high load variability produced in joints with tenon failures.

Table 4-29: Statistical Comparisons of DSFs Between Species (α =0.05)

ANOVA Comparison			p-value	Rank		
WO-11-1	to	DF-11-1	0.563	WO-11-1	=	DF-11-1
WO-11-2	**to**	**DF-11-2**	**0.005**	**WO-11-2**	**<**	**DF-11-2**
WO-4-1	to	DF-4-1	0.528	WO-4-1	=	DF-4-1
WO-4-2	to	DF-4-2	0.075	WO-4-2	=	DF-4-2

4.2.4.3 Comparison of DSFs between Tenon Length

Table 4-30 shows the results of the single factor ANOVA regarding the influence of joint tenon length on the of DSFs between joint groups with similar details. DSFs of Douglas-fir joints with 11-inch tenons with two keys were significantly greater than Douglas-fir joints with four-inch tenons with two keys. No other significant differences existed for DSFs between joint groups regarding tenon length. However, joints with 11-inch tenons produced greater DSFs that joints with four-inch tenon for other joint groups, although not statistically. The significant difference in DSFs between the Douglas-fir joints with two keys indicated that the models were most conservative when predicting joint load with key failures than the load of joints with tenon failures. However, the single key strength values used for joint load predictions was similar in SG to the less dense white oak keys in joints with one key. If the key SG used for predictions was closer to that of white oak keys in joints with two keys, predictions would be greater and DSFs lower or less conservative. Therefore, these results are inconclusive.

Table 4-30: Statistical Comparisons of DSFs Between Tenon Length (α =0.05)

ANOVA Comparison			p-value	Rank		
WO-11-1	to	WO-4-1	0.384	WO-11-1	=	WO-4-1
WO-11-2	to	WO-4-2	0.144	WO-11-2	=	WO-4-2
DF-11-1	to	DF-4-1	0.119	DF-11-1	=	DF-4-1
DF-11-2	**to**	**DF-4-2**	**0.001**	**DF-11-2**	**>**	**DF-4-2**

4.2.4.4 Comparison of DSFs between Number of Keys

Table 4-31 shows the results of the single factor ANOVA regarding the influence of the number of keys on the DSFs between joint groups with similar details. Significant differences in DSFs existed between each joint group considering the number of keys, except for Douglas-fir joints with four-inch tenons. Douglas-fir joints with four-inch tenons with two keys had greater DSFs than with one key, however these values were not significantly different likely due to high COVs. Greater DSFs for white oak and Douglas-fir joints with 11-inch tenons with two keys than with one key was likely due to the greater SG of the keys in joints with two keys than in the joints with one key, since one value of key bending, bearing, and shear strength were used for predictions. Greater key SG is associated with stronger bending, bearing, and shear properties. Two Douglas-fir joints with 11-inch tenons with one key produced tenon failures, which may have also contributed to the lower DSFs since the two joints that produced tenon failures had the lowest DSFs in the respective group as shown in Appendix B. Greater DSFs of white oak and Douglas-fir joints with four-inch tenons with two keys than with one key, although not significantly different for the Douglas-fir joints, suggested that tenon failures in joints with two keys produced more conservative design load predictions than with one key.

Table 4-31: Statistical Comparisons of DSFs Between Number of Keys (α =0.05)

ANOVA Comparison			p-value	Rank		
WO-11-1	**to**	**WO-11-2**	**0.002**	**WO-11-1**	**<**	**WO-11-2**
WO-4-1	**to**	**WO-4-2**	**0.048**	**WO-4-1**	**<**	**WO-4-2**
DF-11-1	**to**	**DF-11-2**	**0.000**	**DF-11-1**	**<**	**DF-11-2**
DF-4-1	to	DF-4-2	0.679	DF-4-1	=	DF-4-2

4.2.4.5 DSFs of Joints with Ipe keys

Table 4-32 shows DSFs of joints retested with ipe keys. Horizontal key shearing (Z_{K_v}) was predicted for each joint retested with ipe keys considering allowable load predictions. Each joint experienced key bending and slight crushing, except for WO-11-1-4 which experienced tenon split spreading and shearing of a single shear plane followed by relish failure and DF-11-1-4 which experienced tenon relish failure. DSFs ranged from 4.54 to 5.60. The lower DSFs for WO-11-1-4, 4.54, and DF-11-1-4, 4.64, were likely due to tenon failures. DSFs for ipe keyed

joints were generally greater than white oak keyed joints which suggested that key failure predictions were more conservative for single key failure rather than simultaneous key failure, more seen in white oak keys. Joints with denser keys than the mortise and tenon members, such as white oak joints with ipe keys, produced more of one type of key failure rather than simultaneous key failures which supports the TFEC 1-10 about using keys with SG greater than or equal to the that of joint members.

Table 4-32: DSFs of Joints retested with Ipe Keys

Joint(s)	C/T Ratio(s)	AVG (COV)
WO-11-1	5.11, 5.30, 4.54[1]	4.98 (7.9%)
WO-11-2-2	5.06	
DF-11-1-4	4.64	
DF-11-2-2	5.60	

[1] Individual Values of WO-11-1-2,3, and 4 respectively

4.2.5 Alternative Design Values (ADV) of Experimental Ultimate Joint Load/ Design Recommendations from Kessel and Augustin (1996)

This section compares the predicted allowable (design) joint load to experimental joint load adjusted by design recommendations from Kessel and Augustin (1996) to predict alternative design values (ADV). ADV values were calculated by dividing experimental average ultimate joint group loads by the three design recommendations to obtain a minimum ADV. Design recommendations for a joint group included the minimum of the average group ultimate joint load divided by 3.0, average load supported by the joint group at a displacement of 1.5mm (<1/16"), and the minimum group ultimate joint load divided by 2.25. Each ADV represents the alternative design load as a single value for joint groups. The minimum ADV values were governed by the average group ultimate joint load divided by 3.0, except for Douglas-fir joint groups with four-inch tenons with one and two keys, which were governed by the minimum group ultimate joint load divided by 2.25.

Table 4-33 shows the ADV values, reproduced average design load predictions with COVs (for side-by-side comparisons against ADVs), and percent differences between ADVs and average predicted joint design loads. COVs were not given for ADVs since only one value was obtained per joint group. ADVs were developed for all joint groups with white oak keys, and white oak joints with 11-inch tenons with one ipe key since more than one joint was tested per group. ADVs ranged from 984 to 5,220 lbs and were greatest for white oak and Douglas-fir joints with 11-inch tenons with two keys and white oak joints with 11-inch tenons with one ipe key. ADVs were least for white oak and Douglas-fir joints with four-inch tenons with one key. Allowable design load predictions were greatest for white oak and Douglas-fir joints with 11-inch tenons with two keys and white oak joints with 11-inch tenons with one ipe key.

Table 4-33: ADV values of Joints with White Oak and Ipe Keys

Joint Group	ADV Load Value, lbs	Allowable Prediction, lbs Average (COV, %)	% Difference [4]
WO-4-1	1,570 [2]	1,550 (2.8)	1.3%
WO-4-2	4,050 [2]	3,110 (2.3)	30.2%
WO-11-1	2,610 [2]	2,360 (9.8)	10.6%
WO-11-2	5,120 [2]	3,540 (5.8)	44.6%
DF-4-1	984 [3]	1,240 (3.4)	-20.6%
DF-4-2	1,990 [3]	2,500 (1.7)	-20.4%
DF-11-1	2,390 [2]	2,070 (4.8)	15.5%
DF-11-2	5,220 [2]	2,990 (2.1)	74.6%
WO-11-1 [1]	5,100 [2]	3,090 (10.3)	65.0%

[1] Joints retested with ipe keys

[2] ADV governed by average ultimate joint load/ 3.0

[3] ADV governed by minimum ultimate joint load/ 2.25

[4] % Difference = (ADV - Allowable)/ Allowable x 100%

For joints with white oak keys, percent differences between ADVs and design load predictions were greatest for white oak and Douglas-fir joints with 11-inch tenons with two keys (44.6% and 74.6%, respectively), where every joint produced key bending and crushing failures. One key bending, bearing, and shear strength value was used for all white oak keys for joint load predictions and the average SG of key stock most closely resembled keys in joints with one key which were less dense than white oak keys in two keyed joints. This may also explain the high percent differences for white oak and Douglas-fir joints with 11-inch tenons with two keys, between ADVs and governing allowable load predictions, compared to joints with 11-inch tenons with one key. Douglas-fir joints with 11-inch tenons with two keys had the greatest percent difference (74.6%) which is indicative of the lower perpendicular-to-grain bearing strength of the Douglas-fir mortise members, compared to white oak, that greatly influenced allowable joint load predictions. Therefore, NDS compression perpendicular-to-grain values of Douglas-fir bearing strength could be used to substitute 5% offset yield bearing strength divided by a reduction factor of 5.0 (see Section 4.2.1.4). White oak joints with 11-inch tenons with one

ipe key also produced high percent differences between ADVs and design load predictions (65.0%). Although, only two of three white oak joints with 11-inch tenons with one ipe key failed in key bending and slight crushing, one joint produced a tenon relish failure, however key bending failure was initiated upon the tenon relish failure. Denser keys and softer joint members produced more conservative results (greatest percent differences between ADV and allowable predictions) than softer keys and denser joint members. For instance, Douglas-fir joints with 11-inch tenons with two white oak keys produced the greatest percent differences and white oak joints with ipe keys produced greater percent differences than white oak joints with 11-inch tenons with two white oak keys which produced greater percent differences than white oak joints with 11-inch tenons with one white oak key (which were less dense than white oak keys in joints with two keys).

Joints with four-inch tenons generally produced the least percent differences between ADVs and design joint load predictions, except for white oak joints with four-inch tenons with two keys. White oak joints with four-inch tenons with one and two keys produced larger ADVs than design load predictions while Douglas-fir joints with four-inch tenons with one and two keys produced larger design load predictions than ADVs. This indicates that model predictions for white oak tenon failures (much tenon splitting) were more conservative than for Douglas-fir tenons failures (more single plane shearing).

4.3 Conclusions

This paper compared governing ultimate and allowable predicted joint load to ultimate experimental joint load. Joint load predictions were developed by incorporating input strength test results and NDS values into models. Ultimate load predictions were compared to experimental ultimate load in the form of C/T (calculated/ tested) ratios to validate the models. Minimum allowable (design) load predictions were compared to experimental ultimate load to establish design safety factors (DSFs). Alternative design values (ADVs) were developed by adjusting experimental ultimate load by design recommendations from Kessel and Augustin (1996) which were compared to design load predictions.

Material Tests

Bearing specimens of the mortise and tenon members and keys showed that average experimental 5% offset yield strengths, divided by the appropriate reduction factor, could be supplemented by NDS compression parallel- and perpendicular-to-grain values.

Ultimate and Allowable Joint Load Predictions

Joints with four inch tenons were predicted to have tenon relish failures, while joints with 11-inch tenons were predicted to have horizontal key shear failures. Joints with four-inch tenons with two keys were predicted to have approximately twice the load than with one key due to double the amount of shear planes. Joints with 11-inch tenons with two keys were predicted to have approximately one-and-a-half times the load than with one key due to 50% more total key width. White oak joints with four-inch tenons were predicted to have greater load than Douglas-fir joints with four-inch tenons due greater experimental parallel-to-grain shear strength of white oak tenon input specimens and greater allowable shear strength for white oak in the NDS. White oak joints with 11-inch tenons were predicted to produce greater load than Douglas-fir joints with 11-inch tenons due the lower experimental perpendicular-to-grain bearing strength of Douglas-fir mortise member input specimens. Load optimization of these joints can be achieved by increasing the number of keys (greater number of tenon shear planes) and total bearing area on the keys (increased key width), while reducing tenon net-section area. Increasing total key bearing area (width), for a given tenon thickness and key depth, would increase key bearing, bending, and shear strength since the combined key width would increase. Increased number of

tenon shear planes (greater shear area) may also allow a reduction in tenon length, if individual key width is also reduced to avoid increasing key resistance relative to relish resistance, constructing a brittle joint. High ultimate load predictions of mortise and key bearing models indicated that the definition of bearing, as the maximum load within 0.5 inches of deformation, could be decreased since no joint component experienced bearing deformations of 0.5 inches upon failure.

C/T Ratios of Minimum Ultimate Predicted Joint Load/ Actual Ultimate Load

Each C/T ratio showed non-conservatively predicted joint load due to unaccounted failure types when developing models. Non-conservative predictions (high C/T ratios) in joints with four-inch tenons were due to tenon splitting, tenon split spreading, single shear plane failure, and relish failure of one of two keys in joints with two keys, where simultaneous failure of each tenon shear plane was assumed. Non-conservative predictions in joints with 11-inch tenons where primarily due to simultaneous key bending and crushing, where models predicted key failures independently. Predictions for white oak joints with 11-inch tenons with two keys produced significantly greater C/T ratios than Douglas-fir joints with the same details due to softer bearing surfaces of the Douglas-fir mortise members. Softer bearing surfaces permitted more key bending and less crushing that better sustained key-section geometry, where harder surfaces of the white oak mortise members generated more key crushing which 'pinched' the keys at the mortise and tenon shear plane interfaces, altering key-section geometry. The differences in C/T ratios in white oak joints, regarding tenon length, suggested that key failure predictions produced greater error than tenon failures. However, the opposite was true for Douglas-fir joints with two keys due to the relatively low C/T ratios caused by lower bearing strength of the Douglas-fir mortise members used for predictions. For joints with white oak key failures, C/T ratios were greater for white oak and Douglas-fir joints with one key than with two keys due to greater specific gravity of two keys versus one key and since a single value of key bending, bearing, and shear strength was used for predictions that more closely matched the specific gravity of keys used in joints with one key. Indicating further need to reduce key failure predictions for ultimate load. Ipe keys showed key bending with less crushing than white oak keys. C/T ratios for ipe keyed joints were generally lower than white oak keyed joints suggesting that key failure predictions were more accurate for predicting joint load with single

key failure (seen more in ipe keys), rather than simultaneous key failures (seen more in white oak keys with bending and more crushing).

DSFs of Experimental Ultimate Joint Load/ Minimum Allowable Predicted (Design) Load

The only significant difference in DSFs between joint group species comparisons existed between white oak and Douglas-fir joints with 11-inch tenons with two keys due to softer bearing surfaces of the Douglas-fir mortise members that permitted more key bending and less crushing and better sustained key-section geometry, where harder surfaces generated more key crushing which 'pinched' the keys at the mortise and tenon shear plane interfaces, altering key-section geometry. White oak and Douglas-fir joints with 11-inch tenons with two keys had greater DSFs than with one key due to greater specific gravity of two keys versus one key and since a single value of key bending, bearing, and shear strength was used for predictions. White oak and Douglas-fir joints with four-inch tenons with two keys had greater DSFs than joints with one key suggesting that tenon failures in joints with two keys produced more conservative allowable joint load predictions than joints with one key. DSFs for ipe keyed joints suggested that key failure predictions were more conservative for predicting joint load with single key failure rather than simultaneous key failures, more seen in white oak keys with bending and crushing.

ADVs of Ultimate Joint Load/ Recommendations from Kessel and Augustin (1996)

White oak joints with four-inch tenons produced larger ADVs than design load predictions while Douglas-fir joints with four-inch tenons produced larger design load predictions than ADVs. Therefore, allowable predictions for joints with tenon splitting and relish failures of white oak joints were more conservative than single shear plane and relish failures of Douglas-fir joints. Denser keys and softer joint members produced more conservative results (greatest percent differences) than softer keys and denser joint members. For instance, Douglas-fir joints with 11-inch tenons with two white oak keys produced the greatest percent differences and white oak joints with ipe keys produced greater percent differences than white oak joints with 11-inch tenons with two white oak keys which produced greater percent differences than white oak joints with 11-inch tenons with one white oak key. White oak keys in joints with two keys were denser than white oak keys in joints with one key.

Chapter 5: Summary and Conclusions

5.1 Summary

Investigation of the tensile strength of through-tenon keys in mortise and tenon joints was performed by measuring load and stiffness of white oak and Douglas-fir joints with four- and 11-inch tenons with one and two keys, and comparing the results to mathematical models developed from the NDS (AF&PA 2005) and TR-12 (AF&PA 1999). Specific objectives included: develop models to predict ultimate and allowable joint load, measure joint load and stiffness and behavioral characteristics, compare joint load and stiffness based on species and details, measure material properties of mortise and tenon members and keys to develop joint load predictions using models, compare model predictions to experimental results for validation, and determine effects of joint species and details on such comparisons. A total of 40 joints were tested with white oak keys and six were retested with ipe keys. Material property specimens were cut from mortise and tenon members and key stock and included tension, shear, and bearing parallel-to-grain, bearing perpendicular-to-grain, bending, moisture content, and specific gravity. Ultimate material strength was used for ultimate joint load predictions while NDS ASD strength values and experimental 5% offset yield material strengths, divided by NDS reduction factors, were used for allowable joint load predictions. Governing ultimate load predictions were compared to experimental ultimate joint load to develop C/T (calculated/tested) ratios to validate the models. Governing allowable load predictions were compared to experimental ultimate load to develop DSF (design safety factors). Experimental ultimate joint load values were also adjusted by design recommendations from Kessel and Augustin (1996) to obtain ADV (alternative design values) which were compared to governing allowable joint load predictions.

5.2 Conclusions

5.2.1 Chapter 3 Conclusions

Joint Response Comparisons between Species

- In general, white oak joints with greater specific gravity had load and stiffness responses equal to or greater than Douglas-fir joints. However, differences in moisture content of the samples complicated these comparisons.

Joint Response Comparisons between Tenon Length

- Four-inch tenons displayed brittle failures involving the tenon, and 11-inch tenons displayed ductile failures involving the keys.
- In general, joints with 11-inch tenons had load and stiffness responses greater than or equal to joints with four-inch tenons since joints with 11-inch tenons often utilized the entire key resistance where joints with four-inch tenons did not due to tenon failure.

Joint Response Comparisons between Number of Keys

- In general, joints with two keys had load and stiffness responses greater than or equal to joints with one key.
- Joints with four-inch tenons with two keys had twice the shear planes causing greater load and stiffness responses than joints with four-inch tenons with one key.
- Joints with 11-inch tenons with two keys had greater load and stiffness responses than joints with 11-inch tenons with one key, due to greater total key width in joints with two keys. Key strength properties between keys in joints with one and two keys were confounded to where white oak keys in joints with two keys had greater specific gravity (greater strength properties) than white oak keys in joints with one key.
- Many significant differences were found among load and stiffness responses between joint groups with one and two white oak keys after normalizing responses to key width. Differences in the specific gravity of the keys for use in one- and two-key joints were significantly different, affecting these comparisons.

Joints Retested with Ipe Keys Compared to Joints Originally Tested with White Oak Keys

- Joints with ipe keys had greater load and generally greater stiffness than the same joints originally tested with white oak keys due to greater specific gravity (greater strength properties) of ipe keys.
- When a keyed through-tenon joint produces key failure, joint stiffness is reduced upon installation of replacement keys due to the original key failure pre-deforming the mortise bearing surface causing reliance of joint stiffness on replacement key bending stiffness, even if the replacement keys are denser than the original. Replacement keys should be cut to match crushed surfaces of the mortise member to eliminate loss of joint stiffness, however, special care is needed to make certain that tenon load would be greater than replacement keys, to avoid the constructing a brittle joint.
- For joints producing key failures, white oak keys experienced key bending and crushing while ipe keys experienced key bending and less crushing due to greater specific gravity.

Comparisons between Key Width-Normalized Joint Load versus Key Specific Gravity

- For joints with ductile failure, good correlations existed between key-width normalized joint load and key specific gravity. Correlations were not as strong between key-width normalized joint stiffness and key specific gravity for white oak joints. This indicated that key specific gravity could be used to predict joint load for given key sizes and appropriately sized tenons. However, it should be noted that denser keys experienced bending and less crushing while less dense keys experienced bending and more crushing, especially in denser (white oak) joints.

5.2.2 Chapter 4 Conclusions

Material Test Results

- Bearing specimens of mortise and tenon members and keys showed that average experimental 5% offset yield strength divided by NDS reduction factors could be supplemented by NDS compression parallel- and perpendicular-to-grain values.

Ultimate and Allowable Joint Load Predictions

- Tenon relish failures were predicted for all joints with four-inch tenons, while horizontal key shear failures were predicted for all joints with 11-inch tenons.
- Joints with four-inch tenons with two keys were predicted to have twice the load than with one key due to twice the amount of shear planes. Joints with 11-inch tenons with two keys were predicted to have one-and-a-half times the load than with one key due to 50% more total key width in joints with two keys.
- White oak joints were predicted to have greater load than Douglas-fir joints due greater experimental and NDS values of parallel-to-grain shear strength for tenon members and perpendicular-to-grain bearing strength for mortise members.
- High net-section tenon joint load predictions, due to great tenon area, suggested that increased joint load could be achieved by increasing the number of keys and total key width, thereby reducing the tenon net-section. Increasing the number of keys increases the number of shear planes allowing a shorter tenon to carry more load due to increased shear area. It should be noted that individual key width should also be reduced to avoid increasing key resistance relative to relish resistance, constructing a brittle joint.
- High ultimate joint load predictions of mortise and key bearing models indicated that the definition of ultimate bearing strength, as the maximum strength within 0.5 inches of deformation, could be decreased since no joint component experienced bearing deformations of 0.5 inches upon failure.

C/T (calculated/ tested) Ratios

- Each C/T ratio showed non-conservatively predicted joint load due to unaccounted failure types when developing models. Non-conservative predictions (high C/T ratios) in joints with four-inch tenons were due to tenon splitting, tenon split spreading, single shear plane failure, and relish failure of one of two keys in joints with two keys, where simultaneous failure of each tenon shear plane was assumed. Non-conservative predictions in joints with 11-inch tenons where primarily due to simultaneous key bending and crushing, where models predicted key failures independently.

- Two Douglas-fir joints with four-inch tenons with two keys produced simultaneous tenon relish failure at both keys producing C/T ratios of 1.55 and 1.20, which indicated that further reduction may be necessary for joints governed by tenon relish failure since these joints failed as predicted and still produced high C/T ratios.
- Non-conservative predictions (high C/T ratios) due to simultaneous key bending and crushing indicated that yield models, such as those used to predict key failure, were not suitable for predicting ultimate joint load and since yield models were originally developed for joints with steel fasteners where fastener crushing does not occur.
- Predictions for white oak joints with 11-inch tenons with two keys produced significantly greater C/T ratios than Douglas-fir joints with the same details due to softer bearing surfaces of the Douglas-fir mortise members. Softer bearing surfaces permitted more key bending and less crushing that better sustained key-section geometry, where harder surfaces of the white oak mortise members generated more key crushing which 'pinched' the keys at the mortise and tenon shear plane interfaces, altering key-section geometry.
- The differences in C/T ratios in white oak joints, regarding tenon length, suggested that key failure predictions produced greater error than tenon failures. However, the opposite was true for Douglas-fir joints with two keys due to the relatively low C/T ratios caused by lower bearing strength of the Douglas-fir mortise members used for predictions.
- For joints with white oak key failures, C/T ratios were greater for white oak and Douglas-fir joints with one key than with two keys due to greater specific gravity of two keys versus one key and since a single value of key bending, bearing, and shear strength was used for predictions that more closely matched the specific gravity of keys used in joints with one key. Indicating further need to reduce key failure predictions for ultimate load.
- Ipe keys showed key bending with less crushing than white oak keys. C/T ratios for ipe keyed joints were generally lower than white oak keyed joints suggesting that key failure predictions were more accurate for predicting joint load with single key failure (seen more in ipe keys), rather than simultaneous key failures (seen more in white oak keys with bending and more crushing).

DSF (design safety factors)

- The only significant difference in DSFs between joint group species comparisons existed between white oak and Douglas-fir joints with 11-inch tenons with two keys due to softer bearing surfaces of the Douglas-fir mortise members. Softer bearing surfaces permitted more key bending and less crushing that better sustained key-section geometry, where harder surfaces generated more key crushing which 'pinched' the keys at the mortise and tenon shear plane interfaces, altering key-section geometry.
- White oak and Douglas-fir joints with 11-inch tenons with two keys had greater DSFs than with one key due to greater specific gravity of two keys versus one key and since a single value of key bending, bearing, and shear strength was used for predictions.
- White oak and Douglas-fir joints with four-inch tenons with two keys had greater DSFs than joints with one key suggesting that tenon failures in joints with two keys produced more conservative allowable joint load predictions than joints with one key.
- DSFs for ipe keyed joints suggested that key failure predictions were more conservative for predicting joint load with single key failure rather than simultaneous key failures, more seen in white oak keys with bending and crushing.

ADV (alternative design values)

- Allowable predictions for joints with tenon splitting and relish failures of white oak joints were more conservative than single shear plane and relish failures of Douglas-fir joints.
- Denser keys and softer joint members produced more conservative predictions than softer keys and denser joint members. For instance, Douglas-fir joints with 11-inch tenons with two white oak keys produced the most conservative predictions and white oak joints with ipe keys produced more conservative predictions than white oak joints with 11-inch tenons with two white oak keys which produced more conservative predictions than white oak joints with 11-inch tenons with one white oak key. White oak keys in joints with two keys were denser than white oak keys in joints with one key.

5.3 Limitations

- All joints and materials were from one company.
- All joints were composed of either white oak or Douglas-fir mortise and tenon members.
- Species was the same for mortise and tenon members in each joint.
- Only five joints per combination of species and details were tested, more joints per combination would have provided more reliable load and stiffness values.
- The moisture content of white oak joints exceeded fiber saturation point and may have behaved in a more brittle manner if tested below fiber saturation point.
- Joints were only tested axial in tension, no axial compression, moment, or shear tests were conducted.
- Joints were tested monotonically.
- Joints were tested to failure in less than one hour and were not tested for load duration.
- Tenons were of one size and only tested at lengths, protruding beyond the backside of the mortise members, of four or 11 inches.
- Joints were only tested with one or two keys.
- All keys were either white oak or ipe.
- Keys were one of two sizes depending on the number used.
- No models were developed for tenon splitting, split spreading, single shear plane failure, or simultaneous key failures since the models were developed prior to joint testing.

5.4 Recommendations for Future Work

- Testing of joints other than white oak and Douglas-fir would be useful in determining load and stiffness of other species for use as through-tenon keyed joints.
- Joints with different species for mortise and tenon members should be tested. Timber frames often use different species between posts and beams. Different species of mortise and tenon members in a joint would verify how models predict the load of such joints.
- Joint groups, with greater than five joints of same species and detail should be tested for more reliable load and stiffness values.
- Seasoned white oak joints should be tested to verify if joints behave in a more brittle manner than when unseasoned.
- Moment, shear, and axial compression tests on through-tenon keyed joints should be performed to verify such load and stiffness properties of the joints. Axial compression could verify if and when loosening of key(s) occur.
- Cyclic loading of through-tenon keyed joints would provided useful information regarding repetitive loading events such as wind and seismic conditions. Cyclic loading would also provide useful information for obtaining appropriate key dimensions, such as key slope, to prevent loosening of the keys in such loading events.
- Load duration testing of through-tenon keyed joints would provide information for appropriate reduction factors considering different loading durations.
- Different tenon lengths and number of keys should be tested to determine optimum tenon size, for given key sizes, to establish balanced joint details where tenon and key failures would occur simultaneously. For instance: would increasing the number of keys, and thus tenon shear planes, allow for less tenon length, for a given key size and/or specie?
- Joints with long tenons to induce key failure, with different sized keys (different length, width, height and slope), should be tested to determine various key failure behaviors.
- Joints with short tenons to induce tenon relish failure should be tested to determine if NDS equations, using triangular shear plane stress distributions, are adequate for predicting joint load with tenon relish failures since two Douglas-fir joints with four-inch tenons with two keys produced C/T ratios of 1.20 and 1.55 and displayed simultaneous tenon relish failure at each key.

- Key species other than white oak or ipe, at given sizes, should be tested to verify model accuracy and precision for such keys and to determine any further trends related to various key-failure governing joint loads and key specific gravities exist.
- Models should be developed for predicting tenon splitting (possibly as two eccentrically loaded tension members reinforced with perpendicular-to-grain tension strength of the tenon over the key(s)), tenon split spreading, single shear plane failure (similar to tenon splitting), and simultaneous key bending and crushing. These failures may show accurate prediction with strut-and-tie models.
- Models should be rerun to predicted 5% offset yield load, of joints with ductile failure, to verify accuracy in predicting yield instead of ultimate load that produced high C/T ratios.
- A shear-bending model should also be developed for keyed through-tenon joints to determine if such model accurately predicts joint load as evidence of key shearing was seen in a few keys also showing indications of vertical shear.
- Since mortise and key perpendicular-to-grain bearing models showed relatively high predictions, redefinition of ultimate bearing strength should be determined for ultimate strength predictions, instead of defining it as the maximum stress within 0.5 inches of deformation (maybe maximum stress within 0.3, 0,2... inches of deformation).
- Effects of key tightening/pretensioning on joint load and stiffness should be tested.

It should be noted that future testing of through-tenon keyed joints may be accomplished using planks for mortise and tenon members instead of timbers, as previously suggested by Dr. Robert Brungraber. Planks must be reinforced to eliminate tenon splits spreading into the rest of the plank representing the tenon member and to avoid mortise plank splitting from key failure, as a mortise split was seen in a 6x8 white oak mortise member. Using planks instead of timbers would reduce cost and time associated with fabrication and would eliminate concerns of high moisture content.

References

American Forest and Paper Association (AF&PA). 1996. *Load and Resistance Factor Design Manual for Engineered Wood Construction*, American Forest and Paper Association, Washington, D.C.

American Forest and Paper Association (AF&PA). 1997. National Design Specification for Wood Construction. American Forest and Paper Association, Washington, D.C.

American Forest and Paper Association (AF&PA). 1999. General Dowel Equations for Calculating Lateral Connection Values - Technical Report 12. American Forest and Paper Association, Washington, D.C.

American Forest and Paper Association (AF&PA). 2005. National Design Specification for Wood Construction. American Forest and Paper Association, Washington, D.C.

American Society of Agricultural Engineers, Standards, 46th Ed.1999. EP484.2 Diaphragm design of metal-clad, wood-frame rectangular buildings. St. Joseph, Michigan.: ANSI/ASAE

ASTM D 5764-97. 2004a. Standard Test Method for Evaluating Dowel-Bearing Strength of Wood and Wood-Based Products. American Society of Testing and Materials, West Conshohocken, PA.

ASTM D 5652-95. 2004b. Standard Test Methods for Bolted Connections in Wood and Wood-Based Products. American Society of Testing and Materials, West Conshohocken, PA.

ASTM D 4442-92. 2004c. Standard Test Methods for Direct Moisture Content Measurement of Wood and Wood-Base Materials. American Society of Testing and Materials, West Conshohocken, PA.

ASTM D 2395-02. 2004d. Standard Test Method for Specific Gravity of Wood and Wood-Based Materials. American Society of Testing and Materials, West Conshohocken, PA.

ASTM D 143-94. 2004e. Standard Test Methods for Small Clear Specimens of Timber. American Society of Test and Materials, West Conshohocken, PA.

ASTM D 2555-03. 2004f. Standard Test Method for Establishing Clear Wood Strength Values. American Society of Testing and Materials, West Conshohocken, PA.

Beer, F. P., E. R. Johnston, Jr., and J. T. DeWolf, eds. 2006. *Mechanics of Materials.* 4th ed. New York: McGraw-Hill.

Benson, T. 1999. Timber Frame. Newtown, Connecticut: The Taunton Press

Benson, T. and J. Gruber, eds. 1980. *Building The Timber Frame House: The Revival of a Forgotten Craft.* New York: Fireside, Simon & Schuster Inc.

Brungraber, R. L. 1985. "Traditional Timber Joinery: A Modern Analysis." Ph.D. diss., Stanford University.

Brungraber, R. L. 2009. Personal Phone Call Communication with Lance Shields.

Bulleit, W. M., L. B. Sandberg, M. W. Drewek, and T. L. O'Bryant. January 1999. "Behavior and Modeling of Wood-Pegged Timber Frames," *Journal of Structural Engineering*, Vol. 125, No. 1: 3-9.

Carradine, D. M. 2000. "Methodology for the Design of Timber Frame Structures Utilizing Diaphragm Action." Master's Thesis. Virginia Polytechnic Institute and State University, Blacksburg, Virginia.

Church, J. R., and B. W. Tew. 1997. Characterization of Bearing Strength Factors in Pegged Mortise and Tenon Connections. *Journal of Structural Engineering* 123 (3): 326-332.

DeStefano, J. February 2008. TFEC 1-07 Standard for Design of Timber Frame Structures. Structure Magazine. p47. http://www.structuremag.org/ (accessed August 27, 2010).

Drewek, M.W. 1997. "Modeling the Behavior of Traditional Timber Frames." Master's Thesis. Michigan Technology University, Houghton, Michigan.

Erikson, R. G., and R. J. Schmidt. 2003. "Behavior of Traditional Timber Frame Structures Subjected to Lateral Load." Ph.D. Dissertation, University of Wyoming, Laramie, Wyoming.

ENV 2005-1-1 Eurocode-5. 2004. Design of Timber Structures, Part 1. Comite Europeen de Normalisation, Brussels, Belgium

Finkenbinder, D. E. 2007. "An Experimental Investigation of Structural Composite Lumber Loaded by a Dowel in Perpendicular of Grain Orientation and Yield and Capacity." Master's Thesis., Virginia Polytechnic Institute and State University, Blacksburg, Virginia, 2007.

Fischetti, D. C. (P.E.). 2009. *Structural Investigation of Historic Buildings*. Hoboken, New Jersey: John Wiley & Sons, Inc.

Goldstein, E. W. 1999. *Timber Construction: For Architects and Builders.* New York, NY: McGraw-Hill.

Harding, N. and A. H. R. Fowkes. 1984. "Bolted Timber Joints," Proceedings, Pacific Timber Engineering Conference, Auckland, New Zealand, Vol. III: 872-883.

Hill, T., J. Shanks, J. Scott, and P. Walker. February 2007. Testing and Analysis of a traditional oak frame. *Structures & Buildings* 160 (SB1): 23-29.

Jensen, J.L., P. J. Gustafsson, and H. J. Larsen. 2003. A Tensile Fracture Model for Joints with Rods or Dowels Loaded Perpendicular to Grain. CIB-W18 meeting thirty-six, paper 36-7-9, Colorado, USA.

Johansen, K. W. 1949. Theory of Timber Connection. *International Association for Bridge and Structural Engineering Publication*, Vol. 9, 249-262.

Kessel, M. H., M. Speich, and F. J. Hinkes. 1988. "The Reconstruction of an Eight-Floor Timber Frame House at Hildesheim (FRG)," *International Conference on Timber Engineering*: 415-451.

Kessel, M. H., and R. Augustin. December 1995. "Load Behavior of Connections with Oak Pegs," *Timber Framing 38*: 6-9.

Kessel, M. H., and R. Augustin. March 1996. "Load Behavior of Connections with Pegs II," *Timber Framing 39*: 6-9.

Miller, J. F. 2004. "Capacity of Pegged Mortise and Tenon Joints." Master's Thesis., University of Wyoming, Laramie, Wyoming.

Miller, J. F. 2009a. "Capacity of Pegged Connections," *Timber Frame Engineering Council, Technical Bulletin No. 2009-01*: 1-10.

Miller, J. F. October 3, 2009b. E-mail message to Lance Shields.

National Forest Products Association (NFPA). 1986. National Design Specification, Washington, D.C.

National Forest Products Association (NFPA). 1991. National Design Specification for Wood Construction. Washington, D.C.

Nehil, T., and A. Warren. December 2007. "Basic Issues in Timber Frame Engineering," *Timber Framing 86*: 16-23.

Nehil, T., and A. Warren. March 2008. "Basic Issues in Timber Frame Engineering II," *Timber Framing 87*: 6-9.

O'Bryant, T. L. 1996. "Modeling the behavior of pegged timber connections," Master's Thesis., Michigan Technology University, Houghton, Michigan.

O'Connell, T. D. and P. M. Smith. January 1999. "The North American Timber Frame housing industry," *Forest Products Journal*, Vol. 49, Iss. 1: 36-42.

Patel, M. C. 2009. "Investigation of Single and Two Bolt Connections Perpendicular to Grain in Laminated Veneer Lumber." Master's Thesis., Virginia Polytechnic Institute and State University, Blacksburg, Virginia.

Salmon, C. G., J. E. Johnson, and F. A. Malhas. 2009. *Steel Structures: Design and Behavior*, 5th. Ed. New Jersey: Pearson Prentice Hall.

Sandberg, L. B., W. M. Bulleit, and E. H. Reid. June 2000. "Strength and Stiffness of Oak Pegs in Traditional Timber-Frame Joints," *Journal of Structural Engineering*, Vol. 126, No. 6: 717-723.

Sangree, R. H., and B. W. Schafer. January 2009. "Experimental and numerical analysis of stop-splayed traditional timber scarf joint with key." *Construction and Building Materials*. Vol. 23, Iss. 1: 376-385.

Schmidt, R. J., and C. E. Daniels. 1999. "Design Considerations for Mortise and Tenon Connections," Master's Thesis., University of Wyoming, Laramie, Wyoming.

Schmidt, R. J., and G. F. Scholl. 2000. "Load Duration and Seasoning Effects on Mortise and Tenon Joints," Master's Thesis., University of Wyoming, Laramie, Wyoming.

Schmidt, R. J., and R. B. MacKay. 1997. "Timber Frame Tension Joinery," Master's Thesis, University of Wyoming, Laramie, Wyoming.

Schmidt, R. J., R. B. MacKay, and B. L. Leu. October 1996. "Design of Joints in Traditional Timber Frame Buildings." Proceedings, International Wood Engineering Conference, Vol. 4, pp. 240-247, New Orleans, LA. 28-31.

Shanks, J. D., P. Walker. September 6, 2005. "Experimental performance of mortice and tenon connections in green oak.," *The Structural Engineer*: 40-45.

Smart, J. V. 2002. "Capacity Resistance and Performance of Single-Shear Bolted and Nailed Connections: An Experimental Investigation," Master's Thesis., Virginia Polytechnic Institute and State University, Blacksburg, Virginia.

Sobon, J., and R. Schroeder. 1984. *Timber Frame Construction: All about Post-and-Beam Building.* Pownal, Vermont: Storey Books.

Soltis, L.A. and T. L. Wilkinson. 1987. Bolted-Connection Design. General Technical Report FPL-GTR-54, USDA, Forest Service, Forest Products Laboratory, Madison, WI.

Soltis, L. A., and T. L. Wilkinson. 1991. "United States Adaptation of European Yield Model to Large-Diameter Dowel Fastener Specification." Proceedings of the 1991 International timber engineering conference; 1991 September 2-5; London. London: TRADA; 3.43-3.49. Vol. 3.

Timber Frame Business Council (TFBC). 2010. Personal Phone Call Communication with Lance Shields.

Timber Frame Engineering Council (TFEC). 2007. Standard for Design of Timber Frame Structures and Commentary, TFEC 1-07. Timber Frame Engineering Council, Becket, MA.

Timber Frame Engineering Council (TFEC). 2010. Standard for Design of Timber Frame Structures and Commentary, TFEC 1-2010. Timber Frame Engineering Council, Becket, MA.

Trayer, G.W. 1932. The Bearing Strength of Wood Under bolts. Technical Bulletin No. 332. USDA. Washington, D.C.

Van der Put, T.A.C.M. and A. J. M. Leijten. 2000. Evaluation of Perpendicular to Grain Failure of Beams Caused by Concentrated Loads at Joints. CIB-W18 meeting thirty-three, paper 33-7-7, Delft, The Netherlands.

Weaver, D. A. 1993. "Modeling the behavior of traditionally connected timber frames," Master's Thesis, Michigan Technological University, Houghton, Michigan.

Wilkinson, T. L. July 1993. "Bolted Connection Design Values Based on European Yield Model," *Journal of Structure Engineering,* Vol. 119, No. 7: 2,169-2,186.

Appendix A - Initial Joint Defects (White Oak Joints)

White Oak Joints	Tenon Splits (Full thickness Check or Shake)			Tenon Checks				Slight Decay in Pith, over Key	Shake(s) in Tenon
	Split(s) in Tenon Center	Tenon Split over Key(s)	Tenon Split over/ near Key Shear Plane(s)	Tenon Check(s)	Check(s) in Tenon Center	Check over Key(s)	Check over/ near Key Shear Plane(s)		
WO-4-1-1 [1]								■	
WO-4-1-2								■	
WO-4-1-3		■				■			
WO-4-1-4		■							
WO-4-1-5		■				■			
WO-4-2-1									
WO-4-2-2						■		■	
WO-4-2-3 [1]							■		■
WO-4-2-4		■							
WO-4-2-5							■		
WO-11-1-1									
WO-11-1-2 [1]									
WO-11-1-3									
WO-11-1-4			■				■		
WO-11-1-5									
WO-11-2-1	■		■						
WO-11-2-2				■					
WO-11-2-3									
WO-11-2-4 [1]					■				
WO-11-2-5	■		■					■	

[1] Documentation not available for defect identification immediately prior to testing

Appendix A - Initial Joint Defects (Douglas-fir Joints)

Douglas-fir Joints	Tenon Splits (Full thickness Check or Shake)			Tenon Checks				Slight Decay in Pith, over Key	Shake(s) in Tenon
	Split(s) in Tenon Center	Tenon Split over Key(s)	Tenon Split over/ near Key Shear Plane(s)	Tenon Check(s)	Check(s) in Tenon Center	Check over Key(s)	Check over/ near Key Shear Plane(s)		
DF-4-1-1									
DF-4-1-2									
DF-4-1-3									
DF-4-1-4									
DF-4-1-5									
DF-4-2-1									
DF-4-2-2									
DF-4-2-3									
DF-4-2-4									
DF-4-2-5									
DF-11-1-1									
DF-11-1-2									
DF-11-1-3									
DF-11-1-4									
DF-11-1-5									
DF-11-2-1 [1]									
DF-11-2-2									
DF-11-2-3									
DF-11-2-4									
DF-11-2-5									

[1] Documentation not available for defect identification immediately prior to testing

Appendix A - Initial Joint Defects (Joints with Ipe Keys)

Joints retested with Ipe Keys	Tenon Splits (Full thickness Check or Shake)			Tenon Checks				Slight Decay in Pith, over Key	Shake(s) in Tenon
	Split(s) in Tenon Center	Tenon Split over Key(s)	Tenon Split over/ near Key Shear Plane(s)	Tenon Check(s)	Check(s) in Tenon Center	Check over Key(s)	Check over/ near Key Shear Plane(s)		
WO-11-1-2-IPE [1]									
WO-11-1-3-IPE									
WO-11-1-4-IPE									
WO-11-2-2-IPE									
DF-11-1-4-IPE [1]									
DF-11-2-2-IPE [1]									

[1] Documentation not available for defect identification immediately prior to testing

Appendix B - White Oak Joint Responses, C/T Ratios, DSFs, & ADVs

White Oak Joints	Proportional-limit Load	5% Offset Yield Load	Ultimate Load	Stiffness	Load at 1.5mm	K1 [1]	K2 [2]	K3 [3]	C/T Ratio	DSF	ADV
WO-4-1-1	3,000	N/A	5,740	88,900	5,050				1.43	3.55	
WO-4-1-2	1,800	N/A	3,527	82,100	N/A				1.92	2.26	
WO-4-1-3	2,500	N/A	5,506	98,800	4,200				1.47	3.57	
WO-4-1-4	1,900	N/A	3,621	48,000	2,830	1,567	3,778	1,568	1.79	2.42	1,567
WO-4-1-5	2,300	N/A	5,106	62,700	3,030				1.45	3.31	
Average	**2,300**	**N/A**	**4,700**	**76,100**	**3,778**				**1.61**	**3.02**	
COV, %	**21.1**	**N/A**	**22.4**	**27.0**	**27.6**				**14.1**	**21.0**	
WO-4-2-1	6,200	N/A	10,845	179,300	9,130				1.69	3.38	
WO-4-2-2	6,000	12,050	13,631	134,200	7,360				1.08	4.50	
WO-4-2-3	6,000	N/A	9,923	148,600	7,850				1.33	3.25	
WO-4-2-4	5,900	N/A	12,963	185,100	9,450	4,045	8,558	4,410	1.22	4.14	4,045
WO-4-2-5	5,000	12,920	13,312	169,800	9,000				1.12	4.24	
Average	**5,820**	**12,485**	**12,135**	**163,400**	**8,558**				**1.29**	**3.90**	
COV, %	**8.1**	**4.9**	**13.6**	**13.1**	**10.5**				**19.0**	**14.2**	
WO-11-1-1	3,300	7,180	8,535	99,600	5,000				1.89	3.82	
WO-11-1-2	2,700	6,480	8,266	99,000	4,770				2.09	3.38	
WO-11-1-3	3,200	6,790	8,201	110,300	5,020				1.98	3.63	
WO-11-1-4	3,100	6,240	7,471	106,800	4,570	2,605	4,652	2,931	2.36	2.75	2,605
WO-11-1-5	2,500	5,720	6,595	80,500	3,900				2.26	3.10	
Average	**2,960**	**6,482**	**7,814**	**99,240**	**4,652**				**2.12**	**3.34**	
COV, %	**11.6**	**8.5**	**10.1**	**11.6**	**9.9**				**9.2**	**12.7**	
WO-11-2-1	8,800	15,980	17,071	166,400	10,250				1.40	4.59	
WO-11-2-2	5,700	12,950	14,800	199,600	9,620				1.60	4.38	
WO-11-2-3	4,600	11,790	14,650	202,400	9,300				1.71	3.86	
WO-11-2-4	5,300	12,520	15,211	193,800	9,620	5,123	9,698	6,511	1.55	4.53	5,123
WO-11-2-5	6,600	13,150	15,109	192,800	9,700				1.56	4.41	
Average	**6,200**	**13,278**	**15,368**	**191,000**	**9,698**				**1.56**	**4.35**	
COV, %	**26.2**	**12.0**	**6.4**	**7.5**	**3.6**				**7.1**	**6.6**	

[1] K1 = Average ultimate joint load/ 3.0 (from Kessel and Augustin 1996)

[2] K2 = Average load at 1.5mm of displacement (from Kessel and Augustin 1996)

[3] K3 = Minimum ultimate joint load/ 2.25 (from Kessel and Augustin 1996)

Appendix B - Douglas-fir Joint Responses, C/T Ratios, DSFs, & ADVs

Douglas-fir Joints	Proportional-limit Load	5% Offset Yield Load	Ultimate Load	Stiffness	Load at 1.5mm	K1 [1]	K2 [2]	K3 [3]	C/T Ratio	DSF	ADV
DF-4-1-1	1,900	N/A	2,213	53,600	N/A				3.06	1.69	
DF-4-1-2	2,100	N/A	2,702	55,400	N/A				2.34	2.22	
DF-4-1-3	2,870	N/A	3,610	98,700	N/A				1.87	2.93	
DF-4-1-4	3,568	N/A	3,568	98,200	N/A	1,112	4,300	984	1.68	2.91	984
DF-4-1-5	2,900	N/A	4,582	83,800	4,300				1.28	3.84	
Average	**2,668**	**N/A**	**3,335**	**77,940**	**4,300**				**2.05**	**2.72**	
COV, %	**25.3**	**N/A**	**27.4**	**28.5**	**N/A**				**33.4**	**29.9**	
DF-4-2-1	4,800	N/A	6,609	145,400	N/A				1.78	2.59	
DF-4-2-2	5,700	N/A	8,689	116,700	7,350				1.55	3.51	
DF-4-2-3	4,400	N/A	6,852	138,500	N/A				1.87	2.80	
DF-4-2-4	3,600	N/A	4,468	117,100	N/A	2,457	7,075	1,986	2.35	1.77	1,986
DF-4-2-5	5,200	N/A	10,234	117,200	6,800				1.20	4.07	
Average	**4,740**	**N/A**	**7,370**	**126,980**	**6,800**				**1.75**	**2.95**	
COV, %	**16.9**	**N/A**	**29.7**	**10.9**	**N/A**				**24.2**	**29.9**	
DF-11-1-1	2,800	N/A	6,257	67,500	4,020				2.12	3.17	
DF-11-1-2	4,000	6,850	7,739	81,300	4,550				1.70	3.93	
DF-11-1-3	3,400	N/A	7,413	81,800	4,500				1.85	3.37	
DF-11-1-4	2,700	6,700	7,242	93,500	4,900	2,388	4,624	2,781	1.98	3.50	2,388
DF-11-1-5 [4]	4,300	N/A	N/A	80,800	5,150				N/A	N/A	
Average	**3,440**	**6,775**	**7,163**	**80,980**	**4,624**				**1.91**	**3.49**	
COV, %	**20.6**	**1.6**	**8.9**	**11.4**	**9.3**				**9.4**	**9.2**	
DF-11-2-1	4,100	14,720	16,191	126,400	6,400				1.15	5.52	
DF-11-2-2	5,000	13,960	16,395	183,400	9,220				1.16	5.57	
DF-11-2-3	6,900	14,920	15,636	175,200	10,200				1.25	5.22	
DF-11-2-4	8,700	15,050	16,502	172,200	10,100	5,215	8,884	6,000	1.17	5.34	5,215
DF-11-2-5	5,400	10,950	13,500	165,800	8,500				1.49	4.50	
Average	**6,020**	**13,920**	**15,645**	**164,600**	**8,884**				**1.24**	**5.23**	
COV, %	**30.0**	**12.3**	**8.0**	**13.5**	**17.5**				**11.5**	**8.3**	

[1] K1 = Average ultimate joint load/ 3.0 (from Kessel and Augustin 1996)

[2] K2 = Average load at 1.5mm of displacement (from Kessel and Augustin 1996)

[3] K3 = Minimum ultimate joint load/ 2.25 (from Kessel and Augustin 1996)

[4] Testing Error: Joint test mistakenly terminated prior to reaching ultimate strength and ruptured when adjusting the testing machine

Appendix B - Ipe Keyed Joint Responses, C/T Ratios, DSFs, and ADVs

Joints Retested with Ipe Keys	Proportional-limit Load	5% Offset Yield Load	Ultimate Load	Stiffness	Load at 1.5mm	K1 [1]	K2 [2]	K3 [3]	C/T Ratio	DSF	ADV
WO-11-1-2-IPE	5,200	14,870	15,234	154,600	8,600				1.27	5.11	
WO-11-1-3-IPE	6,600	14,550	15,005	139,900	7,540				1.24	5.30	
WO-11-1-4-IPE	6,200	15,360	15,625	155,000	8,900	5,096	8,347	6,669	1.26	4.54	5,096
Average	**6,000**	**14,927**	**15,288**	**149,833**	**8,347**				**1.26**	**4.98**	
COV, %	**12.0**	**2.7**	**2.1**	**5.7**	**8.6**				**1.2**	**7.9**	
WO-11-2-2-IPE	9,300	19,570	20,789	188,500	7,850				1.27	5.06	
DF-11-1-4-IPE	5,100	12,360	12,519	188,000	9,200				1.37	4.64	
DF-11-2-2-IPE	9,200	19,730	21,130	84,600	3,640				1.08	5.60	

[1] K1 = Average ultimate joint load/ 3.0 (from Kessel and Augustin 1996)

[2] K2 = Average load at 1.5mm of displacement (from Kessel and Augustin 1996)

[3] K3 = Minimum ultimate joint load/ 2.25 (from Kessel and Augustin 1996)

Appendix C - Joint Load-Deformation Plots

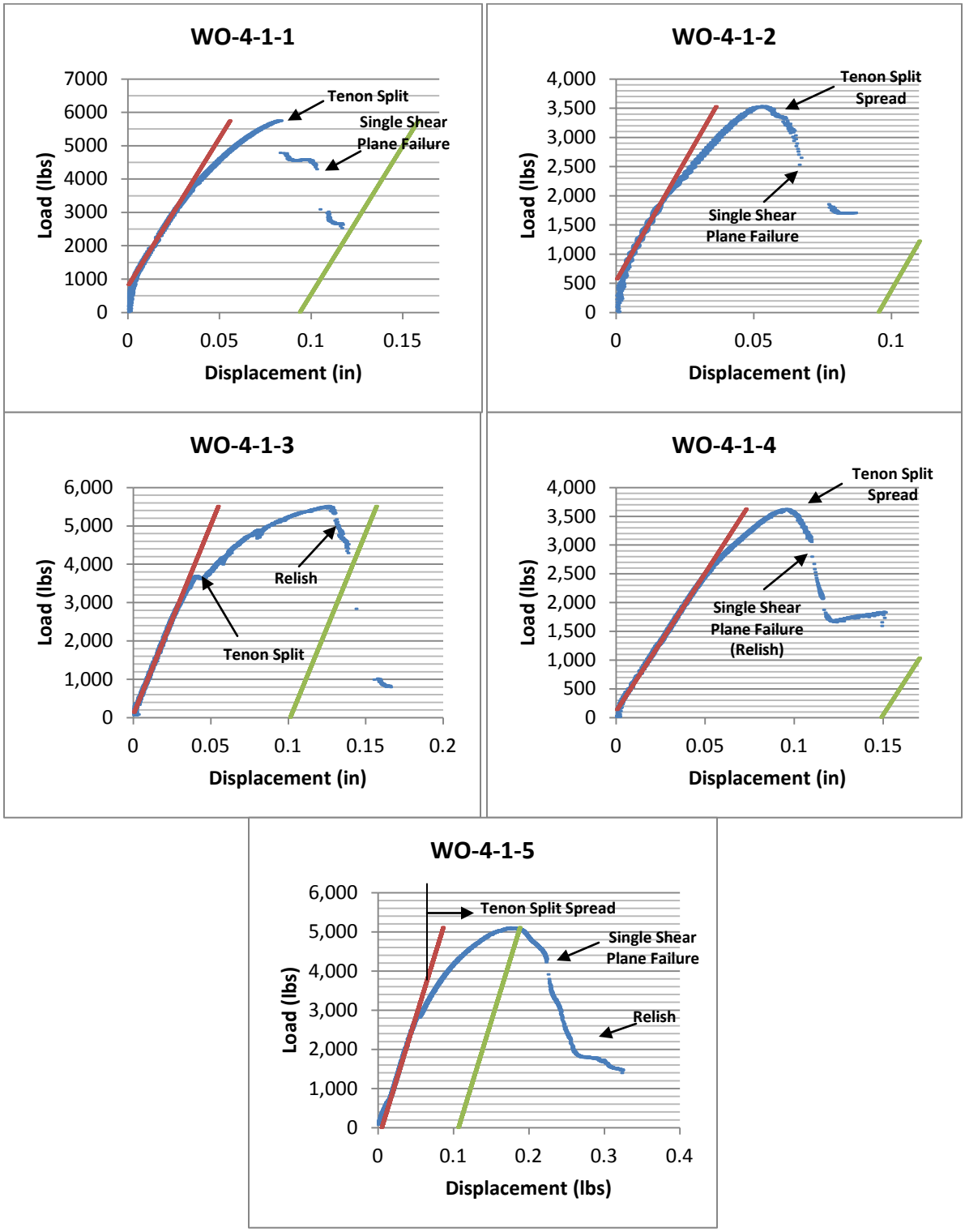

Appendix C

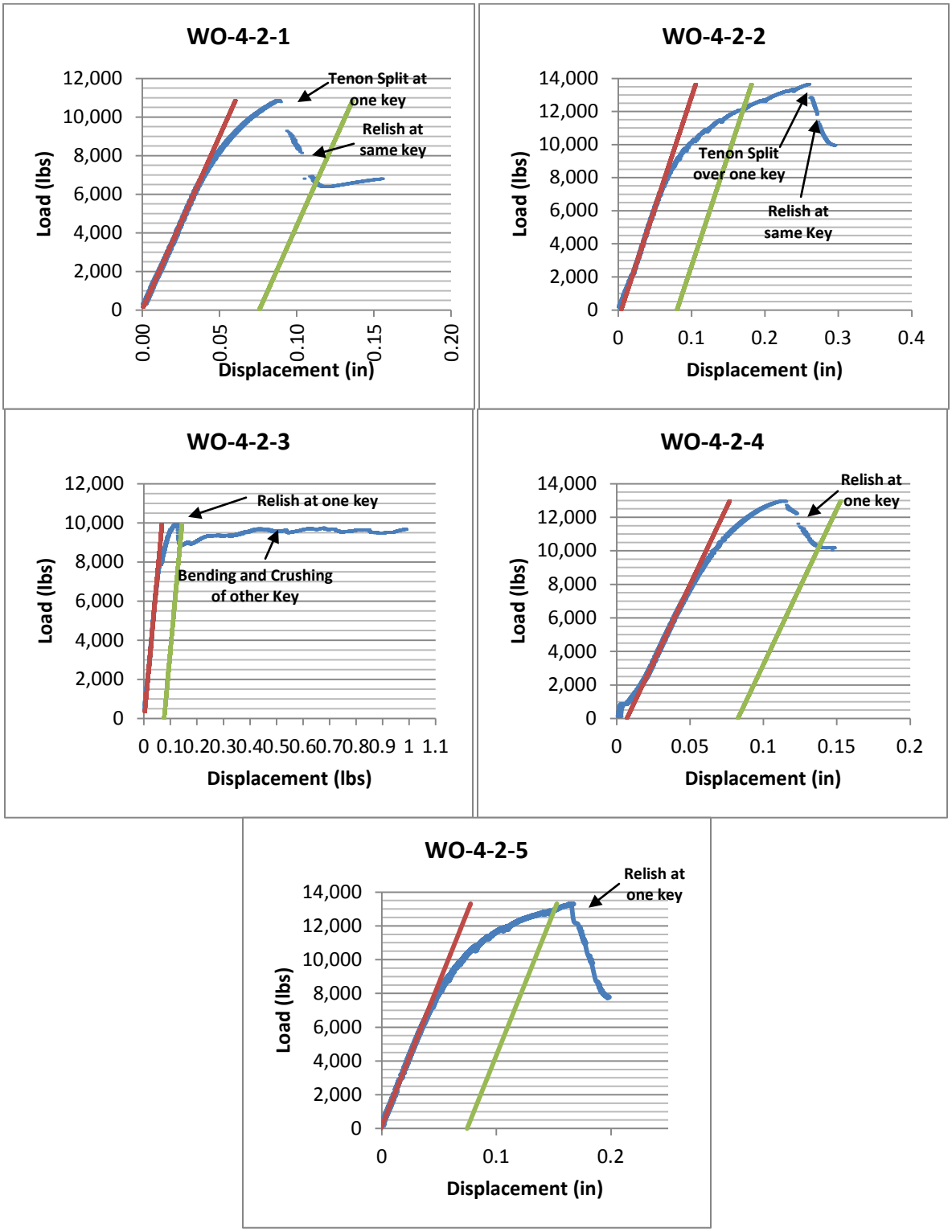
WO-4-2-1
Load (lbs)
12,000
10,000
8,000
6,000
4,000
2,000
0
0.00
0.05
0.10
0.15
0.20
Displacement (in)
Tenon Split at one key
Relish at same key
WO-4-2-2
Load (lbs)
14,000
12,000
10,000
8,000
6,000
4,000
2,000
0
0
0.1
0.2
0.3
0.4
Displacement (in)
Tenon Split over one key
Relish at same Key
WO-4-2-3
Load (lbs)
12,000
10,000
8,000
6,000
4,000
2,000
0
0 0.10.20.30.40.50.60.70.80.9 1 1.1
Displacement (lbs)
Relish at one key
Bending and Crushing of other Key
WO-4-2-4
Load (lbs)
14,000
12,000
10,000
8,000
6,000
4,000
2,000
0
0
0.05
0.1
0.15
0.2
Displacement (in)
Relish at one key
WO-4-2-5
Load (lbs)
14,000
12,000
10,000
8,000
6,000
4,000
2,000
0
0
0.1
0.2
Displacement (in)
Relish at one key

Appendix C

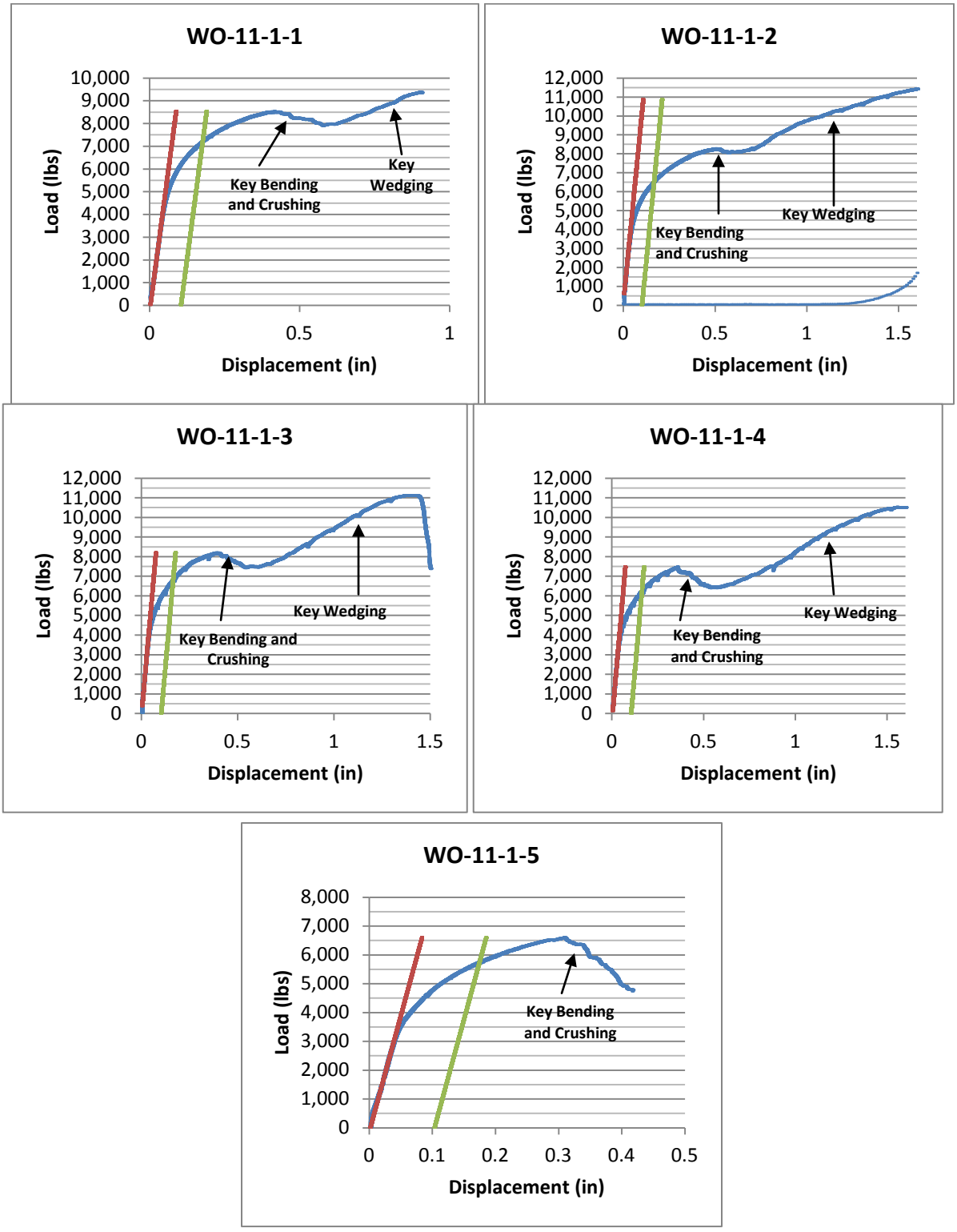
WO-11-1-1
Load (lbs)
10,000
9,000
8,000
7,000
6,000
5,000
4,000
3,000
2,000
1,000
0
0
0.5
1
Displacement (in)
Key Bending and Crushing
Key Wedging
WO-11-1-2
Load (lbs)
12,000
11,000
10,000
9,000
8,000
7,000
6,000
5,000
4,000
3,000
2,000
1,000
0
0
0.5
1
1.5
Displacement (in)
Key Bending and Crushing
Key Wedging
WO-11-1-3
Load (lbs)
12,000
11,000
10,000
9,000
8,000
7,000
6,000
5,000
4,000
3,000
2,000
1,000
0
0
0.5
1
1.5
Displacement (in)
Key Bending and Crushing
Key Wedging
WO-11-1-4
Load (lbs)
12,000
11,000
10,000
9,000
8,000
7,000
6,000
5,000
4,000
3,000
2,000
1,000
0
0
0.5
1
1.5
Displacement (in)
Key Bending and Crushing
Key Wedging
WO-11-1-5
Load (lbs)
8,000
7,000
6,000
5,000
4,000
3,000
2,000
1,000
0
0
0.1
0.2
0.3
0.4
0.5
Displacement (in)
Key Bending and Crushing

Appendix C

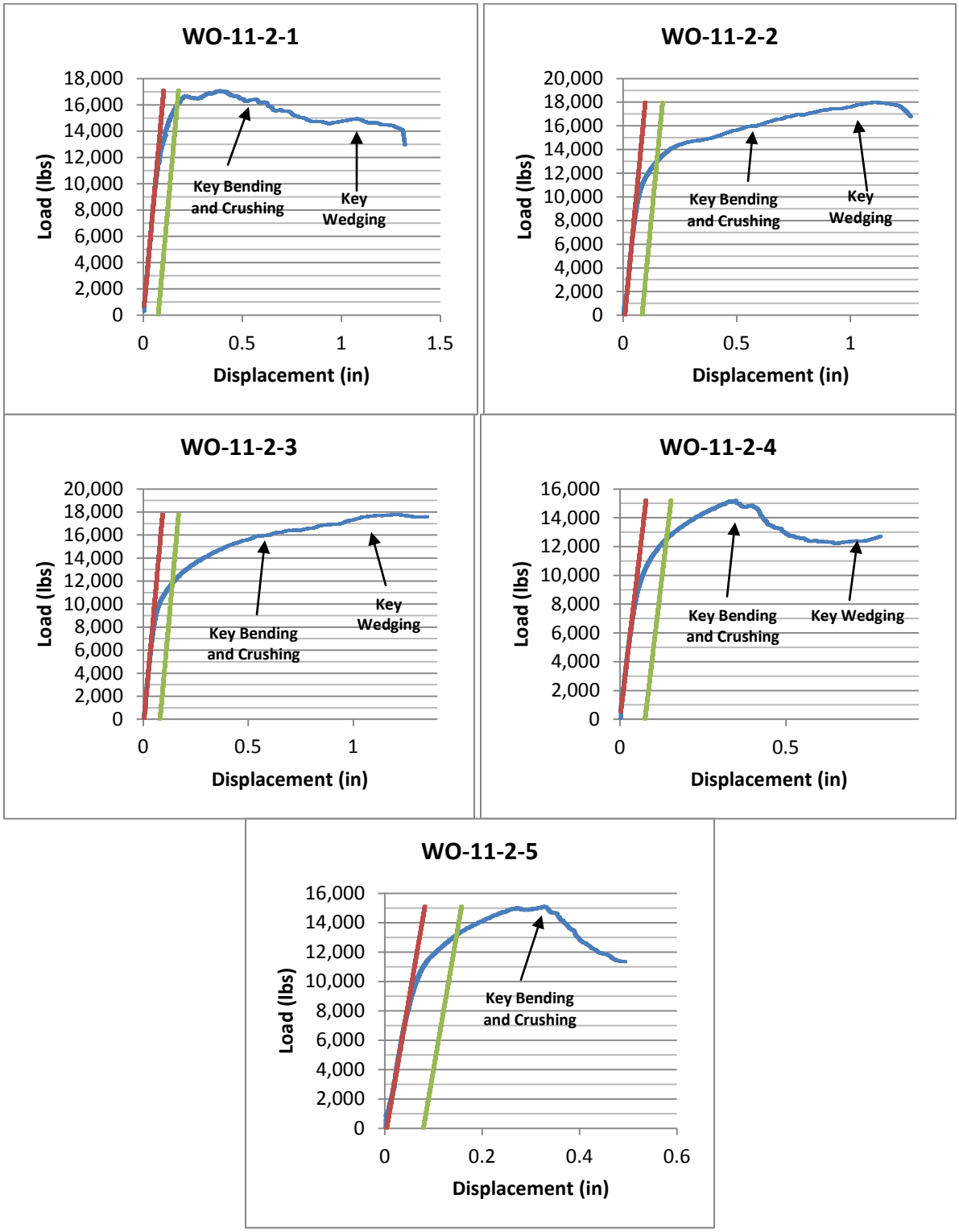
WO-11-2-1
Load (lbs)
18,000
16,000
14,000
12,000
10,000
8,000
6,000
4,000
2,000
0
0
0.5
1
1.5
Displacement (in)
Key Bending and Crushing
Key Wedging
WO-11-2-2
Load (lbs)
20,000
18,000
16,000
14,000
12,000
10,000
8,000
6,000
4,000
2,000
0
0
0.5
1
Displacement (in)
Key Bending and Crushing
Key Wedging
WO-11-2-3
Load (lbs)
20,000
18,000
16,000
14,000
12,000
10,000
8,000
6,000
4,000
2,000
0
0
0.5
1
Displacement (in)
Key Bending and Crushing
Key Wedging
WO-11-2-4
Load (lbs)
16,000
14,000
12,000
10,000
8,000
6,000
4,000
2,000
0
0
0.5
Displacement (in)
Key Bending and Crushing
Key Wedging
WO-11-2-5
Load (lbs)
16,000
14,000
12,000
10,000
8,000
6,000
4,000
2,000
0
0
0.2
0.4
0.6
Displacement (in)
Key Bending and Crushing

Appendix C

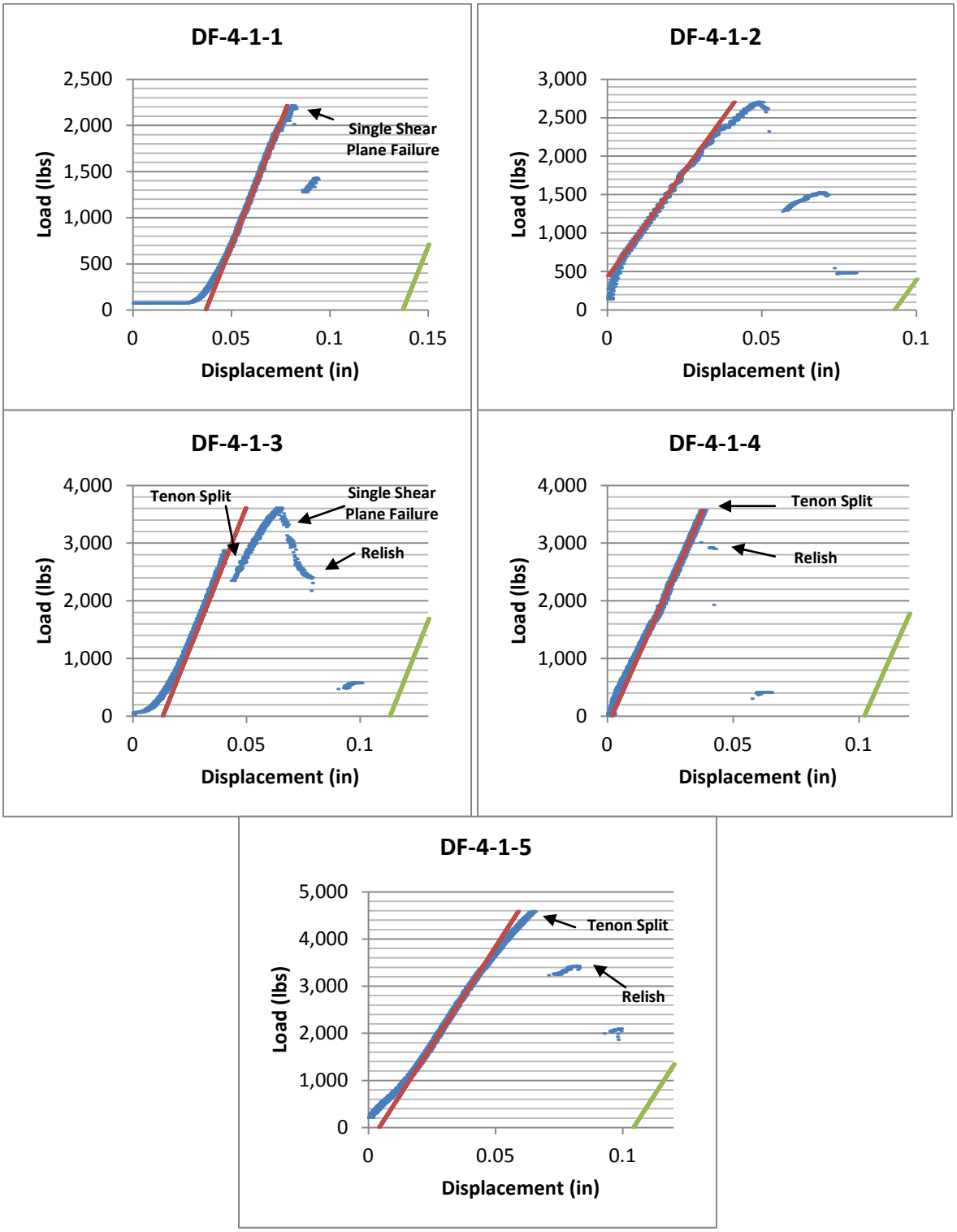
DF-4-1-1
Load (lbs)
2,500
2,000
1,500
1,000
500
0
0
0.05
0.1
0.15
Displacement (in)
Single Shear
Plane Failure
DF-4-1-2
Load (lbs)
3,000
2,500
2,000
1,500
1,000
500
0
0
0.05
0.1
Displacement (in)
DF-4-1-3
Load (lbs)
4,000
3,000
2,000
1,000
0
0
0.05
0.1
Displacement (in)
Tenon Split
Single Shear
Plane Failure
Relish
DF-4-1-4
Load (lbs)
4,000
3,000
2,000
1,000
0
0
0.05
0.1
Displacement (in)
Tenon Split
Relish
DF-4-1-5
Load (lbs)
5,000
4,000
3,000
2,000
1,000
0
0
0.05
0.1
Displacement (in)
Tenon Split
Relish

Appendix C

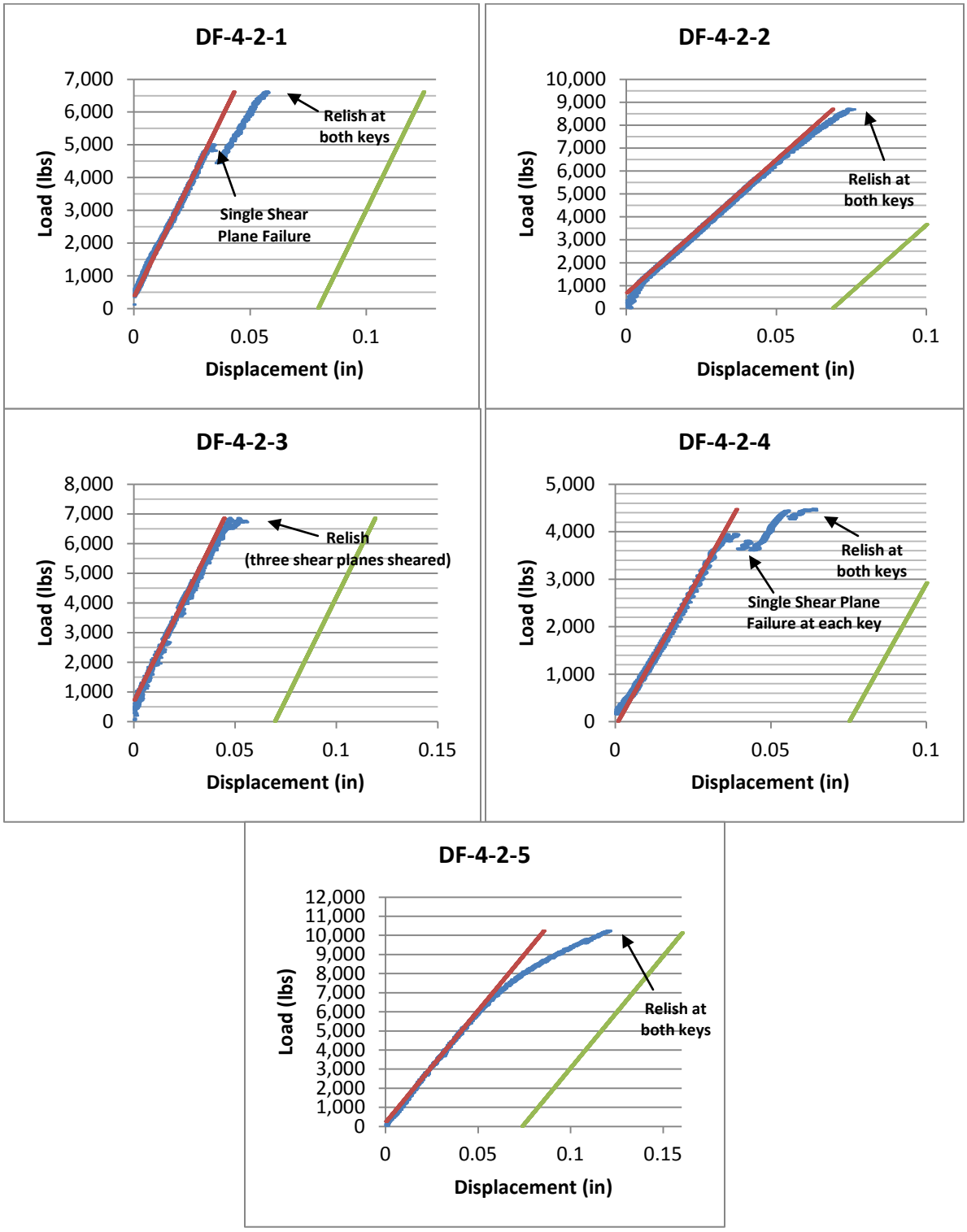
DF-4-2-1
Load (lbs)
7,000
6,000
5,000
4,000
3,000
2,000
1,000
0
0
0.05
0.1
Displacement (in)
Relish at both keys
Single Shear Plane Failure
DF-4-2-2
Load (lbs)
10,000
9,000
8,000
7,000
6,000
5,000
4,000
3,000
2,000
1,000
0
0
0.05
0.1
Displacement (in)
Relish at both keys
DF-4-2-3
Load (lbs)
8,000
7,000
6,000
5,000
4,000
3,000
2,000
1,000
0
0
0.05
0.1
0.15
Displacement (in)
Relish
(three shear planes sheared)
DF-4-2-4
Load (lbs)
5,000
4,000
3,000
2,000
1,000
0
0
0.05
0.1
Displacement (in)
Relish at both keys
Single Shear Plane Failure at each key
DF-4-2-5
Load (lbs)
12,000
11,000
10,000
9,000
8,000
7,000
6,000
5,000
4,000
3,000
2,000
1,000
0
0
0.05
0.1
0.15
Displacement (in)
Relish at both keys

Appendix C

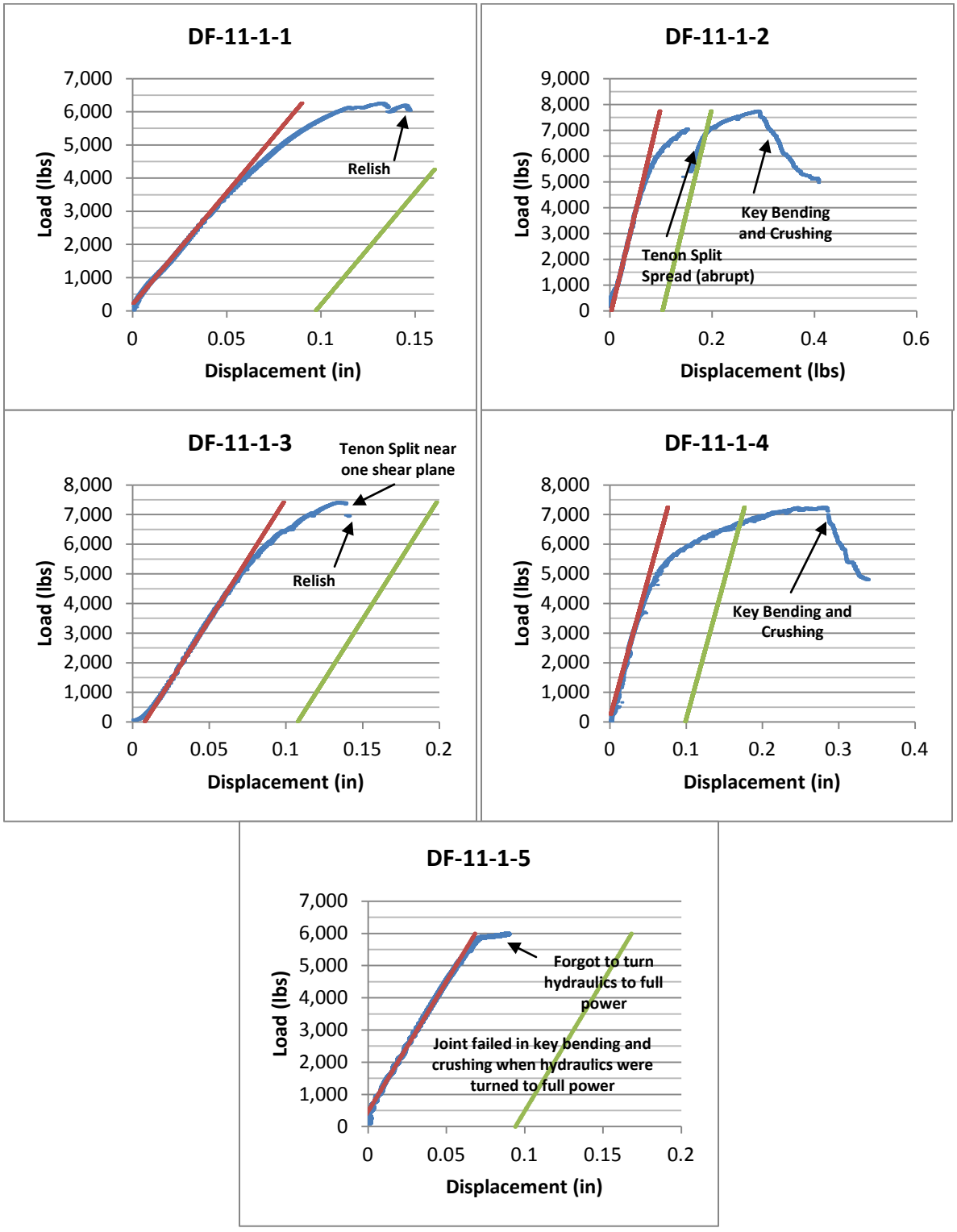
DF-11-1-1
Load (lbs)
Displacement (in)
Relish
DF-11-1-2
Load (lbs)
Displacement (lbs)
Key Bending and Crushing
Tenon Split Spread (abrupt)
DF-11-1-3
Load (lbs)
Displacement (in)
Tenon Split near one shear plane
Relish
DF-11-1-4
Load (lbs)
Displacement (in)
Key Bending and Crushing
DF-11-1-5
Load (lbs)
Displacement (in)
Forgot to turn hydraulics to full power
Joint failed in key bending and crushing when hydraulics were turned to full power

Appendix C

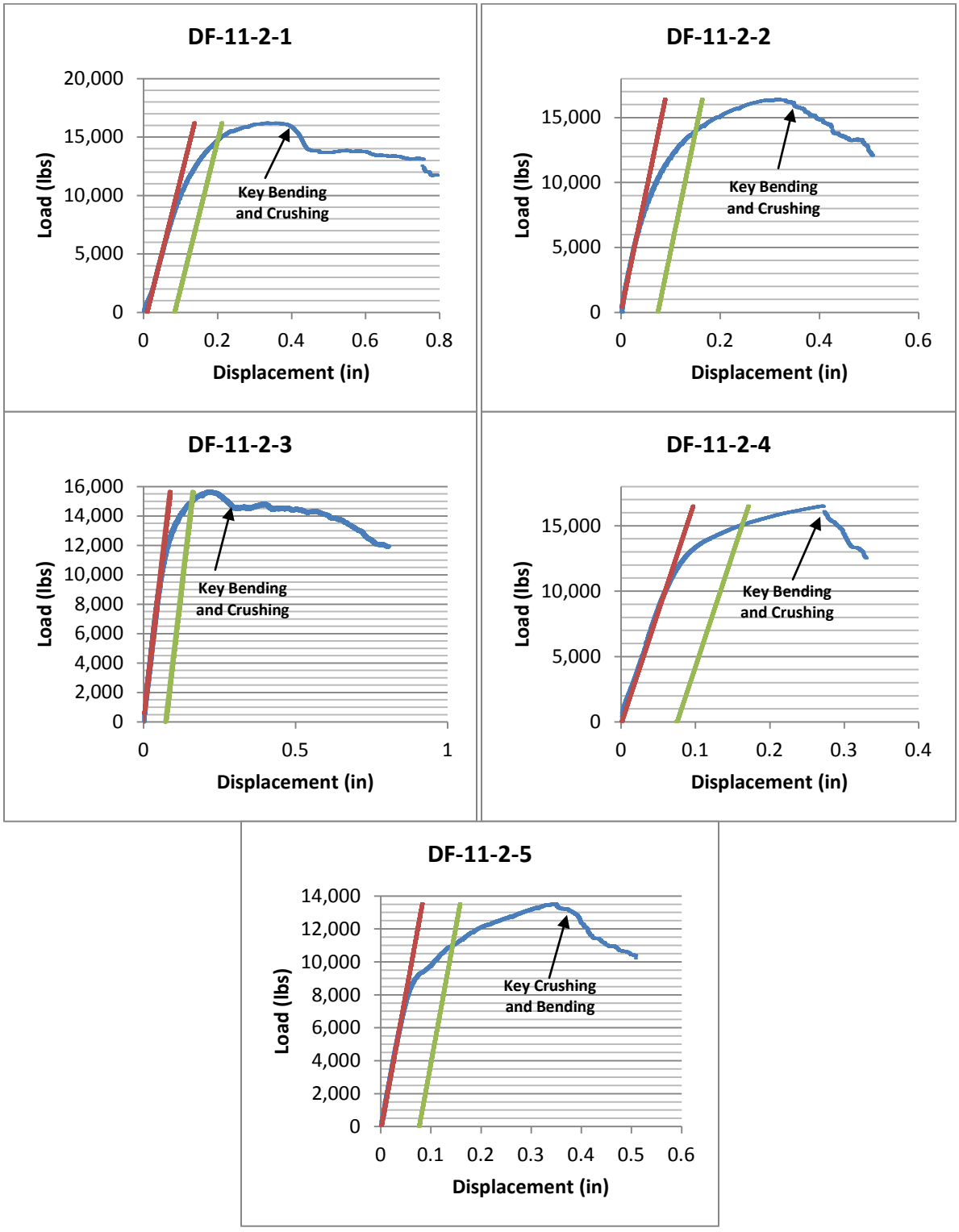
DF-11-2-1
Load (lbs)
20,000
15,000
10,000
5,000
0
0
0.2
0.4
0.6
0.8
Displacement (in)
Key Bending and Crushing
DF-11-2-2
Load (lbs)
15,000
10,000
5,000
0
0
0.2
0.4
0.6
Displacement (in)
Key Bending and Crushing
DF-11-2-3
Load (lbs)
16,000
14,000
12,000
10,000
8,000
6,000
4,000
2,000
0
0
0.5
1
Displacement (in)
Key Bending and Crushing
DF-11-2-4
Load (lbs)
15,000
10,000
5,000
0
0
0.1
0.2
0.3
0.4
Displacement (in)
Key Bending and Crushing
DF-11-2-5
Load (lbs)
14,000
12,000
10,000
8,000
6,000
4,000
2,000
0
0
0.1
0.2
0.3
0.4
0.5
0.6
Displacement (in)
Key Crushing and Bending

Appendix C

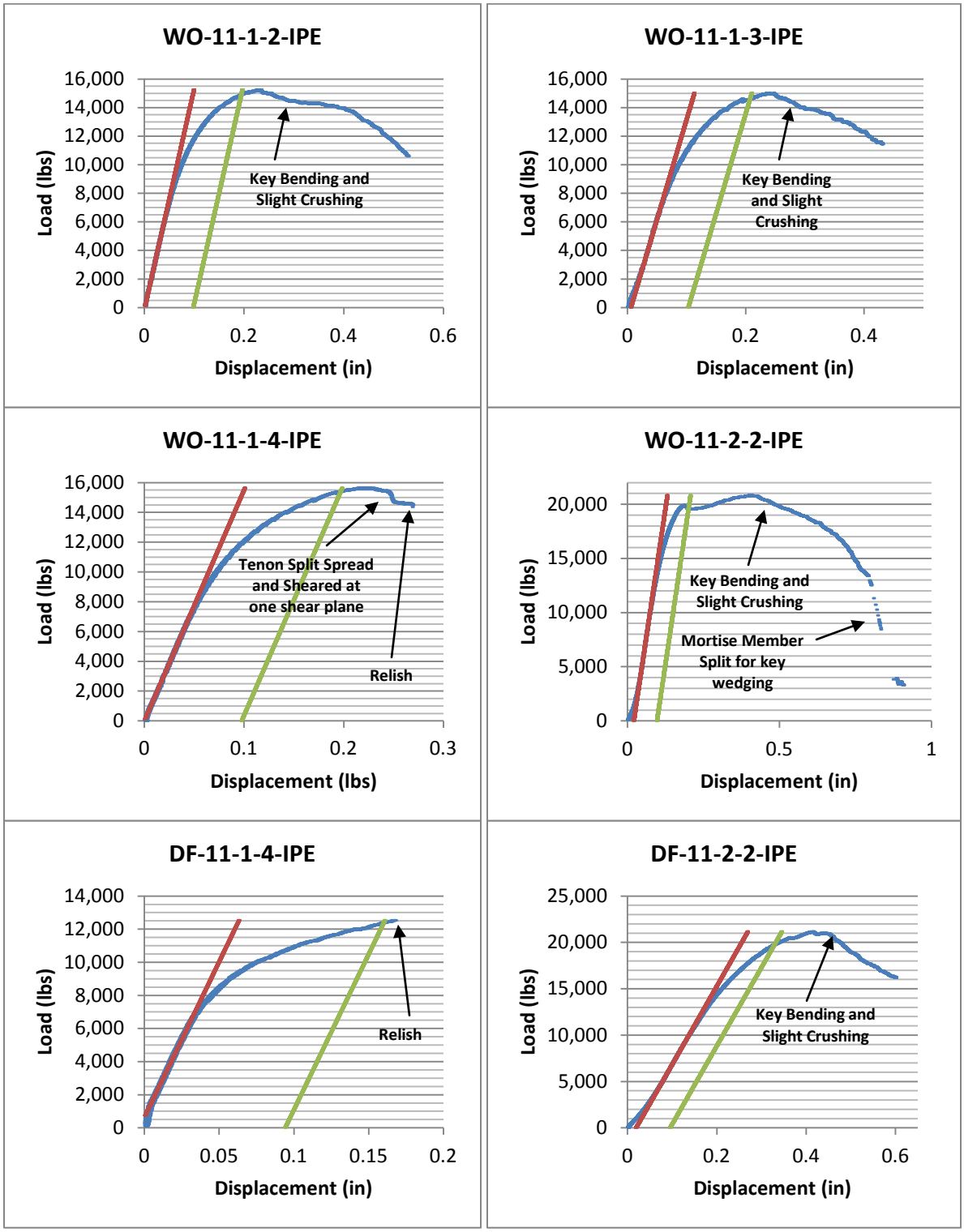
WO-11-1-2-IPE
Load (lbs)
16,000
14,000
12,000
10,000
8,000
6,000
4,000
2,000
0
0
0.2
0.4
0.6
Displacement (in)
Key Bending and Slight Crushing
WO-11-1-3-IPE
Load (lbs)
16,000
14,000
12,000
10,000
8,000
6,000
4,000
2,000
0
0
0.2
0.4
Displacement (in)
Key Bending and Slight Crushing
WO-11-1-4-IPE
Load (lbs)
16,000
14,000
12,000
10,000
8,000
6,000
4,000
2,000
0
0
0.1
0.2
0.3
Displacement (lbs)
Tenon Split Spread and Sheared at one shear plane
Relish
WO-11-2-2-IPE
Load (lbs)
20,000
15,000
10,000
5,000
0
0
0.5
1
Displacement (in)
Key Bending and Slight Crushing
Mortise Member Split for key wedging
DF-11-1-4-IPE
Load (lbs)
14,000
12,000
10,000
8,000
6,000
4,000
2,000
0
0
0.05
0.1
0.15
0.2
Displacement (in)
Relish
DF-11-2-2-IPE
Load (lbs)
25,000
20,000
15,000
10,000
5,000
0
0
0.2
0.4
0.6
Displacement (in)
Key Bending and Slight Crushing

Appendix D - Moisture Content (MC) and Specific Gravity (SG) of Mortise and Tenon Members and Keys

	Tenon Member		Mortise Member		Key (A)		Key (B)	
Joint	MC	SG	MC	SG	MC	SG	MC	SG
WO-4-1-1	66.7%	0.79	65.6%	0.80	19.3%	0.70	N/A	N/A
WO-4-1-2	59.0%	0.76	46.9%	0.71	19.4%	0.70	N/A	N/A
WO-4-1-3	55.9%	0.81	63.4%	0.75	21.2%	0.70	N/A	N/A
WO-4-1-4[1]	59.4%	0.76	53.3%	0.75	12.9%	0.61	N/A	N/A
WO-4-1-5	61.4%	0.83	51.8%	0.76	18.3%	0.64	N/A	N/A
WO-4-2-1	64.6%	0.79	65.0%	0.78	19.4%	0.78	19.5%	0.78
WO-4-2-2	65.4%	0.80	64.6%	1.10	22.6%	0.75	21.8%	0.77
WO-4-2-3	66.1%	0.81	43.6%	0.72	18.8%	0.79	19.1%	0.79
WO-4-2-4	67.5%	0.76	58.3%	0.85	18.6%	0.81	17.9%	0.84
WO-4-2-5	67.1%	0.76	52.8%	0.80	17.9%	0.79	18.0%	0.79
WO-11-1-1	66.9%	0.78	64.6%	0.82	19.3%	0.70	N/A	N/A
WO-11-1-2	67.7%	0.74	64.9%	0.79	21.3%	0.70	N/A	N/A
WO-11-1-3	72.5%	0.80	58.0%	0.84	20.0%	0.67	N/A	N/A
WO-11-1-4	62.9%	0.73	56.7%	0.77	18.9%	0.64	N/A	N/A
WO-11-1-5	65.5%	0.73	56.1%	0.88	19.2%	0.65	N/A	N/A
WO-11-2-1	56.8%	0.75	68.4%	0.78	16.5%	0.80	15.9%	0.80
WO-11-2-2	54.9%	0.77	62.1%	0.76	19.4%	0.81	20.6%	0.79
WO-11-2-3	66.7%	0.78	62.9%	0.79	19.6%	0.68	19.8%	0.67
WO-11-2-4	63.4%	0.77	51.2%	0.75	18.7%	0.80	19.2%	0.80
WO-11-2-5	57.1%	0.77	62.7%	0.79	18.0%	0.78	18.0%	0.79
DF-4-1-1	18.9%	0.47	14.1%	0.46	14.2%	0.66	N/A	N/A
DF-4-1-2	18.8%	0.43	15.8%	0.54	15.1%	0.70	N/A	N/A
DF-4-1-3	16.8%	0.48	13.7%	0.49	14.2%	0.70	N/A	N/A
DF-4-1-4	18.4%	0.47	14.6%	0.45	13.7%	0.72	N/A	N/A
DF-4-1-5	16.5%	0.45	18.5%	0.60	14.6%	0.70	N/A	N/A
DF-4-2-1	13.7%	0.53	14.2%	0.46	15.2%	0.80	14.6%	0.79
DF-4-2-2	18.5%	0.43	14.7%	0.44	14.3%	0.68	14.8%	0.69
DF-4-2-3	18.1%	0.44	18.7%	0.55	14.4%	0.69	14.2%	0.68
DF-4-2-4	14.2%	0.52	14.0%	0.48	14.2%	0.82	14.2%	0.82
DF-4-2-5	18.9%	0.44	14.8%	0.45	13.2%	0.65	13.3%	0.66
DF-11-1-1	11.9%	0.46	14.3%	0.48	14.6%	0.66	N/A	N/A
DF-11-1-2	16.1%	0.46	13.4%	0.48	14.1%	0.66	N/A	N/A
DF-11-1-3	14.0%	0.47	14.5%	0.46	14.3%	0.70	N/A	N/A
DF-11-1-4	17.6%	0.58	15.1%	0.53	15.1%	0.63	N/A	N/A
DF-11-1-5	12.2%	0.53	14.7%	0.47	14.5%	0.70	N/A	N/A
DF-11-2-1	16.2%	0.50	14.0%	0.49	14.1%	0.81	14.1%	0.78
DF-11-2-2	21.3%	0.47	18.3%	0.56	15.2%	0.79	15.4%	0.77
DF-11-2-3	22.8%	0.47	15.7%	0.56	15.5%	0.80	15.6%	0.80
DF-11-2-4	23.7%	0.58	14.6%	0.46	14.5%	0.79	14.4%	0.80
DF-11-2-5	16.5%	0.45	11.1%	0.45	13.4%	0.64	13.6%	0.65
WO-11-1-2-IPE	67.7%	0.74	64.9%	0.79	12.3%	1.03	N/A	N/A
WO-11-1-3-IPE	72.5%	0.80	58.0%	0.84	10.4%	1.04	N/A	N/A
WO-11-1-4-IPE	62.9%	0.73	56.7%	0.77	13.2%	1.03	N/A	N/A
WO-11-2-2-IPE	54.9%	0.77	62.1%	0.76	13.0%	1.01	12.8%	1.01
DF-11-1-4-IPE	17.6%	0.58	15.1%	0.53	12.0%	1.02	N/A	N/A
DF-11-2-2-IPE	21.3%	0.47	18.3%	0.56	10.2%	1.04	10.2%	1.03

[1]Key was misplaced and tested for MC/SG over one week after associated joint members

Appendix E - Joint Load Predictions (Model Nomenclature)

Z,NT:	Tenon Net-section Tension (at keyholes)
Z,Im:	Tenon Parallel-to-grain Keyhole Bearing
Z,RT:	Tenon Row Tear-out/ Tenon Relish
Z,GT :	Tenon Group Tear-out/ Block Shear
Z,Is:	Mortise Bearing
Z,IIIm M,T:	Key Bending considering bearing strength of Mortise and Tenon only
Z,IIIm K:	Key Bending considering bearing strength of Mortise, Tenon, and Key(s)
Z,Im-k:	Key Bearing against Tenon Keyhole
Z,Is-k:	Key Bearing against Mortise Member
Z,Kv:	Key Horizontal Shear

Appendix E - Ultimate Joint Load Predictions

Joint Group	Tenon							Mortise	Key				
	Z,NT (lbs)	Z,Im (lbs)	Z,RT (lbs)	Z,GT (a) (lbs)	Z,GT (b) (lbs)	Z,GT (c) (lbs)	Z,GT (d) (lbs)	Z,Is (lbs)	Z,IIIm (M,T) (lbs)	Z,IIIm (K) (lbs)	Z,Im - K (lbs)	Z,Is - K (lbs)	Z,Kv (lbs)
WO-4-1-1	268,364	25,134	**8,231**	138,297	N/A	N/A	N/A	50,858	18,077	17,584	22,116	58,960	16,500
WO-4-1-2	138,802	19,630	**6,756**	72,779	N/A	N/A	N/A	51,044	17,523	17,523	21,753	58,500	16,093
WO-4-1-3	129,979	23,078	**8,097**	69,038	N/A	N/A	N/A	50,381	18,144	17,976	22,131	58,816	16,516
WO-4-1-4	175,272	20,162	**6,488**	90,880	N/A	N/A	N/A	44,547	16,755	16,755	21,159	57,710	15,372
WO-4-1-5	158,029	18,589	**7,392**	82,711	N/A	N/A	N/A	50,033	17,009	17,009	21,475	58,143	15,604
AVG	174,089	21,319	**7,393**	90,741	N/A	N/A	N/A	49,373	17,502	17,370	21,727	58,426	16,017
COV,%	31.9	12.7	**10.5**	30.8	N/A	N/A	N/A	5.5	3.5	2.8	1.9	0.9	3.2
WO-4-2-1	95,419	30,517	**18,295**	N/A	39,417	74,296	67,418	108,208	26,461	25,217	32,455	86,798	23,544
WO-4-2-2	93,517	27,718	**14,674**	N/A	36,480	71,712	64,999	82,845	26,019	26,019	32,452	87,130	23,868
WO-4-2-3	87,771	34,010	**13,220**	N/A	34,566	66,424	61,169	80,552	26,991	26,673	32,289	86,495	24,476
WO-4-2-4	69,936	32,243	**15,761**	N/A	30,045	55,653	49,990	85,265	27,056	27,056	32,438	85,829	24,812
WO-4-2-5	61,603	33,081	**14,969**	N/A	26,810	49,762	44,206	66,883	25,575	25,455	32,347	85,811	23,357
AVG	81,649	31,514	**15,384**	N/A	33,464	63,569	57,556	84,751	26,421	26,084	32,396	86,412	24,011
COV,%	18.4	7.9	**12.1**	N/A	15.1	16.6	17.4	17.6	2.4	3.0	0.2	0.7	2.6
WO-11-1-1	228,333	24,246	32,183	130,258	N/A	N/A	N/A	51,783	17,652	17,239	21,784	58,603	**16,152**
WO-11-1-2	180,302	24,783	27,113	103,707	N/A	N/A	N/A	66,970	19,440	18,385	22,203	59,389	**17,256**
WO-11-1-3	113,755	25,858	30,743	72,249	N/A	N/A	N/A	51,121	18,399	17,717	21,645	58,350	**16,251**
WO-11-1-4	116,015	24,296	30,780	73,397	N/A	N/A	N/A	64,626	20,523	19,537	21,636	59,387	**17,626**
WO-11-1-5	230,104	20,477	31,470	130,787	N/A	N/A	N/A	40,728	16,280	16,280	21,511	57,336	**14,917**
AVG	173,702	23,932	30,458	102,080	N/A	N/A	N/A	55,046	18,459	17,831	21,756	58,613	**16,440**
COV,%	33.0	8.5	6.4	28.3	N/A	N/A	N/A	19.6	8.8	6.9	1.2	1.5	**6.5**
WO-11-2-1	208,754	29,680	56,740	N/A	93,903	171,591	151,328	86,785	26,186	26,008	31,709	84,193	**23,826**
WO-11-2-2	150,055	26,338	51,485	N/A	73,510	128,030	111,783	84,427	25,842	25,842	32,261	87,092	**23,720**
WO-11-2-3	204,778	33,351	71,762	N/A	100,514	176,026	152,646	116,976	28,844	26,970	33,232	87,212	**24,993**
WO-11-2-4	111,665	35,888	60,538	N/A	65,316	106,888	88,490	70,469	26,384	25,772	32,071	86,256	**23,644**
WO-11-2-5	163,441	30,233	55,232	N/A	78,449	140,224	120,945	71,573	25,708	25,708	32,185	86,948	**23,608**
AVG	167,739	31,098	59,151	N/A	82,338	144,552	125,038	86,046	26,593	26,060	32,292	86,340	**23,958**
COV,%	24.1	11.8	13.1	N/A	17.7	20.3	21.8	21.8	4.8	2.0	1.8	1.5	**2.4**
DF-4-1-1	188,545	22,406	**6,776**	97,660	N/A	N/A	N/A	27,897	14,187	14,108	21,622	56,656	13,211
DF-4-1-2	221,623	22,452	**6,330**	113,977	N/A	N/A	N/A	28,396	14,626	14,515	21,396	57,254	13,291
DF-4-1-3	124,489	23,438	**6,757**	65,623	N/A	N/A	N/A	44,625	17,189	16,888	21,508	56,721	15,492
DF-4-1-4	169,259	23,600	**5,984**	87,622	N/A	N/A	N/A	24,672	13,997	13,811	21,457	57,291	12,648
DF-4-1-5	123,193	23,211	**5,851**	64,522	N/A	N/A	N/A	22,172	13,835	13,689	21,425	57,169	12,577
AVG	165,422	23,021	**6,339**	85,881	N/A	N/A	N/A	29,552	14,767	14,602	21,482	57,018	13,444
COV,%	25.6	2.4	**6.7**	24.7	N/A	N/A	N/A	29.8	9.4	9.0	0.4	0.5	8.8
DF-4-2-1	131,965	56,459	**11,738**	N/A	47,887	95,816	89,926	37,939	22,303	20,804	32,050	84,810	19,527
DF-4-2-2	87,202	36,319	**13,473**	N/A	34,812	65,863	61,007	38,410	21,631	21,179	31,281	85,112	19,432
DF-4-2-3	157,391	39,232	**12,806**	N/A	57,089	113,108	107,240	32,730	20,857	20,316	31,810	85,133	18,663
DF-4-2-4	147,312	42,992	**10,481**	N/A	52,184	105,610	99,748	33,488	21,144	20,386	31,954	84,947	18,721
DF-4-2-5	75,493	34,158	**12,284**	N/A	29,823	57,954	52,658	38,611	21,723	21,545	32,291	86,493	19,777
AVG	119,872	41,832	**12,157**	N/A	44,359	87,670	82,116	36,236	21,532	20,846	31,877	85,299	19,224
COV,%	30.5	21.1	**9.3**	N/A	26.1	27.9	29.3	7.9	2.6	2.5	1.2	0.8	2.6
DF-11-1-1	113,480	25,787	17,763	65,622	N/A	N/A	N/A	27,834	14,550	14,175	21,670	57,006	**13,280**
DF-11-1-2	175,779	24,423	19,594	97,687	N/A	N/A	N/A	26,798	14,293	14,028	21,529	57,400	**13,145**
DF-11-1-3	98,496	33,023	24,501	61,499	N/A	N/A	N/A	31,348	15,950	14,971	21,597	57,013	**13,715**
DF-11-1-4	215,666	31,034	27,931	121,799	N/A	N/A	N/A	36,295	16,268	15,328	21,706	57,253	**14,352**
DF-11-1-5	124,072	28,366	25,956	75,014	N/A	N/A	N/A	31,834	15,394	14,740	21,555	57,408	**13,809**
AVG	145,499	28,526	23,149	84,324	N/A	N/A	N/A	30,822	15,291	14,648	21,612	57,216	**13,660**
COV,%	33.6	12.5	18.6	29.9	N/A	N/A	N/A	12.2	5.6	3.7	0.3	0.3	**3.5**
DF-11-2-1	102,387	36,185	48,736	N/A	55,728	95,395	79,058	33,223	20,601	20,288	32,175	84,559	**18,623**
DF-11-2-2	89,614	30,875	46,421	N/A	51,334	84,701	70,474	35,332	20,697	20,697	31,999	84,629	**19,000**
DF-11-2-3	102,007	28,416	58,878	N/A	62,107	98,778	82,057	43,195	20,824	20,824	32,296	85,065	**19,499**
DF-11-2-4	81,621	28,321	53,882	N/A	51,889	83,614	66,755	38,686	21,066	21,066	32,236	85,121	**19,352**
DF-11-2-5	122,168	37,076	50,259	N/A	62,967	109,461	92,567	42,863	22,219	21,728	32,000	86,162	**20,137**
AVG	99,560	32,175	51,635	N/A	56,805	94,390	78,182	38,660	21,082	20,921	32,141	85,107	**19,322**
COV,%	15.4	13.1	9.4	N/A	9.7	11.3	13.0	11.5	3.1	2.5	0.4	0.8	**2.9**
WO-11-1-2-IPE	180,089	23,416	23,673	101,881	N/A	N/A	N/A	62,744	24,891	24,891	41,118	109,058	**19,364**
WO-11-1-3-IPE	113,371	24,535	27,402	70,386	N/A	N/A	N/A	48,469	24,491	24,491	40,253	108,435	**18,629**
WO-11-1-4-IPE	115,336	23,269	27,365	71,350	N/A	N/A	N/A	60,825	25,847	25,847	40,614	109,552	**19,677**
AVG	136,265	23,740	26,146	81,206	N/A	N/A	N/A	57,346	25,076	25,076	40,662	109,015	**19,223**
COV,%	28	3	8	22	N/A	N/A	N/A	14	3	3	1	1	**3**
WO-11-2-2-IPE	152,316	**26,436**	48,017	N/A	72,482	127,850	112,399	83,866	34,394	34,394	63,467	169,567	26,712
DF-11-1-4-IPE	214,954	30,078	27,525	121,240	N/A	N/A	N/A	35,280	22,589	22,589	41,235	109,078	**17,168**
DF-11-2-2-IPE	89,614	31,464	45,175	N/A	50,711	84,078	70,163	36,006	30,417	30,417	63,914	169,039	**22,716**

Governing Predictions Bolded and Shaded

Appendix E - Allowable Joint Load Predictions

Joint Group	Tenon							Mortise	Key				
	Z,NT (lbs)	Z,Im (lbs)	Z,RT (lbs)	Z,GT a (lbs)	Z,GT b (lbs)	Z,GT c (lbs)	Z,GT d (lbs)	Z,Is (lbs)	Z,IIIm (M,T) (lbs)	Z,IIIm (K) (lbs)	Z,Im - K (lbs)	Z,Is - K (lbs)	Z,Kv (lbs)
WO-4-1-1	12,199	6,030	**1,616**	6,907	N/A	N/A	N/A	4,584	2,954	2,722	2,838	7,566	2,272
WO-4-1-2	12,071	4,907	**1,559**	6,815	N/A	N/A	N/A	4,940	3,011	2,837	2,792	7,507	2,318
WO-4-1-3	12,207	5,437	**1,543**	6,875	N/A	N/A	N/A	4,538	2,974	2,777	2,840	7,548	2,268
WO-4-1-4	11,718	5,041	**1,496**	6,607	N/A	N/A	N/A	4,054	2,779	2,620	2,715	7,406	2,174
WO-4-1-5	11,724	4,267	**1,544**	6,634	N/A	N/A	N/A	4,792	2,882	2,775	2,756	7,461	2,304
AVG	11,984	5,137	**1,552**	6,768	N/A	N/A	N/A	4,581	2,920	2,746	2,788	7,498	2,267
COV,%	2.1	12.7	**2.8**	2.1	N/A	N/A	N/A	7.3	3.1	3.0	1.9	0.9	2.5
WO-4-2-1	9,347	7,250	**3,207**	N/A	4,569	7,986	6,958	11,963	4,802	4,379	4,165	11,139	3,641
WO-4-2-2	9,622	6,651	**3,031**	N/A	4,514	8,139	7,068	7,040	4,315	4,137	4,164	11,181	3,380
WO-4-2-3	9,498	7,919	**3,058**	N/A	4,554	8,002	7,026	8,265	4,645	4,301	4,144	11,100	3,570
WO-4-2-4	9,239	7,536	**3,133**	N/A	4,495	7,878	6,867	6,790	4,332	4,078	4,163	11,014	3,385
WO-4-2-5	9,316	7,763	**3,139**	N/A	4,492	7,963	6,904	6,218	4,217	3,966	4,151	11,012	3,291
AVG	9,405	7,424	**3,114**	N/A	4,525	7,993	6,965	8,055	4,462	4,172	4,157	11,089	3,453
COV,%	1.6	6.7	**2.3**	N/A	0.8	1.2	1.2	28.7	5.6	4.0	0.2	0.7	4.2
WO-11-1-1	12,174	5,826	6,220	9,197	N/A	N/A	N/A	4,746	2,912	2,683	2,795	7,520	**2,235**
WO-11-1-2	12,169	5,807	6,228	9,198	N/A	N/A	N/A	5,849	3,208	2,934	2,849	7,621	**2,449**
WO-11-1-3	11,991	6,155	6,126	9,059	N/A	N/A	N/A	4,688	3,018	2,763	2,778	7,488	**2,257**
WO-11-1-4	12,051	6,074	6,111	9,081	N/A	N/A	N/A	8,098	3,828	3,337	2,776	7,621	**2,716**
WO-11-1-5	11,897	5,119	6,108	9,002	N/A	N/A	N/A	4,019	2,763	2,607	2,760	7,358	**2,130**
AVG	12,057	5,796	6,159	9,108	N/A	N/A	N/A	5,480	3,146	2,865	2,792	7,522	**2,357**
COV,%	1.0	7.0	1.0	1.0	N/A	N/A	N/A	29.3	13.2	10.1	1.2	1.5	**9.8**
WO-11-2-1	9,317	6,725	12,260	N/A	9,055	12,522	9,186	10,324	4,751	4,476	4,069	10,804	**3,717**
WO-11-2-2	9,353	5,909	12,210	N/A	9,083	12,481	9,218	7,056	4,239	4,139	4,140	11,176	**3,381**
WO-11-2-3	9,637	8,116	12,648	N/A	9,366	12,920	9,502	11,961	5,150	4,609	4,265	11,192	**3,798**
WO-11-2-4	9,293	8,370	12,272	N/A	9,053	12,513	9,173	6,694	4,367	4,049	4,116	11,069	**3,361**
WO-11-2-5	9,460	7,126	12,332	N/A	9,108	12,684	9,284	7,032	4,365	4,133	4,130	11,158	**3,429**
AVG	9,412	7,249	12,345	N/A	9,133	12,624	9,272	8,613	4,574	4,281	4,144	11,080	**3,537**
COV,%	1.5	14.0	1.4	N/A	1.4	1.5	1.5	27.7	8.2	5.7	1.8	1.5	**5.8**
DF-4-1-1	13,395	5,601	**1,306**	7,350	N/A	N/A	N/A	2,908	2,379	2,250	2,775	7,271	1,905
DF-4-1-2	13,133	5,613	**1,218**	7,175	N/A	N/A	N/A	3,259	2,544	2,393	2,746	7,347	1,981
DF-4-1-3	13,373	5,859	**1,233**	7,303	N/A	N/A	N/A	4,195	2,857	2,642	2,760	7,279	2,193
DF-4-1-4	13,104	5,900	**1,226**	7,165	N/A	N/A	N/A	3,538	2,628	2,450	2,754	7,352	2,029
DF-4-1-5	13,331	5,803	**1,195**	7,263	N/A	N/A	N/A	2,685	2,425	2,292	2,749	7,336	1,901
AVG	13,267	5,755	**1,235**	7,251	N/A	N/A	N/A	3,317	2,567	2,405	2,757	7,317	2,002
COV,%	1.0	2.4	**3.4**	1.1	N/A	N/A	N/A	17.8	7.4	6.4	0.4	0.5	6.0
DF-4-2-1	10,803	14,115	**2,548**	N/A	4,714	8,638	7,759	4,114	3,683	3,355	4,113	10,883	2,844
DF-4-2-2	10,180	9,080	**2,474**	N/A	4,514	8,139	7,347	4,934	3,894	3,624	4,014	10,922	3,008
DF-4-2-3	10,414	9,808	**2,446**	N/A	4,577	8,284	7,496	3,746	3,552	3,333	4,082	10,925	2,765
DF-4-2-4	10,399	10,748	**2,529**	N/A	4,579	8,350	7,489	4,082	3,688	3,422	4,101	10,901	2,840
DF-4-2-5	10,532	8,540	**2,512**	N/A	4,560	8,485	7,546	4,962	3,924	3,686	4,144	11,099	3,059
AVG	10,466	10,458	**2,502**	N/A	4,589	8,379	7,527	4,368	3,748	3,484	4,091	10,946	2,903
COV,%	2.2	21.1	**1.7**	N/A	1.6	2.3	2.0	12.6	4.2	4.6	1.2	0.8	4.3
DF-11-1-1	13,552	6,447	5,032	9,292	N/A	N/A	N/A	3,195	2,512	2,335	2,781	7,315	**1,976**
DF-11-1-2	13,412	6,106	5,022	9,217	N/A	N/A	N/A	3,153	2,492	2,328	2,763	7,366	**1,970**
DF-11-1-3	13,421	8,256	5,030	9,226	N/A	N/A	N/A	4,544	3,000	2,657	2,772	7,316	**2,200**
DF-11-1-4	13,350	7,758	5,016	9,183	N/A	N/A	N/A	3,719	2,700	2,446	2,786	7,347	**2,071**
DF-11-1-5	13,400	7,091	5,046	9,223	N/A	N/A	N/A	4,046	2,769	2,512	2,766	7,367	**2,126**
AVG	13,427	7,132	5,029	9,228	N/A	N/A	N/A	3,731	2,695	2,456	2,773	7,342	**2,068**
COV,%	0.6	12.5	0.2	0.4	N/A	N/A	N/A	15.8	7.7	5.6	0.3	0.3	**4.8**
DF-11-2-1	10,630	9,046	10,036	N/A	8,274	12,392	9,452	4,489	3,768	3,531	4,129	10,851	**2,931**
DF-11-2-2	10,523	7,719	9,883	N/A	8,244	12,162	9,383	4,496	3,728	3,547	4,106	10,860	**2,944**
DF-11-2-3	10,424	7,104	10,087	N/A	8,382	12,129	9,403	5,078	3,694	3,537	4,144	10,916	**2,995**
DF-11-2-4	10,478	7,080	10,067	N/A	8,236	12,309	9,357	5,155	3,889	3,722	4,137	10,923	**3,088**
DF-11-2-5	10,242	9,269	9,887	N/A	8,116	12,013	9,179	4,894	3,840	3,577	4,106	11,057	**2,998**
AVG	10,459	8,044	9,992	N/A	8,250	12,201	9,355	4,822	3,784	3,583	4,125	10,922	**2,991**
COV,%	1.4	13.1	1.0	N/A	1.2	1.2	1.1	6.5	2.1	2.2	0.4	0.8	**2.1**
WO-11-1-2-IPE	12,155	5,487	5,437	8,796	N/A	N/A	N/A	5,480	4,328	4,328	8,080	21,431	**2,981**
WO-11-1-3-IPE	11,951	5,840	5,460	8,706	N/A	N/A	N/A	4,445	4,229	4,229	7,910	21,309	**2,833**
WO-11-1-4-IPE	11,981	5,817	5,433	8,707	N/A	N/A	N/A	7,622	5,081	5,081	7,981	21,528	**3,444**
AVG	12,029	5,715	5,444	8,736	N/A	N/A	N/A	5,849	4,546	4,546	7,991	21,423	**3,086**
COV,%	0.9	3.5	0.3	0.6	N/A	N/A	N/A	27.7	10.3	10.3	1.1	0.5	**10.3**
WO-11-2-2-IPE	9,494	5,931	11,388	N/A	8,715	12,166	9,105	7,009	5,946	5,946	12,472	33,322	**4,106**
DF-11-1-4-IPE	13,306	7,519	4,943	9,125	N/A	N/A	N/A	3,615	3,947	3,947	8,103	21,435	**2,620**
DF-11-2-2-IPE	10,523	7,866	9,618	N/A	8,111	12,029	9,317	4,582	5,774	5,774	12,560	33,218	**3,776**

Governing (Design) Predictions Bolded and Shaded

Appendix F - Model Input Specimen Test Strength Results

Tension Parallel-to-grain (Tenon)

Specimen	Ultimate Strength (psi)	MC	SG
WO-4-1-1	24,639	47.3%	0.77
WO-4-1-2	12,879	47.5%	0.69
WO-4-1-3	11,926	46.8%	0.86
WO-4-1-4	16,753	43.8%	0.67
WO-4-1-5	15,097	48.8%	0.91
WO-4-2-1	11,433	49.5%	0.83
WO-4-2-2	10,885	55.7%	0.85
WO-4-2-3	10,350	50.3%	0.78
WO-4-2-4	8,478	52.5%	0.81
WO-4-2-5	7,406	49.4%	0.79
WO-11-1-1	21,007	49.0%	0.79
WO-11-1-2	16,594	46.8%	0.77
WO-11-1-3	10,625	51.6%	0.78
WO-11-1-4	10,782	46.5%	0.79
WO-11-1-5	21,662	49.4%	0.76
WO-11-2-1	25,094	32.2%	0.81
WO-11-2-2	17,969	39.7%	0.85
WO-11-2-3	23,798	44.2%	0.79
WO-11-2-4	13,458	45.8%	0.77
WO-11-2-5	19,351	44.4%	0.69
DF-4-1-1	17,454	14.6%	0.48
DF-4-1-2	20,926	13.5%	0.49
DF-4-1-3	11,543	15.2%	0.43
DF-4-1-4	16,017	14.9%	0.46
DF-4-1-5	11,459	14.2%	0.43
DF-4-2-1	15,147	12.3%	0.53
DF-4-2-2	10,622	13.0%	0.45
DF-4-2-3	18,740	13.6%	0.45
DF-4-2-4	17,565	12.4%	0.54
DF-4-2-5	8,888	16.4%	0.43
DF-11-1-1	10,383	11.4%	0.49
DF-11-1-2	16,251	15.0%	0.41
DF-11-1-3	9,100	10.1%	0.47
DF-11-1-4	20,032	16.1%	0.51
DF-11-1-5	11,481	12.0%	0.50
DF-11-2-1	11,944	13.6%	0.47
DF-11-2-2	10,560	16.1%	0.51
DF-11-2-3	12,134	19.8%	0.49
DF-11-2-4	9,659	17.7%	0.46
DF-11-2-5	14,791	13.3%	0.51

Appendix F

Shear Parallel-to-grain (Tenon)

Specimen	Ultimate Strength (psi)	MC	SG
WO-4-1-1	1,671	39.5%	0.80
WO-4-1-2	1,421	37.1%	0.70
WO-4-1-3	1,721	43.8%	0.82
WO-4-1-4	1,423	41.0%	0.76
WO-4-1-5	1,570	43.0%	0.88
WO-4-2-1	1,871	Missing	0.85
WO-4-2-2	1,588	55.1%	0.88
WO-4-2-3	1,418	52.2%	0.82
WO-4-2-4	1,650	51.4%	0.76
WO-4-2-5	1,564	52.7%	0.80
WO-11-1-1	1,697	46.0%	0.80
WO-11-1-2	1,428	44.9%	0.72
WO-11-1-3	1,646	59.8%	0.79
WO-11-1-4	1,652	42.1%	0.77
WO-11-1-5	1,690	45.0%	0.71
WO-11-2-1	1,518	40.8%	0.81
WO-11-2-2	1,383	38.5%	0.81
WO-11-2-3	1,861	45.9%	0.81
WO-11-2-4	1,618	44.9%	0.70
WO-11-2-5	1,469	39.6%	0.73
DF-4-1-1	1,370	15.3%	0.48
DF-4-1-2	**1,372**	**10.8%**	**0.42**
DF-4-1-3	1,447	13.7%	0.43
DF-4-1-4	1,289	14.4%	0.42
DF-4-1-5	1,293	14.2%	0.44
DF-4-2-1	1,216	12.2%	0.51
DF-4-2-2	1,438	13.3%	0.42
DF-4-2-3	1,382	13.9%	0.41
DF-4-2-4	1,094	10.7%	0.43
DF-4-2-5	1,291	15.8%	0.47
DF-11-1-1	932	11.3%	0.45
DF-11-1-2	1,030	13.3%	0.47
DF-11-1-3	1,286	10.6%	0.42
DF-11-1-4	1,470	13.7%	0.51
DF-11-1-5	1,358	12.2%	0.50
DF-11-2-1	1,282	13.2%	0.45
DF-11-2-2	1,240	15.7%	0.44
DF-11-2-3	1,541	18.4%	0.54
DF-11-2-4	1,413	16.5%	0.49
DF-11-2-5	1,342	13.7%	0.45

Tested after others

Appendix F

Bearing Parallel-to-grain (Tenon)

Specimen	5% Offset Yield Strength (psi)	Ultimate Strength (psi)	MC	SG
WO-4-1-1	5,810	6,054	44.5%	0.81
WO-4-1-2	4,807	4,807	43.8%	0.71
WO-4-1-3	5,235	5,555	46.7%	0.83
WO-4-1-4	5,076	5,076	39.2%	0.75
WO-4-1-5	4,234	4,611	46.8%	0.86
WO-4-2-1	4,760	5,009	42.4%	0.81
WO-4-2-2	4,367	4,550	49.9%	0.80
WO-4-2-3	5,226	5,611	51.4%	0.80
WO-4-2-4	4,950	5,295	49.8%	0.72
WO-4-2-5	5,114	5,448	53.8%	0.79
WO-11-1-1	5,699	5,929	43.8%	0.77
WO-11-1-2	5,573	5,946	48.5%	0.73
WO-11-1-3	6,059	6,364	46.9%	0.80
WO-11-1-4	5,982	5,982	42.4%	0.74
WO-11-1-5	5,071	5,071	42.6%	0.72
WO-11-2-1	4,519	4,986	33.8%	0.77
WO-11-2-2	3,903	4,349	43.0%	0.78
WO-11-2-3	5,204	5,346	45.7%	0.79
WO-11-2-4	5,561	5,961	48.1%	0.78
WO-11-2-5	4,718	5,004	39.3%	0.76
DF-4-1-1	5,520	5,520	15.3%	0.46
DF-4-1-2	5,590	5,590	14.6%	0.45
DF-4-1-3	5,805	5,805	14.2%	0.45
DF-4-1-4	5,859	5,859	14.7%	0.46
DF-4-1-5	5,771	5,771	14.1%	0.45
DF-4-2-1	9,384	9,384	10.9%	0.45
DF-4-2-2	6,185	6,185	14.8%	0.47
DF-4-2-3	6,570	6,570	15.4%	0.44
DF-4-2-4	7,167	7,167	12.2%	0.49
DF-4-2-5	5,635	5,635	15.8%	0.44
DF-11-1-1	6,339	6,339	10.9%	0.48
DF-11-1-2	6,043	6,043	14.4%	0.46
DF-11-1-3	8,145	8,145	11.2%	0.51
DF-11-1-4	7,616	7,616	14.0%	0.53
DF-11-1-5	7,010	7,010	12.7%	0.51
DF-11-2-1	5,991	5,991	14.1%	0.45
DF-11-2-2	5,140	5,140	16.3%	0.43
DF-11-2-3	4,687	4,687	17.8%	0.49
DF-11-2-4	4,680	4,680	16.1%	0.44
DF-11-2-5	6,172	6,172	14.1%	0.48

Appendix F

Bearing Perpendicular-to-grain (Mortise)

Specimen	5% Offset Yield Strength (psi)	Ultimate Strength (psi)	MC	SG
WO-4-1-1	2,071	4,595	42.5%	0.68
WO-4-1-2	2,249	4,648	37.2%	0.68
WO-4-1-3	2,055	4,563	37.0%	0.75
WO-4-1-4	1,871	4,112	33.3%	0.74
WO-4-1-5	2,195	4,584	37.8%	0.74
WO-4-2-1	3,671	6,641	45.3%	0.69
WO-4-2-2	2,152	5,065	44.3%	0.73
WO-4-2-3	2,545	4,961	36.7%	0.70
WO-4-2-4	2,107	5,292	44.0%	0.74
WO-4-2-5	1,930	4,152	36.1%	0.82
WO-11-1-1	2,157	4,707	32.2%	0.77
WO-11-1-2	2,623	6,007	49.0%	0.73
WO-11-1-3	2,140	4,667	41.5%	0.74
WO-11-1-4	3,632	5,797	39.3%	0.71
WO-11-1-5	1,867	3,784	41.0%	0.78
WO-11-2-1	3,266	5,491	49.3%	0.79
WO-11-2-2	2,158	5,164	42.9%	0.76
WO-11-2-3	3,653	7,145	45.9%	0.73
WO-11-2-4	2,067	4,352	46.3%	0.76
WO-11-2-5	2,154	4,385	48.6%	0.75
DF-4-1-1	1,367	2,623	10.4%	0.43
DF-4-1-2	1,516	2,642	12.3%	0.52
DF-4-1-3	1,970	4,191	9.8%	0.49
DF-4-1-4	1,645	2,294	11.6%	0.44
DF-4-1-5	1,251	2,066	15.3%	0.54
DF-4-2-1	1,292	2,383	12.0%	0.41
DF-4-2-2	1,544	2,404	11.0%	0.43
DF-4-2-3	1,172	2,048	15.4%	0.55
DF-4-2-4	1,280	2,100	11.2%	0.47
DF-4-2-5	1,528	2,378	12.5%	0.43
DF-11-1-1	1,493	2,601	11.5%	0.47
DF-11-1-2	1,463	2,487	11.3%	0.52
DF-11-1-3	2,123	2,929	11.8%	0.44
DF-11-1-4	1,730	3,377	12.7%	0.54
DF-11-1-5	1,877	2,954	12.8%	0.42
DF-11-2-1	1,414	2,093	11.8%	0.48
DF-11-2-2	1,415	2,224	14.2%	0.57
DF-11-2-3	1,590	2,705	13.2%	0.49
DF-11-2-4	1,613	2,421	11.6%	0.45
DF-11-2-5	1,513	2,650	11.5%	0.43

Appendix F

Bending (Keys) - White Oak						
Specimen	5% Offset Yield Strength (psi)	Ultimate Strength (psi)	MC	SG	Ring Orientation	Rings per Inch
1	8,435	11,866	10.3%	0.64	R/T	15
2	6,000	8,170	11.6%	0.64	R	15
3	7,524	10,159	11.4%	0.71	R/T	12
4	8,538	12,148	12.0%	0.67	T	9
5	9,231	11,640	11.4%	0.65	R	14
6	7,226	8,942	11.2%	0.68	R/T	17
7	6,893	10,382	11.8%	0.70	R	15
8	7,274	9,910	11.4%	0.64	T	17
9	8,342	11,796	10.8%	0.64	R/T	?
10	9,892	13,280	10.1%	0.71	R	14
11	11,138	15,042	10.8%	0.68	R/T	13
12	8,229	11,981	11.5%	0.67	T	14
13	7,909	10,915	11.6%	0.65	R	13
14	8,144	11,597	11.6%	0.65	R/T	13
15	8,183	11,265	11.6%	0.63	R/T	15
16	7,123	9,795	11.3%	0.65	R/T	13
17	8,222	11,782	11.4%	0.69	R/T	12
18	8,355	11,402	11.3%	0.68	T	18
19	7,662	10,567	12.1%	0.68	T	12
20	8,364	11,427	11.0%	0.77	R	9
21	7,095	9,480	11.3%	0.68	R	12
22	7,305	10,350	11.7%	0.64	T	13
23	8,036	11,420	10.9%	0.65	R/T	14
24	7,145	9,413	10.4%	0.63	R/T	13
25	7,490	10,292	11.1%	0.64	R/T	14
26	8,122	11,147	11.3%	0.65	R/T	14
27	8,594	11,698	11.6%	0.65	R/T	12
28	7,930	11,190	11.4%	0.65	R/T	13
AVG	**8,014**	**11,038**	**11.3%**	**0.66**	(R - Radial)	
COV	**12.3%**	**12.3%**	**4.2%**	**4.6%**	(T - Tangential)	

Appendix F

Bending (Keys) - Red Oak						
Specimen	5% Offset Strength (psi)	Ultimate Strength (psi)	MC	SG	Ring Orientation	Rings per Inch
1	12,718	16,118	11.1%	0.67	T	6
2	11,836	15,576	10.8%	0.69	R	6
3	12,082	16,944	10.9%	0.68	R	6
4	9,022	12,538	10.8%	0.61	T	9
5	11,105	15,092	11.2%	0.75	R	8
6	11,475	15,485	10.6%	0.65	T	6
7	13,538	18,562	11.3%	0.71	R	6
8	13,201	16,790	11.7%	0.69	T	6
9	11,505	15,946	11.8%	0.67	T	5
10	14,580	21,077	11.0%	0.74	R	6
11	14,259	17,705	11.0%	0.73	R/T	7
12	13,405	17,887	11.4%	0.67	T	6
13	12,807	16,724	10.9%	0.68	T	5
14	11,645	15,362	11.0%	0.66	R	6
15	13,039	16,688	11.5%	0.68	R	6
16	12,159	16,659	10.9%	0.65	R/T	5.5
17	10,611	15,671	10.8%	0.65	R	8
18	12,868	18,053	11.4%	0.67	R	6
19	11,394	15,493	11.4%	0.60	R	8
20	8,331	13,457	10.5%	0.60	R	7
21	12,028	16,144	10.2%	0.65	R	6
22	13,447	17,547	9.6%	0.67	T	5
23	12,261	16,405	10.2%	0.64	R	6
24	11,314	15,603	10.2%	0.64	R	6
25	11,648	16,276	10.9%	0.65	R/T	6
26	12,976	17,003	11.1%	0.71	R/T	5
27	13,737	19,324	11.0%	0.73	R/T	7
28	14,704	20,257	11.0%	0.73	R/T	7
AVG	**12,275**	**16,657**	**10.5%**	**0.67**	(R - Radial)	
COV	**12.0%**	**10.8%**	**21.9%**	**5.9%**	(T - Tangential)	

Appendix F

Bending (Keys) - Black Walnut						
Specimen	5% Offset Strength (psi)	Ultimate Strength (psi)	MC	SG	Ring Orientation	Rings per Inch
1	13,155	15,667	9.4%	0.64	R/T	4
2	9,059	11,715	9.9%	0.63	R	4
3	12,046	17,477	10.0%	0.60	T	16
4	9,144	13,380	10.3%	0.57	T	5
5	11,817	16,803	10.4%	0.57	T	18
6	9,709	13,052	10.0%	0.60	T	4
7	9,578	12,976	9.8%	0.57	R/T - R	5
8	13,103	18,342	9.7%	0.63	R-T	6
9	6,877	10,384	9.4%	0.57	R/T-T	3
10	12,534	17,651	9.6%	0.64	R	11
11	13,082	17,274	9.8%	0.63	R/T	12
12	9,654	13,567	8.3%	0.57	T	6
13	9,874	14,021	9.8%	0.66	T	5
14	8,398	11,924	8.8%	0.56	T-R/T	4
15	12,851	17,882	9.7%	0.63	R/T	10
16	10,828	16,990	10.0%	0.64	R-R/T	9
17	12,327	15,782	9.8%	0.62	T	7
18	13,840	18,560	10.0%	0.63	R/T	10
19	12,166	16,477	10.1%	0.63	T	10
20	8,033	12,033	9.8%	0.60	T-R	6.5
21	11,547	16,076	10.0%	0.59	R-R/T	4.5
22	9,367	13,418	9.7%	0.55	T	4.5
23	14,275	19,005	9.9%	0.64	T	12
24	12,259	16,980	10.1%	0.61	T	12
25	12,598	16,741	10.1%	0.57	T	6
26	10,521	14,652	10.2%	0.62	R	6
27	12,926	18,501	10.2%	0.63	R	12
28	12,318	16,579	9.5%	0.60	R/T	10
AVG	**11,210**	**15,497**	**9.8%**	**0.61**	(R - Radial)	
COV	**17.3%**	**15.7%**	**4.4%**	**5.0%**	(T - Tangential)	

Appendix F

Bending (Keys) - Cherry						
Specimen	5% Offset Strength (psi)	Ultimate Strength (psi)	MC	SG	Ring Orientation	Rings per Inch
1	12,084	16,113	9.4%	0.61	T	8
2	11,289	15,530	8.5%	0.69	T	11
3	11,667	16,295	8.4%	0.69	T	6
4	8,135	11,372	8.5%	0.55	R/T	6.5
5	12,172	14,785	8.0%	0.62	R	6
6	12,530	15,652	9.6%	0.57	T-R/T	4.5
7	10,921	15,425	9.9%	0.58	T	5
8	12,450	17,458	8.7%	0.59	R/T	4
9	10,823	14,226	9.4%	0.63	T-R/T	3.5
10	12,575	16,069	9.1%	0.58	R/T	4
11	12,208	16,939	8.9%	0.60	R/T	3.5
12	11,960	16,697	10.1%	0.56	T-R/T	5
13	10,611	13,750	8.7%	0.59	T	8
14	8,231	9,708	8.2%	0.56	T	10
15	11,781	16,757	9.4%	0.58	T	5
16	13,791	18,451	8.7%	0.66	T	5
17	8,275	9,769	7.6%	0.61	R/T	3.5
18	9,528	11,801	8.7%	0.54	T-R/T	6
19	13,741	17,508	8.5%	0.61	R/T	5
20	12,170	13,335	8.1%	0.55	T-R/T	4.5
21	6,387	8,480	8.9%	0.54	R/T	6
22	11,169	15,324	9.1%	0.65	R	13
23	12,277	15,429	9.2%	0.59	R-R/T	3.5
24	13,222	17,616	8.0%	0.56	T	5
25	13,030	16,471	9.0%	0.56	R	4
26	11,463	16,748	7.8%	0.65	T-R/T	5
27	11,179	15,070	8.9%	0.72	R	4
28	13,057	16,029	8.5%	0.56	T	6
AVG	**11,383**	**14,957**	**8.8%**	**0.60**	(R - Radial)	
COV	**15.8%**	**17.2%**	**7.0%**	**8.1%**	(T - Tangential)	

Appendix F

Bending - Key (IPE)					
Specimen	5% Offset Strength (psi)	Ultimate Strength (psi)	MC	SG	Ring Orientation
1	17,932	22,116	8.3%	1.06	T
2	21,658	25,959	8.4%	0.99	T
3	14,993	19,005	8.5%	1.06	R
4	19,303	24,764	8.8%	1.04	R
AVG	**18,472**	**22,961**	**8.5%**	**1.04**	(R - Radial)
COV	**15.1%**	**13.4%**	**2.5%**	**3.4%**	(T - Tangential)

Appendix F

Bearing Perpendicular-to-grain (Keys) - White Oak						
Specimen	5% Offset Strength (psi)	Ultimate Strength (psi)	MC	SG	Ring Orientation	Rings per Inch
1	3,490	5,793	8.6%	0.78	R/T	6.5
2	2,925	5,686	8.2%	0.73	R/T	11
3	3,422	5,103	9.7%	0.69	R	9
4	3,452	4,839	7.8%	0.69	R/T	12
5	3,796	5,102	8.9%	0.74	R	10
6	3,731	5,913	8.3%	0.64	R/T	9
7	3,976	5,118	7.3%	0.71	R	12
8	3,133	5,678	8.5%	0.71	R/T	10
9	3,277	4,453	9.7%	0.91	R/T	8
10	4,036	6,463	7.6%	0.74	R	9
11	3,568	5,052	7.3%	0.72	R/T	9
12	3,533	5,034	8.7%	0.80	R	11
13	3,796	4,965	7.9%	0.73	R	11
14	3,229	4,978	7.9%	0.80	R/T	10
15	3,209	4,809	8.9%	0.72	R	12
16	3,325	5,242	7.7%	0.72	R/T	9
17	3,186	5,473	8.9%	0.62	R/T	11
18	3,207	5,449	9.4%	0.63	R/T	13
19	3,057	5,549	10.2%	0.63	R/T	13
20	2,999	5,459	7.6%	0.62	R/T	11
21	3,279	5,471	7.2%	0.65	R/T	14
22	3,626	5,271	8.3%	0.69	R/T	11
23	3,214	5,337	8.3%	0.65	R/T	13
24	3,940	5,413	8.5%	0.73	R	9
25	3,260	5,398	9.9%	0.63	R/T	12
26	3,349	5,504	7.1%	0.76	R	7
27	3,273	5,176	8.5%	0.76	R/T	9
28	3,411	5,439	7.5%	0.77	R/T	9
AVG	**3,418**	**5,327**	**8.4%**	**0.71**	(R - Radial)	
COV	**8.7%**	**7.4%**	**10.2%**	**9.2%**	(T - Tangential)	

Appendix F

Bearing Perpendicular-to-grain (Keys) - Red Oak						
Specimen	5% Offset Strength (psi)	Ultimate Strength (psi)	MC	SG	Ring Orientation	Rings per Inch
1	4,377	8,113	6.2%	0.78	R	9
2	4,581	8,746	7.4%	0.81	R	9
3	4,411	8,008	9.4%	0.84	R	7
4	4,397	7,755	9.0%	0.84	R	7
5	4,673	8,444	8.4%	0.84	R	7
6	4,360	8,038	7.4%	0.85	R	8
7	4,473	8,058	6.8%	0.85	R	7
8	4,667	7,957	7.5%	0.80	R	8
9	3,989	7,769	8.0%	0.82	R	6
10	4,258	7,434	7.3%	0.80	R	8
11	4,369	7,643	6.9%	0.80	R	6
12	4,174	7,864	8.1%	0.85	R	6.5
13	4,447	8,029	6.7%	0.89	R	7
14	5,215	8,526	6.1%	0.88	R	7
15	4,573	8,379	8.3%	0.81	R	7
16	5,027	8,788	8.7%	0.80	R	8
17	5,875	7,615	7.3%	0.90	R	7
18	5,450	8,864	8.1%	0.83	R	7
19	5,630	10,278	7.7%	0.77	R	7
20	4,032	9,813	6.5%	0.70	R	8.5
21	5,150	10,175	6.3%	0.74	R	8
22	5,052	8,017	7.2%	0.82	R	7
23	4,129	9,445	6.4%	0.71	R	7
24	3,967	9,512	6.7%	0.73	R	7
25	5,143	8,510	6.5%	0.77	R	7
26	4,868	8,703	6.1%	0.79	R	8
27	5,218	9,678	6.1%	0.78	R	8
28	4,893	8,878	6.0%	0.82	R	6
AVG	**4,693**	**8,537**	**7.3%**	**0.81**	(R - Radial)	
COV	**10.8%**	**9.3%**	**13.1%**	**6.1%**	(T - Tangential)	

Appendix F

Bearing Perpendicular-to-grain (Keys) - Black Walnut						
Specimen	5% Offset Strength psi	Ultimate Strength psi	MC	SG	Ring Orientation	Rings per Inch
1	2,660	4,350	6.6%	0.54	T-R/T	4
2	3,047	5,194	9.0%	0.58	R-R/T	3
3	3,374	5,750	8.7%	0.59	R	3.5
4	3,389	6,362	8.0%	0.62	T-R/T	4
5	3,694	6,088	7.1%	0.62	R/T	4
6	3,900	6,041	6.5%	0.59	T-R/T	3.5
7	4,942	6,516	6.3%	0.66	R	3.5
8	4,442	7,358	8.2%	0.69	R-R/T	3
9	3,883	6,381	8.4%	0.68	T-R/T	3
10	3,366	5,352	9.0%	0.65	T	3.5
11	3,482	5,254	8.1%	0.57	T	4
12	3,196	4,607	7.6%	0.61	T	3.5
13	4,219	6,031	7.4%	0.65	R-R/T	4
14	3,554	4,871	6.4%	0.57	T	3
15	3,308	5,026	7.8%	0.59	T	3.5
16	3,641	6,551	7.9%	0.59	T	4
17	3,337	5,458	8.2%	0.60	R-R/T	3
18	3,984	6,964	6.9%	0.63	T-R/T	5
19	3,895	6,996	6.6%	0.63	R/T	7.5
20	3,888	6,700	6.4%	0.61	T-R/T	7
21	4,781	6,823	5.9%	0.62	T-R/T	7
22	4,580	7,719	6.3%	0.67	R-R/T	7
23	4,349	7,414	6.8%	0.65	R/T	7
24	3,697	6,288	6.5%	0.64	T-R/T	7.5
25	3,894	6,597	6.9%	0.68	T	5
26	3,840	6,722	6.0%	0.63	T-R/T	7
27	4,107	6,922	6.1%	0.66	T-R/T	6
28	4,188	6,964	5.6%	0.66	T-R/T	7
AVG	**3,809**	**6,189**	**7.2%**	**0.62**	(R - Radial)	
COV	**13.9%**	**14.4%**	**13.8%**	**6.3%**	(T - Tangential)	

Appendix F

Bearing Perpendicular-to-grain (Keys) - Cherry						
Specimen	5% Offset Strength psi	Ultimate Strength psi	MC	SG	Ring Orientation	Rings per Inch
1	6,806	9,869	5.0%	0.64	R	5
2	2,453	4,801	5.5%	0.57	T-R/T	4
3	3,263	6,954	6.1%	0.60	R	3.5
4	2,320	4,784	5.7%	0.59	R/T	5
5	3,607	6,679	5.5%	0.58	R	4
6	3,248	6,587	5.4%	0.53	R	4
7	3,324	6,498	5.3%	0.54	R	4.5
8	3,681	6,697	4.9%	0.60	R/T	3.5
9	5,238	8,499	5.7%	0.59	R	4
10	3,431	6,404	5.4%	0.57	R/T	3.5
11	2,564	5,161	5.5%	0.54	R/T	4.5
12	5,386	7,087	5.5%	0.55	R	4.5
13	3,310	6,516	5.5%	0.55	R-R/T	6
14	4,036	6,009	5.4%	0.56	T-R/T	4
15	5,312	10,637	5.7%	0.63	R	4
16	4,609	9,026	5.2%	0.63	R	4.5
17	4,423	8,388	5.5%	0.61	R	4
18	6,113	8,505	5.7%	0.62	R	4.5
19	4,438	8,693	5.7%	0.64	R	4.5
20	4,268	8,547	5.5%	0.58	R	4
21	6,033	8,274	4.7%	0.64	R	5
22	5,899	8,799	5.7%	0.62	R	4
23	5,536	6,885	5.1%	0.59	R-R/T	4
24	5,967	7,222	5.2%	0.65	R-R/T	4
25	3,428	7,012	5.4%	0.62	R-R/T	4
26	3,568	6,854	5.4%	0.64	R-R/T	5
27	6,279	8,054	5.1%	0.66	R	4
28	5,430	9,168	5.2%	0.62	R	4.5
AVG	**4,428**	**7,450**	**5.4%**	**0.60**	(R - Radial)	
COV	**29.1%**	**19.6%**	**5.6%**	**6.4%**	(T - Tangential)	

Appendix F

Bearing Perpendicular-to-grain Bearing - Key Bearing (IPE)					
Specimen	5% Offset Strength psi	Ultimate Strength psi	MC	SG	Ring Orientation
1	9,434	9,727	5.4%	0.98	T
2	10,706	10,792	5.7%	1.01	T
3	10,811	10,997	5.9%	1.05	T
4	10,083	10,247	6.1%	1.02	T
AVG	**10,259**	**10,441**	**5.8%**	**1.01**	(R - Radial)
COV	**6.2%**	**5.5%**	**5.1%**	**3.0%**	(T - Tangential)

Appendix F

Shear Parallel-to-grain (Keys) - White Oak					
Specimen	Ultimate Strength (psi)	MC	SG	Shear Surface Ring Orientation	Rings per Inch
1	2,087	11.0%	0.77	T	6.5
2	1,917	11.1%	0.68	T-R/T	9
3	1,653	10.6%	0.65	R/T	9
4	1,851	11.6%	0.66	R/T	17
5	1,701	11.6%	0.66	R	14
6	2,194	10.8%	0.75	R/T	7
7	1,849	11.7%	0.63	R/T	15
8	1,656	10.9%	0.69	R-R/T	8
9	1,804	11.5%	0.65	R-R/T	13
10	1,915	11.6%	0.63	R/T	16
11	1,488	11.8%	0.65	R	14
12	1,839	11.9%	0.66	R	13
13	1,856	11.6%	0.65	R/T	16
14	1,986	11.1%	0.68	T-R/T	8
15	1,797	11.2%	0.69	T-R/T	8
16	1,898	11.1%	0.78	T	6
17	2,044	11.2%	0.68	R/T	9
18	1,921	11.7%	0.68	R/T	15
19	2,092	11.0%	0.73	R-R/T	7
20	2,208	11.0%	0.74	R/T	7
21	1,834	11.0%	0.67	R-R/T	10
22	1,931	11.7%	0.71	T-R/T	7
23	2,327	11.0%	0.78	R/T	7
24	2,143	11.7%	0.73	T	6
25	1,910	11.1%	0.69	T-R/T	8
26	1,872	11.7%	0.64	R/T	15
27	1,909	11.2%	0.67	R/T	9
28	1,911	11.6%	0.64	R/T	15
AVG	**1,914**	**11.3%**	**0.69**	(R - Radial)	
COV	**9.5%**	**3.1%**	**6.5%**	(T - Tangential)	

Appendix F

Shear Parallel-to-grain (Keys) - Red Oak					
Specimen	Ultimate Strength (psi)	MC	SG	Shear Surface Ring Orientation	Rings per Inch
1	1,660	11.8%	0.60	R	7
2	1,892	12.5%	0.69	R	8.5
3	1,889	12.4%	0.70	R/T	8
4	1,630	11.6%	0.60	R	8
5	2,063	11.9%	0.68	R	7
6	1,964	13.3%	0.72	R-R/T	7
7	1,720	13.4%	0.70	R	9
8	1,501	13.0%	0.67	R	8
9	1,630	12.4%	0.59	R	8
10	1,665	13.5%	0.71	R	8
11	1,541	13.4%	0.70	R	7
12	2,059	13.2%	0.74	R/T	9
13	1,599	11.8%	0.61	R	7.5
14	1,582	12.5%	0.66	R	7
15	1,851	12.3%	0.71	R-R/T	9
16	1,678	11.6%	0.60	R	7
17	1,675	11.9%	0.62	R	7
18	1,952	12.8%	0.69	R	7
19	1,660	12.4%	0.59	R	8
20	1,891	12.9%	0.77	R	7
21	1,650	11.5%	0.61	R	7
22	1,965	12.4%	0.70	R	7.5
23	1,755	13.0%	0.68	R	7
24	1,626	11.7%	0.62	R	8
25	2,130	12.1%	0.71	R-R/T	9
26	1,760	12.5%	0.68	R	7
27	1,837	12.8%	0.67	R	8
28	1,392	11.7%	0.60	R	7
AVG	**1,758**	**12.4%**	**0.66**	(R - Radial)	
COV	**10.5%**	**5.1%**	**7.7%**	(T - Tangential)	

Appendix F

Shear Parallel-to-grain (Keys) - Black Walnut					
Specimen	Ultimate Strength (psi)	MC	SG	Shear Surface Ring Orientation	Rings Per Inch
1	1,786	11.1%	0.54	T	12
2	1,630	10.6%	0.61	R	8
3	1,642	10.7%	0.62	R/T	8
4	1,456	10.6%	0.59	R	10
5	1,645	11.1%	0.54	T	11.5
6	1,562	10.6%	0.60	R	5
7	1,736	10.7%	0.65	R/T	5.5
8	1,428	10.7%	0.56	T	10
9	1,643	11.1%	0.55	T	12
10	1,956	9.1%	0.65	T	5
11	1,665	10.5%	0.63	R/T	9
12	1,592	10.2%	0.61	R	9
13	1,435	10.9%	0.60	R	5
14	1,633	10.7%	0.55	R/T	10.5
15	1,632	11.2%	0.62	T	8
16	1,855	10.9%	0.64	R/T	8
17	1,636	11.1%	0.55	T	11
18	1,927	10.6%	0.67	R/T	8
19	1,659	10.7%	0.61	R	6
20	1,544	10.3%	0.60	R	10
21	1,642	10.9%	0.55	T	10
22	1,521	10.7%	0.61	R	5
23	2,040	10.3%	0.63	R/T	6
24	1,561	11.0%	0.55	T	11
25	1,073	10.7%	0.60	R	11
26	1,941	11.0%	0.55	T	10
27	1,375	10.7%	0.59	R	9
28	1,676	10.4%	0.63	R/T	6
AVG	**1,639**	**10.7%**	**0.60**	(R - Radial)	
COV	**12.1%**	**3.7%**	**6.5%**	(T - Tangential)	

Appendix F

Shear Parallel-to-grain (Keys) - Cherry					
Specimen	Ultimate Strength (psi)	MC	SG	Shear Surface Ring Orientation	Rings per Inch
1	1,521	9.9%	0.59	T	5.5
2	1,283	10.1%	0.56	T	6
3	1,417	9.1%	0.59	R-R/T	6
4	1,394	8.8%	0.56	R	5
5	1,524	9.2%	0.60	R	4
6	1,598	8.3%	0.61	R/T	4
7	1,387	9.3%	0.59	R	5
8	802	9.0%	0.57	R	5
9	1,366	9.0%	0.57	R-R/T	5
10	1,280	8.9%	0.57	R-R/T	4
11	1,279	9.2%	0.59	R	3.5
12	1,561	9.0%	0.56	R-R/T	4.5
13	1,378	10.2%	0.59	T	6
14	1,777	10.1%	0.58	T	6
15	1,958	11.0%	0.68	T	7.5
16	1,338	11.0%	0.66	T	7
17	1,800	10.7%	0.66	T	9
18	1,672	10.0%	0.59	T	5
19	2,018	11.0%	0.67	T	6
20	1,524	8.4%	0.58	R/T	5
21	1,555	8.3%	0.58	R/T	5
22	1,444	10.3%	0.58	T	7
23	1,580	8.9%	0.60	R	4
24	1,543	10.1%	0.70	T	8.5
25	1,645	10.6%	0.62	T	3.5
26	1,781	10.5%	0.69	T	5
27	1,151	8.8%	0.57	R/T	4.5
28	1,577	8.6%	0.58	R	3.5
AVG	**1,505**	**9.6%**	**0.60**	(R - Radial)	
COV	**16.4%**	**9.1%**	**7.0%**	(T - Tangential)	

Appendix F

Shear Parallel-to-grain - Key Shear (IPE)			
Specimen	Ultimate Strength (psi)	MC, %	SG
1	2,224	7.2%	0.98
2	2,759	7.9%	0.99
3	2,746	7.3%	0.98
4	2,491	8.5%	1.00
5	2,792	9.1%	1.01
6	2,991	8.1%	1.00
AVG	**2,667**	**8.0%**	**1.00**
COV	**10.1%**	**8.9%**	**1.3%**